MOLECULAR CHARACTERISATION OF ETHYLENE BIOSYNTHESIS DURING LEAF ONTOGENY IN WHITE CLOVER (*Trifolium repens* L.)

A thesis presented in partial fulfillment of the requirements
for the degree of

Doctor of Philosophy

at

Massey University

SANG DONG YOO

1999

Dedication

This thesis is dedicated to my mother

Dong-Sook Kim

and to my wife

Young hee Cho

Abstract

Ethylene (C_2H_4) biosynthesis has been investigated during leaf ontogeny in white clover (*Triforium repens* L. cv. Glassland challenge, genotype 10F) with a particular emphasis on the production of the hormone in the apex and newly initiated leaves (designated as leaves 1 and 2). In these developing tissues, a relatively higher rate (5 to 6-fold) of ethylene production (0.5 to 0.9 nL C_2H_4 $gFwt^{-1}$ hr^{-1}) was associated with a higher accumulation (1.5-fold) of 1-aminocyclopropane-1-carboxylate (ACC), when compared with mature green leaves.

Genes encoding the ethylene biosynthetic enzymes, ACC synthase (ACS) and ACC oxidase (ACO) have been cloned to characterise ethylene biosynthesis at the molecular level. The partial protein-coding regions of ACS genes have been cloned using reverse transcriptase-dependent polymerase chain reaction (RT-PCR) with degenerate nested primers using cDNA templates from RNA isolated either the apex or leaf 2. These ACS genes were identified and designated as TRACS1, TRACS2 and TRACS3. TRACS1 (680 bp) is 72% and 64% homologous to TRACS2 (674 bp) and TRACS3 (704 bp), respectively, and TRACS2 and TRACS3 are 63% homologous, in terms of nucleotide sequence. TRACS1 shows highest homology with PS-ACS2, an ACS cloned from etiolated pea (*Pisum sativum*) seedlings which is induced by IAA and wounding. TRACS2 shows highest homology with MI-ACS1, an ACS cloned from mature mango (*Mangifera indica*) fruit. TRACO3 shows highest homology with VR-ACS7, an ACS cloned from etiolated hypocotyls of mung bean (*Vigna radiata*) and also PS-ACS1, an ACS cloned from etiolated pea seedlings which is induced by IAA, but not by wounding.

The TRACS3 gene was expressed as a 1.95 kb transcript mainly in the apex and newly initiated leaves as determined by northern analysis. TRACS1 has not been detected in the tissues examined. The expression of TRACS2 has not been determined.

Three ACO genes, comprising *ca.* 1100 bp of the protein-coding region and 3'-untranslated region (3'-UTR) have been cloned using a combination of RT-PCR and 3'-rapid amplification of cDNA ends (3'-RACE), and designated as TRACO1, TRACO2 and TRACO3. Comparison

of a 813 bp protein-coding region of TRACO1, generated by RT-PCR using degenerate primers on cDNA templates from RNA isolated from the apex shows 77% and 75% homology to the protein-coding region sequences of TRACO2 (804 bp) and TRACO3 (816 bp), respectively, generated by RT-PCR using degenerate primers on cDNA templates from RNA isolated from leaf 2. The TRACO2 and TRACO3 protein-coding region sequences show 84% homology. The technique of 3'-RACE generated 3'-UTR sequences of 301 bp (TRACO1), 250 bp (TRACO2), and 92 bp (TRACO3) each amplified using mRNA extracted from the apex. The 92 bp 3'-UTR of TRACO3 has been shown to be a truncated version of a 324 bp sequence amplified from TRACO3 expressed in senescent leaf tissue of white clover (Dr. D. Hunter, IMBS, Massey University, *personal communication*), and it is this full-length version that was used in further experiments. The 3'-UTR sequences of the three ACO genes are more divergent, when compared with the protein-coding regions, showing 61%, 55%, and 59% homology between TRACO1 and TRACO2, TRACO1 and full-length TRACO3, and TRACO2 and full-length TRACO3, respectively. Using these 3'-UTR sequences as gene-specific probes, Southern analysis revealed that the three ACO genes are encoded by distinct genes in the white clover genome.

Northern analysis, using either protein-coding regions or 3'-UTRs as probes, determined that the TRACO1 gene was expressed as a 1.35 kb transcript almost exclusively in the apex and the TRACO2 gene was expressed as a 1.35 kb transcript mainly in newly initiated leaves and mature green leaves, with maximum expression in newly initiated leaves. This pattern of gene expression coincides with the high rate of ethylene production from the apex and newly initiated leaves in white clover. The apex tissue-specific TRACO1 gene was also detected in axillary buds, and the mature leaf-associated TRACO2 gene was expressed in other mature vegetative tissues, including internodes, nodes and petioles. Both TRACO1 and TRACO2 genes are highly expressed in roots.

TRACO3 gene expression was not detected in apex and mature green leaf tissues examined using the 3'-UTR gene-specific probe, but two transcripts (1.17 kb and 1.35 kb) were visualised using the protein-coding region probe and with an extended exposure time.

ACO enzyme activity, *in vitro*, was highest in just fully expanded mature green leaves (leaf 3 and leaf 4) during leaf ontogeny in white clover. Apex, axillary bud and floral bud tissues show a relatively higher enzyme activity, when compared with mature nodes and internode tissues, but lower than that measured in petiole tissue. Highest activity of ACO, *in vitro*, has been detected in root extracts.

Polyclonal antibodies, raised against the TRACO1 gene product expressed in *E. coli*, recognised a high molecular weight (*ca.* 205 kD) protein complex with highest accumulation in the apex. This complex was also detected in axillary bud, floral bud, and leaf 1 tissue. Immunoaffinity-based purification of the *ca.* 205 kD protein was carried out to obtain sufficient protein for amino acid sequencing. However, no sequence was obtained.
Polyclonal antibodies, raised against the TRACO2 gene product in *E. coil*, recognised ACO protein (*ca.* 36 kD) in newly initiated leaves and mature green leaves as well as petioles and roots. This recognition pattern coincides with ACO enzyme activity, *in vitro*, as well as TRACO2 gene expression in the tissue.

Expression of the TRACO2 and TRACO3 genes has been characterised in response to a combination of wounding, ethylene, indole-3-acetic acid (IAA), aminoethoxyvinylglycine (AVG), and 1-methylcyclopropene (1-MCP) treatments using mature green leaves. Expression of TRACO2 gene is enhanced in response to ethylene and IAA. Ethylene-induced TRACO2 gene expression was not blocked by 1-MCP. Expression of TRACO3 was induced in response to wounding in mature green leaves. Wound-induced TRACO3 gene expression was not induced by the ethylene produced in the leaf tissue, indicating ethylene-independent ACO expression in the wounded leaves. Induction of either TRACO2 by IAA treatment or TRACO3 by wounding was delayed with AVG treatment of mature green tissue, suggesting that changes in ACS activity in the tissue is associated with induction of ACO gene expression.

Acknowledgment

I would like to thank Dr. Michael T. McManus and Professor Paula E Jameson for their valuable advice and deep understanding throughout my Ph.D. period. In particular, Dr. McManus has been patient and inspiring, and has been an excellent role model as a scientist. I cannot thank you enough, Michael. Professor Jameson has been supportive and I thank you for giving me a once in a life time chance of meeting Michael. I also thank Dr. Veit for valuable discussion throughout.

I thank my first lab teacher, Dr. Butcher for giving me such a flying start.
Lyn has been wonderful both for understanding and for helping out in many aspects. Especially, I thank you for your patient listening. Dr. Don, my lab partner, I appreciate deeply your generous help throughout. It's been a great pleasure being with you.

I thank Deming for assisting my write up, Richard for the phylogenetic tree analysis, Leon for assistance with scanning, Nena for helping out with the *in situ* hybridisation and Carmel for much technical advice. Thank you very much all!

Ranier and Angelika, I thank you for sharing friendship. You've been so nice to me and my wife. Dan! Well, what can I say? Thanks anyway.

I would like to thank my great lab mates, Greg, Kusmin, Huaibi, Trish, Celia, Simone, Nigel, Robert H, Don, Suzanne. Thank you all!

I would like to thank Institute of Molecular BioSciences, Massey University for the opportunity to use laboratories and other facilities. I would like to thank to Dr. Mike Hay, Grasslands, AgResearch, for financial support. I would also like to thank NZSPP and IMBS for travel grants to attend 16th International Congress of Plant Growth Substances and Annual NZSPP meetings.

Table of Contents

Chapter 2. Materials and Methods

List of figures

List of tables

Abbreviation

$A_{260\ nm}$	absorbance in a 1 cm light path at 260 nm
ACC	1-aminocyclopropane-1-carboxylate
ACO	ACC oxidase
ACS	ACC synthase
AE	after excision
Amp^{100}	ampicilin (100 mg / mL)
AOA	aminoethoxyacetic acid
APS	ammonium persulphate
ATP	adenosine-5'-triphophate
AVG	aminoethoxyvinylglycine
BCIP	5-bromo-4-chloro-3-indolyl-phosphate
BSA	bovine serum albumin
ca.	approximately
CBB	Coomassie Brilliant Blue
CER	constitutive ethylene response
CHX	cycloheximide
CNBr	cyanogen bromide
DATP	2'-deoxyadenosine-5'-triphosphate
DCTP	2'-deoxycytidine-5'-triphosphate
DMF	N',N'-dimethyl formamide
DMSO	dimethyl sulphoxide
DNA	deoxyribonucleic aicd
DTT	dithiothreitol
DTTP	2'-deoxythymidine-5'-triphosphate
EDTA	ethylenediaminetetraacetic acid
EIN	ethylene insensitive

EMS	ethylmethane sulfonate
ERE	ethylene responsive element
Fwt	fresh weight
GACC	1-(gamma-L-glutamylamino)cyclopropane-1-caboxylate
GC	gas chromatography
hr	hour
IAA	indole-3-acetic acid
kb	kilo-pairs
kD	kilo-dalton
LB	Luria-Bertani (media)
MAbs	monoclonal antibodies
MACC	1-(malonylamino)cyclopropane-1-carboxylate
1-MCP	1-methylcyclopropene
min	minute
MOPS	Na[3-(N-morpholiono)propanesulphonic aicd
MTA	5'-methylthioadenosine
NaOAc	sodium acetate
NBT	*p*-nitro blue terazolium chloride
Ni-NTA	nickel-nitrilotriacetic acid
PA	1,10-phenanthroline
PAbs	polyclonal antibodies
PAGE	polyacrylamide gel electrophoresis
PCR	polymerase chain reaction
pH	$-\log[H^+]$

pI	isoelectro-point
PLP	pyrodoxyl phosphate
PVDF	polyvinyliden difluoride
PVPP	polyvinyl polypyrrolidone
3'-RACE	3'-rapid amplification of cDNA ends
RNase	ribonuclease
RO	reverse osmosis
RPA	ribonuclease protection assay
RT-PCR	reverse transcriptase-dependent PCR
s.e.	standard error of the mean
SAG	senescence-associated gene
SAM	S-adenosylmethionine
SA-PMP	Streptavidine Magne Sphere® Paticles
SDS	Sodium dodesyl sulphate
TEMED	*N,N,N',N*-tetramethylethylenediamine
Tris	tris(hydroxymethyl)aminomethane
U	units
UTR	untranslated region
UV	ultra violet
V	volt (m^2 kg s^{-3} A^{-1})
W	watt (m^2 kg s^{-3}) = VA
YE-elicitor	yeast-extracted elicitor

Chapter 1. Introduction

1.1. Overview

Ethylene (C_2H_4) was the first endogenous regulator of plant growth and development identified chemically (Abeles *et al.*, 1992; Bleecker, 1999) and the biochemistry and molecular biology of the ACC-dependent ethylene biosynthesis has been well characterised in higher plants (Mckeon *et al.* 1995). More recently, our understanding of the action of the ethylene has also been advanced at the molecular level using ethylene-responsive mutants of *Arabidopsis thaliana* (Bleecker, 1999; Chang and Shockey, 1999). Together, these studies suggest that the regulation of both the biosynthesis of and sensitivity to ethylene in a plant tissue governs many physiological responses to developmental or environmental stimuli.

In the pasture legume white clover (*Trifolium repens* L.), leaf senescence-associated ethylene biosynthesis has been characterised at the physiological, biochemical and molecular levels (Butcher, 1997; Hunter, 1998). In this thesis, the molecular basis of ethylene biosynthesis during early leaf development has been characterised and compared with biosynthesis during the later leaf senescence stage. To do this, genes encoding the key ethylene biosynthetic enzymes, ACC synthase and ACC oxidase have been cloned and their expression patterns studied in developing leaf tissues. Also, these ethylene biosynthetic genes have been further characterised to determine some of the factors, which may regulate their expression, with the aim of the understanding how ethylene biosynthesis is controlled during leaf ontogeny in white clover.

1.2 Ethylene in plant biology

Ethylene (C_2H_4) is a chemically simple molecule known to regulate many biological functions in plants. This hydrocarbon gas, well known as a fruit-ripening regulator (Lelievre *et al.*, 1997), is biologically active at a concentration as little as 10 nL L^{-1} in air (Reid, 1995). Almost all plant tissues are able to produce or respond to ethylene, which has been shown to regulate many aspects of the growth and development in higher plants (Mattoo and Suttle, 1991; Abeles *et al.*, 1992). These include:

- the breaking of seed dormancy in some species to enhance seed germination, and also the regulation of plumular expansion from some spring buds (Abeles, 1973; Ketring, 1977; Brewley and Black, 1994; Kepczynski and Kepczynska, 1997),

- the well characterised ethylene response in seedlings grown in the dark, termed the triple response: seedlings, when exposed to 1 $\mu L\ L^{-1}$ exogenous ethylene in the dark, display shortened and thickened stems with exaggerated apical hooks, when compared with seedlings grown without ethylene (Guzman and Ecker, 1990). This ethylene-induced apical hook structure seems to facilitate the emergence of germinating seedlings through the soil (Harpham *et al.*, 1991),

- mediating apparently opposite effects (to the triple response) on light-grown seedlings, such as enhancing hypocotyl elongation and promoting emergence of the first true leaf (Smalle and Van Der Straeten, 1997),

- the promotion of shoot and leaf epinastic growth, and also regulation of the position of root hair growth initiation (Dolan, 1997),

- playing an important role in sex determination in some species, e.g. cucumber (*Cucuminus sativus*; Trebitsh *et al.*, 1997),

- the promoting action in leaf and flower senescence and abscission, with modification of the spectrum of pigment in plant organs (Reid, 1995; Smalle and Van Der Straten, 1997; O'Neil, 1997; Johnson and Ecker, 1998),

- the mediation of environmental signals. For instance, ethylene is thought to be a key regulator of the growth of rice (*Oryza sativa*) internodes in a submerged environment (Kende, 1983; Kende *et al.*, 1998) and also for the growth of corn (*Zea mays*) roots in response to a hypoxic environment (Drew, 1997), and

- the mediation of signals for abiotic and biotic stresses to modify plant defense mechanisms (O'Donnell *et al.*, 1996; Morgan and Drew, 1997; Bowles, 1998; Ohtsubo *et al.*, 1999).

All these roles for ethylene during plant growth and development underline how complex the mechanisms must be which regulate ethylene biosynthesis and its signal transduction pathway in higher plants (Johnson and Ecker, 1998).

1.3 Ethylene perception and signal transduction

Understanding of ethylene action in higher plants has progressed rapidly with studies on ethylene perception and signal transduction using *A. thaliana* (Kieber and Ecker, 1993; Ecker, 1995; Bleecker and Schaller, 1996; Kieber 1997a; 1997b; Bleecker *et al.*, 1998; Fluhr, 1998; Johnson and Ecker, 1998; McGrath and Ecker, 1998; Solano and Ecker, 1998; Woeste and Kieber, 1998).

1.3.1 Ethylene responsive mutants

Ethylene signaling mutants have been isolated using the altered triple response of etiolated seedlings in mutagenized lines of *A. thaliana* (Bleecker *et al.*, 1988; Guzman and Ecker 1990; Van Der Straeten *et al.*, 1993).

Ethylene insensitive (EIN) mutants show a reduced or no response to exogenous ethylene at *ca.* 100 $\mu L\ L^{-1}$ and *etr1, ein2, ein3, ein4, ein5, ein6* and *ein7* have been reported as members of this class of mutations. For example, *etr1* mutants conferred insensitivity to endogenous ethylene as well as exogenous ethylene and showed abnormal growth and development (Bleecker *et al.*, 1988). The hypocotyls of the mutant elongated with ethylene in a similar way to wild types grown without ethylene in the dark. The rosette size was 25% enlarged and the timing of flowering (determined by bolting) and leaf senescence was delayed about one to two weeks in mutants, when compared with wild types. As well, seeds of the mutants showed relatively lower rate of germination under the same conditions. Therefore, the *etr1* phenotype showed typical ethylene insensitivity in many aspects of plant development.

In contrast, constitutive ethylene response (CER) mutants show the triple response in etiolated seedlings grown without added ethylene, and these are categorized into two sub-classes, according to their capacity for ethylene production.

Seedlings of one class of CER mutants produce higher amounts of ethylene in the dark, when compared with wild type. The constitutive triple response of these mutant seedlings appears to be caused by this overproduction of endogenous ethylene, and *eto1, eto2, eto3,* and *eto4* belong to this class of CER mutants. Recently, characterisation of *eto2* has revealed that the mutant has a defect in a gene encoding for the ethylene biosynthetic enzyme, ACC synthase (ACS5). The point mutation near to the carboxyl terminal of ACS5 in *eto2* modifies the enzyme to be produced as a hyperactive form, which is responsible for the higher ethylene production by the mutant (Vogel *et al.*, 1998).

The second class of CER mutants, designated as constitutive triple response (e.g. *ctr1*), does not produce higher ethylene production in the dark, when compared with wild types, but still displays the triple response without ethylene treatment (Kieber *et al.*, 1993). The mutant phenotype displayed a short hypocotyl, a compact inflorescence, and a reduced root system without ethylene treatment and hence the phenotype was similar to that observed in wild type responding to ethylene treatment. From the recessive nature of the *ctr1* mutant, it is proposed that the mutant has an impaired negative regulator affecting on the ethylene signal transduction pathway in *A. thaliana.*

In addition, the construction of double mutants provided a means of identifying the order of gene products in the ethylene signal transduction pathway (Roman *et al.*, 1995). *Ctr1* is epistatic to *etr1* and *ein4*, so the double mutant *etr1* or *ein4* with *ctr1* always shows the *ctr1* phenotype. Whereas *ein2, ein3, ein5, ein6* or *ein7* show an epinastic relationship to *ctr1,* indicating that these mutants have defects in genes working down-stream of *ctr1*.

Since the first ethylene insensitive dominant mutant (*etr1*) was reported a decade ago (Bleecker *et al.*, 1988), cloning and characterisation of genes from these various mutants has proceeded rapidly. This has led to more of an understanding of the molecular basis of ethylene perception,

and subsequent signal transduction to the nucleus: events which underlie the ethylene response in higher plants.

1.3.2 Ethylene perception

Cloning the ETR1 gene using a map-based approach revealed that this gene encodes a two-component signal transducer present in prokaryotes and eukaryotes (Chang *et al.*, 1993; Chang, 1996). Ethylene perception by ETR1 was demonstrated by a [C^{14}]-ethylene displacement assay using the protein overexpressed in yeast (Schaller and Bleecker, 1995; Bleecker and Schaller, 1996). The ethylene-binding activity (perception) of the ETR1 is mediated through a transition metal, copper (Cu I) located in the second hydrophobic motif at N-terminal end of the protein (Rodriguez *et al.*, 1999). This transition metal (copper) mediated ethylene binding activity of ETR1 has been further supported by cloning a gene encoding a copper-transporting P-type ATPase from the *ran1* mutant (*responsive to antagonist 1*). This mutant is sensitive to an ethylene action inhibitor, *trans*-cyclooctene (Hirayama *et al.*, 1999). Because the gene product is proposed to deliver copper to create a functional ethylene receptor such as ETR1. The ETR1 protein has been further characterised biochemically showing that it acts as a homodimer (Schaller *et al.*, 1995), and contains intrinsic histidine-kinase activity (Gamble *et al.*, 1998). Taken together, the ETR1 gene product has been proposed as a functional ethylene receptor (Chang and Myerowitz, 1995; Bleecker *et al.*, 1998; Bleecker, 1999).

However, the lack of recessive mutants for *etr1* suggested that this class of gene might be functionally redundant in *A. thaliana* (Ecker, 1995). To elucidate this further, intensive screening of mutagenized *A. thaliana* lines for *etr1* class mutants, and also low stringency screening of cDNA libraries using cloned ethylene receptor genes (ETR1) as probes, was undertaken to identify gene homologues (Hua *et al.*, 1995; Sakai *et al.*, 1998; Hua *et al.*, 1998). All together, five members of a putative ethylene receptor gene family were cloned and designated as ETR1, ETR2, ERS1, ERS2 and EIN4. The structure of each of these genes is very similar and the deduced amino acids are highly conserved, particularly at the N-terminus, which includes the membrane-spanning regions for ethylene binding (Fig. 1.1).

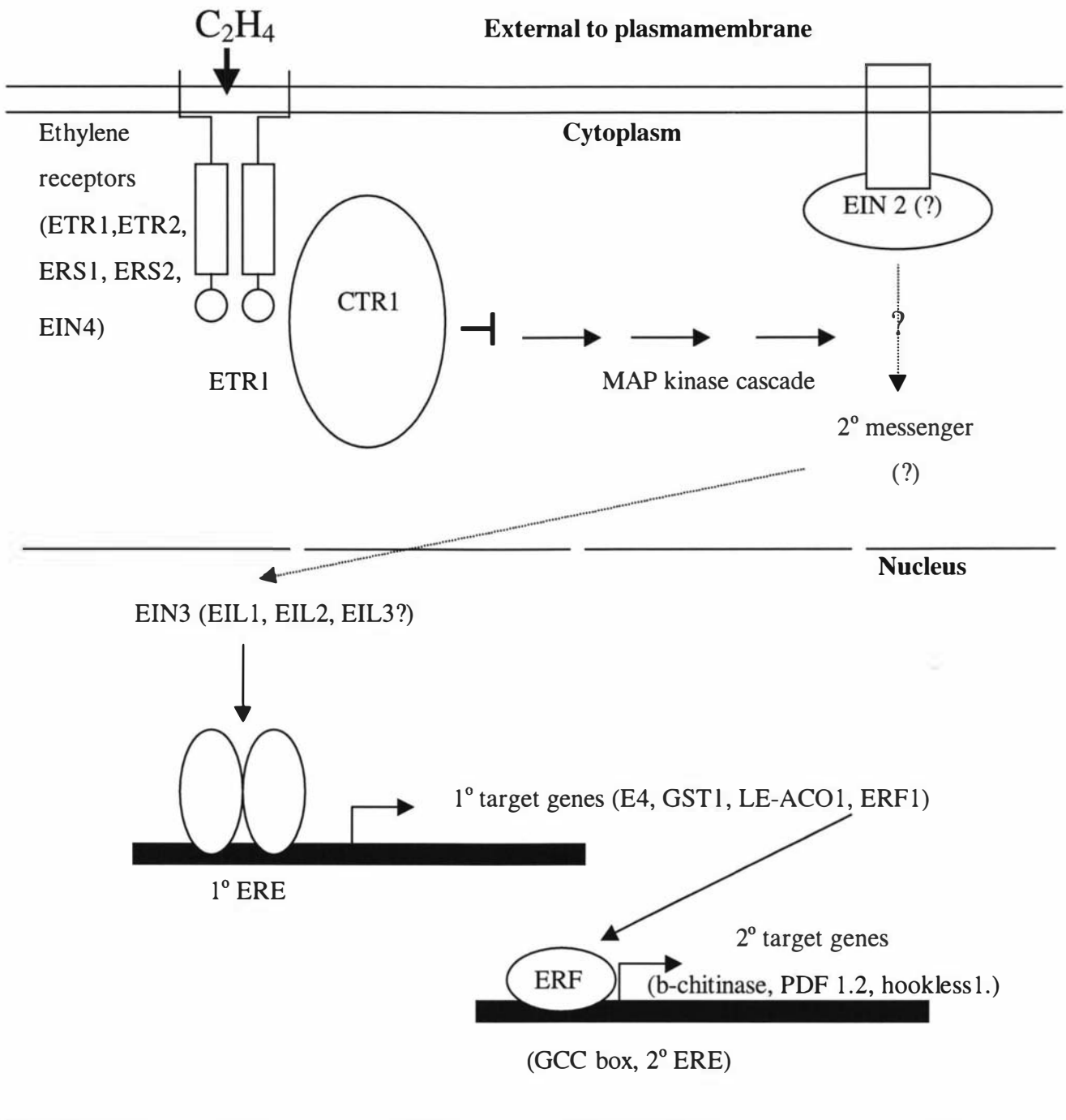

Figure 1.1 Hypothetical model of ethylene signaling in *A. thaliana* (modified from Chao *et al.*, 1997 and Solano *et al.*, 1998).

Suppressor intragenic lines of these dominant mutants were further screened to identify recessive counterparts of these mutants (Hua and Myerowitz, 1998). Loss-of-function mutants of *etr1*, *etr2* and *ein4* (EMS mutagenized lines) and *ers2* (T-DNA insertional lines) were isolated with phenotypes, which mimicked the wild-type etiolated seedling growth in response to ethylene (short hypocotyls and roots). These mutants expressed non-functional truncated proteins, so that it was unable to detect full-length proteins by western analysis.

A quadruple mutant was constructed with the four loss-of-function mutants of *etr1, etr2, ein4* and *ers2* and displayed a constitutive ethylene response, rather than a defective response (Hua and Myerowitz, 1998). This result suggests that knocking out ethylene receptors leads to a constitutive ethylene response, which also explains why the original screening of mutant lines could not isolate loss-of-function lines for ethylene perception (a knock-out mutant is indistinguishable from wild types in the presence of ethylene). In summary, active ethylene receptors or receptor complexes in wild type *A. thaliana* appear to repress ethylene signaling in air. With the addition of ethylene, these receptors switch to an inactive state in terms of the repressor function, and downstream signaling is initiated.

1.3.3. Ethylene signal transduction

From the determination of epistatic relationships, the gene product of CTR1 is positioned to act down stream of ETR1 (Fig. 1.1). The CTR1 gene was cloned by screening T-DNA insertional lines of *A. thaliana* (Kieber, 1993). The deduced amino acid sequence of the gene has identity to Raf-like protein kinases with a highly conserved protein motif for an intrinsic Ser-Thr protein kinase at the carboxyl end of the protein. Biochemical analysis of the CTR1 gene product using the yeast two hybridisation system and *in vitro* affinity assays demonstrated that the CTR1 protein is able to interact physically with ETR1 or ERS1 protein (Clark *et al.*, 1998). This implies that CTR1 can associate with ethylene receptor complex, and phosphorylation of CTR1 may also be directly controlled by the phosphorylation status of the ethylene receptor, which is dependent on the presence of ethylene.

The notion that ethylene receptors act as suppressors of signaling without ethylene suggests that, in the absence of ethylene-binding, a receptor complex may associate with CTR1 and

mediate the suppression. In the presence of ethylene, a receptor complex may lose the CTR1 association, and the receptor complex activates the ethylene signaling downstream pathway. In this case, signaling between receptors and CTR1 may not require a direct involvement of phosphotransfer as was speculated originally (Bleecker, 1999) (Fig 1.1).

The CTR1 gene sequence is highly similar to an activator of mitogene-activating protein (MAP) kinase cascade (a Raf-like protein kinase; Wurgler-Murphy and Saito, 1997). So, a possible involvement of protein phosphorylation or dephosphorylation in ethylene signaling has been studied using basic PR1 gene expression in tomato (*Lycopersicon esculentum*; Raz and Fluhr 1993), ACC oxidase (VR-ACO1) gene expression in mung bean (*Vigna radiata*) hypocotyls (Kim *et al.*, 1997a) and ACC oxidase (PS-ACO1) gene expression in pea (*Pisum sativum*) epicotyls (Kwak and Lee, 1997). These studies show that each expression of ethylene-induced genes might be mediated by a unique mechanism of ethylene signaling, including protein phosphorylation and/or protein dephosphorylation (Fig. 1.1).

As well, a possible involvement of Ca^{2+} as a secondary messenger in ethylene signaling has been implicated from studies with ethylene responsive genes (Raz and Fluhr, 1992; Kwak and Lee, 1997; Jung *et al.*, 1999). The involvement of a secondary messenger (as a divalent cation) in ethylene signaling pathway has been further supported by the characterisation of the EIN2 gene in *A. thaliana* (Alonso *et al.*, 1999). This gene sequence encodes for a membrane-embedded protein with substantial homology to the Nramp family of proteins, which are known as transporters of a variety of divalent cations in many other organisms. So, in that study, EIN2 is proposed to function as a sensor of divalent cations, which may act as secondary messengers in the ethylene signaling pathway (Fig.1.1).

Taken together, these studies suggest that ethylene perceived at the receptor is transmitted through a pathway, involving protein phosphorylation and/or dephosphorylation with recruiting or sensing secondary messengers (probably Ca^{2+}) (Fig. 1.1).

1.3.4. Ethylene responses in the nucleus

The ethylene signal perceived by receptors has to be transmitted into the nucleus, where ethylene-responsive genes are transcribed. The cloning and characterisation of EIN3 (together with EILs; Chao *et al.*, 1997) and ERF1 (Solano *et al.*, 1998) in *A. thaliana* has led to the proposal that a cascade of transcription acts as a regulatory mechanism for expression of ethylene responsive genes.

In the cascade, EIN 3 gene expression is activated by ethylene and the activation is independent of protein synthesis (Chao *et al.*, 1997). The EIN3 product binds specifically to primary ethylene responsive elements identified in the 5'-regulatory regions in genes of GST1 (Itzhaki *et al.*, 1994), E4 (Montgomery *et al.*, 1993), LE-ACO1 (Blume and Grierson, 1997) and ERF1 (Solano *et al.*, 1998) and acts as a transcriptional activator. One of the primary responsive genes is ethylene responsive factor 1 (ERF1), also a transcription activator, which binds to a secondary ethylene responsive element, the so called GCC box, identified in the 5'-regulatory regions of b-chitinase (Shinsh *et al.*, 1995), PDF 1.2 (Penninckx *et al.*, 1996) and Hookless1 (Lehman *et al.*, 1996). ERF1 activates the transcription of these genes so as to generate the ethylene response (Fig. 1.1).

During the last decade, studies on ethylene signaling have led to a clearer picture of ethylene perception on the plasma membrane, and the signal transduction pathway which leads to ethylene-responsive gene expression in the nucleus (Fig. 1.1). Over a similar period of time, significant parallel advance in the ethylene biosynthetic pathway, particularly the genes which encode the key enzymes, have also been made.

1.4 Ethylene biosynthesis in higher plants

The biosynthesis of ethylene is considered classically to begin from S-adenosyl-methionine (SAM), which is derived from the amino acid methionine by the action of SAM synthetase. SAM is then converted by ACS to methylthio-adenosine (MTA) and ACC, the immediate precursor of ethylene. ACC is then oxidized to CO_2, HCN and ethylene by a complex enzymatic reaction catalyzed by ACO (Yang and Hoffman, 1984; Kende, 1993; Zarembinski and Theologis, 1994; Fluhr and Mattoo, 1996; Imaseki, 1999).

The cyanide product is readily degraded to β-cyanoalanine and asparagine by β-cyanoalanine synthase (Yip and Yang, 1988; Manning, 1988). A high correlation between activation of ACC oxidase and β-cyanoalanine synthase, in accordance with the high level of asparagine accumulation, supports this detoxification mechanism of the cyanide product.

This ethylene biosynthetic pathway allows high rates of ethylene production without depleting methionine in cells, and is achieved by recycling MTA (produced by the activity of ACS) back to methionine through the Yang cycle. Therefore, the 4-carbon skeleton of methionine from which ethylene is derived is conserved (Fig.1.2).

1.4.1 SAM synthetase

SAM synthetase (EC 2.5.1.6) is the enzyme which converts methionine to SAM. It is not usually proposed as an enzyme controlling ethylene production in higher plants, because SAM is a universal substrate participating in a range of reactions including polyamine biosynthesis (Evens and Malmberg, 1989), and transmethylation of proteins, carbohydrates, lipids and nucleic acids (Tabor and Tabor, 1984). It is also known that only a minor portion of cellular SAM is utilised for ACC production in higher plants (Yu and Yang, 1979).

Recent molecular characterisation of SAM synthetase genes has revealed that they are encoded by a multigene family. The gene family members have been shown to be expressed differentially during ethylene-mediated senescence of carnation (*Dianthus caryophyllus*) petals (Woodson *et al.*, 1992) and also during ethylene dependent ripening of kiwifruit (*Actinidia chinesis*; Whittaker, *et al.*, 1997). Nevertheless, gene expression and enzyme activity of SAM synthetase appears to be coordinated primarily to maintain a certain level of SAM in cells (Fluhr and Mattoo, 1996).

1.4.2 ACC synthase (ACS)

1.4.2.1 Biochemical studies of ACS

ACC synthase (EC 4.4.1.14) is a pyridoxal phosphate (PLP) requiring enzyme and is inactivated by aminoethoxy acetic acid (AOA) or AVG, which act as a competitive inhibitor for PLP (Yang and Hoffman, 1984).

Figure 1.2 Ethylene biosynthetic pathway in higher plants (modified from Yang and Hoffman, 1984).

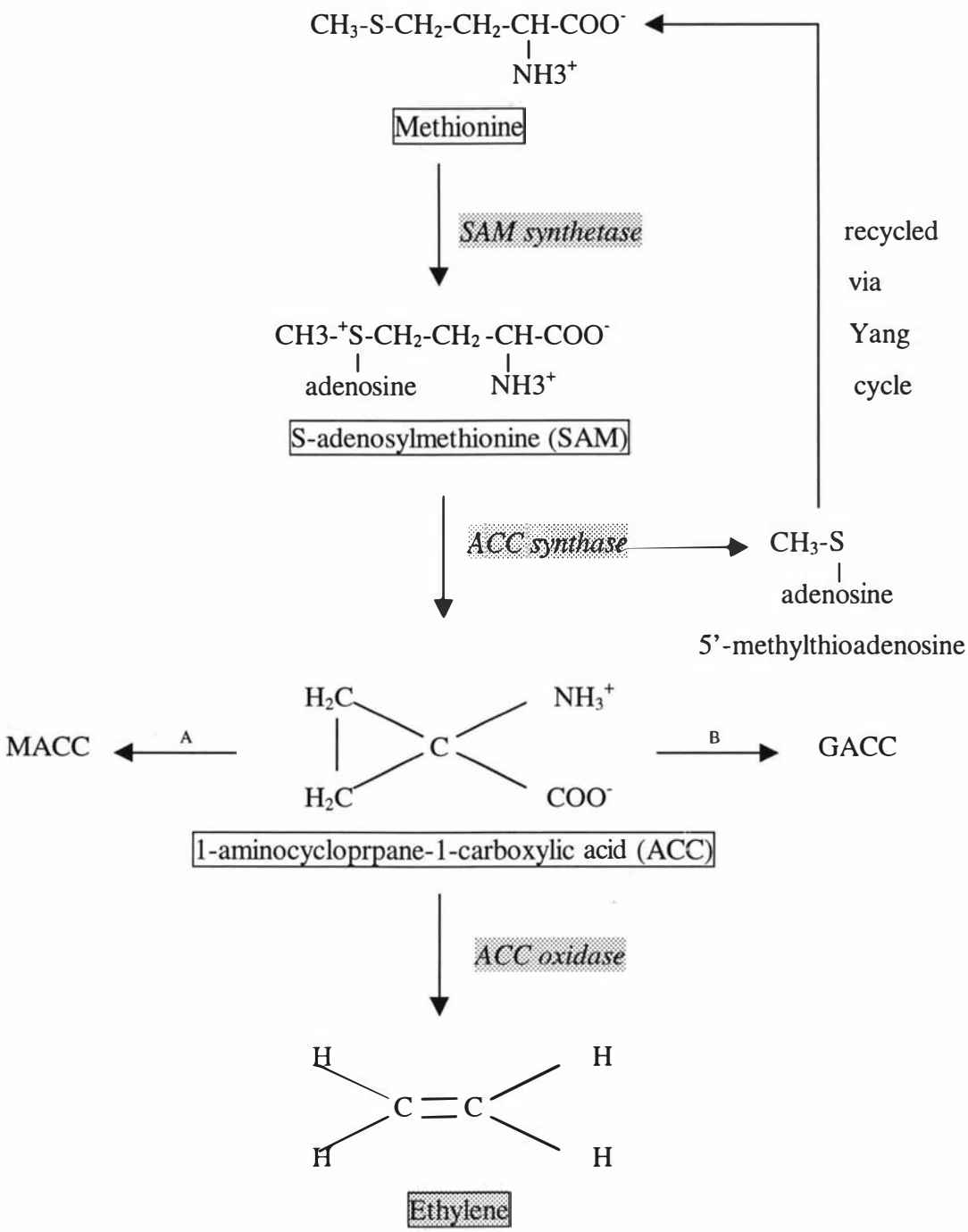

[A] Malonyl ACC transferase

[B] Glutamyl ACC transferase

A partial protein sequence of the active sites from tomato and apple (*Malus sylvestris*) ACS was determined using an active site-probing technique with $NaB_3H^3_4$ or Ado[^{14}C]Met. This analysis revealed that the sequences showed only 1 residue difference out of 11 amino acids between two species (Yip *et al.*, 1990). In the labeled peptide, a sequence of Ser-Leu-Ser-Lys was identified and this is well-conserved in the active sites of other PLP-requiring enzymes such as asparate aminotransferase (AATase). ACS shows high substrate specificity for SAM and affinity to its substrate is also high with a Km range from 12 to 60 μM (Imaseki, 1999).

Progress in the purification of ACS had been slow because the protein exists in low abundance in most plant tissues, and is unstable *in vivo* as well as *in vitro*(Yang and Dong, 1993; Fluhr and Mattoo, 1996). Therefore, early attempts to isolate the enzyme were mainly carried out with plant systems known to produce a large amount of ethylene, such as ripening climacteric fruits, wounded tissues, or tissues treated with other hormones (e.g. auxin or cytokinin) (Bleecker *et al.*, 1986; 1988; Metha *et al.*, 1988; Nakajima *et al.*, 1988; Yip *et al.*, 1990; Yip *et al.*, 1991; Dong *et al.*, 1991).

Low protein expression of ACS isoforms

Purification and characterisation of ACS was facilitated by the production of monoclonal antibodies (MAbs) raised against partially purified enzyme (Bleecker *et al.*, 1986; Bleecker *et al.*, 1988; Mehta *et al.*, 1988; Yip *et al.*, 1990; Dong *et al.*, 1991; Yip *et al.*, 1991). The MAbs were able to recognise ACS proteins of either 50 kD (pI 5.3 and 9) (Bleecker *et al.*, 1986; 1988) or 67 kD (pI 7) (Mehta *et al.*, 1988) in tomato fruit extracts. Using an immuno affinity gel coupled with the specific ACS MAbs, Bleecker *et al.* (1986) achieved a more than 2000-fold purification of ACS and calculated that ACS was present as less than 0.0001% of total protein in the pericarp of ripening tomato fruits.

Wound-induced ACS in tomato fruits was also detected using labeling, *in vivo,* of the proteins with [S^{35}]-methionine, followed by MAb recognition (Bleecker *et al.*, 1986). Time course experiments after wounding indicated that the synthesis of ACS protein was triggered *de novo* and radioactive-labeled ACS was detectable 2 hr after wounding (Bleecker *et al.*, 1988). When ACS protein accumulation was maximal (after 3 hr), the percentage of radioactivity

incorporated into ACS reached 0.04% of total radioactivity incorporation. However, its enzyme activity, *in vivo*, decreased rapidly, so that enzyme activity was not detectable even when the radioactively labeled ACS accumulation was high after 5 hr after wounding.

MAbs have also been produced against apple ACS (Yip *et al.*, 1991). Western analysis using these MAbs showed that these antibodies recognised both native and AdoMet-inactivated forms of ACS in apple fruit (Dong *et al.*, 1991), but failed to immunoprecipitate ACS using protein extracts from ripe tomato and avocado (*Persea americana*) fruits or auxin-treated mung bean hypocotyls. The MAbs were effective at immuno-precipitating the enzyme isolated from ripening pear (*Pyrus communis*) fruits. These observations indicate that apple ACS is immunologically related to the pear fruit enzyme but not to those from tomato fruit, avocado fruit, and mung bean hypocotyls.

The immunologically distinct characteristics of ACS in plants suggests that the enzyme exists as isoforms, but the activity of the enzyme in many different plants is known to have similar biochemical characteristics (e.g. Km and cofactor requirements) (Fluhr and Mattoo, 1996; Imaseki, 1999).

Rapid inactivation of ACS enzyme activity during catalysis

ACS enzyme activity decays rapidly *in vivo* and *in vitro* during catalysis, and SAM-dependent inactivation has been proposed as a mechanism (Satoh and Esashi, 1986; Satoh and Yang, 1988; Kim and Yang, 1992). Satoh and Esashi (1986) demonstrated the substrate-dependent inactivation of the enzyme in mung bean hypocotyls. As such, when a partially purified tomato ACS protein was incubated with [3,4-^{14}C]-SAM and then analysed by SDS-PAGE, only one radioactively labeled protein band was discerned and confirmed as ACS based on immuno-precipitation by MAbs raised against tomato ACS (Satoh and Yang, 1988). From these results, a mechanism was proposed that the inactivation process involved the formation of an ACS-SAM complex, which is then transformed into an intermediate. Because of the proposed high reactivity of the intermediate, it is speculated that a fragment of the SAM molecule may covalently link to the active site of ACC synthase and lead to the irreversible inactivation of enzyme activity. In addition, this SAM-dependent inactivation has been shown using *E. coli*-

expressed tomato ACS protein, with the time of inactivation dependent upon SAM concentration (Li *et al.*, 1992). This enzyme inactivation was also shown to be dependent on an ATP–requiring mechanism in tomato fruit tissue, because uncoupling agents of oxidative phosphorylation significantly reduced the rate of inactivation of ACS enzyme activity (Kim and Yang, 1992).

However, another suggestion is that the rapid inactivation of ACS activity, at least *in vivo*, is regulated by phosphorylation and dephosphorylation of the enzyme, or of proteins regulating the inactivation of enzyme activity, rather than inactivation through a SAM-ACS suicidal complex (Spanu *et al.*, 1990; Spanu *et al.* 1994).

Using elicitor treated tomato leaf discs and cell in culture, a competitive inhibitor (AVG) of the PLP-binding process was shown not to be able to delay the inactivation of ACS enzyme activity, *in vivo* (Spanu *et al.*, 1990). This result suggests that the decay of ACS enzyme activity, *in vivo*, is not related to the irreversible binding of ACS protein to its substrate (SAM). Spanu *et al.* (1994) also demonstrated, using the same cell culture system, that the elicitor-induced up-regulation of ACS and ACO enzyme activities was blocked by an inhibitor of translation (cycloheximide; CHX), but only ACO enzyme activity was affected by an inhibitor of RNA synthesis (cordycephin). Therefore, ACO enzyme activity was more likely regulated at a transcriptional level, whereas ACS enzyme activity appeared to be also controlled at a post-transcriptional level. When cell cultures were treated together with elicitors and K252a (as staurosporine-type inhibitor of protein kinase), ACS enzyme activity was not up-regulated. In contrast, addition of Caulyne (an inhibitor of protein phosphatase1 and 2a) alone could increase the enzyme activity in the culture, so changes in protein phosphorylation appear to be required for ACS enzyme activity. With and without AVG (an inhibitor of ACS activity), changes of ACS enzyme activity, *in vivo*, in response to inhibitors of protein kinase and phosphatase in culture cells treated with elicitors were rapid and occurred in a consistent manner: i.e. a phosphorylation process was required for ACS enzyme activity.

Taken together, the rapid inactivation of ACS activity, *in vivo*, is most likely to be regulated at the post-transcriptional level, such as phosphorylation and dephosphorylation status of the enzyme or associated regulatory proteins.

So, two possibilities have been proposed to explain the rapid inactivation of ACS activity and it still remains to be shown which mechanism (or both) is the most critical regulator of ACS enzyme activity, *in vivo*.

1.4.2.2 Molecular studies of ACS

Cloning and expression studies of ACS genes

The first ACS clone was isolated by immuno-screening a cDNA expression library made from mRNA isolated from zucchini (*Cucurbita pepo*) fruit with polyclonal antibodies (PAbs) raised against partially purified ACS (Sato and Theologis, 1989). The deduced amino acid sequence from this ACS clone, as well as a partial amino acid sequence obtained from 5000-fold purified tomato ACS (Van Der Straeten et al., 1990) were then used for the design of oligonucleotides to be used as probes for the subsequent screening of cDNA (Van Der Straeten *et al.*, 1990; Olson *et al.*, 1991) or genomic DNA libraries (Huang *et al.*, 1991; Rottmann *et al.*, 1991).

Since then, divergent ACS gene families have been reported from many plant species, including *A. thaliana* (Liang *et al.*, 1992, Van Der Straeten *et al.*, 1992; Arteca and Arteca, 1999), tomato (Van Der Streten *et al.*, 1990; Olson *et al.*, 1991; Rottman *et al.*, 1991; Yip *et al.*, 1992; Lincoln *et al.*, 1993; Oetiker *et al.*, 1997; Shiu *et al.*, 1998), Mung bean (Botella *et al.*, 1992a; Botella *et al.*, 1992b; Kim *et al.*, 1992; Botella *et al.*, 1993; Kim *et al.*, 1997), zucchini (Sato and Theologis, 1989; Huang *et al.*, 1991), rice (Zarenmbinski and Theologis, 1993), potato (Desfano-Beltran *et al.*, 1995; Schlagnhaufer *et al.*, 1995), kiwifruit (Whittacker *et al.*, 1997), carnation (Park *et al.*, 1992; Henskens *et al.*, 1994), and orchid (O'Neil *et al.*, 1993).

A. The ACS multigene family in tomato plants

In tomato, a model plant for studies on climacteric fruit-ripening, substantial progress has been made in the characterisation of the ACS gene family (Van Der Straeten *et al.*, 1990; Olson *et*

al., 1991; Rottmann *et al.*, 1991; Yip *et al.*, 1992; Lincoln *et al.*, 1993; Olson *et al.*, 1995; Shiu *et al.*, 1998; Nakastsuka *et al.*, 1998).

Two ACS genes were identified using oligonucleotide probes constructed from the N-terminus of partially purified enzyme from tomato pericarp (Van Der Straeten *et al.*, 1990). One cDNA (originally designated as pVV4A; now LE-ACS2) contains a 1.9 Kb insert with a single open reading frame (*ca.* 55 kD) and the other one, a partial cDNA clone (originally pVV4B; now LE-ACS4) differs from the first one in 18 % of its bases. Genomic Southern blotting suggested that pVV4A (LE-ACS2) and pVV4B (LE-ACS4) are encoded by two different genes, but are probably tandemly arranged in the tomato genome. The complete nucleotide and deduced amino acid sequences of LE-ACS4 show highly conserved regions to LE-ACS2, but these are surrounded by regions of low homology, especially at the 5' and 3' ends (Olson *et al.*, 1991).
Rottman *et al.* (1991) identified two cDNA clones of ACS (ptACC2, now LE-ACS2 and ptACC4, now LE-ACS4) and an additional four genomic clones (LE-ACS1A, LE-ACS1B, LE-ACS3, and LE-ACS4) by screening a genomic library using ptACC2 as probe. LE-ACS1A and LE-ACS1B are 96 % identical in their coding regions, whereas the identity of the other clones as deduced amino acid sequences to each other varied between 50 and 70%.

Yip *et al.* (1992), using degenerate oligonucleotide primers corresponding to conserved regions flanking the active-site domain of ACS genes, amplified ACS cDNA fragments by PCR from mRNA isolated from tomato fruit and cells in suspension culture. Sequencing of the PCR products identified four distinct cDNA fragments encoding ACS homologues. The pBTAS1 (LE-ACS2) and pBTAS4 (LE-ACS4) sequences were obtained from fruit mRNA, whereas the cell culture mRNA yielded three sequences, pBTAS1, pBTAS2 (LE-ACS3) and pBTAS3 (LE-ACS5).
In addition, particular members of the ACS gene family have been identified in plant tissues exposed to various environmental stimuli. For example, LE-ACS7 was cloned both by RT-PCR using cDNA templates from mRNA isolated from flooded root tissue, and also by screening a genomic library of tomato (Shiu *et al.* 1998).

Taken all together, eight members of the ACS gene family have been identified in tomato and categorised into three groups based on their sequence homology. LE-ACS1a, LE-ACS1b and LE-ACS6 in class I, LE-ACS2 and LE-ACS4 in class II, and LE-ACS3, LE-ACS5 and LE-ACS7 in class III (Shiu *et al.*, 1998) (Table 1.1).

Table 1.1 Expression of Tomato ACS genes in response to various stimuli.

TOMATO ACS (LE-ACS)			
		Elicitor-treated cultured cells	Expression in plant organs
CLASS I[a]	1A	No detection (Group III[b])	vegetative tissue
	1B	Low expression (Group II)	vegetative tissue
	6	High expression (Group I)	vegetative tissue
CLASS II	2	High expression (Group I)	fruits/C_2H_4/wound-inducible
	4	Low expression (Group II)	fruits/C_2H_4/wound-inducible
CLASS III	3	Low expression (Group III)	vegetative tissue/flooding-inducible
	5	High expression (Group I)	vegetative tissue/IAA/CK[c]-inducible
	7	Low expression (Group II)	vegetative tissue flooding- /wound-inducible

[a]Classes are based on nucleotide sequence homology (Shiu *et al.*, 1998)

[b]Groups are based on responses to elicitors in cultured cells (Oetiker *et al.*, 1997)

[c]CK: cytokinin

B. Characterisation of differential ACS gene expression in tomato plants

Gene expression studies have shown that both LE-ACS2 and LE-ACS4 transcripts increase in ripening fruits (Olson *et al.*, 1991; Lincoln *et al.*,1993). Exogenous ethylene initiated the ripening process with a concomitant induction of these ripening related ACS genes in a dose-dependent manner in mature fruits. The LE-ACS2 transcript was primarily responsive to by wounding of the pericarp tissue of ripening fruits, whereas LE-ACS4 transcript was up-regulated only partially (Olson *et al.*, 1991; Lincoln *et al.*, 1993).

Using the highly sensitive ribonuclease protection assay (RPA) with PCR products encoding protein-coding regions of tomato ACS genes, Yip *et al.* (1992) demonstrated a consistent pattern of differential gene expression. The pBTAS1 (LE-ACS2) transcript accumulated during ripening and in response to wounding of tomato fruits, but was only slightly induced in response to auxin (IAA) in tomato vegetative tissue. The induction of pBTAS4 (LE-ACS4) expression was also associated with fruit ripening, but was unresponsive to applied auxin in vegetative tissue. In contrast, the expression of pBTAS2 (LE-ACS3) and pBTAS3 (LE-ACS5) was promoted by auxin treatment of vegetative tissue, but they were absent from fruit tissues of tomato. Expression of pBTAS2 (LE-ACS3) was moderately dependent on wounding, but pBTAS3 (LE-ACS5) was unresponsive to this stimulus.

LE-ACS3 expression was rapidly induced in roots within 1 hr after flooding treatment, and that was followed by LE-ACS2 expression at a latter stage (after 10 hr)(Olson *et al.*, 1995). The expression of LE-ACS7, which was already present in roots tissue before treatment, was also induced further just after flooding (within 1 hr) and then disappeared by 3 hr (Shiu *et al.*, 1998). This expression of the LE-ACS7 gene was also increased by wounding in leaf tissue, but only transiently, and before the wounding-induced ethylene production peak. This transient induction in response to external stimuli such as flooding or wounding has been suggested as a factor responsible for imparting competence to the tissue to respond to the subsequent exposure to ethylene.

Expression of the LE-ACS6 gene was detected in pre-ripening tomato fruits but down-regulated by ethylene treatment of the fruit at this developmental stage (Nakatsuka *et al.*, 1998). However, the gene was not expressed in ripening tomato fruit, but up-regulated by 1-MCP treatment of the ripening fruits. The results suggest that LE-ACS6 expression may be under negative-feedback control by ethylene. Therefore, when an ethylene action inhibitor blocks the ethylene signaling pathway, any repression may be released and LE-ACS6 gene expression is induced.

C. Regulatory mechanism in expression of tomato ACS genes

The regulation of ACS gene expression in tomato has been extended further by the analysis of promoter sequences (Lincoln *et al.*, 1993; Olson *et al.*, 1995; Shiu *et al.*, 1998). Sequences of LE-ACS2 and LE-ACS4 (ripening fruit-specific, ethylene and wound-responsive ACS genes) indicated some potential *cis*-acting regulatory elements for ethylene responsiveness, wounding and anaerobiosis together with the presence of EmBP1, GBF-1, and OCSBF-1 motifs (Lincoln *et al.*, 1993). DNA sequences in the promoter region of LE-ACS3 (a flooding- and wound-responsive ACS gene) revealed putative *cis*-elements for anaerobic responses, root specific expression, and the chloroplast DNA binding factor 1 (Olson *et al.*, 1995). The presence of complex DNA elements confirms that the expression of these genes will be responsive to various stimuli.

Analysis of LE-ACS7 revealed that its promoter was very similar to a wound responsive ACS [ST-ACS2 identified as an ACS gene in potato, *Solanum tuberosum* (Desfano-Beltran *et al.*, 1995], and it was also tagged by a Sol3 transposon element (Shiu *et al.*, 1998). This transposon element has been identified previously in polygaracturonase genes (Montgomery *et al.*, 1993), and has been reported to be a positive regulator of gene expression in tomato fruits. So, a possible regulatory mechanism mediated by the transposon has been suggested for LE-ACS7 expression.

Alternative RNA splicing induced by flooding has also been proposed as another regulatory mechanism for LE-ACS3 gene expression (Olson *et al.*, 1995). Probes comprising protein-

coding regions of LE-ACS3 hybridised to two RNA transcripts from flooded root tissues at all time points sampled. When the first intron and third intron of LE-ACS3 were used separately as probes for northern analysis, the probe corresponding to the third intron hybridised to the higher molecular weight RNA species extracted from flooding-treated samples, indicating that flooding may inhibit the splicing process of the LE-ACS3 transcript. It was thus speculated that the induction of splicing failure for the LE-ACS3 transcript by flooding stress may trigger changes in stability or translatability of the ACS gene transcripts, and so act as a control point in the regulation of ACS activity in the tissue.

D. Post-transcriptional regulation of tomato ACS gene expression

Many studies have shown that transcriptional activation of ACS correlates with an increase of ACS enzyme activity, and this normally leads to higher ethylene production. However, some reports claim that in tomato this is not always the case. Enhanced ethylene production in cultured tomato cells treated with elicitors is one instance in which the accumulation of ACS transcripts cannot simply explain the increase in ACS activity (Spanu *et al.*, 1993; Oetiker *et al.*, 1997). Spanu *et al.* (1993) reported that, in pathogen (*Phytophthora infestans*)-infected leaf tissue of tomato, ACS activity increased steadily and reached a maximum four days after infection. Accumulation of LE-ACS2 transcript correlated well with the increased level of ACS activity in the infected tissue. In tomato cells in culture, ACS activity also increased in response to a yeast-extracted elicitor (YE-elicitor), and reached maximal activity at 90 min after the elicitor treatment (Spanu *et al.*, 1993). When the cells were treated with cordycepin (an inhibitor of RNA synthesis) 15 min before elicitor treatment, the increase of ACS activity was not affected by the inhibitor treatment, and reached maximal activity at 120 min after the elicitor treatment. This suggests that the increase of ACS activity here may not be related to the transcriptional activation of specific ACS genes. Gene expression studies with LE-ACS2, pBAT3 (LE-ACS5) and LE-ACS4 were also carried out with cultured cells treated with elicitor. LE-ACS2 (an ACS gene induced by the pathogen infection in leaf tissue) hybridised to two bands of 1.9 kb and 1.6 kb with a temporal difference in expression. However, LE-ACS2 hybridised to only one of the two bands (1.6 kb) in RNA extracted from the culture cells treated with the elicitor and the RNA synthesis inhibitor (cordycepin). LE-ACS5 hybridised to

a band of 1.6 kb only, and its hybridisation was induced by elicitors, but reduced by the RNA synthesis inhibitor. The expression of LE-ACS4 was not detected in any of systems used.

In summary, expression of different ACS genes was differentially induced by elicitors in cultured tomato cells and these were also differentially sensitive to an inhibitor of mRNA synthesis (cordycepin). Furthermore, the discrepancy between the changes of ACS gene expression and ACS activity, when an RNA synthesis inhibitor was added, suggested that post-transcriptional regulation of ACS plays an important role in controlling ACS enzyme activity in this system.

A more detailed study has been undertaken in cultured tomato cells using the RPA assay with seven members of the ACS multigene family (Oetiker *et al.*, 1997). The induction pattern of ACS gene expression by elicitor was categorised to three groups. Group I genes were induced and accumulated to a high level in the system (LE-ACS2, LE-ACS5 and LE-ACS6). Group II genes were expressed in a constitutive manner or induced weakly (LE-ACS1B, LE-ACS3 and LE-ACS4). However, LE-ACS1A was not detected in the cell culture system, and was categorised into Group III. The overall level of transcript accumulation of ACS genes appeared unrelated to the biosynthetic rate of ethylene, supporting the notion that an increase of ACS activity in the system might not be solely controlled by the transcriptional activation of ACS genes.

Together, it is interesting to note that sequences of tomato ACS genes predominantly expressed in vegetative and fruit tissues are clustered into separate groups based on nucleotide sequence homology. The ACS genes may be functionally redundant in tomato plants, but their expression appears to be highly coordinated in an organ- and development-specific manner (Table 1.1).

E. The ACS multigene family in mung bean

Seven members of the ACS gene family have been identified in mung bean and the differential expression of each member has been examined thoroughly (Botella *et al.*, 1992a; Botella *et al.*,

1992b; Kim *et al.*, 1992; Botella *et al.*, 1993; Kim *et al.*, 1997). A well-characterised model system for the study of ethylene biosynthesis is the mung bean hypocotyl (Yoon *et al.*, 1997; Yu *et al.*, 1998) and auxin (IAA)- and cytokinin-induced ACS activity is especially well studied in this system (Yoshii and Imaseki 1981; Yoshii and Imaseki, 1982).

More recently, Yoon *et al.* (1997) characterised the differential induction of VR-ACS1 (pAIM1 in Botella *et al.*, 1992b) and VR-ACS6 (pMBA1 in Kim *et al.*, 1992) gene expression in mung bean hypocotyls in response to IAA. Both ACS genes were specifically induced by a single treatment of 100 μM IAA. However, the induction kinetics in response to IAA differed between the two ACS genes. The induction of VR-ACS1 expression was weak and transient until 30 min after IAA treatment and then disappeared. However, the induction of VR-ACS6 began 30 min after IAA treatment and expression remained at a high level until 6 hr after the treatment. VR-ACS1 expression was also induced by CHX, but VR-ACS6 was not affected. The pattern of VR-ACS6 gene expression is consistent with earlier physiological data of auxin-induced ethylene production, in terms of dosage response and interaction with other plant hormones, such as suppression by ABA and enhancement by cytokinin (Yoshii and Imaseki, 1981). So, the induction of VR-ACS6 is proposed to be most likely responsible for the IAA-induced ethylene production in this tissue. Also, further analysis of a 1 612 bp DNA sequence in the promoter region of VR-ACS6 revealed some DNA sequence motifs conserved in IAA-responsive genes, supporting IAA-induced VR-ACS6 gene expression (Yoon *et al.*, 1999). In tobacco plants transformed with a fusion construct of the VR-ACS6 promoter and the GUS reporter gene, GUS activity was induced by applied IAA in a dose-dependent manner. All these confirm that VR-ACS6 gene expression is responsive to IAA to produce IAA-induced ethylene in mung bean plants.

F. ACS multigene in *Arabidopsis thaliana*

Arabidopsis thaliana is frequently used as a model plant for studies of plant development, because of its short generation time and small genome (Meyrowitz, 1989; Smyth, 1990), which will be entirely sequenced by the year 2000 (Meinke *et al.*, 1998; Gibbs, 1999).

The cloning and characterisation of ACS genes in *A. thaliana* has also been undertaken with Liang *et al.* (1992) first reporting five divergent ACS genes (ACS1, ACS2, ACS3, ACS4 and

ACS5). These genes were identified by screening a genomic library with heterologous cDNA probes from zucchini (pACC1) and tomato (ptACC2), and also using PCR amplification from *A. thaliana* genomic DNA with degenerate oligonucleotide primers. Among the five members, enzyme activity of ACS2 was confirmed by an ACC assay of *E. coli* transformed with the gene. Liang *et al.* (1995) also reported that the sequences of ACS1 and ACS3 of *A. thaliana* are highly homologous to each other. Indeed, the ACS3 gene was identified as a truncated version of the ACS1 gene, missing the fourth exon. Chromosomal localisation of the five numbers of the ACS multigene family in *A. thaliana* placed each member on a different chromosome, so the truncation of ACS3 was proposed to have occurred during the translocation of ACS1 to another chromosome (Liang, 1995). Abel *et al.* (1995) reported that ACS4 was specifically induced by applied IAA at a concentration as low as 100 nM in etiolated seedling of *A. thaliana*. This response to IAA was rapid (within 25 min), but defective in the auxin resistant mutant lines of *A. thaliana* (*axr1, arx2,* and *aux1*), supporting the proposal that the induction of ACS4 gene expression is mediated by IAA. As well, the promoter of ACS4 contains four sequence motifs, which are highly homologous to functionally defined auxin-responsive *cis*-elements. However, gene expression was insensitive to CHX, suggesting that gene induction does not require protein synthesis *per se.* In addition, ACS5 appeared to be induced in response to a low level of cytokinin (50 μM) (Vogel, *et al.*, 1998). The function of the ACS5 gene was characterised further using an ethylene over-production mutant, *eto2*, which displays an exaggerated triple response in etiolated *A. thaliana* seedlings with an accompanying over production of ethylene. The mutant, *eto2* has a single base pair insertion in the 3' end of ACS5, which gives rise to a truncated ACS protein with the loss of 11 amino acids at the carboxyl terminal. This truncation is proposed to cause a hyperactivation of ACS activity and leads the higher production of ethylene in the mutant. Recently, ACS6 was isolated using RT-PCR and screening of a cDNA library made from mRNA isolated from *A. thliana* seedlings (Arteca and Arteca, 1999). This gene appears to be responsible for touch-inducible ethylene production in light-grown plants.

In summary, cloning and characterisation of ACS genes have shown that each member of the ACS gene family is differentially induced by different signals and regulated at both the transcriptional and post-transcriptional levels to manipulate ACS activity in higher plants.

Molecular characterisation of ACS genes using heterologous expression systems

Due to the extremely low level of ACS gene expression in plant tissues and the rapid decay of ACS enzyme activity *in vitro* and *in vivo*, purification and biochemical characterisation of the protein has been difficult. Therefore, ACS protein, over-expressed in and purified from *E. coli* cells has been used for structure-function analyses of the enzyme (White *et al.*, 1994; Li and Mattoo, 1994; Li *et al.*, 1996; Li *et al.*, 1997; Huxtable *et al.*, 1998; Tarun and Theologis, 1998; Tarun *et al.*, 1998; Zhou *et al.*, 1998).

An ACS gene cloned from apple fruit (pETACS1) was over-expressed in *E. coli* and characterised using a continuous assay system involving the detection of 5'-methyl-thioadenosine (a product of ACS activity) by adenosine deaminase (White *et al.*, 1994). Based on the high sequence homology between ACS and AATase, three amino acid residues known to be important for AATase activity were examined by site-directed mutagenesis. Lys273Ala and Arg407Lys mutant proteins lost enzyme activity dramatically, indicating that these two amino acids play an important role in ACS function. Tyr233Phe mutant protein, however, demonstrated a 24 fold increase in Km, but ACS activity was not entirely lost, suggesting that Tyr233 is not a critical residue for ACS function, but has some role in controlling the catalytic reaction rate. In that study, the Tyr233 residue was proposed to orient the PLP cofactor, so that the imine group of the internal aldimine is perpendicular to the attacking α-amino group of AdoMet.

Because of difficulties in making crystals of ACS proteins purified from plant organs, due to its low expression and labile nature, a cDNA pool of mis-sense mutants of tomato LE-ACS2 was constructed using a combination of PCR-based random mutagenesis and a genetic screening method using the *E coli* Ile auxotroph genome-transformed with ACC deaminase (Tarun *et al.*, 1998). In this system, three classes of mutants were identified based on enzyme activity and

protein accumulation in *E. coli* cells. Mutant proteins in class I showed an almost equal protein accumulation when compared with wild type, but most enzyme activity was lost. About 89% of mutations in this class had substitution at one out of 11 amino acid residues which are conserved in AATase. Interestingly, in terms of specific amino acids, the substitution at Tyr92 with a Phe or Trp caused a loss of most activity, but 30 to 35% activity remained when His or Leu were substituted, suggesting that the basic nature of amino acid in this position is important for enzyme function. In addition, mutations at one of Tyr205-Asn-Pro207, which are not conserved in AATases, also belonged to class I. It was suggested that a mutation at one of these three amino acid residues might hamper the functionality of the conserved amino acid at Asn209. Although Asp37 and Cys236 residues are not conserved in ACS sequences in other plants, mutations at these residues also caused a complete loss of the enzyme activity, suggesting that these two amino acids may be important for LE-ACS2 activity specifically. Taken together, all mutated residues in class I may be related either to the catalytic site or to protein folding, which are important for ACS functionality.

Mutant proteins in class II lost *ca.* 50% enzyme activity, but protein accumulated to as similar level to the wild type (Tarun *et al.*, 1998). These mutated proteins were also tolerated to non-conservative substitution of particular residues, suggesting that these amino acids are not necessary for enzyme function. Try240 is highly conserved in ACS sequences reported from many plant species, but substitutions at Tyr240 were tolerated. This result is consistent with the observation in which a mutation at the equivalent trypsin (Tyr233) in apple ACS did not result in loss of entire activity (White *et al.*, 1994).

Mis-sense mutants in class III were not expressed in bacterial cells (Tarun *et al.*, 1998). It was speculated that these substitutions either might change the stability of the expressed protein to become more susceptible to protease-mediated degradation, or *E. coli* cells might be incapable of expressing class III mutated proteins, due to the substitutions introducing codon usage limitations. Even though expression of eukaryotic proteins in prokaryotic hosts has certain limitations in terms of interpretation, data gained from such experiments and the predicted protein secondary structures based on the protein sequence are shedding light on structure-function relationships of ACS proteins.

ACS protein is also reported to act as a dimer in plant tissue, and this has also been examined using ACS proteins expressed in *E. coli* (Li and Mattoo, 1994; White *et al.*, 1994; Li *et al.*, 1997; Tarun and Theologis, 1998). Determination of tomato recombinant LE-ACS2 proteins revealed a molecular weight of 96 ± 5.7 kD using gel filtration column chromatography and 54 kD using SDS-PAGE in reducing conditions, indicating that native form of ACS might be a dimer comprising 54 kD subunits (Li and Mattoo, 1994). This was also demonstrated with apple ACS expressed in *E. coli* (White *et al.*, 1994). Using a cross-linking reagent (glutaraldehyde), an apple recombinant ACS protein was purified as a dimer of 104 kD (subunit molecular weight 52 kD), supporting the view that ACS protein may act as a dimer.

In another approach, an apple recombinant ACS protein mutated at Tyr85Ala or Lys273Ala lost enzyme activity completely. However, a mixture of the two mutant proteins which would replace the mutated amino acid residue in one subunit of a putative protein dimer, restored *ca.* 15% of wild type ACS activity (Li *et al.*, 1997), suggesting that ACS is functional as a dimer or higher-order oligomers. This has also been confirmed by negative or positive complementation effects of mutated and wild type tomato ACS proteins expressed in *E. coli*, which suggests further that ACS has an inter-subunit or shared arrangement for its active sites and the enzyme functions as a dimer (Tarun and Theologis, 1998). A preliminary study of crystallised ACS protein from apple further enforces the notion, by showing an ACS dimer as the functional form. It is most likely that ACS proteins act or at least exist as a dimer in the native state of apple fruit tissue (Hohenester *et al.*, 1994).

Native ACS proteins are often smaller (by *ca.* 8-9 kD) when compared with calculated protein sizes from the full length genes in several plant species, including tomato (Edelman and Kende, 1990; Van Der Straeten *et al.*, 1990), zucchini (Nakajima *et al.*, 1990) and winter squash (Sato *et al.*, 1991).

The biological significance of the truncated ACS protein was addressed using recombinant tomato LE-ACS2 in *E. coli* (Li and Mattoo, 1994). Enzyme assay demonstrated that Arg429 was necessary to preserve the enzyme function. However, truncation up to Ser439 or Phe433 from the C-terminal end of the protein resulted in *ca.* 2- to 4-fold increase of ACS enzyme

activity. This portion of the protein (Ala428-Gly440) contains an Arg/Lys-rich motif. When these Arg residues were replaced with Ala, the mutated protein lost ACS activity dramatically. In contrast, when Arg and Lys were replaced with Val and Gly, the mutated protein gained activity, suggesting that positively charged amino acids in this region play some controlling role in enzyme activity. Therefore, truncation of carboxyl end of ACS protein is proposed to be one of the regulatory processes to gain hyperactive forms of the enzyme to produce a large amount of ACC (and ethylene), probably during periods of high ethylene production (e.g. fruit ripening or organ senescence). However, this notion of hyperactivity caused through C-terminal truncation has been challenged in another report using mutated recombinant LE-ACS2 proteins where its activity associated with the truncated protein was demonstrated to be similar to that of the wild type enzyme (Tarun *et al.*, 1998).

Deletion studies in the N-terminal portion of the protein have also been carried out using the LE-ACS2 gene, and Tyr27 was observed to be critical to maintain intact enzyme activity (Li *et al.*, 1996). However, truncation up to the first 12 N-terminal amino acids both in wild type and carboxyl terminal truncated mutant proteins increased ACS enzyme activity, *in vivo,* and, *in vitro.* The double truncation of ACS reduced the Km from 0.28 mM to 0.042 mM SAM, which is close to ACS activity, *in vivo.*

In summary, it is proposed that monomeric truncated ACS may catalyse higher enzyme activity, and the non-conserved regions of N- and C- terminal of ACS proteins may affect this enzyme activity (Li *et al.*, 1996). However, characterisation of eukaryotic ACS proteins in prokaryotic cells may limit this interpretation again.

Even though such structure-function analyses of ACS have progressed rapidly, the structural basis of ACS catalysis is still uncertain. It is anticipated that more evidence will be acquired from a three dimensional structure obtained from crystallised ACS proteins (Hohenester *et al.*, 1994).

ACS appears to be encoded for by a comparatively large gene family in higher plants, the members of which are differentially expressed in response to a variety of stimuli (Yang and Dong, 1993; Kende, 1993; Zarembinski and Theologis, 1994; Fluhr and Mattoo, 1996; Imaseki, 1999). Also, more recent evidence from mutant analysis and protein characterisation of recombinant ACS proteins suggest that ACS activity is regulated at the post-transcriptional level as well as the transcriptional level. Nevertheless, it is the general notion that the close relationship between the increase of ACS activity and ethylene production has positioned the enzymatic reaction as the rate-determining step in ethylene biosynthetic pathway in higher plants (Yang and Hoffman, 1984; Zarembinski and Theologis, 1994; Imaseki, 1999).

However, ACC, the product of ACS activity, is not always converted to ethylene in plant tissue. This immediate precursor of ethylene (ACC) can be sequestered to an inactive form which may also regulate the rate of ethylene production in higher plants.

1.4.3 Conjugation of ACC

An increased level of ACC in plant tissues can be sequestered to prevent overproduction of ethylene by N-malonylation or gamma-glutamyl-transfer (Yang and Hoffman, 1984; Reid, 1995; Martin *et al.*, 1995). A malonyltransferase enzyme controls the ACC conjugation process by using malonyl-CoA as malonyl donor (Yang and Hoffman, 1984). The enzyme isolated from mung bean hypocotyl demonstrated malonylation of a broad range of substrates, including ACC, AEC, non-polar D-amino acids (D-methionine, D-phenylalanine, and D-alanine) and amino-isobutyric acid. Consequently, when mung bean hypocotyls were fed with D-amino acids, ethylene production increased. This is because the level of available ACC for conversion to ethylene was increased due to competition of D-amino acids with ACC in the malonylation reaction (Su *et al.* 1985).

Even though malonylation of ACC is a reversible reaction, current evidence suggests that 1-(malonylamino)cylopropane-1-carboxylate (MACC) is not readily hydrolysed to provide ACC for ethylene production *in vivo* (Reid, 1995). For example, during germination of peanut seeds containing a high level of MACC, most of the ethylene produced was from ACC synthesized *de novo,* rather than the hydrolyzed products of MACC (Yang and Hoffman, 1984). Less than

2% of ethylene was converted from the hydrolyzed products, when compared to ethylene produced from newly synthesised ACC. In addition, during ripening of tomato fruits, the activity of N-ACC malonyl-transferase increased just after the ethylene burst, and the enzyme is also induced in response to ethylene treatment of the fruit at any fruit developmental stage (Martin and Saftner, 1995). This ethylene-induced activation of N-ACC malonyl-transferase activity has led to the proposition that the enzyme might act as a negative regulatory component in ethylene production in fruit tissues.

Taken together, malonyl-ACC appears not to be source of ACC, *in vivo,* but may be important in controlling the rate of ethylene production since the formation of the conjugate causes depletion of ACC levels and so reduces ethylene production (Reid, 1995).

One-(gamma-L-glutamylamino)-cyclopropane-1-carboxylic acid (GACC) has also been reported as an ACC-conjugated form, catalysed by gamma-glutamyl-transpeptidase (GGT) in a glutathione concentration-dependent manner (Martin *et al.*, 1995). The conjugating activity was calculated as 10 to 50 times higher than N-malonyl-transferase activity in tomato fruits. However, the activity was not responsive to ethylene, unlike N-malonyl transferase. Therefore, GACC is proposed as one of main conjugated forms in tomato fruit when sufficient GSH tripeptide (the substrate of gamma-glutamyl-transpeptidase) is available. However, Peiser and Yang (1998) have challenged whether GACC is an authentic major conjugate form of ACC in tomato fruit tissue because GACC is only detectable in ripening tomato fruit and not in any other plant organs producing high ethylene production. This lack of universality may imply that it is not a general form of ACC conjugation, but may be specific to ripening tomato fruit tissue. Peiser and Yang (1998) also pointed out that the biological function of GGT is as a hydrolase rather than a peptide-transferase. Together, these undermine the significance of GACC conjugation.

1.4.4 ACC oxidase (ACO)

In contrast to ACC synthase, ACC oxidase was thought to be expressed in a constitutive manner in many plant tissues, because ACC, when included in the growth medium or infiltrated into plant tissues, is readily converted to ethylene (Yang and Hoffmann, 1984). Nevertheless,

recent studies using molecular analysis suggest that ACO expression is also increased when ethylene production is maximised, (e.g. fruit ripening; Kende, 1993). Thus changes in ACO activity has been suggested to constitute an extra tier of control for ethylene biosynthesis in higher plants.

1.4.4.1 Identification of genes encoding ACO and recovery of ACO activity, *in vitro*

From the observation of reduced ethylene production in transgenic plants transformed with an antisense construct of a ripening-related cDNA (pTOM13), Hamilton *et al.* (1990) suggested that the gene encoded an enzyme involved in ethylene biosynthesis. Subsequently, the pTOM13 gene and related sequences (pTOM5) were shown to exhibit ethylene-forming enzyme (EFE or ACO) activity, when these cDNAs were expressed in yeast (Hamilton *et al.*, 1991) or in *Xenopus laevis* oocytes (Spanu *et al.* 1991), respectively. The gene product of pTOM13, when expressed in yeast, displayed similar characteristics to ethylene-forming activity found in plant tissue, in that it converted the ACC analogue, 1-amino-2-ethylcyclopropane-1-carboxylic acid (AEC) to 1-butene in preference to the *trans*-isomer. Further, activity was strongly inhibited by cobalt ions (Co^{2+}) and 1,10-phenanthroline (PA; a metal chelator).

The DNA sequence of pTOM13 and related cDNAs showed a comparatively high homology to flavonone 3-hydroxylase genes (Hamilton *et al.*, 1990). Since it had been known that flavonone 3-hydroxylase enzyme activity, *in vitro*, required ascorbate and iron (Fe^{2+}) as cofactors, when these cofactors were added to protein extracts from melon (*Cucumis melo*) fruits, complete recovery of the enzyme activity, *in vitro,* was demonstrated (Ververidis and John, 1991). These cofactors, therefore, were found to be essential for the assay of ACO activity, *in vitro,* and the failure of previous attempts to assay enzyme activity was presumed to be caused by loss of these cofactors during protein extraction from plant tissue. Subsequently, ACO activity, *in vitro*, from apple was reported to be increased by the presence of CO_2 (as HCO_3^-) in the enzyme activity assay mixture (Fernandez-Maculet and Yang, 1992). With protein extracts from melon fruits, the activating effects of HCO_3^- and CO_2 in the assay mixture were compared, and CO_2 rather than HCO_3^- was reported as the activating form in the assay *in vitro* (Smith and John, 1993).

1.4.4.2 Biochemical studies

Biochemical characterisation of ACO

Once ACO activity, *in vitro*, was fully recovered from crude protein extracts using appropriate cofactors (Fe^{2+} and ascorbate), purification and characterisation of the enzyme from many plant species has progressed rapidly especially from fruits, such as apple (*Malus domestica* ; Dong *et al.*, 1992; Kuai and Dilley, 1992; Dupille, *et al.*, 1993; Pirrung *et al.*, 1993), avocado (McGarvey and Christoffersen, 1992), pear (Vioque and Castellano, 1994; Vioque and Castellano, 1998), banana (*Musa* AAA group; Moya-Leon and John, 1995) and citrus (*Citrus rediculata*; Dupille and Zacarias, 1996).

The requirement for cofactors (ascorbate and Fe^{2+}) for ACO activity, *in vitro*, is a general phenomenon applying to both dicot (e.g. tomato) and monocot (e.g. banana) plant species (John, 1997). Ascorbate cannot be replaced with any other 2-oxoacid, and hence when 2-oxglutarate instead of ascorbate was added to the assay mixture extracted from pear fruits, most of the enzyme activity *in vitro* was lost (Vioque and Castellano, 1994). Also, when an ion chelator [ethylenediaminetetraacetic acid (EDTA) or PA] was added to an assay mixture from citrus, ACO activity, *in vitro*, was lost, confirming that a metal ion (Fe^{2+}) serves as an essential cofactor (Dupille and Zacarias, 1996). The requirement of iron cannot be replaced with any other divalent metal ions, such as Zn, Mg, Mn, and Cu. Dupille *et al.* (1993) purified ACO protein from apple and demonstrated that the ACO protein did not contain a prosthetic-heme group for binding Fe^{2+}. Instead, His177, Asp179, His211 and His234 are proposed as the Fe^{2+} binding site from studies using recombinant ACO proteins (Lay *et al.*, 1996; Shaw *et al.*, 1996; Kayrzhanova *et al.*, 1997; Zhang *et al.*, 1997; Tayeh *et al.*, 1999).

The activating effect of CO_2 for ACO activity has also been reported from protein extracts of many plant species (John, 1997). Enzyme activity, *in vitro*, extracted from citrus peel was maximum with 30 mM of HCO_3^- in the assay mixture (Dupille and Zacarias, 1996). However, from the observation of an increase in ACO activity, *in vitro*, with CO_2 (14%), the activating component in the assay mixture for pear fruit extracts was proposed to be CO_2 rather than HCO_3^- (Vioque and Castellano, 1994), in common with the observation from melon fruits (Smith and John, 1993).

ACO activity, *in vitro*, demonstrates very similar characteristics when compared with activity, *in vivo* (John, 1997). Inhibitors of the ACO activity, *in vivo*, such as aminoisobutyric acid (AIB) and Co^{2-}, severely inhibit enzyme activity, *in vitro* (McGarvey and Christoffersen, 1992; Kuai and Dilley, 1993; Vioque and Castellano, 1994). Also *trans*-AEC is preferentially converted to 1-butene, compared to its *cis*-isomers (McGarvey and Christoffersen, 1992; Kuai and Dilley, 1993). These characteristics are often used to confirm authentic ACO mediated ethylene biosynthesis in assay systems *in vitro*.

Based on the well-characterised properties of ACO activity, *in vitro*, purification of ACO protein from several fruits has been achieved (Smith *et al.*, 1992; Dong *et al.*, 1992; Dupille *et al.*, 1993; Pirrung *et al.*, 1993; Moya-Leon and John, 1995). In apple fruits, ACO protein was purified 170-fold by four (Dong *et al.*, 1992) or 180-fold by five purification steps (Dupille *et al.*, 1993). A 20 amino acid sequence was obtained from the purified protein, which matched a peptide sequence deduced from pAE12 (an apple ACO cDNA) (Dong *et al.*,1992). Pirrung *et al.* (1993), however, reported that only a 20- to 30-fold purification was enough to isolate the enzyme to homogeneity from apple fruits, suggesting that expression of the enzyme in this tissue might be relatively high.

The purified ACO enzyme has been used to determine the stoichiometry of the ACO enzymatic reaction (Figure 1.3).

$$ACC\ (C_4NO_2H_2) + O_2 + AH_2 \xrightarrow{Fe^{2+},\ CO_2} C_2H_4 + CO_2 + HCN + A + 2H_2O$$

Figure 1.3 Ethylene forming reaction catalyzed by ACO.
AH_2: Ascorbate reduced form
A: Ascorbate oxidised form

The purified apple ACO protein by Dong *et al.* (1992) was determined to be 35 kD using SDS-PAGE, but 39 kD with gel filtration. The ACO protein purified by Pirrung *et al.* (1993) was

calculated as 35331.8+5 amus by electrospray-mass spectroscopy, which is 52 amus different from the mass calculated from the deduced amino acid sequence of the cDNA encoding an apple ACO (pAE12). From these observations, the ACO protein is proposed to exist as a monomer in apple fruit. Pirrung *et al.* (1993) speculated that the size discrepancy they observed using mass spectroscopy may be due to N-acetylation of the protein.

Characterisation of recombinant ACO proteins

To understand the mechanism of the ethylene forming reaction mediated by ACO further, recombinant ACO proteins expressed in *E. coli* have been used to study the enzyme from tomato (Zhang *et al.*, 1995), apple (Shaw *et al.*, 1996; Kadyrzhanova *et al.*, 1997) and kiwi fruit (Lay *et al.*, 1996). Activity, *in vitro*, of tomato recombinant enzyme requires addition of ascorbate and Fe^{2+} as cofactors, is enhanced by CO_2, and discriminated *trans*-isomers from *cis*-isomers of AEC to produce 1-butene (Zhang *et al.*, 1995).

When the recombinant tomato ACO protein was treated with diethyl pyrocarbonate (DEPC), the protein lost activity rapidly (Zhang *et al.*, 1995). However, enzyme activity was maintained in DEPC-treated extracts if these were co-treated with ACC, ascorbate, and Fe^{2+}. This observation suggests that DEPC might alter histidine residues, which may be critical for binding substrates. However, Fe^{2+} alone in the mixture was not able to maintain enzyme activity, suggesting that although ACO protein can bind Fe^{2+} via its His residues, ACC and ascorbate stabilise the ACO-Fe^{2+} complex against DEPC inactivation. This involvement of histidine residues during DEPC-induced inactivation of the recombinant tomato ACO protein was also supported from data achieved by spectroscopic changes during enzyme inactivation (Tayeh *et al.*, 1999).

In addition, site-specific mutagenesis of His or Asp residues has been used to examine the possibility that these amino acid residues may act as Fe^{2+}-binding ligands during ACO catalysed reactions (Zhang *et al.*, 1997; Tayeh *et al.*, 1999). Mutations at His177, Asp179, His211 and His234 demonstrated a total loss of activity, meaning that these residues are essential for ACO activity. This effect was also observed in recombinant ACO protein from apple (Shaw *et al.*,

1996; Kayrzhanova *et al.*, 1997) and kiwifruit (Lay *et al.*, 1996). Metal Catalytic Oxidation (MCO) fragmentation experiments using the recombinant tomato ACO confirmed His177 and Asp179, but not His 234 as the Fe^{2+}-binding sites (Zhang *et al.*, 1997).

The activation of ACO activity by CO_2 via carbamylation was also tested using site-specific mutagenesis of recombinant ACO proteins from apple and kiwifruit (Lay *et al.*, 1996; Kadyrzhanova *et al.*, 1997). Seven lysine residues, conserved among ACO sequences from various plant species, were targeted as mutational sites to examine their possible involvement as CO_2 activation sites. With the exception of Lys158, none of the other lysine residues tested (Lys177, 199, 230, 292, and 296) resulted in impaired enzyme activity (Kadyrzhanova *et al.*, 1997). However, the ACO activity loss by the Lys158Leu mutation was not reconfirmed by Lys158Glu, Lys158Gln or Lys158Arg mutations, suggesting that the loss of enzyme activity by the Lys158Leu mutation might be specific to this particular substitution, probably through a conformational change in the protein. This was also reported for a Lys158Ala mutation of recombinant ACO protein of kiwifruit, and its activity loss appeared to be related to disruption of an essential structural unit of the protein, and not by interrupting CO_2 carbamylation (John *et al.*, 1997). Therefore, CO_2 carbamylation via specific Lys residues may not be the activating mechanism of ACO activity by CO_2.

The inactivation mechanisms of ACO protein during catalysis have also been characterised using recombinant tomato ACO proteins. Barlow *et al.* (1997) proposed separate mechanisms for inactivation of ACO protein. The inactivation of enzyme activity was increased by pre-incubation of the protein with Fe^{2+} and ascorbate, but this could be reduced by co-incubation with catalase. However, if ACC was added together with Fe^{2+} and ascorbate, the inactivation was further increased. Catalase could not reduce this inactivation, but saturating levels of CO_2 (supplied as 10 mM bicarbonate) were effective. This study suggests that ACO protein appears to be inactivated via a relatively slow partial unfolding of the catalytically active conformation, via oxidative damage mediated by hydrogen peroxidase (which is catalase protectable), and via oxidative damage to the active site, resulting in partial proteolysis (catalase unprotectable).

Tissue localisation of ACO

Before ACO activity, *in vitro*, was successfully recovered (Ververidis and John, 1991), loss of activity, *in vitro*, from cell homogenates was assumed to be caused by the loss of membrane integrity during protein extraction. Thus ACO protein was proposed as a membrane-bound protein (Mattoo and White, 1991). Even though this has proven not to be the case (activity is dependent on the inclusion of appropriate cofactors), in some cases polyvinylpolypyrrolidone (PVPP) or Triton X-100 are needed in the extraction buffer to fully recover enzyme activity from apple and pear fruits (Kuai and Dilley, 1993; Vioque and Castellano, 1994). This may indicate that ACO is membrane-bound in plant cells. So, the question as to whether ACO protein is a membrane-bound enzyme or localised in any particular organelle in plant cells was examined when antibodies against ACO became available (Reinhardt *et al.*, 1994; Rombaldi *et al.*, 1994; Charng *et al.*, 1998; Ramassamy *et al.*, 1998).

The subcellular location of the protein has been determined in tomato suspension-cultured cells using cell fractionation techniques, followed by immunoblot analysis (Reinhardt *et al.*, 1994). Using a MAb raised against a tomato ACO expressed in *E. coli* cells, ACO protein was shown to be absent from the vacuole and not bound to the membrane, but localised mostly in the cytoplasm of the cell. This was further confirmed from electron microscopic studies using immunogold-labeled antibodies, which indicated a cytoplasmic localisation of ACO protein (Charng *et al.*, 1998). As such, a preliminary study of the translation of apple ACO, *in vitro* revealed that the ACO protein was neither processed nor partitioned to the microsomal membrane, indicating that ACO protein is a cytoplasmic protein (Charng *et al.*, 1998).

However, another suggestion is that ACO proteins also exist in the extra-cellular space, more precisely at the periplasm of fruit cells in apple and tomato (Rombaldi *et al.*, 1994; Ramassamy *et al.*, 1998). Evidence from immuno-localisation studies using polyclonal antibodies, raised either against a synthetic peptide, designed from antigenic sites on ACO protein or pTOM13 protein expressed in *E. coli* demonstrated that the antigen-antibody complexes existed primarily in cell walls of apple and tomato fruit (Rombaldi *et al.*, 1994). With highly reduced detection from transgenic tomato fruits transformed with an antisense pTOM13 construct, the antibody

detection in the cell walls was confirmed as authentic ACO recognition. In addition, proteinase K-treated protoplasts of apple culture cells showed much less detection of the antigen by western analysis, supporting the proposal that the enzyme is present in the extracellular space in fruit cells (Ramassamy *et al.*, 1998).

Although most observations (including analysis of ACO gene sequences, which lack any known sequence-motif for extracellular targeting) indicate that the location of ACO protein is cytoplasmic, it has to be examined further whether this protein is also able to be secreted via a non-traditional mechanism of protein transport and is present in the extracellular space of plant cells.

Evidence for the occurrence of ACO isoforms

From the biochemical characterisation of ACO protein extracted from many plant species, evidence has emerged that the enzyme exists as more than one isoform in plants (McGarvey and Christoffersen, 1992; Vioque and Castellano, 1994; Dupille and Zacarias, 1996; Finlayson *et al.*, 1997)

From avocado fruits, two fractions, designated as EFE1 and EFE2, were identified with ACO activity after differential ammonium sulphate precipitation (McGarvey and Christoffersen, 1992). The demonstration of typical stereo-specificity of substrate and the inhibitory effect of 2-AIB confirmed EFE1 and EFE2 as authentic ACO proteins. Further analysis of EFE1 demonstrated a relatively low Km (32 μM) for ACC with a pH optimum of 7.5 to 8.0.

ACO activity, *in vitro*, extracted with 0.8% (v/v) Triton X-100 from pear fruits had two optimal temperatures at 28 °C and 38 °C (Vioque and Castellano, 1994). In common with pear ACO protein, citrus ACO activity, *in vitro*, which became detectable after passage of the crude extract through a Sephadex G-25 column, demonstrated two optimal temperatures for activity at 35 °C and 45 °C (Dupille and Zacarias, 1996). Both studies implied that there might be two different isoforms of ACO in these extracts.

Further evidence for the occurrence of ACO isoforms has been reported from the assay of enzyme activity, *in vitro*, using protein extracts from leaf and root tissues of corn (*Zea mays*) and sunflower (*Halianthus annus*) (Finlayson *et al.*, 1997). Biochemical characteristics

including Km for O_2, CO_2, and ascorbate in protein extracts from the two different organs suggested that the enzyme present in leaf tissue is distinct from one in root tissue (i.e. these are organ-specific isoforms of ACO), regardless of its plant origin. The high Km for CO_2 and ascorbate and the low Km for O_2 in root extracts, compared to those in leaf extracts suggests that the two different isoforms of ACO protein have evolved to adapt to the environment to which each organ is exposed.

1.4.4.3 Molecular studies

Since pTOM13 and its related cDNA sequences were identified as genes encoding authentic ACO protein (Hamilton *et al.*, 1990; Hamilton *et al.*, 1991; Spanu *et al.*, 1991), the occurrence of ACO genes has been screened for various plants. From studies thus far, the ACO gene family has been shown to comprise two to four members (Tang *et al.*, 1993; Kim and Yang, 1994; Pogson *et al.*, 1995; Barry *et al.*, 1996; Lasserre *et al.*, 1996; Liu *et al.*, 1997; Brandstatter and Kieber, 1998; Kim *et al.*, 1998).

A. Identification of ACO genes in plant species

In *A. thaliana*, an ACO gene (AT-ACO1) has been cloned by screening a cDNA library with pTOM13 (Gomez-Lim *et al.* 1993) and another ACO gene has been identified by Brandstatter and Kieber (1998) using differential display PCR (DD-PCR). Searching expressed sequence tag (EST) clones for ACO gene sequences revealed, however, that more than two genes encode ACO protein in *A. thaliana* (Bennet *et al.*, 1998). Four ACO genes (ACO1, ACO2, ACO3 and ACO4), sharing 80% nucleotide sequence homology in their coding regions, were isolated from petunia (*Petunia hybrida*; Tang, 1993). The 5'-regulatory regions of these ACO genes show divergence, but contain some conserved functional sequence motifs, including the TATA box. Kim and Yang (1994) isolated putative ACO clones by screening a cDNA library constructed with mRNA extracted from mung bean hypocotyls, using a combination of apple (pAE12) and tomato (pTOM13) ACO cDNAs as probes. Two of these ACO genes, designated as pVR-ACO1 and pVR-ACO2, show high homology in their coding regions, but high divergence in their 3'-untranslated regions. Pogson *et al* (1995) reported the identification of two cDNA clones (ACC Ox1 and ACC Ox2) isolated from senescent florets of broccoli

(*Brassica oleracea*). Genomic Southern analysis indicated that these two clones represent two distinct genes in the broccoli genome. Three ACO genes (LEACO1, LEACO2, and LEACO3) have been identified in tomato (Barry *et al.*, 1996). The 3'-untranslated regions (UTRs) of the tomato ACO genes are so divergent that these 3'-UTRs have been used as gene-specific probes for northern studies to analyse the differential expression of ACO genes in various tissues at different stages of development. The characterization of the 5'-regulatory regions of the tomato ACO genes using inverse-PCR revealed a 420 bp direct repeat in the up-stream region of LE-ACO1, which resembles a retrotransposon (Blume *et al.* 1997). Also, two copies of this transposable element are identified in the 5'-regulatory region and the third intron of LEACO3. Three genes, designated as CM-ACO1, CM-ACO2 and CM-ACO3, were identified from melon (Lasserre *et al.*, 1996). The CM-ACO1 gene has three introns, whereas CM-ACO2 and CM-ACO3 have two introns. The DNA sequence of CM-ACO1 show 59% and 75% homology with those of CM-ACO2 and CM-ACO3, respectively, while CM-ACO2 and CM-ACO3 show 59% homology. All these genes displayed considerable divergence in their 5'- and 3'-untranslated regions. In sunflower, three ACO genes (ACCO1, ACCO2, and ACCO3) were cloned by a combination of cDNA library screening with *Brassica napus* ACO cDNA probes and RT-PCR amplification with degenerate primers (Liu *et al.* 1997). Southern analysis confirmed the presence of three or four ACO genes in the genome. Also, by screening a cDNA library constructed from tobacco mosaic virus (TMV)-infected leaves of tobacco (*Nicotiana glutinosa*) by RT-PCR, three ACO genes have been cloned and designated as pNG-ACO1, pNG-ACO2 and pNG-ACO3 (Kim *et al.*, 1998). High sequence homology (78 to 81%) is evident in the coding regions of these tobacco ACO genes, but high divergence in their 3'-untranslated regions is also observed.

One ACO gene has been cloned using PCR-based screening of a cDNA library, constructed with RNA extracted from submerged rice internodes (Mekhedov and Kende, 1996). The gene was confirmed as encoding a functional ACO protein, as its enzymatic activity was proven by transformation into yeast as a sense construct, and also as an anti-sense construct (with no corresponding activity). However, from the characterisation of identified cDNA clones (eight of them), it was observed that although all clones encoded the same ACO gene, they contained

different lengths of 3'-UTR, probably caused by alternative polyadenylation. So, it may be that alternative polyadenylation of a single ACO gene in rice might substitute for an ACO multigene family observed in other plant species.

B. Expression of ACO genes in plant tissues

The expression of ACO activity was thought to be constitutive in plant tissues (Yang and Hoffman, 1984). However, ACO gene expression studies have demonstrated that this constitutive expression of ACO in plant tissue is not due to a single gene, but represents differential expression of a small multigene family in a spatial and a temporal manner (Gomez-Lim *et al.*, 1993; Kim and Yang, 1994; Pogson *et al.*, 1995; Barry *et al.*, 1996; Lasserre *et al.*, 1996; Liu *et al.*, 1997; Brandstatter and Kieber, 1998; Kim *et al.*, 1998).

In vegetative tissue of *A. thaliana*, AT-ACO1 has been shown to be constitutively expressed (Gomez-Lim *et al.* 1993). Gene expression is also elevated by wounding, and treatment of tissue with ACC (10 mM), iron (Fe^{2+}; 0.2 M) and ethylene (as 1 mM ethrel). Although such detailed characterisation was carried out with this particular ACO gene only, Brandstatter and Kieber (1998) reported that another ACO gene was induced by the application of a low concentration of cytokinin (50 μM) in *A. thaliana* seedlings. Therefore, at least two different ACO genes are expressed in vegetative tissues of *A. thaliana.*

In mung bean hypocotyl, northern analysis demonstrated significant expression of pVR-ACO1 in all parts of the seedlings, and a basal level expression of the pVR-ACO2 (Kim and Yang, 1994). Expression of pVR-ACO1 was further increased by excision-induced wounding, but decreased with 5 μM methyl-jasmonate treatment. The ACC Ox1 gene in broccoli was expressed in both senescent vegetative and reproductive tissues, but expression of this gene was not responsive to the plant hormones, ABA or ethylene (added as propylene) (Pogson *et al.*, 1995). The ACC Ox2 was, however, expressed only in reproductive tissues, and was responsive to ABA or ethylene. Even though both transcripts appeared not to be induced by wounding, the level of ACC Ox2 transcript increased rapidly after harvest. It was suggested, therefore, that expression of the ACC Ox2 gene might cause high ethylene production after harvest, which may control the loss of chlorophyll in florets of broccoli.

The expression of ACO genes in tomato has been thoroughly characterised by Grierson and colleagues (Barry *et al.*, 1996; Barry *et al.*, 1997). When divergent gene-specific 3'-UTR clones of the three tomato ACO genes (LEACO1, LEACO2, and LEACO3) were used as probes in northern analysis, both LEACO1 (pTOM 13) and LEACO3 (pTOM 5) transcripts were shown to accumulate during senescence of leaves, fruits and flowers. All three ACO genes were expressed during flower development with spatially-regulated accumulation patterns. LEACO1 was expressed predominantly in the petals, stigma and style, LEACO2 expression was mainly restricted to tissues associated with the anther cone, and LEACO3 transcripts accumulated in all of the floral organs examined, except the sepals.

Expression of ACO genes in melon has been characterised using semi-quantitative RT-PCR. All three genes were expressed in etiolated hypocotyls at a relatively high level. A positive correlation was found between the expression of CM-ACO1 and measurable ACO enzyme activity in senescent leaves and fruits, and gene expression was responsive to ethylene and wounding in non-senescent leaf tissue. CM-ACO3 was expressed mainly in mature green leaves and in developing floral tissue (Lasserre *et al.* 1996; Lasserre *et al.* 1997).

In sunflower, RT-PCR-based gene expression studies indicated that the ACCO3 gene transcript might be responsible for the basal level of ethylene production in all plant parts (Liu *et al.* 1997). In contrast, ACCO1 and ACCO2 were expressed predominately in roots and aerial parts of the plant, respectively. The ACCO1 gene was also expressed more highly in rapidly dividing cells, such as apical buds and root tips, when compared with expression in hypocotyls and cotyledons. This may indicate that ethylene plays a role during early growth and development of sunflower tissues.

In tobacco, pNG-ACO1 and pNG-ACO 3 gene expression was highly induced in roots, and also in senescent leaves, whereas pNG-ACO2 was constitutively expressed in leaves and stems (Kim *et al.*, 1998). Upon treatment of vegetative tissue with various stress factors (TMV infection, wounding, salicylic acid, Cu_2SO_4, ethylene and methyl-jasmonate), the expression of pNG-ACO1 and pNG-ACO3 was up-regulated, whereas pNG-ACO2 expression was unresponsive, and remained constitutively expressed in vegetative tissues.

C. Transgenic plant analysis

Differential accumulation of ACO transcripts during plant growth and development has also been examined at the transcriptional level using transgenic plants containing ACO promoter: GUS transcriptional fusion (Blume and Grierson, 1997; Lasserre *et al.*, 1997). Using three types of the fusion from –124 bp, -396 bp and -1825 bp to +97 bp (designated as ACO1-124, ACO1-396 and ACO1-1825, respectively), the promoter region of LEACO1 has been characterised in tobacco (*Nicotiana plumbaginifolia*) and tomato plants (Blume and Grierson, 1997). GUS activity driven by the ACO1-124 sequence was not expressed in any tobacco tissue, but was high in ripening tomato fruit tissue. This observation implied that the sequence between -124 and +97 might contain minimal fruit-ripening specific elements which are operative in tomato. GUS expression driven by the ACO1-396 sequence closely paralleled lowed mRNA expression of LEACO1 in non transformed tomato (Barry *et al.*, 1996). Thus in transgenic tomato, GUS expression increased significantly during fruit ripening, leaf and flower senescence and abscission, and was induced by wounding, by pathogen infection, and by treatment with methyl-jasmonate or 1-aminobutyric acid. Both tomato and tobacco plants transformed with ACO1-1825 displayed a very similar pattern to each other, indicating that the mechanism of transcriptional activation of the ACO gene seems to be well conserved between the two plant species, probably mediated by similar developmental signals and *cis*-acting sequences. The ACO1-1825 construct showed a slightly higher basal level of GUS-expression in young, immature organs, compared with ACO1-396 transgenic plants, suggesting that additional positive and/or negative regulatory elements might be located upstream of nucleotide-396. In addition to GUS expression corresponding to mRNA expression of LEACO1 in wild type tomato, additional expression of the reporter gene was also detected in pollen and seed endosperm in transgenic tomato.

The expression of ACO genes in melon has also been examined further in tobacco (*Nicotiana tobaccum*) plants transformed with GUS fusion constructs of the 0.7 kb and 2.2 kb upstream regions of CM-ACO1 and CM-ACO3, respectively (Lasserre *et al.*, 1997). In seedlings, CM-ACO1-GUS expression was induced weakly in vascular tissues, whereas the CM-ACO3-GUS expression increased strongly in cotyledons, indicating that the expression of CM-ACO3 may be involved in early leaf development. During tobacco leaf senescence, the CM-ACO1-GUS

expression increased sharply at the onset of chlorophyll breakdown, which confirmed the expression pattern of the gene in melon (determined by semi-quantitative RT-PCR analysis). The CM-ACO3-GUS expression also remained high at this stage, which conflicted with data of semi-quantitative RT-PCR analysis from melon, which showed expression decreased before de-greening (Lasserre *et al.*, 1997). This discrepancy between the level of CM-ACO3-GUS expression in the transgenic tobacco and the abundance of the gene transcripts in melon was proposed to arise from the stability of the products of the GUS reaction in tobacco tissue. Therefore, the CM-ACO3 promoter appeared to be active in green, fully expanded leaves, and declined before the onset of senescence in leaves.

In developing tobacco flowers, CM-ACO3-GUS expression was high in sepals and petals at all developmental stages. Expression was also localized to the stigma before pollination, then extended to the upper part of the styles after pollination, and then to the anthers. The CM-ACO1-GUS expression was, however, induced weakly in the sepals during flower development. CM-ACO1-GUS expression increased strongly upon treatment with heavy metals, ethylene, wounding, compatible and incompatible plant pathogens, whereas the CM-ACO3-GUS expression was not induced in response to any of these factors. In summary, these experiments on melon ACO promoter activity in tobacco confirmed that ACO mRNA expression detected by semi-quantitative RT-PCR analysis, was regulated at the transcriptional level.

D. Post-transcriptional regulation of ACO gene expression

Changes in ACO enzyme activity, both induced by plant developmental signals or by various external stimuli does not always follow changes in transcript abundance in plants (Kim and Yang, 1994; Liu *et al.*, 1997; Jin *et al.*, 1999). Studies on ethylene-induced VR-ACO1 expression were extended to examine changes in ACO protein levels in mung bean seedlings (Kim and Yang 1994; Jin *et al.*, 1999). In mung bean hypocotyls, VR-ACO1 gene expression, ACO activity, *in vivo*, and ACO protein accumulation (detected by polyclonal antibodies raised against VR-ACO1 protein expressed in *E. coli*), increased in parallel over 2 hr after ethylene treatment. However, the rate of increase in ACO activity, *in vivo*, and ACO accumulation was much slower than the increase of VR-ACO1 transcripts, which suggests that the ethylene-

responsive increase of ACO activity in mung bean hypocotyl is regulated at both the transcriptional and post-transcriptional levels. Studies in roots demonstrated that the induction of VR-ACO1 by ethylene was much higher (when compared with hypocotyls) and the protein accumulation was at the same rate as transcript accumulation. Therefore, it was speculated that ethylene-induced ACO activity, *in vivo*, in roots is regulated mainly at the transcriptional level.

Discrepancies between ACO transcript accumulation and ACO protein accumulation were also reported in sunflowers (Liu *et al.*, 1997). When wounding and treatment with silver ions induced both ACO transcripts and ACO activity in sunflowers, ACO protein accumulation (detected by polyclonal antibodies raised against ACCO1 expressed in *E. coli*) did not correlate with this increase. This observation supports that the notion that ACO activity is controlled at a post-transcriptional level.

E. ACO gene expression and ethylene biosynthesis

In common with ACS, regulation of ACO activity in plant tissues is now proposed as a regulatory step in controlling the rate of ethylene production (Mekhedov and Kende, 1996; Tang and Woodson, 1996; Blume and Grierson, 1997).

Submergence of rice internodes induced ACO activity, *in vitro*, by 8 hr. The increase was smallest in an intercalary meristematic zone (15 mm above node), but rather higher in elongated or differentiated tissues (15 to 45 mm above node) (Mekhedov and Kende, 1996). An increase of an ACO transcript was also detected 4 hr after submergence, with highest induction in the elongated or differentiated tissues. Preliminary expression studies of ACS genes in these tissues did not show any increase in response to submergence. Hence, ACO expression in those tissues was proposed to be an important regulatory step of the ethylene production in response to submergence. ACO controlled ethylene production has also been reported from petunia flowers, which normally senesce after pollination with an associated large increase in ethylene production (Tang and Woodson, 1996). When an immature flower was artificially pollinated, the burst of ethylene was not immediately detected, probably because of a lack of ACO activity expressed at this immature developmental stage. Expression studies of ACO

genes in tomato plants also demonstrated that the transcriptional activation of the LEACO1 gene increased in parallel with ethylene production in most cases (Blume and Grierson, 1997).

However, ACO gene expression has also been shown to be controlled by endogenously or exogenous ethylene (Gomez-Lim *et al.*, 1993; Kim and Yang, 1994; Kim *et al.*, 1997; Bouquin *et al.*, 1997; Liu *et al.*,1997).

AT-ACO1 expression in *A. thaliana* was up-regulated in response to treatment with ACC or the ethylene-releasing chemical, ethrel (at 1 mM) (Gomez-Lim *et al.* 1993). Expression of the VR-ACO1 gene in response to wounding of mung bean hypocotyl was repressed in the presence of 2,5-norbornadiene (NBD; 5000 $\mu L\ L^{-1}$), but expression was restored with ethylene treatment (50 $\mu L\ L^{-1}$) for 7 hr (Kim and Yang, 1994). These results suggest that wound-induced ethylene was the major inducing component of VR-ACO1 gene expression in response to wounding. Using the same system, Kim *et al.* (1997) also demonstrated that the basal constitutive expression of the VR-ACO1 gene was expressed in response to endogenous ethylene, so that this basal ACO gene expression was reduced with NBD treatment in a dose-dependent manner.

Wound-induced ACO gene expression is not always mediated through ethylene. For instance, wounding or silver ion treatment of sunflower hypocotyls increased ACO activity, *in vitro*, ACO mRNA accumulation, and ethylene production (Liu *et al.*, 1997). The ACO genes were, however, unresponsive to ACC, ethylene or auxin treatment of this tissue.

Expression of the CM-ACO1 gene in melon in response to wounding and ethylene (30 $\mu L\ L^{-1}$) was observed (Bouquin *et al.* 1997). The ethylene action inhibitor, 1-methylcyclopropane (1-MCP; 1 $\mu L\ L^{-1}$), inhibited the accumulation of ethylene-induced CM-ACO1 mRNA transcripts in melon leaf tissue or the gene promoter-driven GUS activity in transgenic tobacco plants, but it failed to block the wound-induced CM-ACO1 gene expression. As well, the identification of separate putative *cis*-acting sequence motifs for wounding and ethylene responses within the upstream regions of the CM-ACO1 promoter suggests that this gene is able to respond to both stimuli through different *trans*-acting factors. This result suggests that the induction of CM-

ACO1 expression occurs *via* two separate signal transduction pathways in response to wounding and ethylene treatment.

From these studies of ACO gene and protein expression, it is apparent that changes of ACO activity (along with changes of ACS activity), which are regulated at both the transcriptional and post-transcriptional levels, contribute together to manipulate ethylene production in response to documented wide range of developmental or environmental signals.

1.5 Ethylene biosynthesis and developing tissue in higher plants

1.5.1 Physiological studies

Higher ethylene evolution from developing tissues has been reported from many plant species (Aharoni *et al.*, 1979; Lavee and Martin, 1981; Roberts and Osborne, 1981; Osborne, 1991; Ievinsh and Kreicbergs, 1992).

In tobacco (*Nicotiana tobaccum*), relatively high ethylene production in rapidly expanding leaves, and from senescing leaves, has been reported (Aharoni *et al.*, 1979). Lavee and Martin (1981) also observed that rapidly growing young leaves evolved considerably higher ethylene than mature, non-growing leaves of olive tissues (*Olea europaea*). In bean leaves (*Phaseolus vulgaris*), a rate of 0.1 to 0.4 nL g^{-1}Fwt hr^{-1} of ethylene production was observed from expanding leaves, a basal level (under 0.1 nL g^{-1}Fwt hr^{-1}) of ethylene production was measured from fully expanding annual leaves, and higher ethylene production (above 5 to 6 μL g^{-1}Fwt hr^{-1}) was observed from leaf tissue at the onset of leaf senescence (Osborne, 1991). Roberts and Osborne (1981) characterised ethylene production from developing leaves of *Prunus serrulata,* and showed that the increased production of ethylene followed a higher level of endogenous IAA during initiation and maturation in leaf tissue, whereas this relationship was not observed in senescing leaf or ripening fruit tissues.

Ethylene production has also been reported from cereal seedlings (Ievinsh and Kreicbergs, 1992). Ethylene production from growing coleoptiles of wheat (*Triticum aestivum*), barley (*Hordeum vulgare*) and rye grass (*Secale cerele*) showed a rhythmic pattern with a period of 16 hr and 12 hr, respectively, which is not related to a diurnal response. This rhythmic ethylene

production was detected from coleoptiles while the tissue grows but it ceased after the first leaf emerged and tissue growth ceased.

From these observations, it has been proposed that ethylene produced from developing tissues may have a role in controlling early growth and development. For instance, Lavee and Martin (1981) proposed that ethylene appeared to be involved in the growth processes of olive tissues. Roberts and Osborne (1981) pointed out a positive correlation between auxin content and ethylene production in immature tissues, and suggested that control by the release of a cofactor, which determines the rate of the ethylene biosynthetic enzymes, might be regulated by endogenous auxin. Osborne (1991) suggested that the relatively high rate of ethylene produced from the most rapidly dividing and expanding tissue might well reflect the high endogenous metabolic turnover of the young cells.

Furthermore, the observation of the periodic ethylene production from cereal coleoptiles has shown that the period of maximal production of ethylene correlates with a period of slow growth of the coleoptile tissue, while rapid growth occurs during a period of lower ethylene production (Ievinsh and Kreicbergs, 1992). As well, in *A. thaliana,* the size of rosette leaf increased in an ethylene insensitive genetic background (*etr1*; Bleecker, 1988), whereas it decreased in the constitutive ethylene responsive genetic back ground (*ctr1*; Kieber, 1993), suggesting that endogenous ethylene may inhibit tissue growth during early leaf development.

In sunflower, a biphasic growth response of leaf explants to exogenous ethylene has been observed (Lee and Reid, 1997). Rapid expansion occurred with a low amount (0.01 mM ethephon) of applied ethylene, but slow expansion occurred in response to a higher amount (≥1 mM ethephon) of applied ethylene. The slow expansion of leaf tissues in response to the higher concentration of ethylene was blocked by application of AVG (an inhibitor of ACS) or silver ions (Ag^+; an inhibitor of ethylene action), supporting the notion that this process was controlled by ethylene. The observation that the increase of leaf expansion by a low amount of ethylene suggests that a dividing tissue requires a certain critical level of ethylene during development.

Ethylene involvement in hypocotyl elongation with the concomitant emergence of the first true leaf has been studied using light-grown *A. thaliana* seedlings (Smalle *et al.*, 1997a; Smalle *et al.*, 1997b). Using limited-nutrition medium (LNM), which provides an exaggerated seedling response to applied ACC (ethylene), ACC treatment demonstrated an induction of hypocotyl elongation, caused by cell enlargement. The effect was blocked by treatment with the ethylene action inhibitor Ag^+, or in an ethylene-insensitive genetic background (*etr1*, *ein2*, and *ein4*), suggesting that the added ACC affected seedling development by enhancing ethylene production in the seedlings under light. This ethylene effect was not observed in etiolated seedlings, or in a *ctr1* genetic background. Instead seedlings displayed a reduction of hypocotyl elongation in response to ethylene. IAA application to seedlings grown in the light induced the same effect (hypocotyl elongation with emergence of the first true leaf) as ethylene (Smalle *et al.*, 1997a). This IAA effect is also blocked by Ag^+, suggesting that it may be mediated through IAA-enhanced ethylene production in these seedlings. However, this IAA effect cannot be linked simply to an increase of ACS activity, because an inhibitor of ACS activity (AVG) failed to block the effect. However, it can be related to increased ACO enzyme activity, because Co^{2+} (an inhibitor of ACO activity) did block the effect. These results support the observation of Roberts and Osborne (1981) and lead to speculation that a cofactor, which determines the rate of ethylene biosynthesis and is regulated by endogenous auxin, controls ACO activity in developing tissues, rather than ACS activity.

1.5.2 Molecular studies

The characterisation of ethylene biosynthesis in developing tissues has been studied at the molecular level in *A. thaliana* (Van Der Straeten *et al.*, 1992; Rodrigues-Pousada *et al.*, 1993; Rodrigues-Pousada *et al.*, 1996). Even though ACO activity seems to be an important regulatory factor of ethylene production in developing tissues, early studies were mainly focused on the characterisation of ACS activity, which has long been known as the enzyme controlling the rate-limiting step for ethylene biosynthesis in higher plants (Yang and Hoffman, 1984; Zarembinsky and Theologis, 1994).

In *A. thaliana*, a genomic clone AT-ACS1 (now ACS2; Bennet *et al.* 1998) of the ACS gene family was isolated by screening a genomic library with degenerate oligonucleotide probes, designed from the sequence of an ACS protein purified from mung bean (Van Der Straeten *et al.*, 1992). Expression studies of the ACS2 gene using RT-PCR with gene-specific primers showed mRNA accumulation was higher in young leaves and young flowers, when compared to mature counterparts. Ethylene treatment also led to an induction of ACS2 gene expression in mature leaves. Rodrigues-Pousada *et al.* (1993) examined the temporal and spatial expression of ACS2 using an ACS2 promoter: GUS transcriptional fusion in *A. thaliana*. Higher expression of GUS was observed in young tissues which then switched off in mature tissues, and ACC content (the product of ACS activity) was positively correlated with ACS2-driven GUS activity. ACC oxidase activity, *in vivo*, was also two-fold higher in immature leaves, compared to mature leaves. So both ACS and ACO activities appeared to contribute to a four-fold higher ethylene production from immature leaves, when compared with mature leaves. Rodrigues-Pousada *et al.* (1996) also reported the interaction between endogenous auxin and ACS2-mediated ethylene production in early rosette leaf development of *A. thaliana*. When 2,3,5-triiodobenzoic acid (TIBA) was applied to seedlings to block auxin polar transport, expression of ACS2 was reduced, and when 2-(p-chlorophenoxy)-2-methyl-propionic acid (CMPA; an auxin action inhibitor) was applied, expression of ACS2 in the presence of excessive auxin was demonstrated. Both experiments suggests that a specific member (ACS2) of the ACC synthase multigene family was involved in ethylene production from developing tissues (i.e. young expanding leaves) and that this production might be under the control of auxin (Rodrigues-Pousada *et al.*, 1996).

In etiolated seedling of *A. thaliana,* ACS4 was also reported as another IAA-responsive ACS gene (Abel *et al.*, 1995). The response was rapid (within 25 min) and sensitive to IAA applications as low as 100 nM. Examination of the promoter of ACS4 revealed four sequences motifs, which are highly homologous to functionally defined auxin-responsive *cis*-elements and therefore support the notion of regulation of ACS4 gene expression by IAA. The up-regulation of ACS4 gene expression by IAA was insensitive to CHX, suggesting that it does not require protein synthesis *per se.* Therefore, induction of ACS4 gene expression is proposed to be an

early gene response to IAA (Abel and Theologis, 1996). These early gene transcripts are more likely to be induced by some components already present in cells. From studies with animal cells, these gene products are proposed to be mainly involved in the emergency rescue of cells in response to external stimuli or in events at the initial stage of organ development (Herschman, 1991; Hill and Treisman, 1995). It is interesting to hypothesize here that if specific ACS genes are early IAA response genes, then this may a mechanism by which IAA can control some important events in nascent leaf tissue of higher plants.

The relationship between IAA and the ethylene biosynthetic enzymes, including both ACS and ACO has also been thoroughly studied using pea seedlings (Peck and Kende, 1995; Peck and Kende, 1998). Two cDNA clones encoding ACS, *PS-ACS1* and *PS-ACS2*, have been isolated by screening a cDNA library from mRNA extracted from IAA-treated pea seedlings. Both ACS genes were induced within 30 min after IAA treatment and the induction was specific to IAA. Further, transcript levels were down-regulated at 4hr after IAA treatment. However, the ACO gene cloned from the cDNA library, designated as *PS-ACO1*, was not expressed until 2 hr after IAA treatment. The expression was also induced by applied ethylene, but was reversibly blocked by the ethylene action inhibitor, 2,5-norbornadiene. The pattern of the gene expression highly correlated with enzyme activity, *in vitro*, despite the fact that there was always a basal level of ACO activity in the tissue before IAA treatment. The lag time difference between the induction of ACS and ACO gene expression suggests that the applied IAA may immediately induce the expression of ACS and the catalytic product of the induced enzyme, ACC, is then converted to ethylene by the basal ACO activity in the tissue. This ethylene may then enhance the expression of the ACO genes to further accelerate ethylene production. Taken together, a coordinated induction of specific members of the ACS and probably the ACO gene families might be developmentally regulated to produce ethylene during the early growth and development in higher plants. Further, this induction may be related to the higher level of IAA in the tissue, although the concentration of IAA, *in vivo*, is rarely reported.

1.6 Ethylene biosynthesis in developing tissues of white clover

The model plant used in this study is the perennial forage legume white clover, *Trifolium repens* L. (tribe Trifolieae, sub-family Papilionoideae, Leguminosae; Mabberly, 1993). The structure of the plant and its pattern of vegetative growth and development have been described by Thomas (1987; Fig 1.4). White clover has a prostrate stolon, consisting of internodes separated by nodes. Each node bears a trifoliate leaf with an erect petiole, two root primordia, which may or may not develop and an axillary bud. Roots that do grow out from the root primordia, do so when a moist stratum is available. In terms of development of the axillary bud, either a lateral stolon or a compound flower can develop, or the bud can remain dormant, depending on environmental conditions and the physiological status of the tissue (Thomas, 1987).

In this study, white clover cv. Grassland Challenge genotype 10F is used, which was selected for studies on leaf development after an assessment of several different cultivars of white clover (Butcher, 1997). The growth of white clover in the model system used is maintained by the regular excision of axillary buds, and root development is prevented by growing stolons over a plastic matrix. Eventually, a single stolon develops from a single major root system, with leaves at all developmental stages from initiation at the apex to senescence and necrosis (Fig. 3.1.1).

Basic physiological studies demonstrated that this gradient of leaf development from the developing apex to senescent leaves on a single stolon could be described in terms of chlorophyll content in leaf tissues from each node (Fig. 1.5; from Hunter, 1998). The chlorophyll content increases until leaf 2 (the developing stage). At this stage, the developing apex and newly initiated leaves are expanding rapidly and leaves reach full size at leaf 3. From leaf 3 to leaf 8 (the mature green stage), the chlorophyll content remains essentially at a constantly high level, then decreases after leaf 9 (the senescent stage) as leaves start to senesce with associated chlorophyll degradation. Measurements of ethylene evolution reveal two periods of higher production (Fig. 1.5). This first is from the developing apex, and leaf 1 and 2, while the second is from node 9 and onwards. From leaf 3 to leaf 8, ethylene production

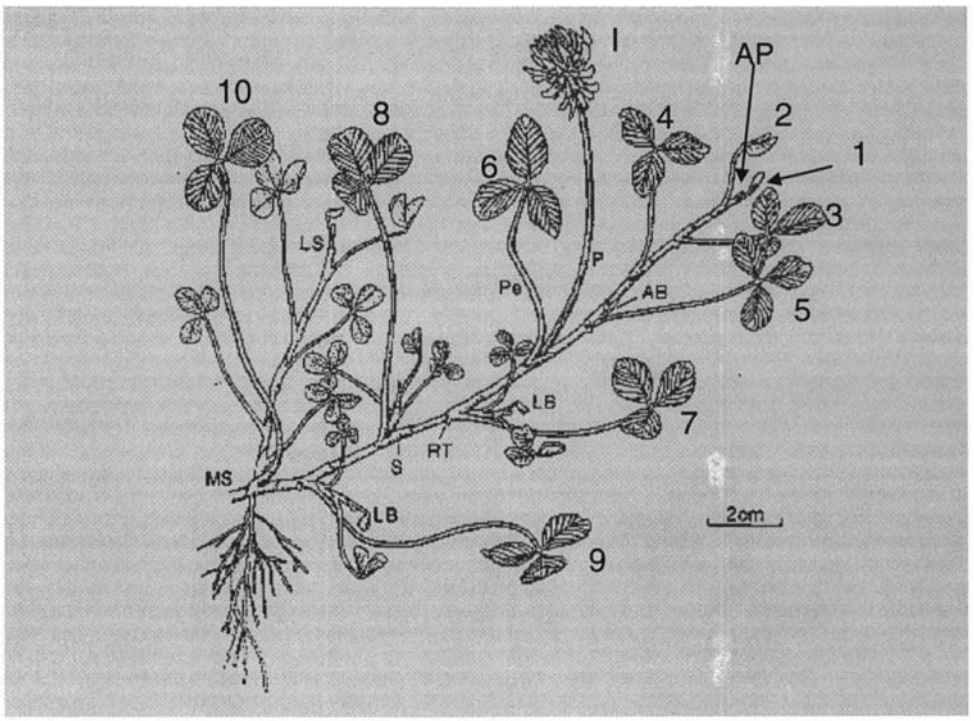

Figure 1.4 Mature structure of white clover (Thomas, 1987). AP, apical bud; AB, axillary bud; MS, main stolon; S, stipule; Pe, petiole; RT, nodal root primordium; I, inflorescence; P, peduncle; LB, lateral bud; LS, lateral stolon. Emerged leaves on the main stolon, and the nodes, bearing them are numbered 1 to 10. This numbering system has been used in this thesis.

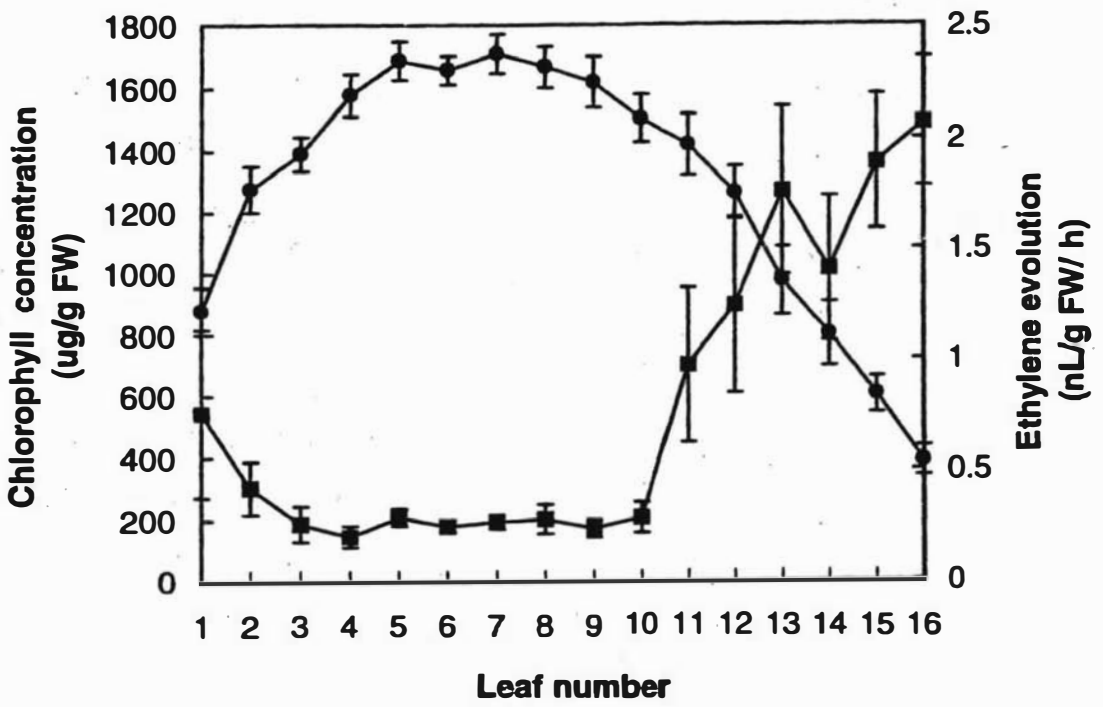

Figure 1.5 Chlorophyll content (-•-) and ethylene production (-▮-) during leaf development in white clover (Hunter, 1998).

remains at a basal level. This pattern of chlorophyll content and ethylene production has also been reported by Butcher (1997).

Together with this physiological analysis, characterisation of ethylene biosynthesis during leaf maturation and senescence has also been studied using this white clover model system (Butcher, 1997; Hunter 1998). Butcher (1997) cloned ACSS, an ACS gene homologue in white clover, using RT-PCR from later mature green leaves, and proposed an active involvement for the ACC-dependent ethylene biosynthetic pathway at the onset of leaf senescence in white clover. Also, two ACO genes, designated as TR-ACO2 and TR-ACO3, were cloned by Hunter (1998) and characterised in terms of gene expression and protein accumulation during leaf maturation and senescence. The differential expression of TR-ACO2 and TRACO3 genes was suggested as a mechanism by which ethylene production during leaf senescence was regulated (Hunter, 1998; Hunter *et al.*, 1999).

It is interesting here to ask how the high ethylene production at two distinct developmental stages is controlled during leaf ontogeny in the white clover model system. Using similar approaches to the previous two studies on leaf senescence-associated ethylene biosynthesis (Butcher, 1997; Hunter, 1998), research in this thesis is concerned with the investigation of the ethylene biosynthesis in early leaf development.

1.7 Aims of research

- Evaluation of ethylene production from the developing apex and newly initiated leaves of white clover

- Cloning of genes encoding the ethylene biosynthetic enzymes, ACS and ACO from developing tissue, analysis of gene sequences and comparison of these with genes expressed in senescent leaf tissue of white clover.

- Characterisation of the expression of ACS and ACO genes during early leaf development in white clover

- Characterisation of the expression of ACO genes in various plant parts of white clover

- Characterisation of the expression of ACO genes in response to wounding and ethylene in mature green leaves of white clover

- Characterisation of ACO protein accumulation using polyclonal antibodies as well as assay of ACO activity, *in vitro,* during early leaf development and in various plant parts of white clover

Chapter 2. Materials and Methods

2.1 Plant material

2.1.1 Clonal propagation of the white clover model growth system

White clover cultivar Grasslands Challenge genotype 10F (AgResearch, Glasslands, Palmerston North, New Zealand) was propagated using the method described by Butcher (1997) with slight modifications.

Apical cuttings, with two or three nodes, were excised from stock plants. The cuttings were placed, with the basal node buried in horticultural-grade bark (bark: peat: pumice = 50:30:20). The cuttings produced roots within 14 to 20 days and then six apical cuttings were transplanted in a line to occupy the outer one third of 30 cm x 45 cm seedling trays, containing potting mix with added nutrients as outlined in Table 2.1 (Fig. 2.1A).

Table 2.1 Composition of potting mix used to propagate white clover.

Ingredient	g / 100 L
Dolomite	300
Agricultural lime	300
Iron Sulphate	50
Osmocote	500

The trays were placed in a glasshouse [Massey University Plant Growth Unit (PGU), Palmerston North, New Zealand] with a temperature range of 21 °C (minimum) to 30 °C (maximum), and irrigation provided by an automatic watering system (watering at 8 am and 5 pm, for 5 min each time). One stolon per cutting was trained over a dry polyethylene surface so as to prevent root growth from primordia at each node. To reduce heat effects in summer, white polyethylene was used as this dry surface (Fig. 2.1). At regular intervals (*ca.* 10 days), any outgrowths from axillary buds were excised to provide one main stolon with leaves from a single root system.

Stock plants of genotype 10F were also grown in the greenhouse to maintain a single genotype for experimental use. To propagate stock plants, apical tips including the leaves distal to node 2 were placed in the horticultural grade barks (bark: peat: pumice = 50:30:20), containing nutrients outlined in Table 2.1. Normally eight apical cuttings were placed in 30 cm x 45 cm trays and the stock plants were maintained in the glasshouse as described above.

Attack (Crop Care Holdings Ltd., Richmond, Nelson, NZ), Pyranica (Mitsubishi Kasei Corporation), and Benlate (Du Pont de Nemours and Co., Inc., Wilmington, Delaware, USA) were used to control aphids and whitefly, mite, and blackspot, respectively.

2.1.2 Harvesting of plant material

As the stolon grows under the conditions described in section 2.1.1, a gradient of leaf development was observed from initiation at the apex through mature green leaves to senescent and then necrotic leaves (cf. Fig. 3.1.1). Three days before harvesting leaf tissue, all axillary structures were removed and the plants left without any further manipulation until harvested. The apex (the apical tip distal to the first emerging leaf), and leaves (leaf blade dissected at the pulvinus) at each node were harvested separately. For some experiments, axillary buds, excised from the axils at nodes 3 and 4 were harvested during the regular pruning for plants. The leaf petiole subtending from nodes 3 and 4 was excised from stolon. Floral buds and open flowers were obtained from leaf axils during early November to January. Internode and node

Figure 2.1 Single stolons of white clover (Grasslands Challenge genotype 10F) grown under the experimental conditions described in section 2.1.1. A, Stolons ready to be harvested; B, The author in one of the glasshouses at the PGU in Massey University (Palmerston North, New Zealand).

A.

B.

tissues were harvested from the mature green developmental stage (nodes 4 to 11) and particular care was undertaken to avoid other tissue contamination such as developing axillary buds and root primordia. All excised plant parts were frozen immediately in liquid nitrogen, and then stored at -80 °C until required.

2.1.3 Treatment of plant tissue

2.1.3.1 Ethylene treatment of detached leaf tissue

Detached mature green leaves (typically 2 g) of white clover were placed in air-tight 2.2 L glass containers. In each container, a double layer of moist paper towers was placed on the bottom to maintain a relative high humidity to prevent tissue dehydration (a separate container was used for each time point). After sealing the glass-lid with petroleum jelly to prevent gas leaking, an appropriate concentration of ethylene (10 $\mu L\ L^{-1}$) was injected through a rubber SUBA-SEAL inserted on the lid. As a control, the same amount of leaf tissue was incubated with 4 g of Purafil™ (Papworth Engineering, Cambridge, New Zealand) and no ethylene was injected.

Glass containers were placed under lights (6X TRUE-LITE® 40W fluorescence tubes) at 20 °C until harvest. At harvest, leaf material was wrapped with aluminum foil, frozen immediately in liquid nitrogen, and stored at -80 °C until required.

2.1.3.2 Ethylene treatment of whole plants

Trays of white clover stock plants (*ca.* eight stolons per tray) were placed in an environment-controlled growth chamber (Contherm Scientific Company, Lower Hutt, New Zealand) for 3 hr before ethylene treatment (Fig. 2.2) with lightening from 8 X TRUE LITE® 40W fluorescence tubes and a constant temperature (25 °C). Ethylene was injected to provide a final concentration of 0.5 or 10 $\mu L\ L^{-1}$, and at appropriate time intervals, leaf material was excised as described in section 2.1.2, wrapped with aluminum foil, frozen in liquid nitrogen immediately, and stored at -80 °C until required. Ethylene was re-injected into the chamber after each harvest. As a control, trays of white clover were placed in the growth chamber and treated in

Figure 2.2 Ethylene treatment of whole plants using the environment-controlled cabinet.

exactly the same manner as the ethylene treatments including equal aeration or sampling periods, but no ethylene was injected.

2.1.3.3 Wounding treatment

Leaves, either detached from or attached to white clover stolons, were punched with forceps to make small holes (diameter = *ca.* 0.1 mm). Leaf tissue was incubated and harvested as discussed in section 2.1.3.1.

2.1.3.4 IAA treatment

Whole plants were treated with IAA using the method described by Peck and Kende (1995). Trays of white clover plants (eight stolons/tray) were treated with 100 µM IAA [pH 6.0, containing 0.05 % (v/v) ethanol, and 0.05 % (v/v) Tween 20] by spraying onto whole plants.
A control was achieved by spraying plants with the same solution but without added IAA.
For some experiments, plants were also treated with IAA solution, containing AVG (section 2.1.3.5). All treated plants were incubated and harvested as described in section 2.1.3.1.

2.1.3.5 AVG treatment

Leaves, either detached from or attached to white clover stolons, were treated with AVG (ReTain™, Nufarm Ltd., Auckland, New Zealand). Excised mature green leaves (typically 2 g) in a 2.2 L glass container (section 2.1.3.1) or attached leaves on stolons in trays (section 2.1.3.2) were sprayed with AVG solution [500 µg L^{-1} ReTain™, containing 0.1% (v/v) surfactant (Freeway-1, 20 g L^{-1})]. At various time intervals, plant tissue was harvested as described in section 2.1.3.1.

2.1.3.6 1-MCP treatment

Whole plants were treated with 1-MCP (EthylBlock™; obtained from Yates NZ Ltd., New Zealand) in the growth chamber used in section 2.1.3.2. Trays of white clover plants (*ca.* 8 stolons per tray) were placed in the growth chamber and the 1-MCP evaporated as a gas from EthylBlock™ with 1 % (w/v) KOH to achieve a final concentration of 20 or 3000 nL L^{-1} of 1-MCP. To do this, 1-MCP was evaporated in 0.48 m^3 (the internal volume of the growth

chamber) by dissolving 0.011 g (for 20 nL L^{-1} 1-MCP) or 1.65 g (for 3000 nL L^{-1}) of EthylBlock powder in 100 mL of 1% (w/v) KOH, according to manufacturer's instruction. Plants were treated for either 0.5 or 1 hr, then aerated, and then treated with an appropriate concentration of ethylene, according to the conditions described in section 2.1.3.2. Plant tissue was harvested before and after 1-MCP treatment, as well as at specific time intervals during ethylene treatment. All plant materials were harvested as described in section 2.1.3.1.

2.2 Physiological analysis of leaf ontogeny

2.2.1 Growth measurement during leaf ontogeny

Leaf fresh weight and leaf area at each node were determined using an AG204 balance (METTLER TOLEDO, Switzerland) and a leaf area meter (LI 3100, LI-COR, NE, USA), respectively.

2.2.2 Chlorophyll quantitation

Chlorophyll measurement was performed using the method as described by Moran and Porath (1980). Sample tissue was powdered in liquid nitrogen with a mortar and pestle, and 50 to 200 mg of the ground material was extracted with 1 ml of chilled N,N-dimethylformamide (DMF) for 16 hr at 4 °C in the dark. The extracts were vortexed briefly and centrifuged at 20 800 x g for 5 min at room temperature. A 200 µL aliquot of the supernatant was made upto 2 mL with DMF in a glass cuvette and the absorbance read at both 647 nm and 665 nm (as 664.5 nm) in an LKB NovaspecII® spectrophotometer (Pharmacia LKB, Biochrom Ltd., Cambridge, England).

Chlorophyll concentrations were calculated on the basis of the formula of Inskeep and Bloom (1985).

$$\text{Chlorophyll A} = 12.7A_{664.5} - 2.79A_{647} \text{ (mg/mL)}$$

$$\text{Chlorophyll B} = 20.7A_{647} - 4.62A_{664.5} \text{ (mg/mL)}$$

$$\text{Total chlorophyll} = 17.9A_{647} - 8.08A_{664.5} \text{ (mg/mL)}$$

2.2.3 Analysis of photosynthetic activity

2.2.3.1 Measurements of CO_2 exchange

Rate of CO_2 gas exchange was measured using the method described by Greer *et al.* (1995). A single trifoliate leaflet from the trifoliate leaf at each node was enclosed within a leaf chamber [Pakinson PLC(B)] and CO_2 gas exchange rate was measured as net photosynthesis rate using a CO_2 detection meter (IRGA and LCA2, ADC Co Ltd., Hoddeson, UK) in an open system.

2.2.3.2 Measurements of chlorophyll florescence

Fluorescence emission from leaf chlorophyll was measured using the method described by Laing *et al.* (1995). For dark-adapted tissue, single leaf-discs (diameter = 10 mm) were excised from the basal portion of leaves at each node (node 2 onwards) and were maintained in a moist environment in a completely dark chamber for 20 min. Chlorophyll fluorescence was measured at room temperature, via the insertion of a fibre-optic cable into the aperture of the chamber, with a pulse amplitude modulated fluorometer (PAM-101, Walz, Effeltrich, Germany). The initial fluorescence, Fo, was measured in the presence of the weak measuring beam while the maximum fluorescence, Fm, was measured during a 1 sec flash at 8 000 μmol $m^{-2}sec^{-1}$. For light-adapted tissue, initial fluorescence, Fo', was measured using a fibre-optic cable exposed to the basal portion of leaf blade attached to stolons in the presence of natural light, and maximum fluorescence, Fm', measured after a 1 sec flash at 8 000 μmol photon m^{-2} sec^{-1}. All data were monitored on a Toshiba T1000 SE computer connected via an A/D convertor (ADC-1, Remote Measurement Systems, Seattle, WA, USA).

Photochemical quenching (qp) and non-photochemical quenching (Npq) were determined based on the formula reported by Reuber *et al.* (1996).

$$pq = (Fm'-Ft) / (Fm'-Fo)$$

$$Npq = (Fm-Fm') / Fm'$$

$$Yield = (Fm'-Ft) / Fm'$$

Where Fo is the minimal fluorescence yield of the dark-adapted sample, and Fm' is the maximal fluorescence yield of the light-adapted sample. Ft is the fluorescence yield at a given time (t).

2.2.4. Ethylene analysis

2.2.4.1 Measurements, *in vitro,* of ethylene production (using excised tissues)

Sample tissue was excised as described in section 2.1.2.1 and enclosed in a 15 mL Vacutainer® tubes (Becton Dickensen Medical, Singapore). The tubes were then placed on layers of moist paper towels and contained within a plastic box (18 L capacity) covered by perforated cling film and incubated for the appropriate time intervals. To collect ethylene, the Vacutainer tubes were sealed with a rubber stopper for 1 hr and 1 mL gas samples were withdrawn from the head space. Ethylene concentration was measured, using a Photo Vac™ as described in section 2.2.4.3.

2.2.4.2 Measurements, *in vivo,* of ethylene production (using intact tissues)

Measurements of ethylene production from intact tissues was performed using the method described by Butcher (1997). Each leaf, except for the apex and leaf 1, was enclosed separately in 30 mL screw top plastic vials with a notch cut in the base to accept the petiole. The apex and leaf 1 were enclosed separately using 16.5 mL plastic containers. A rubber SUBA-SEAL was inserted into the bottom of each container and the space between the petiole and the notch sealed with petroleum jelly. After 1 hr, a 1 mL gas sample was withdrawn from the container though the SUBA-SEAL and ethylene concentration was measured using a Photo Vac™ as described in section 2.2.4.3.

2.2.4.3 Ethylene measurement

Using photo ionisation detector (PID)

Ethylene concentration in 1 mL gas samples was measured using a Photo Vac™ 10S50 (Photo Vac™, Markham, Canada) equipped with a PID. The carrier gas (air) was purified through a Purafil™ (Papworth Engineering, Cambridge, New Zealand) column and supplied at a pressure of 40 psi.

Ethylene at a concentration of 0.101 ppm [BOC gases (NZ) Ltd., Palmerston North, New Zealand] was used as the standard. The retention time of the ethylene peak was *ca.* 0.78-0.82 min and gas elution data was monitored using a Hewlett Packard 3390A integrator. The integrator provided output as ppm values.

Using flame ionisation detector (FID)

Ethylene concentration in 1 mL gas samples was measured using a gas chromatograph (Shimadzu Model GC-8A, Shimadzu Corp. Kyoto, Japan), equipped with FID. A glass column (2.5 m x 3 mm I. D.) prepacked with Porapak-Q (mesh size of 80/100; Alltech Associates Inc., Deerfield, Il., USA) was used for the ethylene analysis. The nitrogen carrier gas was set at a flow rate of 50 mL min^{-1} and the flame of the detector was generated by hydrogen and air at 50 kPa. For measurements, the oven and the injector/detector temperatures were set at 85 °C and 150 °C, respectively.

The retention time of the ethylene peak was *ca.* 1.5 min and data output was recorded as a peak using a Sekonic SS250 chart recorder (Kyoto, Japan). The peak height at the retention time was calculated for ethylene concentration in the sample as a proportion of the peak height (10 cm) of standard ethylene gas, which was at a concentration of 0.99 ± 0.01 ppm [BOC gases (NZ) Ltd., Palmerston North, New Zealand].

2.3 Biochemical analysis

Biochemical reagents used in this thesis, unless specified, were purchased from BDH (BDH Laboratory Supplies, Dorset, England) as analytical grade reagents.

2.3.1 ACC quantitation

2.3.1.1 ACC extraction

Tissue samples (typically 300 to 350 mg) were powdered in liquid nitrogen and extracted with 10 mL of 96 % (v/v) ethanol at 80 °C for 20 min. The extracts were centrifuged at 5 000 x g for 10 min at room temperature and the supernatant was collected. The remaining pellets were again resuspended in 10 mL of 96 % (v/v) ethanol and reextracted at 80 °C for 20 min. The

second extraction was then centrifuged as described before and the two supernatants pooled. The pooled supernatants were than evaporated at 42 °C using a rotary evaporator (Rotovapour; Buchi Laboratoriums, Technik Ag., Flawil/ Schweiz, Switzerland) and the dried extract dissolved in 2 mL water. A half volume (1 mL) of chloroform was added, mixture vortexed, and the two liquid phases separated by centrifugation at 26 000 x g for 10 min at room temperature. The top aqueous layer was collected for ACC assay.

2.3.1.2 Assay of ACC

ACC assay was performed using essentially the method described by Lizarda and Yang (1979), except that a concentration of 50 mM (instead of using 30 mM) of the mercury catalyst was used (Coleman and Hodges, 1991). A 800 µL aliquot of the extracted sample (section 2.3.1.1) was transferred to a 4.5 mL Vacutainer on ice, 100 µL of 500 mM $HgCl_2$ (Sigma Chemicals, St. Louis, USA) added and the tube sealed with a rubber stopper. A 100 µL aliquot of a chilled mixture of 2:1 (v/v) NaOCl:NaOH [3.15%(w/v) NaOCl (Janola®, Reckitt and Coleman NZ Ltd., Auckland, New Zealand) : saturated NaOH] was then injected through the stopper, the tube immediately vortexed for 5 sec, and incubated on ice for 2 min, followed by revortexing for 5 sec. A 1 mL gas sample from the head-space of the tube was then withdrawn for ethylene analysis using a Shimazu gas chromatography (section 2.2.4.3).

2.3.2 Analysis of ACO activity, *in vitro*

2.3.2.1 Protein extraction for assay of ACO activity, *in vitro*

Crude protein extraction without ammonium sulphate fractionation

Tissue samples were powdered in liquid nitrogen and 0.5 g aliquots of the powder were extracted on ice with 2 mL (four volumes) of extraction buffer (100 mM Tris-HCl, pH 7.5, containing 10 % (v/v) glycerol, 30 mM sodium ascorbate and 2 mM DTT). Extraction was performed on ice for 45 min with shaking (120 rpm). The tissue homogenates were then filtered through two sheets of Miracloth (Calbiochem Novabiochem Corporation, La Jolla, CA, USA) into 2 mL microfuge tubes on ice, and the crude protein extract centrifuged at 20 800 x g for 10 min at 4 °C. A 1 mL aliquot of the supernatant was then chromatographed through a

Sephadex G-25 column (section 2.3.2.2) and the eluate used for assay of ACO activity *in vitro* (section 2.3.2.3).

Protein extraction with 30%-90% (w/v) saturated ammonium sulphate fractionation

Tissue samples (typically 2 g) were powdered in liquid nitrogen and mixed with 12 mL (six volumes) of extraction buffer [100 mM Tris-HCl, pH 7.5, containing 10 % (v/v) glycerol, 30 mM sodium ascorbate and 2 mM DTT] and extracted on ice for 45 min with shaking at 120 rpm. The extracts were then filtered through two sheets of Miracloth and centrifuged at 20 800 x g for 10 min at 4 °C. The supernatant was then collected and its volume was adjusted to 30% (w/v) saturated (164 g L^{-1} at 0°C) ammonium sulphate. The mixture was incubated on ice for 30 min with shaking (120 rpm) and then centrifuged at 20 800 x g for 10 min at 4°C. The supernatant was collected and the volume was adjusted to 90% (v/v) saturated (402 g L^{-1} at 0 °C) ammonium sulphate. After 1hr incubation on ice with shaking (120 rpm), the mixture was centrifuged at 20 800 x g for 10 min at 4 °C, the pellet redissolved in 1 mL of resuspension buffer [50 mM Tris-HCl, pH 7.5, containing 2 mM DTT and 10% (v/v) glycerol] and then subjected to Sephadex G-25 column chromatography (section 2.3.2.2). The column eluate was collected and used for assay of ACO activity, *in vitro* (section 2.3.2.3).

2.3.2.2 Sephadex G-25 column chromatography

Sephadex G-25 (Pharmacia Biotech, Uppsala Sweden) was used to desalt ammonium sulphate and also to separate small molecular weight inhibitors from the protein extract. To prepare the column, a 10 mL syringe barrel (Becton Dickensen) were plugged with three layers of GF-A glass microfilter paper (Watman International Ltd., Maidstone, England). The outflow from the column was blocked using parafilm, and Sephadex G-25 resin pre-equilibrated with column buffer [50 mM Tris-HCl, pH 7.5, containing 10% (v/v) glycerol, and 2 mM DTT] was poured and allowed to settle. The column was then placed into a 50 mL centrifuge tube and after removing the parafilm seal, the assembly was centrifuged at 178 x g for 1 min at 4 °C. The column was then transferred into a new 50 mL tube and a 1 mL aliquot of protein extract was applied to the top of the resin and the assembly centrifuged at 178 x g for 1 min at 4 °C. The eluate was then collected from the bottom of the 50 mL centrifuge tube.

2.3.2.3 Assay of ACO activity, *in vitro*

Assay of ACO activity, *in vitro*, was performed in an assay buffer comprising a final concentration of 30 mM Tris-HCl, pH 7.5, containing 2 mM DTT, 30 mM sodium ascorbate, 20 μM $FeSO_4$ and 30 mM $NaHCO_3$. The substrate ACC was added to give a final concentration of 1mM to the assay buffer mixture just before use. To perform each assay, an 800 μL aliquot of assay buffer containing substrate was placed in a reaction tube (4.5 mL Vacutainer tube), pre-equilibrated at 30 °C with shaking at 180 rpm. To start the reaction, a 200 μL aliquot of protein extract was added to the assay buffer, the tube sealed with a rubber stopper, and incubated at 30 °C for 20 min with shaking at 180 rpm. A 1 mL gas sample was then withdrawn from the head space of the reaction tube and analysed using a Shimazu gas chromatography (section 2.2.4.3).

2.3.3 Protein quantitation

Alqiouts (1 μL) of protein extracts were added to 159 μL of distilled water (to give a final volume of 160 μL) in individual wells of a microtitre plate (Nunc™ Brand Product, Nalgen International, Denmark) in triplicate. Forty μL of Bio-Rad protein assay reagent (Bio-Rad Laboratories, Hercules, CA, USA) was then added, the mixture mixed well and the absorbance at 595 nm was determined using an Anthos HTII plate reader (Anthos Labtech Instruments, Salzburg, Austria). A triplicate series of protein standards to give final concentrations of 0, 2, 4, 6, 8 and 10 mg/ml of bovine serum albumin (BSA; Sigma Chemicals) in 160 μL was prepared and assayed as described above. The quantity of protein in each sample was calculated from a protein standard curve made from measurements of the BSA samples.

2.3.4 Protein analysis by SDS-PAGE

SDS-PAGE was performed using basically the method as described by Laemmli (1970).

2.3.4.1 SDS-PAGE using the Bio-Rad mini gel system

The resolving gel was prepared by mixing the ingredients outlined in a table 2.2. The mixture of resolving gel was poured into glass plates assembled using a Bio-Rad Mini-Protein apparatus (Bio-Rad Laboratories) until the mix reached a level *ca.* 1 cm below from the bottom of a well-

forming comb. Water was then layered onto the gel surface, and the gel was left to polymerise for *ca.* 30 min. During polymerisation of the resolving gel, a stacking gel was prepared as outlined in table 2.2.

Table 2.2 Composition of resolving and stacking gels used for SDS-PAGE.

Component	Resolving gel		Stacking gel
	16% (w/v)	10% (w/v)	
		mL	
1. Water	3.5	5	6.5
2. 4 X Resolving gel buffer	2.5	2.5	
2'. 4 X Stacking gel buffer			2.5
3. Acrylamide-bis stock	4	2.5	1
4. APS	0.1	0.1	0.1
5. TEMED	0.01	0.01	0.01

4 X Resolving gel buffer : 1.5 M Tris-HCl, pH 8.8, containing 0.4% (w/v) SDS
4 X Stacking gel buffer : 0.5 M Tris-HCl. pH 6.8, containing 0.4% (w/v) SDS
Acrylamide-bis stock: 40% (w/v) acrylamide-bis (Bio-Rad Laboratories) store at 4 °C
APS : 10% (w/v) ammonium persulphate (Univar, Auburn, NSW, Australia) – aliquots stored at –20 °C
TEMED : N,N,N',N-tetramethylethylenediamine (Reidel-de haen ag seeize, Hannover, Germany)

After polymerisation of the resolving gel, the water layer was discarded, a well-forming comb was inserted and the stacking gel solution added. The stacking gel mix was left for *ca.* 30 min

for gel polymerisation to occur. After polymerisation of the stacking gel, the gel assembly was transferred to the electrophoresis apparatus and gel running buffer [0.25 M Tris 0.2 M glycine buffer, pH 8.3, containing 1 % (w/v) SDS] was added to both inner and outer compartments of gel apparatus. The well-forming comb was removed and protein samples loaded. Protein samples were prepared by mixing the appropriate protein sample with one volume of 2 x gel loading buffer [60 mM Tris-HCl pH 6.8, 20% (v/v) glycerol, 5% (w/v) SDS, 10% (v/v) 2-mercaptoethanol, 0.01% (w/v) bromophenol blue]. The mixture was incubated in a boiling waterbath for 5 min and centrifuged at 20 800 x g for 1 min at room temperature. A 10 µl aliquot of pre-stained molecular weight markers [Low Range (20.5-103 kD) or High Range (43-205 kD), Bio-Rad Laboratories or Pharmacia Biotech] were loaded as required. Electrophoresis was conducted at 200 V for 60 min [10% (w/v) polyacrylamide gels] and 90 min [16% (w/v) polyacryamide gels], respectively.

2.3.4.2 SDS-PAGE using gradient polyacylamide gel

A polyacrylamide gradient from 8 % to 15 % (w/v) gel was prepared using large glass plates (16.5 X 22 cm). Two resolving gel solutions were prepared as outlined in table 2.3. To pour the gradient gel, the high concentration (15%) and low concentration (8%) solutions were poured into the first (closest to the outlet) and the second chamber of a Hoefer SG100 gradient maker (Hoefer Scientific Instruments, San Francisco, CA., USA), respectively. To initiate the gradient, the two solutions were mixed in the first chamber and the gel solution was pumped into the gel plates. After the resolving gel had reached a level equivalent to twice the well depth of the comb, water was layered on the top of the gel, and the gel was stood either at room temperature for *ca.* 2 hr or at 4 ^{o}C overnight to polymerise.

A stacking gel solution was prepared as outlined in table 2.3. After polymerisation of the resolving gel the water layer was discarded, the resolving gel was rinsed briefly with water which was then absorbed totally using a piece of 3MM Chr paper (Watman International Ltd.). After inserting a well-forming comb, the stacking gel solution was poured and left to set for *ca.* 1hr. After placing the gel plates within the gel running apparatus, the comb was removed and protein samples, prepared as described in section 2.3.4.1, loaded. Electrophoresis was

conducted at 65 mA through the stacking gel until samples reached the resolving gel, and after that, 25 mA was used to separate proteins through the resolving gel for *ca.* 6 hr.

Table 2.3 Composition of SDS-PAGE gradient gel (8-15%).

Ingredient	Resolving gel		Stacking gel
	15% (w/v)	8% (w/v)	
		mL	
1. Sucrose	3 (g)		
2. Water	7.5	11	8
3*. 4 X Resolving gel buffer	5	5	
3'*. 4 X Stacking gel buffer			10
4*. Acrylamide-bis stock	7.5	4	2
5. APS	0.2	0.2	0.2
6. TEMED	0.003	0.003	0.02

* Formula of buffers are given in table 2.2.

2.3.4.3 Visualisation of SDS-PAGE gels

Coomassie Brilliant Blue (CBB) staining

After completion of SDS-PAGE, gels were immersed in CBB stain [0.1% (w/v) Coomassie Brilliant Blue R-250, 40% (v/v) methanol, 10% (v/v) acetic acid] for 30 min with gentle agitation and then rinsed several times with 30% (v/v) ethanol until the gel cleared sufficiently to reveal stained protein bands.

When polyvinylidinefluoride (PVDF; Immobilin-P, Millipore Corporation, Bedford, MA, USA) membrane was stained with CBB, a modified stain [0.2% (w/v) Coomassie Brilliant Blue R-250, 20% (v/v) methanol, 0.5% (v/v) acetic acid] was used. Staining was for 10 sec and the membrane was rinsed with 30% (v/v) methanol. After photography or gel documentation, gels were air-dried using a GelAir Support frame system (Bio-Rad Laboratories).

Silver staining

To discern proteins under the limit of visualisation by CBB staining, silver staining was conducted as described by McManus and Osborne (1990a). After electrophoresis or after CBB staining, the polyacrylamide gel was fixed for 45 min in a solution of 50% (v/v) methanol and 10% (v/v) acetic acid, then for 30 min in a solution of 5% (v/v) methanol, 7.5% (v/v) acetic acid, and finally for 45 min in 10% (v/v) glutaraldehyde. The gel was washed thoroughly in distilled water, incubated in a solution of 0.005% (w/v) dithiothreitol (DTT) for 30 min, followed by incubation in a solution of 0.1% (w/v) silver nitrate for 45 min. Protein bands were visualised by immersion of the gel, with constant agitation, in a solution of 0.05% (v/v) of formaldehyde (37%) in 3% (w/v) sodium carbonate. After protein bands were discerned, further staining was stopped by immersion of the gel in a solution of 2.3 M citric acid.

Size estimation of proteins

Protein size was estimated based on the electrophoretic mobility of molecular weight maker proteins. The distance between the origin and the centre of each of the marker proteins was used to plot a calibration curve against the $\log_{10}$ of molecular weight.

2.4 Molecular analysis

The molecular techniques used in this thesis, unless specified, were adopted from methods described by Sambrook *et al.* (1989).

2.4.1 Extraction of nucleic acids

2.4.1.1 Genomic DNA extraction

Genomic DNA was prepared using the method described by Michael *et al.* (1994). Frozen tissue (typically 4 g) was powdered in liquid nitrogen and transferred to 10 mL (2.5 volumes) of extraction buffer [50 mM Tris-HCl, pH 8.0, containing 0.25 M NaCl, 20 mM EDTA, 0.5% (w/v) SDS, 0.35% (v/v) 2-mercaptoethanol (added just before use)]. The mixture was incubated at 60 °C for 5 min, 6 mL of phenol solution (prepared by dissolving 500 g of phenol in 143.5 mL of extraction buffer) added, and the mixture incubated for another 5 min. The mixture was then transferred to a sterile screw-cap centrifuge tube and 6 mL chloroform added, mixed well and then centrifuged at 15 000 x g for 10 min. The supernatant was carefully transferred into a new tube, and 0.35 volumes of 100% (v/v) ethanol was added slowly and then mixed. The mixture was incubated on ice for 15 to 20 min and then centrifuged at 10 000 x g for 10 min at 4 °C. The supernatant was decanted into a new centrifuge tube, an equal volume of isopropanol added and the mixture incubated at room temperature for 15 min. DNA was then pelleted by centrifugation at 10 000 x g for 20 min at 4 °C, the pellet washed with 80% (v/v) and then 100% (v/v) ethanol, and then air dried.

The DNA pellet was resuspended in 3 mL of TE buffer (10 mM Tris-HCl, pH 8, containing 0.1 mM EDTA) and treated with RNase A (1 µg/mL) for 1 hr at 37 °C. The RNase-treated DNA was precipitated with 0.33 volumes of 8 M ammonium acetate and 2.5 volumes of 100% (v/v) ethanol at room temperature for 15 min and then pelleted by centrifugation at 10 000 x g for 20 min. The DNA pellet was washed with 75% (v/v) ethanol, 100% (v/v) ethanol, air dried, and then resuspended in 100 µL of TE buffer (10 mM Tris-HCl, pH 8, containing 0.1 mM EDTA). The extracted DNA was aliquoted in several tubes and kept at -80 °C until required. The quantity of DNA was determined as described in section 2.4.1.3.

2.4.1.2. RNA extraction

Total RNA

Total RNA was isolated using the method described by Van Slogteren *et al.* (1983) with slight modifications. Frozen tissue (typically 1 g) was powdered in liquid nitrogen and transferred

into 5 mL (5 volumes) of lysis buffer [50 mM Tris-HCl, pH 8, containing 50 mM LiCl, 0.5 % (w/v) SDS, 10 mM EDTA, pH 8.0, 50 % (v/v) phenol (prepared by dissolving 500 g of phenol in 143.5 ml buffer (250 mM Tris-HCl, pH 8, containing 100 mM NaCl)]. The extract was homogenised by vortexing for 30 sec and then 2.5 mL (an equal volume to the phenol component) of chloroform : iso-amyl alcohol mixture (24 : 1) added and the mixture vortexed again for 30 sec. The extract was centrifuged at 4 000 x g for 20 min at room temperature, the upper aqueous phase transferred into a fresh 15 ml tube on ice, an equal volume of 4 M LiCl (chilled at -20 °C) added, the mixture vortexed briefly and then stored at 4 °C overnight. The RNA was pelleted by centrifugation at 4 000 x g for 30 min at 4 °C, washed with 70 % (v/v) ethanol, centrifuged briefly, and then air-dried. The RNA pellet was redissolved in 300 µl of 300 mM sodium acetate, pH 5.2, transferred to a microfuge tube, and 2.5 volumes of 100% (v/v) ethanol added. The RNA solution was incubated at -20 °C for 2 hr, and centrifuged at 10 000 x g for 10 min at 4 °C to precipitate RNA. The pellet was washed with 70% (v/v) ethanol twice and dried in a Speed-Vac (Savant, NY, USA) for *ca.* 1 min. The RNA pellet was redissolved in 50 µl of water (RNase-free), aliquoted into several microfuge tubes and stored at -80 °C until required. The quantity of RNA was measured as described in section 2.4.1.3, and the quality of RNA determined using a formaldehyde-denatured agarose gel (section 2.4.3.2).

Poly(A)$^+$mRNA extraction

Messenger RNA was extracted using the biotinylated poly (T) probe and steptavidin magnetic bead-based PolyAT tract System III (Promega, Madison, WI, USA).

Five hundred microgram of total RNA was made up to 500 µL with RNase-free water and incubated at 65 °C for 10 min to denature the secondary structure of RNA. A 3 µL aliquot of the biotinylated 17 mer oligo d(T) primer and 13 µL of 20 X SSC [0.3 M sodium citrate, pH 7.0, containing 3 M NaCl] were added and mixed by swirling with a pipette tip. The solution was allowed to cool down at room temperature for 10 min.

The Streptavidin Magne-Sphere (SA-PMPs) were resuspended by tapping the bottom of the tube, and, after the preservative solution was removed using the magnetic stand for capturing the beads, the SA-PMPs were washed 3 times with 300 µL aliquots of 0.5 X SSC. The SA-

PMPs were then resuspended in 100 µL of 0.5 X SSC and then the RNA preparation was added. The mixture was incubated at room temperature for 10 min to allow binding between the biotin and streptavidin beads. The beads were then washed 4 times, each with 300 µL of 0.1 X SSC, and after the last wash as much wash solution as possible was removed. The poly(A)$^+$RNA was dissociated from the SA-PMPs by resuspending the beads in 100 µL of RNase-free water and the mixture incubated at room temperature for 5 min. The poly(A)$^+$ RNA was then recovered as the supernatant and transferred to a sterile microfuge tube. The SA-PMPs were resuspended in another 150 µL of RNase-free water, incubated at room temperature for 5 min, and poly(A)$^+$RNA collected. Both poly(A)$^+$ RNA samples were pooled, frozen in liquid nitrogen and stored at –80 °C until required. The quantity of poly(A)$^+$mRNA was measured using spectrophotometry at 260 nm (section 2.4.1.3).

2.4.1.3 Nucleic acid quantitation

Nucleic acid concentrations were determined by measuring the absorbance of each solution at 260 nm (A_{260}) using a Shimazu spectrophotometer (Kyoto, Japan). Samples were diluted appropriately and transferred to 1 mL or 200 µL [for poly(A)$^+$RNA] quart cuvettes and measured against a water blank. The nucleic acid concentration was calculated using the formula in Sambrok *et al.*, (1989).

DNA ($\mu g\ mL^{-1}$) = A_{260} X NAF X DF

NAF (Nucleic Acid Factor): 40 for RNA; 50 for DNA

DF (Dilution Factor)

A_{260}/A_{280} ratio was used as a criteria for the purity of nucleic acids. Relatively pure nucleic acids have a ratio of 1.8 (Teare *et al.*, 1997).

2.4.2 Reverse transcriptase dependent polymerase chain reaction

2.4.2.1 Generation of cDNA using reverse transcriptase

Five μg of total RNA in 5 μL of sterile water and 0.5 μg of 17 mer oligo-d(T) primers in 0.5 μL of sterile water were mixed and incubated at 70 °C for 10 min. The mixture was then cooled on ice for 2 min and centrifuged briefly. A reaction buffer (5 X first strand buffer; GIBCO BRL, Life Technologies, USA) was diluted to a final volume of 13.5 μL comprising 50 mM Tris-HCl, pH 8.3, containing 75 mM KCl, 3 mM $MgCl_2$, 10 mM DTT, 0.5 mM dNTP mix, and 10 U of RNase inhibitor (RNasin; GIBCO BRL). The solution was mixed with the RNA preparation and incubated at 42 °C for 2 min, and then centrifuged briefly. Two hundred U (as a 1 μL aliquot) of reverse transcriptase (Superscript II; GIBCO BRL) was added, the reaction mixed using a pipette and then incubated at 42 °C for 50 min. The final volume was then adjusted to 100 μL with sterile water, the preparation was incubated at 70 °C for 15 min, centrifuged at 10 000 x g for 1 min, and stored at -20 °C.

In experiments when the first strand cDNA was used for 3'-RACE, the RT reaction was performed using 5 μL of a 10 μM stock of the oligo-d(T) adapter primer (ADAPdT) (Fig. 2.3), instead of the oligo-d(T) primer. The RNA templates were used with either 1 μg of poly(A)$^+$RNA or 5 μg of total RNA made up to 5 μl in water.

5'-GTGGATCCTACTGCAGCTAATTTTTTTTTTTTTTTT-3'

BamH I Pst I

Figure 2.3 Sequence of the ADAPdT primer.

2.4.2.2 Amplification of cDNAs by PCR

PCR amplification of ACS and ACO genes encoding protein coding regions

Nested PCR reactions were performed with two sets of degenerate oligonucleotide primers (Table 2.4). The mast mix1 was prepared as a 50 μL solution of a 100 μM dNTP mix, 300 nM of the first set of each of forward and reverse primers, and 100 ng of cDNA template. The mast mix2 was prepared as a 50 μl solution of 40 mM Tris-HCl, pH 7.5, containing 200 mM KCl, 3 mM $MgCl_2$, and 3.5 U of DNA polymerase (Expand™, Boehringer Mannheim, Mannheim, German). The PCR mast mix1 was prepared in a thin-walled PCR tube and the mast mix2 in a microfuge tube on ice, and the mast mix2 added to the mast mix1 just before the PCR. The PCR was performed in a Thermal cycler (PTC-200 Peltier Thermal Cycler; MJ Research, Inc., Watertown, MA, USA) for 2 hr 30 min, using 30 cycles of denaturation at 92°C for 1 min, annealing at 42 °C for 1 min, and DNA synthesis at 72 °C for 1 min and 40 sec. After the last cycle, DNA synthesis was extended for 10 min.

The second round PCR reactions were performed using the nested second set of primers (Table 2.4), and 2 μL of the first round PCR products was used as DNA templates (in place of 100 ng of cDNA template in mast mix1). All other components in the mast mix 1 and 2 were as described previously, and PCR performed under the same conditions as described previously.

PCR amplification of ACO genes encoding 3'-untranslated regions

Nested PCR amplification was performed with two sets of gene-specific primers and the adapter primer as the forward and reverse primers, respectively (Table 2.4). The gene-specific primers were designed from a region near to the 3'-end of the coding region, based on the nucleotide sequence generated from the PCR products amplified using degenerate primers.

The mast mix1 and mast mix 2 were prepared as described previously (section 2.4.2.2). This PCR was performed in the PTC-200 Peltier Thermal Cycler (MJ Research), using 30 cycles of denaturation at 92 °C for 1 min, annealing at 55 °C for 1 min, and DNA synthesis at 72 °C for 1 min and 40 sec.

Table 2.4 Primer sequences used for PCR in cloning ACS and ACO genes.

Primers for PCR-degenerate sequences	
ACC synthase	
First round Forward	
(ACSR1F)	GCCGCCTTCATGGGNYTNGCNGARGAAY (1)
Second round Forward	
(ACSR2F)	CTGGATCCGTWYCARGAYTAYCAYGG (1)
Reverse (ACSR6R)	CTCAAGCTTARNSYTRAARCTNGACAT (1)
ACC oxidase	
First round	
Forward (ACOF1)	GTGAATTCGAYGCNTGYSANAAYTGGGG (1)
Reverse (ACOR1)	TCGTCTAGATCRAANCKMGGYTCYTT (1)
Second round	
Forward (ACOF2)	GTGAATTCGCNTGYGARAAYTGGGGHTT (1)
Reverse (ACOR2)	TCGTCTAGAGYTCYTTNGCYTGRAAYTT (1)
Primers for 3'-RACE of ACO genes	
First round PCR-Forward	
TRACO1 (ACOF3)	GATGCTGGTGGCATCATCCTT (2)
TRACO2 (ACOF4)	GTTATCTATCCAGCAACAAC (3)
TRACO3 (ACOF5)	GGTGACCAGCTCGAGGTAAT (3)
Second round PCR-Forward	
TRACO1 (ACOF6)	GGAAGCTTGGTGGCATCATCCTCCTCTT (2)
TRACO2 (ACOF7)	CTATCCAGCAACAACATTGA (3)
Reverse (ADAP)	GTGGATCCTACTGCAGCTAA (3)
Primers for gene-specific probes of ACO genes	
Forward	
TRACO1 (ACOF8)	TGAAGCTATGATGAAAGCAA (2)
TRACO2 (ACOF9)	CTTGGTCAATTGCAACAGT (3)
TRACO3 (ACOF10)	CAAGCTAAGGAACCAAGAT (3)
Reverse (ADAP)	GTGGATCCTACTGCAGCTAA (3)

1), designed by Professor Shang Fa Yang (UC Davis); 2), designed by the author; 3) designed by Dr. D. Hunter (1998)

The second round PCR was performed with the nested second set of primers (Table 2.4) and 2 µl of the first round PCR products added as DNA templates to mast mix 1. All other components in the mast mix 1 and 2 were as described previously and PCR performed under the same conditions as described previously. The PCR products were stored at 4 °C, or –20 °C when longer-term storage was required.

2.4.3 Nucleic acid gel electrophoresis

2.4.3.1 Agarose gel for DNA

An 1.2% (w/v) agarose gel solution was prepared by dissolving the agarose (UltraPURE™ agarose; GIBCO BRL), with heating, in a final volume of 30 mL of 1 X TAE buffer (10 X TAE 0.4 M Tris, 0.2M glacial acetic acid, 10mM EDTA pH 8.0). An aliquot (0.5 µL) of ethidium bromide (stock concentration, 10 mg mL^{-1}) was added to the gel solution after the solution had cooled sufficiently and the gel poured into a horizontal mini gel apparatus (Bio-Rad DNA Mini Sub Cell) with a comb inserted for sample loading wells. The gel mixture was allowed to cool, and then immersed in running buffer (1 X TAE). DNA samples, including molecular size markers (1 Kb DNA ladder; GIBCO BRL), were prepared by the addition of SUDS [10 X SUDS: 0.1 M EDTA, pH 8.0, 50% (v/v) glycerol, 1% (w/v) SDS, 0.025% (w/v) bromophenol blue] at a 1:7 ratio for SUDS:DNA, and DNA samples were then separated at 5 to 10 V cm^{-1} for *ca.* 45 min to 60 min.

2.4.3.2 Agarose-formaldehyde gel for RNA

A 1.2% (w/v) agarose gel was prepared, by dissolving the agarose, with heating, in a final volume of 30 mL of 1 X MSE buffer [10 X MSE: 200 mM Na(3-[N-Morpholino] propanesulphonic acid (MOPS), pH 7.0, containing 50 mM NaOAc, 10 mM EDTA]. After the gel had cooled sufficiently, formaldehyde was added to give a final concentration of 3 % (v/v). Three to 4 µg aliquots of total RNA was made to 15 µL with gel loading buffer [1mL RNA gel loading buffer comprises 212.5 µL of 37% (v/v) formaldehyde, 125 µL MSE (10X), 5 µL ethidium bromide stock solution (section 2.4.3.1) and 625 µL formamide/BB/XC stock solution (Formamide/BB/XC stock solution: 0.01% (w/v) bromophenol blue, 0.01% (w/v) xylene cyanol in formamide)], incubated at 65 °C for at least 15 min, and then cooled on ice

immediately. RNA samples, including molecular size markers (0.24-9.5 Kb RNA ladder; GIBCO BRL) were separated with gel running buffer (1 X MSE, containing 0.22 M formaldehyde) at 80 V for 1.5 hr in a fume hood.

2.4.3.3 Visualisation of nucleic acids on gels

Nucleic acids on gels were visualised using a UV Transilluminator (340 nm; UVP Inc., San Gabriel, CA, USA) and photographed with an Alpha Imager™ 2000 Documentation and Analysis System (Alpha Innnotech Corp., San Leandro, CA, USA).

When DNA fragments were required for further cloning, visualisation of DNA fragments was undertaken using long-wave length UV, instead of the short wave length.

2.4.3.4 Size estimation of nucleic acids

Th size of nucleic acid fragments were estimated using their mobility relative to the mobility of nucleic acids of known molecular size (1 Kb ladder; GIBCO BRL), separated on the same gel.

2.4.4 Cloning of PCR products in *E. coli*

The PCR products were selected by their expected size and recovered from the agarose gel using a Wizard™ Miniprep kit (Promega, Madison, WI, USA), and then the DNA fragments were cloned into the pCR®2.1 vector (Invitrogen, Leek, The Netherlands).

This cloning technique relies on a deoxyadenosine attachment at the 3'-ends of the PCR product by the terminal transferase activity of *Taq* DNA polymerase, which is a complementary to an overhanging 3'-T in the vector, as shown in figure 2.4.

2.4.4.1 DNA purification from the agarose gel

Use Wizard™ mini-column

The DNA recovery process used was described in Technical bulletin #117 (Promega). The DNA fragment of interest was excised from the agarose using a sterile scalpel and weighed in a microfuge tube. Three volumes (by weight) of 6 M NaI were added and the mixture incubated at 55 °C until the gel pieces were completely melted.

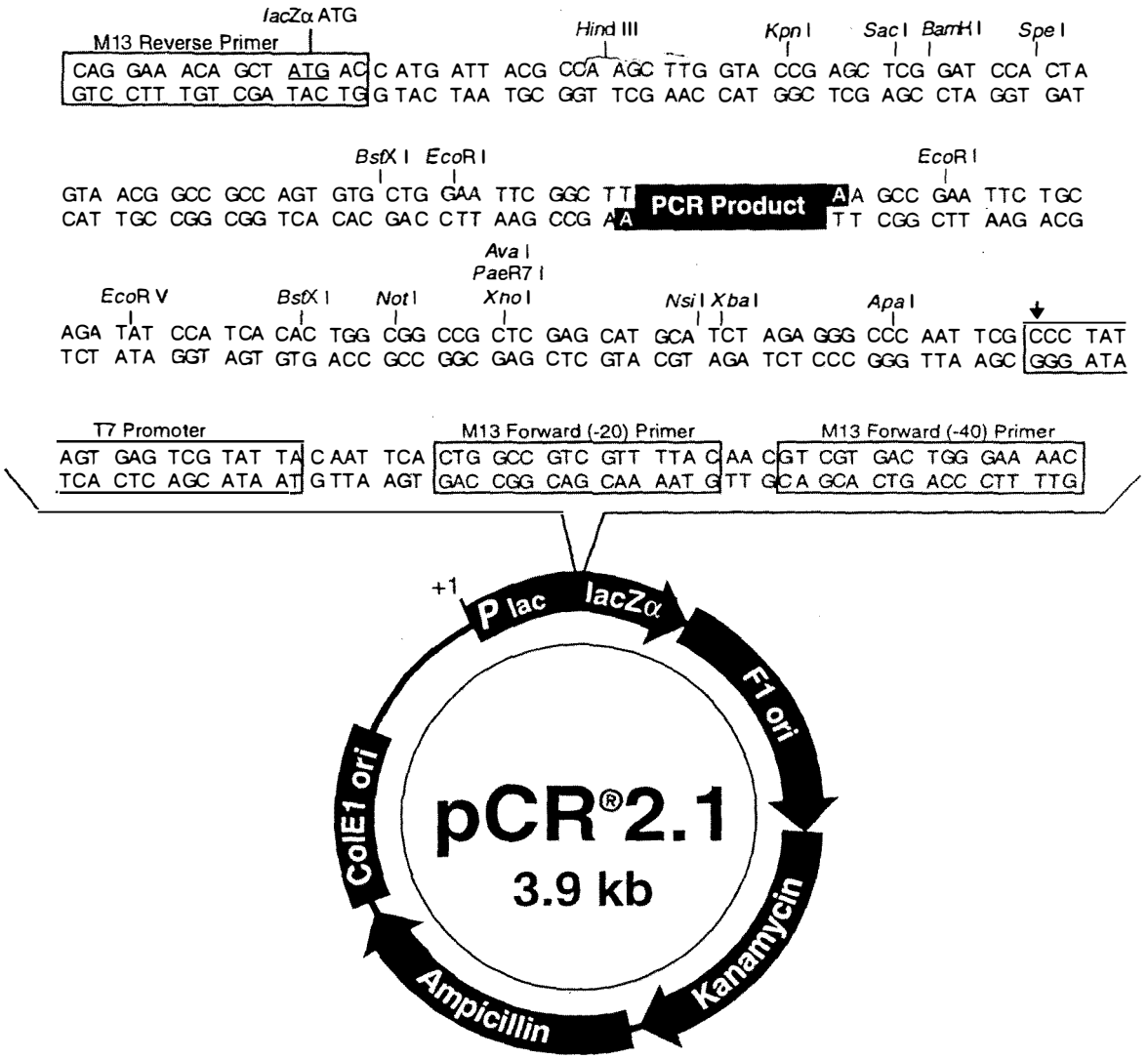

Figure 2.4 Map of the pCR 2.1 vector.

One mL of DNA purification resin (Promega) was added to the melted gel and the mixture incubated at room temperature for 2 min. The mixture was then transferred into a 3 mL syringe barrel attached to a Wizard mini column and the solution passed through the mini-column. The mini column was washed with 2 mL of column wash solution [8.3 mM Tris-HCl, pH 7.5, 80 mM KOAc, 40 μM EDTA, pH 8.0, 55% (v/v) ethanol] and dried by applying air to the column. Any residual wash solution left in the mini-column was removed by centrifugation at 3 800 x g for 1 min at room temperature.

A 50 μL aliquot of water (pre-heated at 70 °C) was then applied to the mini column, incubated at room temperature for 1 min, and then eluted by centrifugation at 10 000 x g for 1 min at room temperature and collected as the DNA solution.

The freeze – squeeze method

The gel slice containing the DNA fragment of interest was frozen in liquid nitrogen, centrifuged at 20 800 x g for 10 min at room temperature and the supernatant collected as the DNA sample. This method is a simple one for recovery of DNA from the gel but the DNA recovery procedure was of sufficient purify to use as the DNA template for ^{32}P labeling.

A slight modification to the method was made which resulted in higher yields. An equal volume of sterile water was added to the excised gel slice before melting at 50 °C for 15 min prior to freezing of the gel in liquid N_2.

2.4.4.2 Ligation of PCR products with pCR 2.1 vector

DNA ligation was performed in a final volume of 20 μL, which comprised 50 ng linearised pCR®2.1 vector (Invitrogen), 150 ng PCR products, 10 U T4 DNA ligase in 1 X ligation buffer (Invitrogen). The mixture was incubated at 14 °C overnight using a PTC-200 Peltier Thermal Cycler (MJ Research).

2.4.4.3 Transformation of *E. coli* with pCR®2.1 vector

Preparation of LB media and LB-Amp^{100} plate

LB growth medium, comprising 1% (w/v) bacto-tryptone (DIFCO Labratories, Detroit, MI, USA), 0.5% (w/v) bacto-yeast extract (DIFCO Labratories), 1% (w/v) NaCl at pH 7, was aliquoted (10 mL) into mini bottles and sterilised at 121 °C (103 kpa) for 15 min. The LB medium was kept at room temperature until required. Ten µL of an ampicilin stock solution (100 mg mL^{-1}) was added to each bottle just before use to provide a LB-Amp^{100} broth.

For LB-Amp^{100} plates, 1.5% (w/v) argar (GIBCO BRL) was added to LB growth medium and the mixture sterilised as before. When the agar medium had cooled down to *ca.* 40 °C, ampicilin was added to give a final concentration of 100 µg mL^{-1} and the medium poured into sterile plates in a lamina flow bench. After solidification, plates were sealed using parafilm and kept at 4 °C until required.

Preparation of competent cells

The *E. coli* cells used for transformation with the pCR®2.1 vector were either TA-Cloning One Shot™ competent cells (Invitrogen) or competent cells prepared from *E. coli* strain DH5α (GIBCO BRL) using the $CaCl_2$ method described below. Competent cells of *E. coli* strain BL21 and TB1 cells, prepared by the $CaCl_2$ method, were used for transformation by the pPROEX vector.

From a single *E. coli* colony, bacterial cells were cultured in 10 mL of LB broth at 37 °C overnight with shaking (225 rpm), and then 0.4 mL of the culture was transferred into 40 mL of fresh LB broth. This broth was incubated at 35 °C until cell growth reached an optical density at 600 nm of 0.4, and the broth then centrifuged at 2 000 x g for 5 min at 4 °C. The bacterial pellet was resuspended in 10 mL of cold 60 mM $CaCl_2$, followed by the addition of a further 10 mL of 60 mM $CaCl_2$, and the cells incubated on ice for 30 min. The cell suspension was centrifuged at 2 000 x g for 5 min at 4 °C, and the cell pellets were then resuspended in 4 mL $CaCl_2$, containing 15% (v/v) glycerol. Aliquots (300 µL) of the cell suspension were transferred to microfuge tubes and stored at -80 °C until required.

***Heat shock transformation of* E. coli**

The ligated pCR®2.1 vector was transformed into *E coli* strain DH5α using the heat-shock method provided with the pCR®2.1 kit (version 2.0; Invitrogen).

Two µL of 0.5 M β-mercaptoethanol was added to a tube of competent cells (300 µL) that had been thawed on ice, the cells were mixed and then 5 µL of the ligation reaction added, and the mixture incubated on ice for 30 min. The cells were then heat-shocked by incubation at 42 °C for 30 sec, immediately cooled on ice for 2 min, and 250 µL of SOC medium [Invitrogen; 2% (w/v) tryptone, 0.5% (w/v) yeast extract, 10 mM NaCl, 10 mM $MgSO_4$, 20 mM glucose] added and the mixture incubated at 37 °C for 1 hr, with shaking at 225 rpm. Cells were pelleted by centrifugation at 8 000 x g for 30 sec at room temperature and resuspended with 200 µL of fresh SOC medium. Aliquots (10 µL and 100 µL) of the cell suspension were then spread onto separate LB-Amp^{100} plates and the plates were incubated at 37 °C overnight.

Single putatively positive colonies were picked using sterile tooth picks and replicated onto a new LB-Amp^{100} plate, which was incubated at 37 °C overnight and kept in 4 °C until required. Colonies of interest on LB-Amp^{100} plates were routinely replicated onto new plates every three to four months.

A glycerol stock of each transformed bacterial colony was made for longer-term storage. To do this, a colony was inoculated into a 10 mL LB-Amp^{100} broth and grown overnight. Bacterial cells were then pelleted by centrifugation at 3 000 x g for 10 min, resuspended in 200 µL of LB broth and 100 µL of the cell suspension added (as 2 x 50 µL aliquots) to a mixture of 200 µL sterile glycerol and 750 µL LB broth. The cells were mixed well, frozen in liquid nitrogen, and stored at -80 °C until required.

2.4.5 Characterisation and sequencing of cloned DNA in *E. coli*

2.4.5.1 Plasmid purification

Plasmid DNA was isolated from transformed *E. coli* using the alkaline lysis method (Sambrook *et al.*, 1989). Individual colonies were replicated in 10 mL LB-Amp^{100} broth and the broth incubated at 37 °C overnight with shaking at 225 rpm. Cells were then pelleted by

centrifugation at 3 000 x g for 10 min at room temperature, air-dried and resuspended in 200 µL of alkaline lysis solution A (25 mM Tris-HCl, pH 8.0, 50 mM glucose, 10 mM EDTA, pH 8.0). After transfer of the cell suspension into a microfuge tube, 400 µL of alkaline lysis solution B [0.2 M NaOH, 1% (w/v) SDS] was added, the contents gently mixed and then incubated on ice for 10 min. Three hundred µL of alkaline lysis solution C (3 M potassium acetate, 2 M glacial acetic acid) was then added, the mixture shaken vigorously and then incubated on ice for 5 min. All cell debris including bacterial proteins and genomic DNA was pelleted by centrifugation at 20 800 x g for 5 min at room temperature, the supernatant transferred into a new microfuge tube and reextracted twice with 500 µL of chloroform. The upper aqueous phase from the two chloroform extracts were transferred into an equal volume of isopropanol to precipitate plasmid DNA. The mixture was then centrifuged at 20 800 x g for 5 min at room temperature and the pellet rinsed with 80% (v/v) ethanol. The pellet was briefly dried in a Speed Vac and resuspended in 40 µL of sterile water or TE buffer (10 mM Tris-HCl, pH 8.0, 0.1 mM EDTA), and then store in -20 °C until used.

2.4.5.2 Digestion of plasmid DNA with restriction enzyme

Aliquots (1 to 4 µl) of plasmid DNA were routinely separated on a 1.2% (w/v) agarose gel (Section 2.4.3.1) to check the yield of plasmid DNA.

One microgram of plasmid DNA was then digested in a reaction mix, containing 5 U of EcoR1 (GIBCO BRL) and 10 µg RNase A (stock solution: 10 mg mL^{-1}; Sigma) in the appropriate 1X restriction enzyme (RE) buffer (GIBCO BRL). The digestion mix was incubated at 37 °C for 1.5 hr and 0.1 volumes of 10 X SUDS added to terminate the digestion. The DNA fragments were then separated and visualised using a 1.2% (w/v) agarose gel (section 2.4.3.1).

2.4.5.3 Sequencing of plasmid DNA in transformed *E. coli*

Plasmid DNA was diluted to a final volume of 100 µL TE buffer (10 mM Tris-HCl, pH 8.0, 0.1 mM EDTA, pH 8.0), containing 50 µg RNase and incubated at 37 °C for 15 min. The plasmid DNA was then purified using a Wizard mini column (section 2.4.4.1) and the concentration of the purified plasmid DNA adjusted to 200 ng μL^{-1} in a final volume of 12 µl. The plasmid

DNA was sent for sequencing to the Massey University DNA Sequencing Centre in the Institute of Molecular BioSciences in Massey University (Palmerston North, New Zealand).
For PCR®2.1 plasmids, the plasmid DNA was sequenced with M13(-20) forward primer / M13 reverse primer using a ABI PRISM™ Dye terminator Cycler Sequencing Ready Reaction Kit with AmpiTaq DNA polymerase (Perkin Elmer, Foster City, CA, USA), and the fragments analysed with an automatic AB PRISM™ 377 DNA sequencer (Applied Biosystems, Foster City, CA, USA).

2.4.6 DNA sequence analysis

2.4.6.1 Sequence alignment

Alignment analysis of DNA sequences was performed using the Align Plus sequence Alignment Program (version 2, Science and Educational Software, State Line, PA, USA). GenBank database searching was performed using a Basic Local Alignment Sequence Tool (NIH Homepage-http://www.ncbi.nlm.nih.gov/blast/blast.cgi?form=1)

2.4.6.2 Sequence phylogenetic analysis

A phylogenetic tree was built (with the aid of Mr. Richard Winkworth, Institute of Molecular BioSciences, Massey University, Palmerston North, New Zealand), using a heuristic search with default parameters of a pre-release β-version of the phylogenetic analysis using parsimony (Paup version 4.0 od64, Sinaur Assoc., Inc. Publishers, Sunderland Massachusetts 1998 Smithonian Institute).

2.4.7 Southern and northern analysis of nucleic acids

2.4.7.1 Southern analysis

Genomic DNA analysis was performed using the downward alkaline transfer method as described by Chomczynski (1992)

Digestion of genomic DNA

Genomic DNA was digested with three REs, EcoRI, Hind III and XbaI (GIBCO BRL). Thirty microgram of DNA was digested at 37 °C overnight in a reaction volume of 300 µL of the

appropriate 1X RE reaction buffer, with 80 U of each RE. After this, an additional 30 units of each restriction enzyme was added and the digest incubated at 37 °C for a further 8 hr. Digested DNA was precipitated with the addition of 150 µL of 8 M ammonium acetate (pH 7.7) and 1 mL of cold 100% (v/v) ethanol, and then incubated at -20 °C overnight. The DNA was collected by centrifugation at 20 800 x g for 20 min, the pellet washed twice with 75% (v/v) ethanol, and dried in a Speed Vac. The DNA pellet was then resuspended in 30 µL of 2 X SUDS gel loading buffer (10 X SUDS see section 2.4.3.1) and incubated at 37 °C for at least 1 hr to dissolve the DNA completely.

Southern gel and blotting

Ten microgram of digested DNA was separated on a 0.8% (w/v) agarose gel (Bio-Rad DNA Sub Cell™) with 1 X TAE running buffer at 20 V overnight (section 2.4.3.1). After electrophoresis for *ca.* 18 hr (the bromophenol blue dye had reached a point 3-3.5 cm away from the gel end), the gel was stained in ethidium bromide solution (0.1 µg mL^{-1}) for 20 min and destained for 20 min in water. The gel was then photographed on a UV-transilluminator attached to an image analyser (section 2.4.3.3).

The gel was then depurinated in 0.25 M HCl for 30 min and then denatured in 0.4 M NaOH, containing 3 M NaCl for 1 hr. The positively charged membrane (Hybond-N^+, Amersham, UK) was wetted in transfer solution (8 mM NaOH, pH 11.4, containing 3 M NaCl) for 10 min. The denatured DNA gel was then immersed in the transfer solution for 15 min and the transfer stack set up as shown in figure 2.5.

DNA on the membrane was post-fixed by UV-crosslinker (UVStratalinker®2400; STRATAGENE, La Jolla, CA, USA) and then neutralised in 50 mM sodium phosphate buffer (pH 7.2) for 10 min. The membrane was sealed in a sterile plastic bag with *ca.* 5 mL of neutralisation buffer and stored at 4 °C until required.

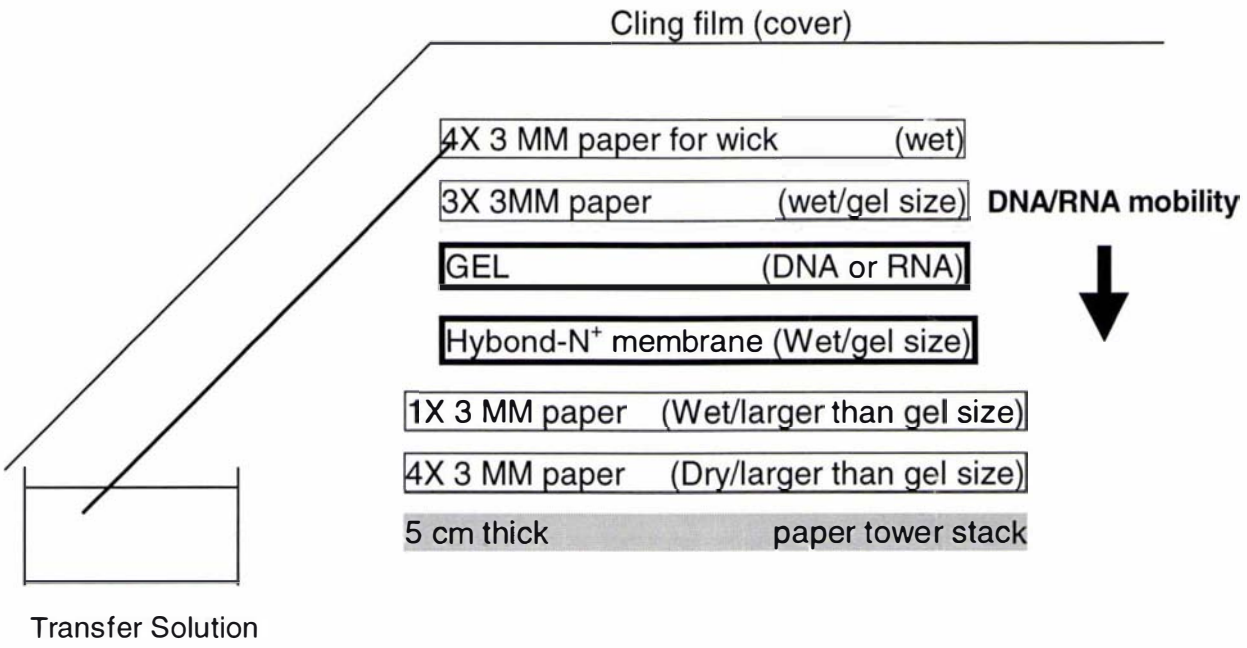

Figure 2.5 Blotting sandwich for the capillary downward method (Chomczynski, 1992).

2.4.7.2 Northern analysis

Agarose- formaldehyde gel

A 1.2% (w/v) agarose gel was prepared, by dissolving the agarose, with heating, in a final volume of 112.5 mL of 1 X MSE buffer (section 2.4.3.2). After the gel had cooled sufficiently, formaldehyde was added to give a final concentration of 3% (v/v).

One and 2 µg of poly(A)$^+$mRNA, or 40 µg of total RNA in 15 µL of RNA gel loading buffer were prepared as described in section 2.4.3.2. RNA samples, including molecular weight markers (0.24-9.5 Kb RNA ladder; GIBCO BRL) were separated with gel running buffer (section 2.4.3.2) at 80 V 3.5 hr.

Northern blotting

After the completion of gel electrophoresis, the gel was photographed using an UV illuminator and image analyser (section 2.4.3.3) and the gel notched to correspond to each molecular marker. The separated poly(A)$^+$mRNA was transferred onto a positively charged nylon membrane (Hybond-N$^+$), using an alkaline transfer solution (8 mM NaOH, 3 M NaCl), using the capillary downward method (Fig. 2.5) for 4 hr. Separated total RNA was transferred to the membrane using 10 X SSPE (20 X SSPE: 0.2 M NaH_2PO_4, pH 7.7, 3.6 M NaCl, 20 mM EDTA, pH 8.0) as transfer buffer with the capillary downward method.

After transfer for 18 hr, the membrane was post-fixed using UV cross-linking (Stratalinker® 2400) and then neutralised in 0.1 M sodium phosphate buffer, pH 7.2, for 10 min. The membrane was sealed in a sterile plastic bag with *ca.* 5 mL neutralisation buffer and stored at 4 ^oC until required.

2.4.7.3 Labeling DNA probes using radioactive dCTP or dATP

Radioactively labeled DNA probes were prepared by random extension using DNA templates prepared from DNA inserts or PCR products amplified with gene specific primers (Table 2.4).

Labeling with [α-P^{32}]-dCTP

DNA labeling was performed with [α-P^{32}]-dCTP (Amersham) using the Ready-To-Go™ DNA labeling kit (Pharmacia Biotech). An aliquot of DNA (25-50 ng) was diluted to 45 µL with sterile water and incubated in a boiling water bath for 3 min, and then cooled on ice for 1 min. After brief centrifugation, the denatured DNA was added to the Ready-to-go beads, the contents mixed thoroughly, and 5 µL of [α-P^{32}]-dCTP (3000 Ci/mmol) added and the mixture incubated at 37 ^oC for 15 min.

After the completion of the labeling reaction, the whole mixture was applied to a ProbeQuant™ Sephadex G-50 Micro Column (Pharmacia Biotech) and centrifuged at 735 x g for 2 min. The solution containing labeled DNA eluted from the column and was incubated in a boiling water bath for 3 min, and then cooled on ice for 1 min. After brief centrifugation, the solution was added to the hybridisation solution (section 2.4.7.4).

Labeling with [α-P^{32}]-dATP

Labeling of 3'-UTR probes was performed with [α-P^{32}]-dATP (Amersham) using the Megaprime™ DNA Labeling kit (Amersham). An aliquot of DNA (25 ng) in 5 µL of water was added to 5 µL of random primer. The mixture was then incubated in a boiling water bath for 5 min and cooled to room temperature. After brief centrifugation, 5 µL of 10 X reaction buffer, 4 µL of each of dTTP, dCTP, and dGTP, 2 µL of DNA polymerase were added, the final volume was adjusted to 45 µL with sterile water, and then 5 µL of [α-P^{32}]-dATP added and the mixture incubated at 37 °C for 10 min. After completion of the labeling reaction, the labeled DNA was purified using ProbeQuant™ Sephadex G-50 Micro Columns as described above and then added to the hybridisation solution (section 2.4.7.4).

2.4.7.4 Hybridization, washing and visualisation

Nylon membranes after DNA and RNA transfer were removed from storage, equilibrated at 65 °C in a final volume of 30 mL of Church-Gilbert (CG) hybridisation buffer [0.25 M sodium phosphate buffer, pH 7.2, containing 7% (w/v) SDS and 1% (w/v) BSA Fraction V, 1 mM EDTA, pH 8; Church and Gilbert, 1984]. Radioactively labeled DNA probes (section 2.4.8.3) were then added and the hybridisation performed overnight at 65 °C. The hybridised membrane was then washed with 20 mM sodium phosphate, pH 7.2, containing 5% (w/v) SDS, 0.5% BSA fraction V, 1 mM EDTA, pH 8.0, at 65 °C for 10 min, then 2 X SSPE, pH 6.5 (section 2.4.7.2), containing 0.1% (w/v) SDS and then 1 X SSPE, pH 6.5, containing 0.1% (w/v) SDS at 65 °C for 20 min each. The membrane was finally washed with 0.1 X SSPE, pH 6.5, containing 0.1% (w/v) SDS at 65 °C for 1 hr.

The hybridised membrane was exposed at –80 °C to X-ray film (XAR-5; East Kodak Company, Rochester, NY, USA) in an X-OMATIC cassette (East Kodak Company), equipped with a single X-OMATIC intensifying film. The film was developed using an AUTOMATIC X-RAY FILM PROCESSOR (100Plus™, All-Pro Imaging, Hicksville, NY, USA) using Kodak developer (HC110) and Rapid Fixer Solution A (East Kodak Company).

2.4.7.5 Stripping nylon membranes

Nylon membranes, once probed and developed, were stripped using the method described by Memelink *et al.* (1994). Boiling stripping solution [0.1 X SSPE (section 2.4.7.2) containing 0.1% (w/v) SDS] was added to the membrane and the solution was shaken until the stripping solution cooled down to room temperature. After discarding the solution, the process was repeated at least three times or until the radioactive counts from the membrane reached background level. The membrane was finally rinsed with 0.1 X SSPE to remove SDS, sealed in a plastic bag, and kept at 4 °C until required

2.4.8 Heterologous protein expression in *E. coli*

2.4.8.1 Protein expression using pPROEX-1 vector

The pPROEX vector system (Fig. 3.3.8; GIBCO BRL) was used in *E. coli* strains DH5α, TB1 and BL21. In-frame PCR products were amplified using the appropriate plasmid DNA as template with ACOFE and ACORH as primers (Fig. 2.6). PCR was performed as described in section 2.4.2.2 at an annealing temperature of 50 °C. The amplification product was checked by sizing on a 1.2% (w/v) agarose gel (Section 2.4.3.1), and then the PCR product was digested with Hind III and EcoRI.

Digestion was performed in a final volume of 30 µL, comprising 20 µL of PCR product, 3 µL of the appropriate 10 X RE buffer and 30 U of Hind III (GIBCO BRL). The mixture was incubated at 37 °C for 2 hr, and then 2 µL of 10X RE buffer, 16 µL sterile water and 20 U of Hind III were added and the mixture incubated at 37 °C for another 2 hr. Digested DNA was precipitated with 75% (v/v) ethanol and 300 mM sodium acetate (pH 5.2) and redissolved in 20 µL sterile water. The Hind III digest was then digested with EcoRI and precipitated using the same procedure as described above. The DNA was then redissolved in 10 µL of sterile water.

The pPROEX vector was also prepared using Hind III and EcoRI digestion. Plasmid DNA was obtained as a final volume of 40 µL (section 2.4.5.1). Each of 20 µL aliquots of plasmid DNA was digested either with Hind III or EcoRI, using a 40 µL digestion mix comprising 40 U RE, 4 µL of the appropriate 10X RE buffer and 20 µg RNase A.

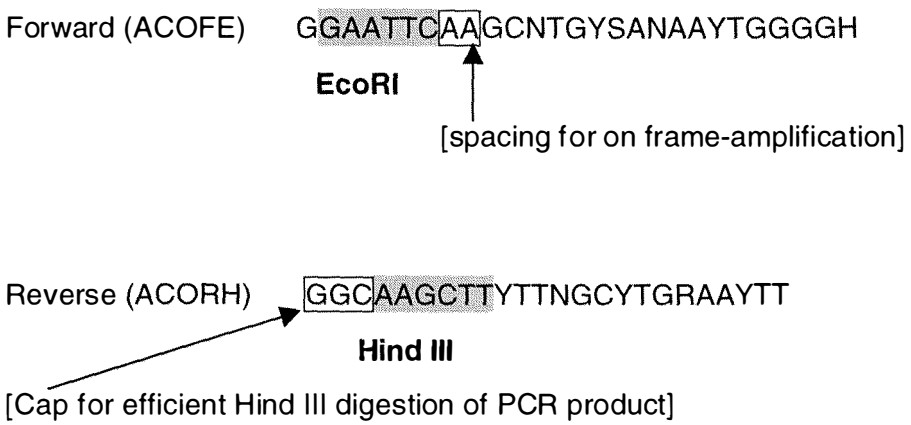

Figure 2.6 Primers for in-frame amplification of ACO gene from white clover (designed by Dr. Michael McManus, IMBS, Massey University, New Zealand).

The mixtures were incubated at 37 °C for 3 hr and a 2 μL aliquot of each digest mix separated on a 1.2% (w/v) agarose gel together with 1 μL of uncut plasmid DNA. When a linearised DNA band was discerned from the digest (to indicate complete digestion), plasmid DNA was precipitated with 75% (v/v) ethanol as described above, resuspended in 20 μL sterile water and digested again with the other enzyme (EcoRI or Hind III as appropriate) using the same conditions as described for the first digestion, but without RNase A. After incubation at 37 °C for 3 hr, the digested DNA was gel purified using the Wizard column (section 2.4.4.1) for subsequent ligation.

For ligation, a mixture of 150 ng of digested PCR product, 2 μL of 10 X ligation buffer [500 mM Tris-HCl, pH 7.6, 100 mM $MgCl_2$, 10 mM ATP, 10 mM DTT, 50% (w/v) polyethylene glycol-800], 10 U of T4 ligase and 50 ng of the digested pPROEX vector and 5 μL of sterile water was incubated at 14 °C. After incubating for *ca.* 18 hr, the ligation mixture was used for transformation of *E. coli* strains DH5α, TB1 and BL21 by the heat-shock method (section 2.4.4.3).

Bacterial cells, transformed with the pPROEX vector, were selected on LB-Amp^{100} plates and positive colonies were inoculated into 10 mL LB-Amp^{100} broth and incubated at 37 °C overnight with shaking at 225 rpm. Plasmid DNA was prepared by alkaline lysis (section 2.4.5.1) and the presence of the correct sized insert after digestion of plasmid DNA with Hind III and EcoRI confirmed by electrophoresis on a 1.2% (w/v) agarose gel (section 2.4.3.1).

2.4.8.2 Preliminary expression of introduced genes in *E. coli*

Transformed cells were cultured at 37 °C overnight with shaking at 225 rpm in 10 mL LB-Amp^{100} broth, a 500 µL aliquot of this overnight-culture was then transferred into a fresh 10 mL LB-Amp^{100} broth and the broth incubated using the same growth conditions for 3 hr. To induce the expression of foreign proteins, isopropyl-β-D-thiogalactopyranoside (IPTG) was added to the cell culture to a final concentration of 0.6 mM, and the cell cultures were grown at 37 °C for another 3 hr, with shaking at 225 rpm. At specific time intervals, 1 mL aliquots were transferred into microfuge tubes and centrifuged at 20 800 x g for 5 min. Proteins were prepared by re-suspending the pellets with 200 µL of 2X SDS-reducing gel loading buffer (section 2.3.4.1). To act as control, a 1 mL aliquot of the overnight culture was also harvested and prepared for protein analysis. A 15 µL aliquot of each sample was separated using 16 % (v/v) SDS-PAGE (section 2.3.4.1). The protein bands were discerned with CBB staining (section 2.3.4.3). In other experiments, IPTG-induced cells were cultured for the purification of expressed proteins using nickel-nitrilotriacetic acid (Ni-NTA) column chromatography (section 2.4.8.3).

2.4.8.3 Purification and characterisation of expressed proteins using Ni-affinity column

Expressed protein from the pPROEX vector (section 2.4.8.2) was purified using the six His repeats attached at the N-terminal of the expressed protein, which have an affinity for the Ni-NTA resin (GIBCO BRL).

IPTG-treated cell cultures were pelleted by centrifugation at 3 000 x g for 10 min, resuspended in four volumes of cell lysis buffer [50 mM Tris-HCl, pH 8.0, containing 2.5% (w/v) SDS, 1% (v/v) 2-mercaptoethanol], transferred to a microfuge tube, and then sonicated on ice six times,

for 10 sec each, at 14 decibel (d.c.b) with a MSE Soniprep 150 Ultrasonic Disintegrator (MSE Sceintific Instruments, Manor Royal, Sussex, England).

A 0.5 mL column of Ni-NTA was prepared in a 5 mL syringe barrel as described for the Sephadex G-25 column (section 2.3.2.2) and the column equilibrated with column equilibration buffer [20 mM Tris-HCl, pH 8.5, containing 100 mM KCl, 20 mM imidazole, 10 mM 2-mercaptoethanol and 10 % (v/v) glycerol]. Protein samples were loaded and the column washed with 5 mL (10 X column volumes) of column equilibration buffer. The column was washed again with 2.5 mL (5 X column volumes) of 20 mM Tris-HCl, pH 8.5, containing 1 M KCl, 10 mM 2-mercaptoethanol, and 10% (v/v) glycerol and then washed with 2.5 mL of the column equilibration buffer. Finally, the column-bound proteins were eluted with 5 mL of elution buffer [20 mM Tris-HCl, pH 8.5, containing 100 mM KCl, 100 mM imidazole, 10 mM 2-mercaptoethanol, and 10 % (v/v) glycerol]. The eluates were collected as 5 x 1 mL fractions, and 20 µl of each fraction was used for protein quantitation (section 2.3.3).

For some experiments, 20 µg of the purified protein was prepared in a final volume of 150 µL comprising 50 mM Tris-HCl, pH 8.0, containing 0.5 mM EDTA, 1 mM DTT and 10 U of rTEV protease (GIBCO BRL). For the reaction, the mixture was incubated at 30 °C for 3 hr.

Prepared proteins were separated using 16% (w/v) SDS-PAGE (section 2.3.4.1) and stained with CBB (section 2.3.4.3). For amino acid sequencing, stained protein bands of interest were excised, placed in water and sent to Ms. Catriona Knight (Department of Biochemistry, University of Auckland, New Zealand).

2.4.8.4 Bulk purification of protein expressed in *E. coli*

Expressed proteins were also purified from larger scale (1 L) cultures. For this 4 x 250 mL LB-Amp^{100} broths were inoculated with 5 mL of 10 mL overnight bacterial cultures and incubated at 37 °C for 3 hr with shaking at 225 rpm. The broth was then treated with IPTG (0.6 mM), incubated for another 3 hr and then centrifuged at 3 000 x g for 10 min at 4 °C. The cell pellets were resuspended in 10 mL of cell lysis buffer (section 2.4.8.3), the cell suspension transferred into 50 mL tubes, sonicated 10 times, for 15 sec each, at 14 d.c.b., decanted

carefully into dialysis membrane (Visking, tubing size 5, 12 to 14 000 kD cutoff; Medicell International Ltd., London, UK; Membranes were prepared by soaking in boiling 10 mM sodium bicarbonate containing 1 mM EDTA for 15 min, and then washing with several changes of sterile water). The protein samples were desalted by dialysis against 2 L of 50 mM Tris-HCl buffer, pH 8, at room temperature for the first 2 hr and then carried out at 4 °C overnight, with at least three changes of the buffer solution.

The expressed proteins were then purified using a 2 mL Ni-NTA resin (section 2.4.8.3) and eluted proteins were collected as 15 x 1 mL fractions. To quantify the protein in each fraction, a 20 µl aliquot of each was used for protein assay (section 2.3.3).

2.5 Immunological analysis

2.5.1 Production of polyclonal antibodies (PAb)

2.5.1.1 Animal immunisation and separation of serum

Two rats were each injected with 400 µL, consisting of an equal volume of the purified TRACO1 protein (80 µg; 2.4.6.4) in PBSalt and Freund's complete adjuvant (DIFCO Laboratories) at the several sites on the animals' back. The immunisation was performed by the staff at the Small Animal Production Unit (SAPU, Massey University, Palmerston North, New Zealand), where the rats were housed. The rats were boosted three times by injecting 400 µL mixture prepared as above, except that Freund's incomplete adjuvant (DIFCO Laboratories) was used at 32 day intervals.

The rat blood was collected before the first injection as a pre-immune serum, and collected after the 3rd boost as the polyclonal antibody 1 (PAb1) serum. After collecting blood, it was allowed to clot at room temperature for 1 hr, and then stored for the clot to contract at 4 °C overnight. The clot was then separated from the side of the tube with a pature pipette and centrifuged at 10 000 x g for 10 min at 4 °C. The supernatant was removed as the serum fraction and stored at –20 °C until use. For some western analysis, antibodies raised against the

gene product of TRACO2 in *E. coli*, were used (PAb2). These were provided by Dr. D. Hunter (IMBS, Massey University).

2.5.1.2 Isolation of immunoglobulin G (IgG) from the PAb1 serum

IgG was isolated using the method described by Johnstone and Thorpe (1986). A saturated ammonium sulphate solution was prepared by dissolving 80 g ammonium sulphate in 100 mL sterile water with heating. After dissolving the salt completely, the solution was cooled on ice for at least 1 hr without agitation to allow crystallisation and the aqueous phase was used as the saturated ammonium sulphate solution. A 10 mL aliquot of PAb1 serum was mixed with the equal volume of PBSalt (50 mM sodium phosphate buffer, pH 7.2, containing 250 mM NaCl). The mixture was then placed on a magnetic stirrer and 20 mL of saturated ammonium sulfate was added slowly in 1 to 2 mL aliquots. Precipitated proteins were collected by centrifugation at 10 000 x g for 15 min at 4 °C, and the supernatant discarded. The pellet was resuspended in 10 mL of 0.07 M sodium phosphate buffer (pH 6.3) and dialysed overnight against 1 L of the resuspension buffer with several changes of the same buffer (the dialysis membrane was prepared as in section 2.4.8.4). The dialysis was performed at room temperature for the first 4 hr, and then carried out at 4 °C overnight.

A 10 mL column was prepared by equilibrating DEAE Sephacel® resin (Pharmacia Biotech) with 0.07 M phosphate buffer (pH 6.3) and then washing with the same buffer several times at room temperature. The dialysed PAb1 was then applied to the column and eluted with the same buffer at room temperature, and 15 x 1 mL fractions collected. Protein content in each fraction was determined by absorbance at 280 nm using a Shimazu spectrophotometer using the relationship A_{280} 1.4 = 1 mg mL^{-1} (McManus and Osborne, 1990a).

2.5.2 Western analysis

Protein samples were extracted (section 2.3.2.1), and separated by SDS-PAGE (section 2.3.4. 1 or 2.3.4.2). The proteins were then transferred onto polyvinylidinefluoride (PVDF; Immobilin-P, Milipore Corporation, Bedford, MA, USA) membrane, using a Trans-Blot

Electrophoretic Transfer Cell (Bio-Rad Laboratories) by assembling the gel-membrane sandwich as depicted in figure 2.7.

After hydration of the PVDF membrane in methanol for 10 min, the transfer sandwich was assembled partially immersed in electroblotting buffer (25 mM Tris, 190 mM Glycine) to avoid trapping air bubbles. Proteins were transferred in the electroblotting buffer at 30 V for 1 hr at room temperature (for mini-gels), or at 20 V for overnight at 4 °C (for gradient gels). After transfer, membranes were blocked in PBST (50 mM sodium phosphate buffer, pH 7.2, 250 mM NaCl, 0.05% (v/v) Tween 20), containing 0.2% (w/v) I-block (Tropix, Bedford, MA, USA) at room temperature for 1 hr, or at 4 °C overnight. The membrane was washed briefly with PBST, incubated with primary antibodies (PAb1 or PAb2; section 2.5.1.1) at a 1:1000 dilution in PBST for 1 hr at 37 °C, and washed three times with PBST, each for 10 min. The membrane was incubated with secondary antibodies (for PAb1, goat anti-rat antibody conjugated with alkaline phosphatase; for PAb2, goat anti rabbit antibody conjugated with alkaline phophatase; Sigma Chemicals) at a 1:10,000 dilution in PBST for 1 hr at room temperature, washed three times with PBST each for 10 min, and then washed twice with 150 mM Tris-HCl (pH 9.7), each for 5 min.

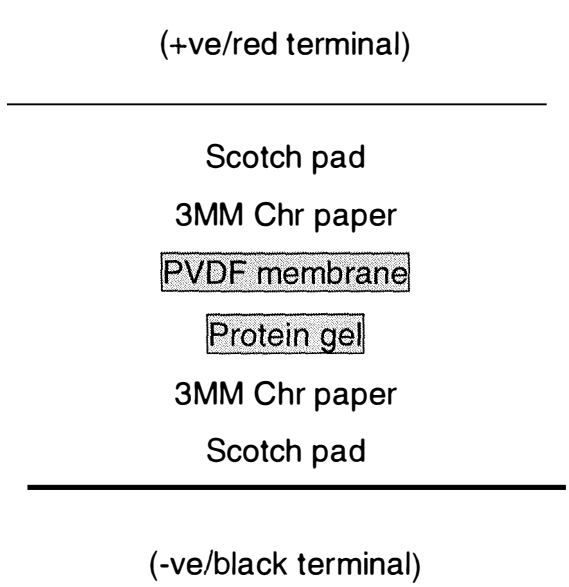

Figure 2.7 Protein transfer sandwich for electro-transfer of protein onto PVDF membrane.

The antigen-antibody complex was visualised using substrates for the secondary antibody-conjugated alkaline phaphatase activity [prepared as 150 mM Tris-HCl, pH 9.7 containing 0.02% (w/v) nitroblue tetrazolium(NBT), 0.01% (w/v) 5-bromo-4-chloro-3-indolylphosphate (BCIP; disolved in dimethyl sulphoxide, DMSO) and 8 mM $MgCl_2$].

When sufficient colour developed, the membrane was washed with excessive reverse-osmosis (RO) water several times and then kept at 4 °C for further photographic record.

2.5.3 Enzyme-linked immuno-sorbent assay (ELISA)

Sample tissue was powdered in liquid nitrogen and four volumes of 50 mM sodium phosphate buffer pH 7.2 was added to extract protein. The slurry was centrifuged at 20 800 x g for 10 min at 4 °C and the supernatant was prepared at a final concentration of 0.1 mg/mL with ELISA coating buffer (50 mM sodium carbonate buffer, pH 9.6). Two hundred µL aliquots of diluted extract was applied to wells of a Nunc-Immuno™ Plate (Nalgene International, Denmark). After incubation overnight at 4 °C, each well was washed three times with PBST and blocked with 100 µL of I-block solution [0.02% (w/v) in coating buffer] for 1 hr at room temperature. Each well was again washed three times with PBST and serial dilutions of purified PAb1 IgG (section 2.4.8.2) applied as 90 µL aliquots. After incubation of the plate at 37 °C for 1 hr, the Pab1 antibodies were washed off and 90 µL aliquots of 2° goat anti-rat antibody-conjugated with alkaline phosphatase (prepared as a dilution of 1:10 000 with PBST; Sigma Chemicals) was applied, the plate incubated for 30 min at 37 °C, and then each well washed three times with PBST.

The plate was developed by the addition of 90 µL aliquots of substrate [0.1% (w/v) p-nitrophenyl phosphate (PNPP; Sigma Chemicals), 3mM $MgCl_2$ in coating buffer] and once sufficient development had occurred, the absorbance was read at 405 nm using an Anthos Htll plate reader.

2.5.4 Immunoprecipitation with Protein G-beads conjugated with PAb1

Crude protein extract (section. 2.3.2.1) were mixed with an equal protein amount of purified PAb1 IgG (section 2.5.1.2) and incubated at 37 °C for 1 hr with rotary mixing. An equal protein amount of protein G beads (Sephadex protein G beads; Pharmacia Biotech) was then

added and the mixture incubated at 37 °C for 45 min as before. The mixture was then centrifuged at 15 000 x g for 5 min at room temperature and the supernatant was discarded carefully. The pellet was washed three times with PBSalt and 20 µL of the pellet was then prepared for SDS-PAGE and separated through 10% (w/v) SDS-PAGE gel, as described in section 2.3.4.1.

2.5.5 Cyanogen bromide (CNBr)-activated column chromatography

An immunoaffinity column was prepared using purified PAb1 IgG (section 2.4.8.2) and CNBr-activated Sepharose 4B (Pharmacia Biotech), according to the method described by McManus and Osborne (1990b). The column resin (typically 1 g) was prepared by suspending the powder (CNBr-activated Sepharose 4B) in 1 mM HCl (resin swelled immediately to 3.5 to 4 mL) and the swollen resin was then washed with five gel volumes of coupling buffer (0.1 M $NaHCO_3$, pH 8.3, containing 0.5 M NaCl). The purified PAb1 IgG, diluted to a concentration of 4 mg/ml in PBSalt, was then added to the gel and the mixture incubated by end-over-end rotation for 1hr. The resin was then poured into a 10 mL syringe barrel plugged with three layers of GF-A glass microfilter paper. Excess IgG was washed off first with five gel volumes of coupling buffer and then with three cycles of five column volumes of 100 mM Tris-HCl (pH 8.0) and five column volumes of 100 mM sodium acetate, pH 4.0. The gel was then washed with a further two cycles of five volumes of 50 mM diethanolamine, pH 11.0, containing 10 mM EDTA and 100 mM NaCl, and five column volumes of 200 mM glycine-HCl, pH 2.5. The gel was washed finally with ten column volumes of PBSalt.

To obtain protein extracts for the immuno-affinity column chromatography, 15 g of apical tissue was extracted in six volume of PBSalt and then subjected to 30-90% (w/v) saturated ammonium sulphate fraction (section 2.3.2.1). The pellet was resuspended with 10 mL of PBSalt and the extract desalted by dialysis against 2 L of PBSalt, containing 0.5 mM PMSF, with three changes, at room temperature for the first 4 hr, and then carried out at 4 °C overnight.

The protein was incubated with the CNBr-activated gel coupled with PAb1 for 2 hr at 37 °C, and then with gentle end-over-end rotation of the column for a further 18 hr at 4 °C. The affinity gel coupled with the plant protein extract was then washed with five column volumes of PBSalt and coupled proteins eluted with two column volumes of 50 mM diethanolamine, pH 11, containing 10 mM EDTA and 100 mM NaCl, and then two column volumes of 200 mM glycine-HCl, pH 2.5. The protein eluate was analysed using 10% (w/v) mini SDS-PAGE (section. 2.3.4.1) or 8-15% (w/v) gradient SDS-PAGE (section 2.3.4.2).

2.6 Statistical analysis

Experimental data collection and statistical analysis were performed with an Excel spread sheet programme (version 5.0; Microsoft, USA).

Chapter 3 Results

Part 1: Physiological and biochemical analysis of clonal growth of white clover

3.1.1 Leaf development of white clover

3.1.1.1 Physiology of leaf development

White clover, under the experimental conditions used in this thesis, grows from one major root as a single stolon with leaves, which show the whole range of developmental stages from initiation at the apex, through mature green to senescence, and then necrosis (Fig. 3.1.1).

Leaf fresh weight and leaf size have been determined initially to characterise the basic physiology of leaf tissue at each developmental stage (Fig. 3.1.2). The values of fresh weight (Fwt) of a trifoliate leaf at each node increased rapidly during leaf expansion (leaf 2 and 3) and reached a maximum level when leaves were fully expanded (leaf 3). The values remained at a constant level of *ca.* 0.17 to 0.22 g during the mature green leaf stage and then decreased gradually after leaf 14 as visible leaf senescence was first observed (based on leaf chlorosis; Fig. 3.1.4).

The size of a trifoliate leaf at each node was determined from leaf 3 (the first fully expanded leaf) using a leaf area meter (Fig. 3.1.2). The mean values of leaf size remained at a constant level of 3.8 to 4.8 cm^2 during the mature green stage (between leaf 3 and leaf 14), but the value decreased after leaf 14 as visible leaf senescence ensued.

The ratio of leaf fresh weight and leaf size at each node was found to increase (Fig. 3.1.3), probably because leaf size decreased dramatically, when compared to fresh weight of trifoliate leaves during leaf ontogeny (Fig. 3.1.3). This trend is also observed when fresh weight of leaf discs (diameter = 10 mm) excised from the basal region of a leaflet of the trifoliate leaf was determined (Fig. 3.1.3). Unlike the fresh weight for trifoliate leaves, the values of the leaf disc fresh weight increased as leaf ages. Thus leaf discs from the oldest leaf (leaf 18) were heavier than any other leaves on the same stolon.

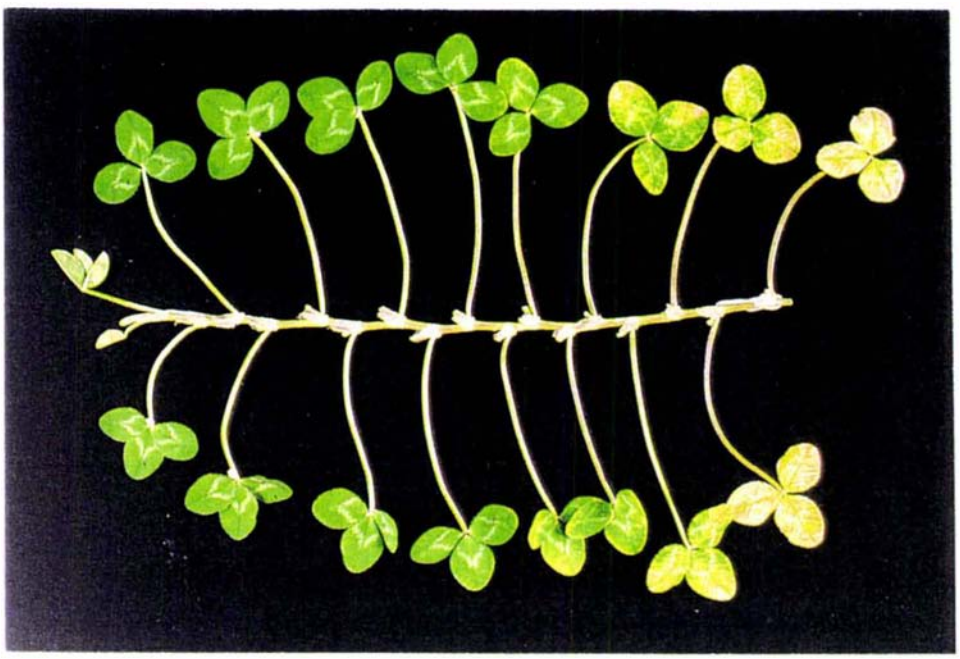

Figure 3.1.1 Stages of leaf development using the stolon growth model system of white clover.

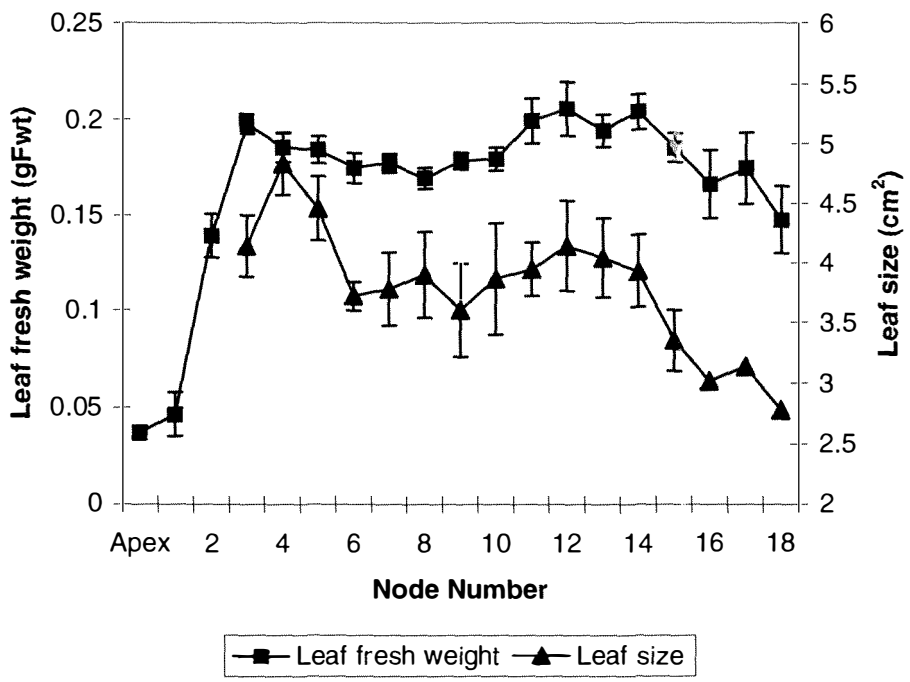

Figure 3.1.2 Changes in fresh weight and size of leaves at each node during leaf ontogeny in white clover. Results are mean values ± s.e., n=5.

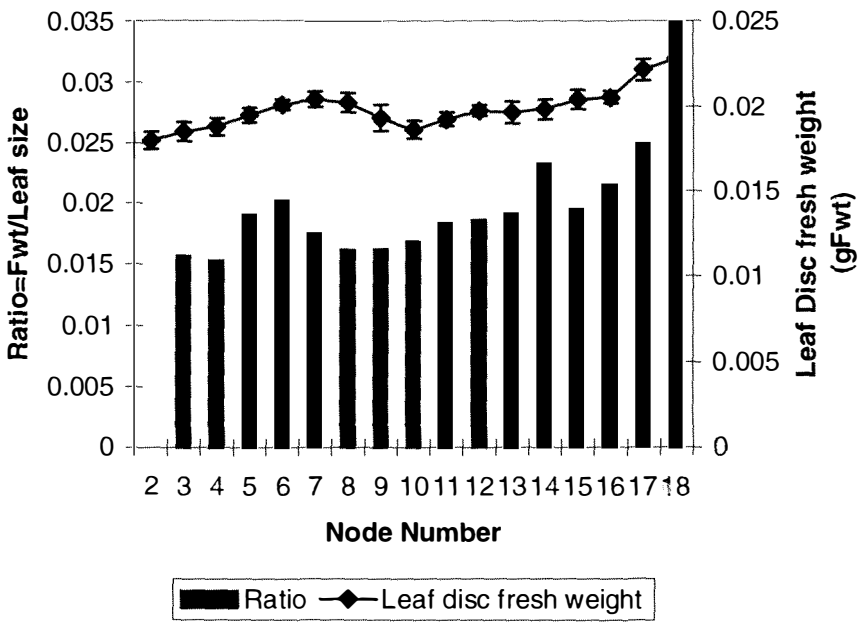

Figure 3.1.3 Changes in the ratio of mean leaf fresh weight / leaf area at each node (from Fig. 3.1.2), and fresh weight of leaf discs excised from the basal portion of the leaf blade at each node. Results of the fresh weight of leaf discs are mean values ± s.e., n=10.

3.1.1.2 Changes in photosynthetic activity during leaf ontogeny in white clover

Each leaf developmental stage on a stolon can be denoted by its rate of photosynthetic activity. Along with measurement of chlorophyll content, which proved to be a simple and reliable indicator (Butcher *et al.*, 1996; Butcher, 1997; Hunter, 1998; Hunter *et al.*, 1999), photosynthetic activity of leaves at each node has been further characterised using two other quantitative methods. One is the measurement of CO_2 gas exchange rate by a single leaf in an open chamber system for a unit time at 25 ^{o}C (photosynthesis rate). The other is the measurement of chlorophyll fluorescence per unit size of leaf, which indicates photochemical (quantum) efficiency of photosynthesis system II (PSII) (Hall, 1993).

Changes in chlorophyll content

Chlorophyll content of leaves at each node was measured (Fig. 3.1.4). The total chlorophyll content increased as leaves expanded (apex to leaf 3), remained at a maximum level of *ca.* 1 700 to 2 000 µg per g fresh leaf tissue during the mature green leaf stage (leaf 4 to 14), and then decreased as leaf senescence progressed (after leaf 14) to reach *ca.* 500 µg per g fresh weight at leaf 18. The values of chlorophyll a and b followed the pattern of total chlorophyll content during the leaf development.

Chlorophyll content was also determined using leaf discs (diameter = 10 mm) excised from basal portion of leaf blades at each odd numbered node (Fig. 3.1.5). Chlorophyll content was highest at leaf 3 and leaf 5, then decreased at leaf 7 and remained more or less constant, even after leaf yellowing is discernable at leaf 14. When it is compared with total chlorophyll in a trifoliate leaf at each node, it is apparent that the chlorophyll content in the excised leaf discs represented most of the chlorophyll in the leaves at the senescent stage of leaf.

As it can also be observed in figure 3.1.1, when a leaf begins to senesce, chlorophyll is lost initially from the margins of its blade, and it remains green around the main veins for longer. Therefore, in leaf discs excised from the basal portion of leaf blade a relatively higher level of chlorophyll content is maintained through the whole programme of leaf development. This portion of leaf tissue was, therefore, used for the measurement of chlorophyll fluorescence to characterise photochemical efficiency of PS II during leaf ontogeny in white clover.

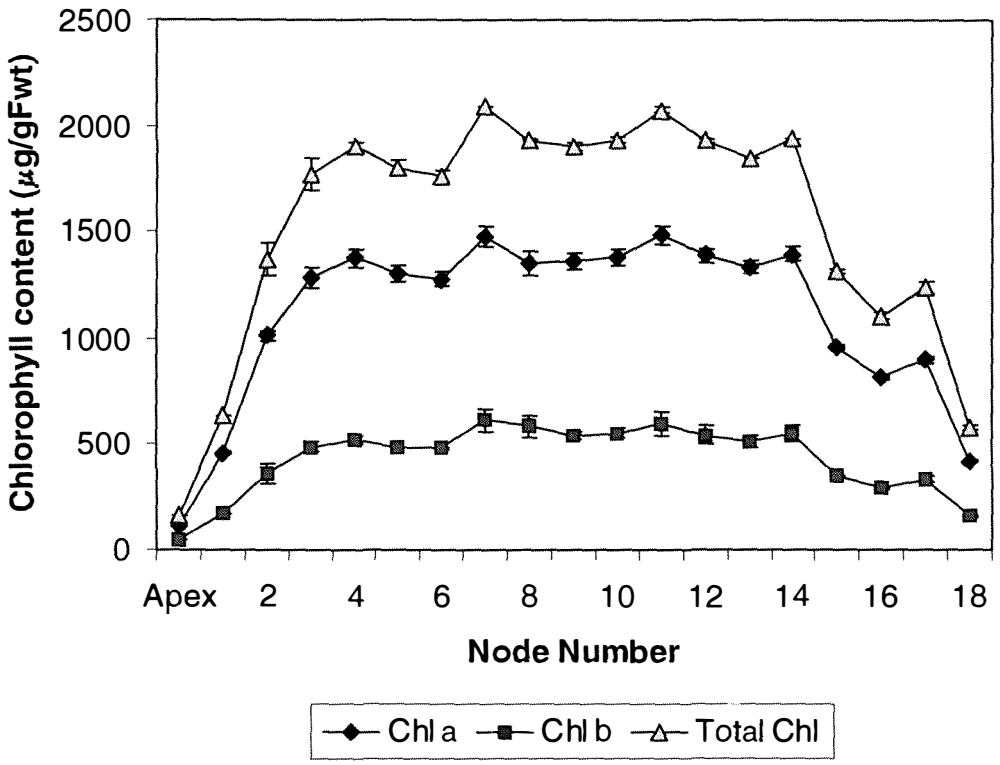

Figure 3.1.4 Changes in chlorophyll content during leaf ontogeny in white clover. Results are mean values ± s.e., n= 3.

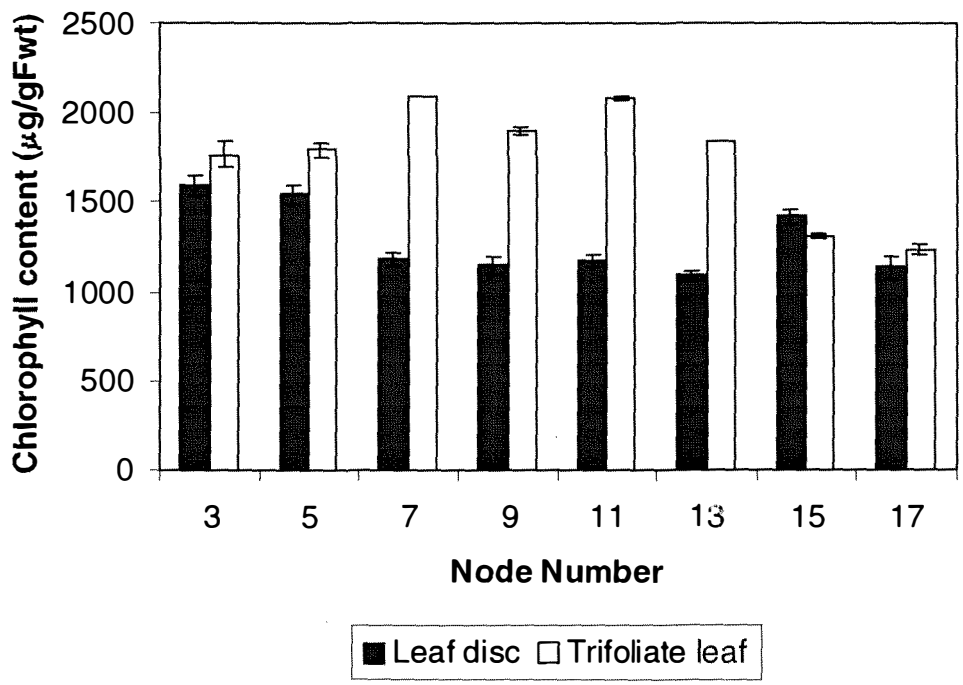

Figure 3.1.5 Changes in total chlorophyll content of each leaf and leaf discs excised from the basal portion of the leaf blade at each odd numbered node along the stolon. Results are mean values ± s.e., n=3.

Photosynthetic activity

Changes in photosynthetic activity during leaf ontogeny have been characterised by measuring the rate of photosynthesis using a CO_2 gas exchange detector (Fig. 3.1.6). The analysis demonstrated that the rate remained high during the mature green leaf stage (leaf 3 to leaf 11) and then decreased after leaf 12. The decrease in CO_2 absorption appeared to be slightly earlier (*ca.* two leaf-stage) than that of chlorophyll content during leaf ontogeny (leaf 14; cf. Fig. 3.1.4).

Photosynthetic activity was also characterised in terms of photochemical efficiency using measurement of chlorophyll fluorescence (Fig.3.1.7). Photochemical efficiency of PSII (photochemical yield) in light–adapted tissues, represented by Fv'/Fm', increased during leaf expansion (leaf 2 to leaf 3), remained high during the mature green stage (leaf 4 to leaf 14), and then decreased as leaf senescence progressed (after leaf 14). This trend quite accurately reflected the total chlorophyll content in leaves at each node.

A further calculation of photochemical efficiency of PSII was made (Table 3.1.1) by using leaf tissues grouped into four different developmental categories [newly initiated expanding leaves (NI; leaf 2 and leaf 3), mature green leaves (leaf 6 and leaf 8), onset of senescent leaves (OS; leaf 13 and leaf 14), and senescent leaves (SL; leaf 16 and leaf 17)].

Fo values (fluorescence emission when all the reaction centres are open for photochemistry) of dark-adapted tissue increased slightly throughout the developmental stages, whereas Ft values (corresponding to Fo value of dark-adapted tissue) of light-adapted tissue remained steady. Fm values (fluorescence emission when all the reaction centres are closed) of dark-adapted tissue increased slightly in OS tissue, and then significantly decreased in SL tissue. Fm' values of light-adapted tissue (corresponding to Fm value of dark-adapted tissue) increased in MG and OS tissues, and then decreased in SL tissue.

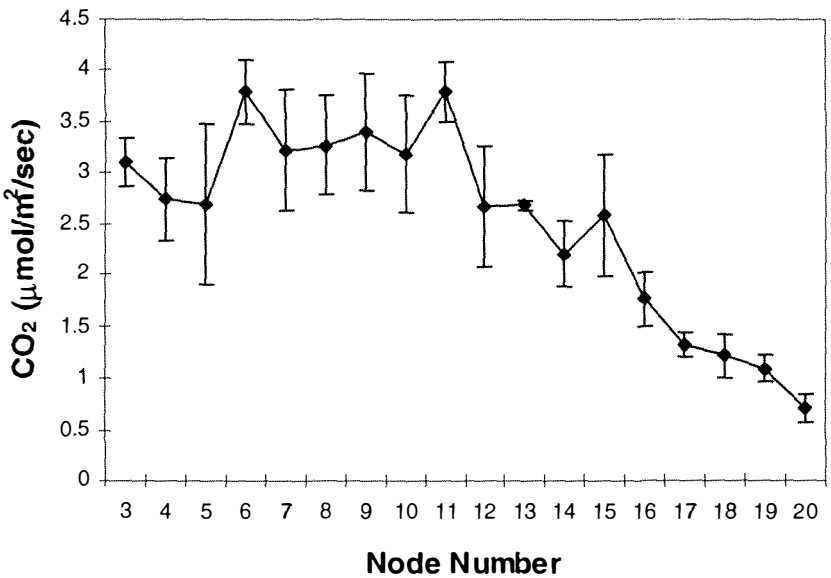

Figure 3.1.6 Changes in photosynthesis rate during leaf ontogeny, measured as CO_2 gas exchange rate per unit time at 25 ^{o}C, using a single trifoliate leaflet. Results are mean values ± s.e., n=5.

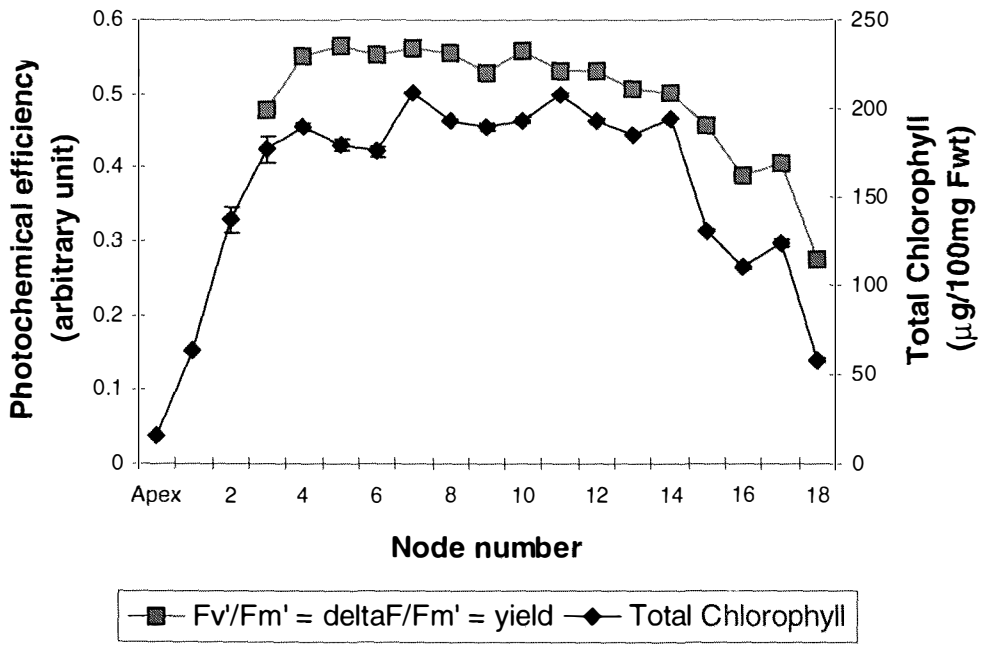

Figure 3.1.7 Changes in the photochemical efficiency of PSII (chlorophyll fluorescence) and total chlorophyll content (from Fig. 3.1.4) during leaf ontogeny in white clover. Results of chlorophyll fluorescence are mean values, n=3. Results of total chlorophyll content are mean values ± s.e., n=3.

	Dark-adapted tissue			Light-adapted tissue		
	Fo	Fv	Fm	Ft	Fv'	Fm'
NI	9.30±0.13	45.66±1.34	54.96±1.46	11.47±0.29	12.46±1.14	23.92±1.30
MG	9.34±0.29	45.28±1.24	54.62±1.51	11.42±0.19	14.29±0.18	25.71±0.28
OS	10.72±0.15	48.55±0.43	59.27±0.52	13.31±0.24	12.64±0.64	25.94±0.71
SL	11.03±0.55	39.32±1.98	50.35±2.47	11.83±0.36	05.25±0.48	17.08±0.74

Table 3.1.1 Chlorophyll fluorescence from dark-adapted (leaf discs excised from leaves) and light-adapted leaf tissues at four major leaf developmental stages: NI, newly initiated leaves (leaf 2 and leaf 3); MG, mature green leaves (leaf 6 and leaf 8); OS, onset of senescence (leaf 13 and leaf 14); SL, senescent leaves (leaf 16 and leaf 17). Results are mean values ± s.e., n=6

Changes in each variable were indicated that total photochemical efficiency of PSII (Fv/Fm) remained constant, whereas photochemical yield (Fv'/Fm') decreased in SL tissue (Fig. 3.1.8). As well, photochemical quenching (qp) did not change during any developmental stage, but non photochemical quenching (Npq) varied at each stage. It was lowest in MG tissue, slightly higher in NI and OS tissues, and highest in SL tissue. Therefore, this result suggests that less photon energy is involved in photochemistry in SL tissue and hence more energy may be lost as other energy forms, e.g. heat or light emission, when compared with non-senescent leaf tissues (Fig. 3.1.8).

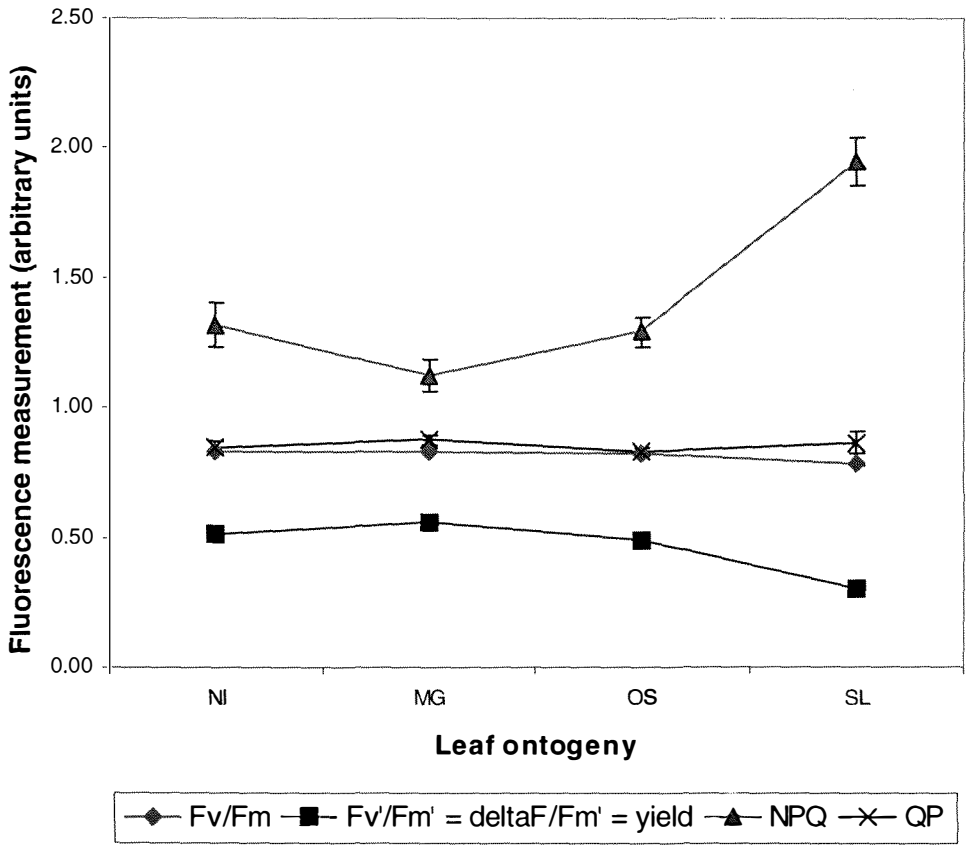

Figure 3.1.8 Changes in the photochemical efficiency of PSII in four major leaf developmental stages: NI, newly initiated leaves (leaf 2 and leaf 3); MG, mature green leaves (leaf 6 and leaf 8); OS, onset of senescence (leaf 13 and leaf 14); SL, senescent leaves (leaf16 and leaf 17). Photochemical efficiency is Fv / Fm and Fv' / Fm' = Yield, with respect to dark-adapted and light-adapted tissues. NPQ and QP are non photochemical quenching and photochemical quenching, respectively. Results are mean values ± s.e., n=6.

3.1.2 Ethylene production in the developing apex and newly initiated leaves

3.1.2.1 Measurement of ethylene production

Ethylene production has been determined from previous studies using this white clover growth system (Butcher, 1997; Hunter, 1998). In this thesis, the significance of ethylene production from the developing apex and newly initiated leaves has been examined further using measurements, both *in vivo* and *in vitro*.

Rates of ethylene production, *in vivo*, from the developing apex, newly initiated leaves (leaf 1 and leaf 2) and a fully expanded mature green leaf (leaf 3) were measured by enclosing stolon-attached leaf tissue in plastic containers and analysing ethylene accumulation for 1 hr (Fig.3.1.9A). A significantly higher rate of ethylene production was observed from the developing apex and a comparatively lower rate of ethylene production was detected from newly initiated leaves (leaf 1 and leaf 2) and a mature green leaf (leaf 3), indicating that a significant amount of ethylene is produced from the developing apex. As well, a relatively higher (although not significant) rate of ethylene production, *in vivo*, was measured from the newly initiated leaf tissue (leaf 1), when compared with fully expanded mature green leaf tissue (leaf 3).

Rates of ethylene production, *in vitro*, from the apex and leaf tissues were also measured using excised tissues and analysing ethylene accumulation for 1 hr (Fig 3.1.9B). The results correlated well with measurements of ethylene production, *in vivo*. A relatively higher rate of ethylene production was observed from developing tissues (the developing apices and leaf 1), when compared with the fully expanded mature green leaf tissue (leaf 3).

Measurement of ethylene production, *in vivo*, is usually considered to be a reliable method for constitutive ethylene production, because there is less chance of contamination of stress-induced ethylene from tissue damage for measurement, *in vitro*. However, in this study, the mean value of ethylene production, *in vitro,* from each sample measured was less variable, when compared with measurements of ethylene production, *in vivo*. The larger variation, represented by a larger standard error, in measurements of ethylene production, *in vivo*, may be

A)

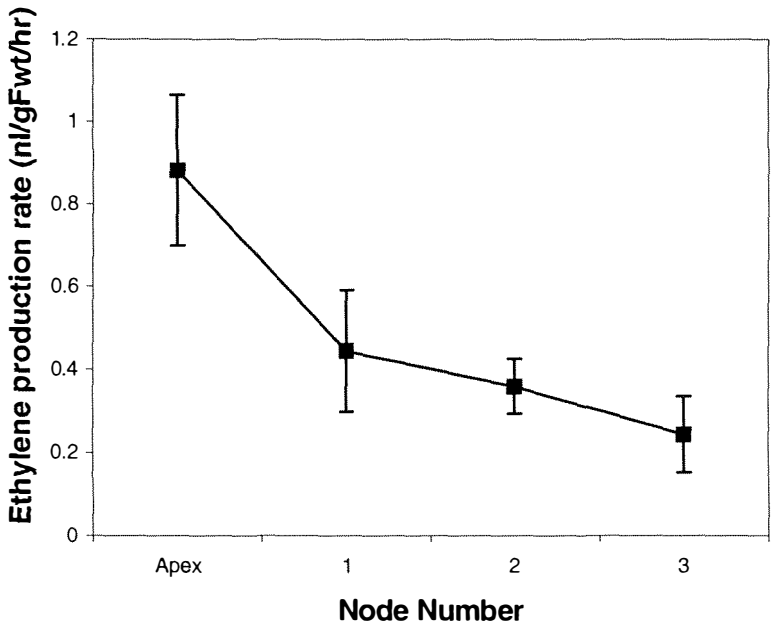

B)

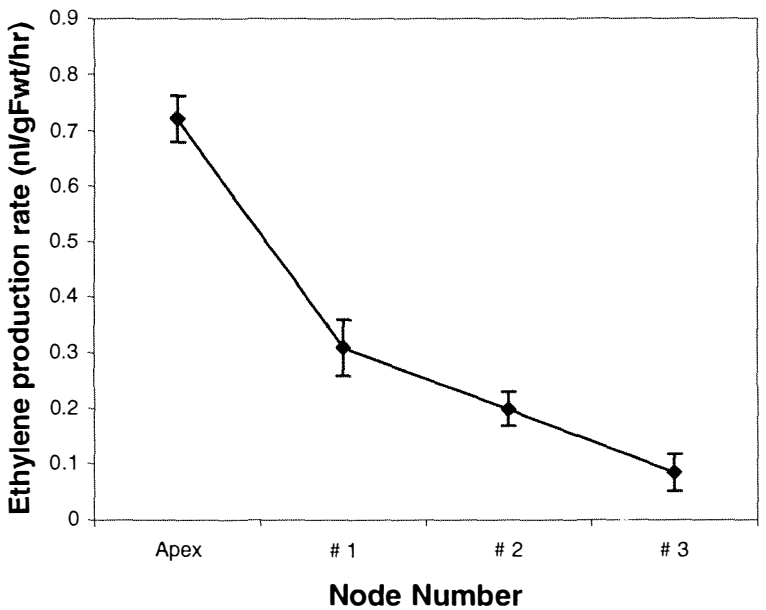

Figure 3.1.9 Measurements, *in vivo* (A) and *in vitro* (B) of ethylene production from developing apices and newly initiated leaves. Results are mean values ± s.e., n=3.

related to the collection of ethylene from intact tissues (It is more difficult to enclose the tissue without gas leakage). Further analysis of ethylene production was, therefore, undertaken using measurements of ethylene production, *in vitro,* over a longer time period.

3.1.2.2 Measurement of ethylene production, *in vitro,* over a longer time period

Rates of ethylene production, *in vitro*, have been measured over the first 11 hr after leaf excision (AE) (Fig.3.1.10). The rate increased over the first 3 hr AE, and then decreased in the apex and newly initiated leaves (leaf 1 and leaf 2). However, the rate in just fully expanded mature green leaves (leaf 3 and leaf 4) decreased more or less steadily throughout the time period. The increased rate of ethylene production, *in vitro*, probably represents stress ethylene production in response to the excision-induced wounding in the apex and newly initiated leaves. Nevertheless, the rate of ethylene production, *in vitro*, was higher in the apex and newly initiated leaves (leaf 1 and leaf 2), when compared with fully expanded mature green leaves (leaf 3 and leaf 4) throughout the time period.

3.1.3 Biochemical characterisation of ethylene biosynthesis in white clover

ACC content (the product of ACS activity) and ACO enzyme activity, *in vitro,* were determined to characterise the biochemistry of higher ethylene evolution from the developing tissues of white clover.

3.1.3.1 ACC content in white clover

ACC content has been measured in various organs of white clover (Fig. 3.1.11). Mean values of ACC content were 2.46 (nL C_2H_4 $gFwt^{-1}$ hr^{-1}) in the developing apex; 2.56 (nL C_2H_4 $gFwt^{-1}$ hr^{-1}) in axillary buds (excised from axils of node 3 and 4); 1.88 (nL C_2H_4 $gFwt^{-1}$ hr^{-1}) in leaf 2; 1.89 (nL C_2H_4 $gFwt^{-1}$ hr^{-1}) in leaf 6, and 11.23 (nL C_2H_4 $gFwt^{-1}$ hr^{-1}) in leaf 12,. In common with ethylene production, ACC content was higher in the developing apex and a newly initiated leaf (leaf 1), when compared with a mature green leaf (leaf 6). Then, ACC content increased (*ca.* 10-fold) in a senescent leaf (leaf 12), which coincides with high ethylene production (cf. Fig. 1.5, data from Hunter, 1998).

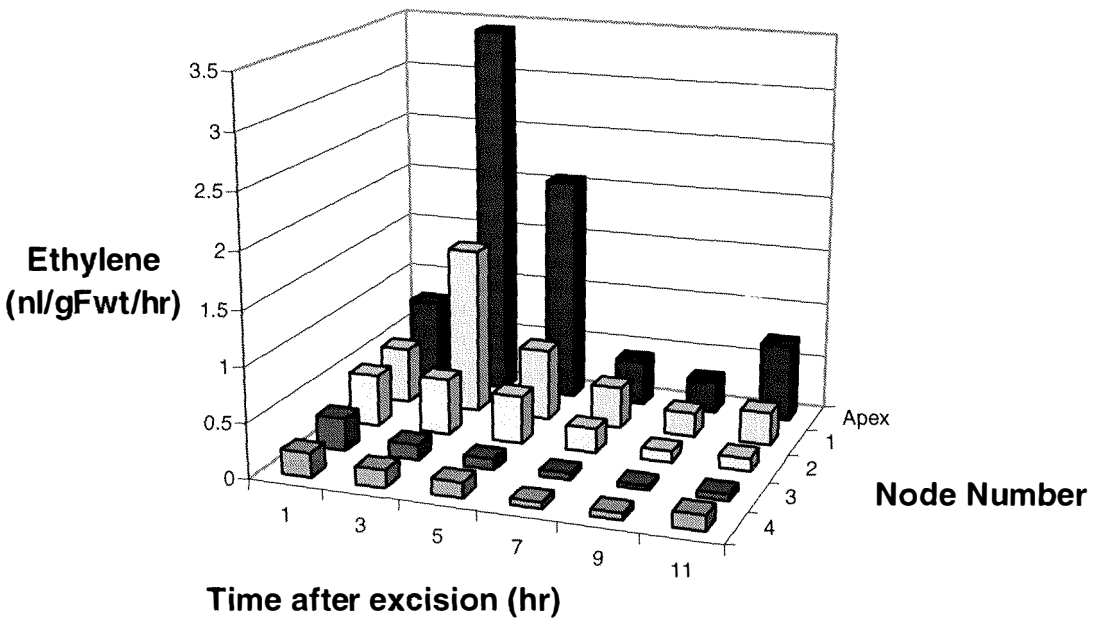

Figure 3.1.10 Measurements of ethylene production, *in vitro*, from developing apices, newly initiated leaves (leaf 1 and leaf 2) and just fully expanded mature green leaves (leaf3 and leaf 4) over 11 hr time course after excision. Results are mean values ± s.e., n=3.

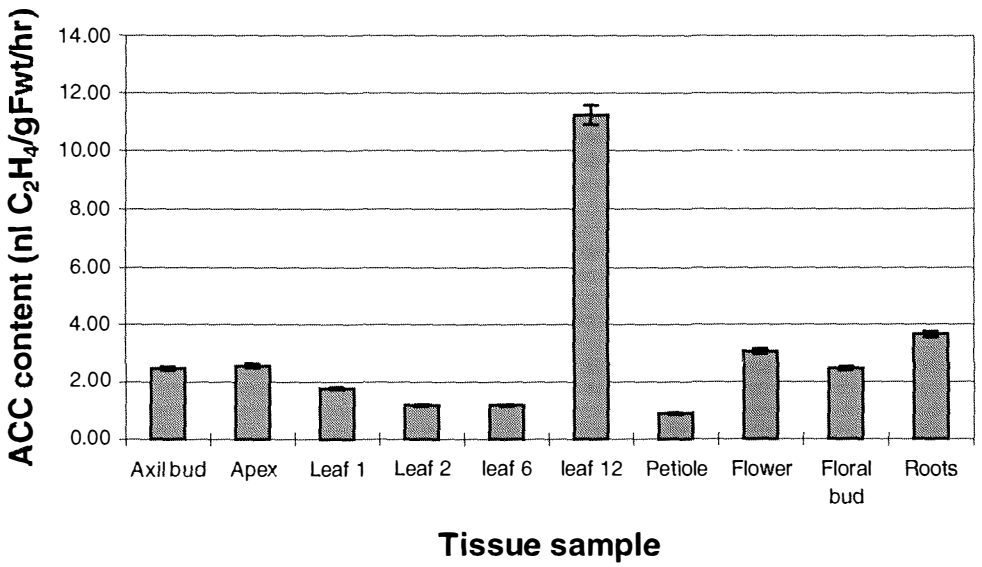

Figure 3.1.11 ACC content in different plant organs of white clover. Results are mean values ± s.e., n=3.

While petiole tissues contained a basal level of ACC (0.89 nL C_2H_4 $gFwt^{-1}$ hr^{-1}), floral bud, flower and root tissues contained a relatively higher level of ACC, ranging from 2.46 to 3.65 (nL C_2H_4 $gFwt^{-1}$ hr^{-1}), when compared with a mature green leaf (leaf 6).

3.1.3.2 ACC oxidase activity *in vitro* in white clover

Hunter (1998) reported optimised conditions for the enzyme assay, *in vitro*, from mature grown leaf extracts, in terms of incubating assay mixtures at 30 °C for 20 min with shaking at 175 rpm to ensure linearity of the reaction. These conditions were confirmed (data not shown) and used for the enzyme activity analysis in this thesis. The assay pH for the enzyme in extracts from different organs [apex, newly initiated leaves (leaf 1 and leaf 2) and a mature green leaf (leaf 3)] was optimised using three different pH values, 6.5, 7, and 7.5 (data not shown). The ACO enzyme activities, *in vitro*, from each protein extract showed a similar trend with activity highest at pH 7.5, except for the apex extract. However, repeated experiments showed no significant difference in activity, *in vitro*, at pH 7 and pH 7.5 from apex extracts (data not shown). This optimisation pH value was also reported by Hunter (1998), and hence pH 7.5 was adopted as the pH for the assay of ACO enzyme activity, *in vitro*.

ACC oxidase enzyme activity during early development and maturation of leaf tissue

ACO activity, *in vitro*, was measured using 30% to 90% (w/v) saturated ammonium sulphate fractionation followed by Sephadex G-25 column chromatography of protein extracts from the developing apex, newly initiated leaves (leaf 1 and leaf 2) and mature green leaves (leaf 3 to 7) (Fig. 3.1.12). ACO enzyme activity, *in vitro*, was highest in just fully expanded mature green leaves (leaf 3 based on total activity and leaf 4 based on specific activity), when compared with the activity determined in developing tissues (the developing apex, leaf 1 and leaf 2) or in later mature green leaves (leaf 5, leaf 6 and leaf 7).

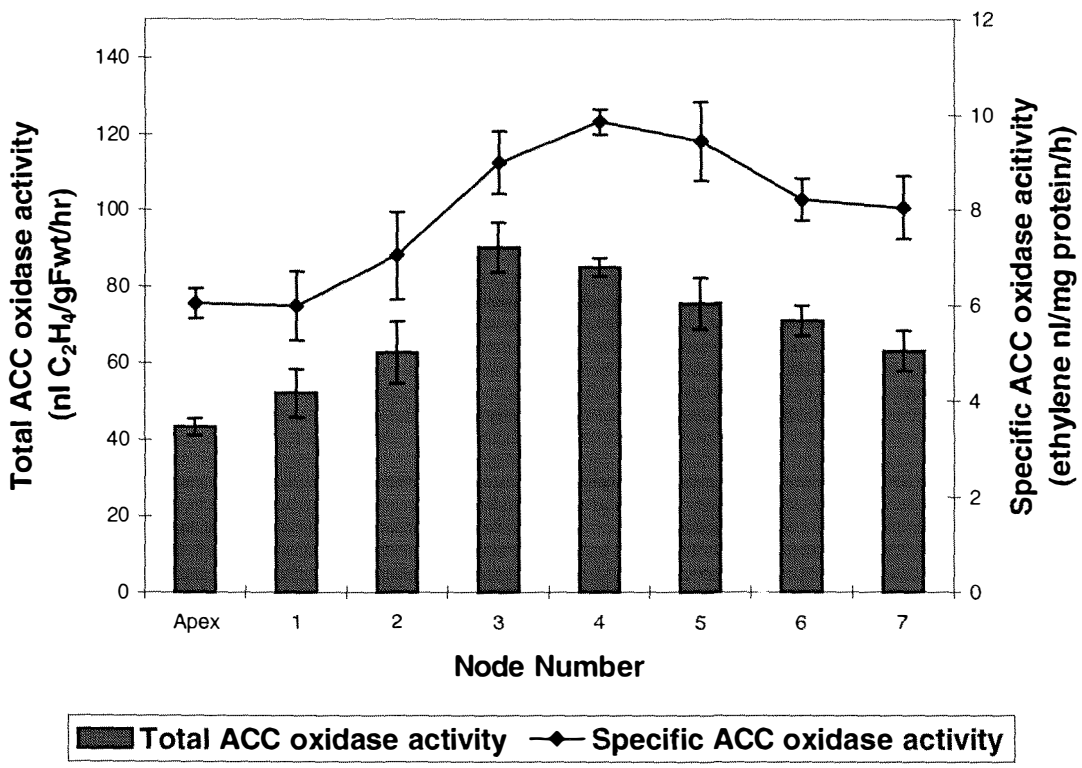

Figure 3.1.12 ACC oxidase activity, *in vitro*, measured in the apex, newly initiated leaves and mature green leaves at pH 7.5. Results are mean values ± s.e., n=3.

ACC oxidase enzyme activity in various plant organs of white clover

ACO enzyme activity, *in vitro*, was also assayed with crude protein extracts (no ammonium sulphate fractionation) from various plant organs of white clover (Fig. 3.1.13), and activity was detected in all extracts tested.

Floral, axillary and apical bud tissue extracts contained a similar level of ACO enzyme activity, *in vitro*, which was relatively higher than activities measured in mature green nodes and internodes. Mature green petioles exhibited even higher enzyme activity, but the highest ACO enzyme activity, *in vitro*, was detected in roots, when compared with any other organ in white clover. Compared with ACC content in these tissues, high ACO enzyme activity, *in vitro*, did not always coincide with high ACC content.

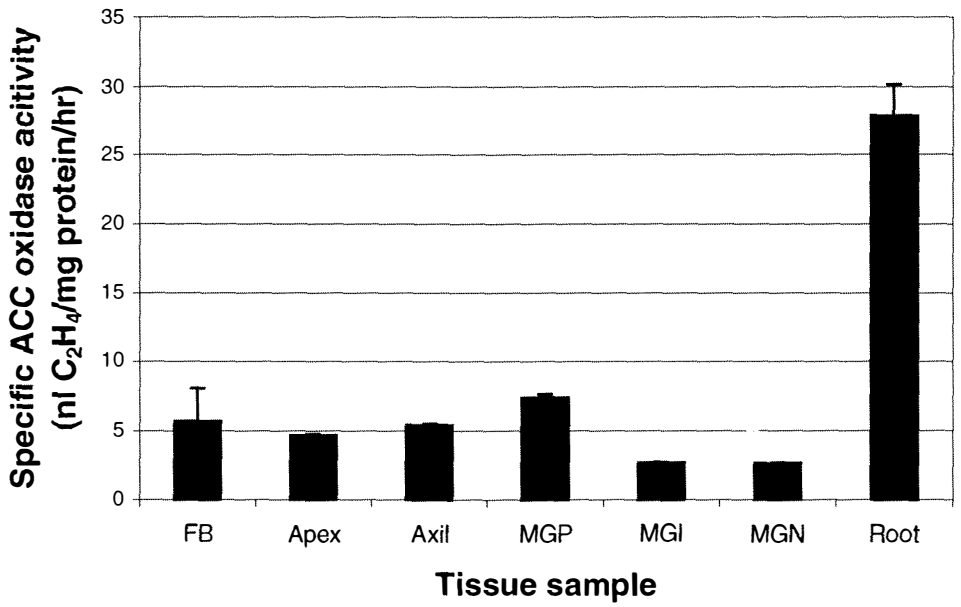

Figure 3.1.13 ACC oxidase enzyme activity, *in vitro,* assayed at pH 7.5 in different plant parts of white clover: FB, floral bud; Apex, apical bud; Axil, axillary bud (excised from axils at node 3 and node 4); MGP, mature green petiole; MGI, mature green internode; MGN, mature green node; and root. Results are mean values ± s.e., n=3.

Part 2: Molecular cloning and characterisation of ACC synthase genes in white clover

3.2.1 ACC synthase genes in developing tissues of white clover

3.2.1.1 Cloning and sequencing of protein-coding regions of putative ACC synthase genes expressed in the developing apex and a newly initiated leaf (leaf 2)

Genes encoding ACC synthase (ACS) expressed in the developing apex and newly initiated leaves of white clover were cloned using RT-PCR with degenerate primers. To amplify the protein-coding region of putative ACS genes in white clover, PCR was performed using cDNA templates generated by reverse-transcriptase (RT) treatment of total RNA isolated from leaf 1 and leaf 2 (Fig. 3.2.1). The primers, ACSR1F and ACSR6R (provided by Professor Shang Fa Yang, UC, Davis; Table 2.4) were used at an annealing temperature of 42 °C. The first round PCR did not amplify any identifiable DNA band, but a smear of DNA was discerned on the gel (Fig. 3.2.1, lane 1 and 2). By using the first round PCR product as template, the second round PCR was performed as a nested PCR with the ACSR2F and ACSR6R degenerate primers (Table 2.4) at the same annealing temperature (42 °C). An amplification product of *ca.* 650 bp was identified (Fig. 3.2.1, lane 3 and 4). However, there were also some other amplified products in this PCR reaction, which appeared as smears on the gel. These products may result from limited amplification at the latter stage of PCR, caused by mismatched primers using the relatively low annealing temperature of 42 °C. Nevertheless, the significant PCR product of *ca.* 650 bp indicated that the two sets of nested degenerate primers were specific enough to amplify putative ACS genes.

In addition, this *ca.* 650 bp PCR product was not amplified if the same amount of RNA (non RT-treated) was used as a template for the first round PCR (Fig. 3.2.2, lane 1). This confirms that the 650 bp DNA band was a genuine RT-PCR product from the tissue.

However, the DNA band of *ca.* 650 bp encoding putative ACS was only amplified by performing two rounds of PCR using ACSR1F and ACSR2F as forward primers for the first

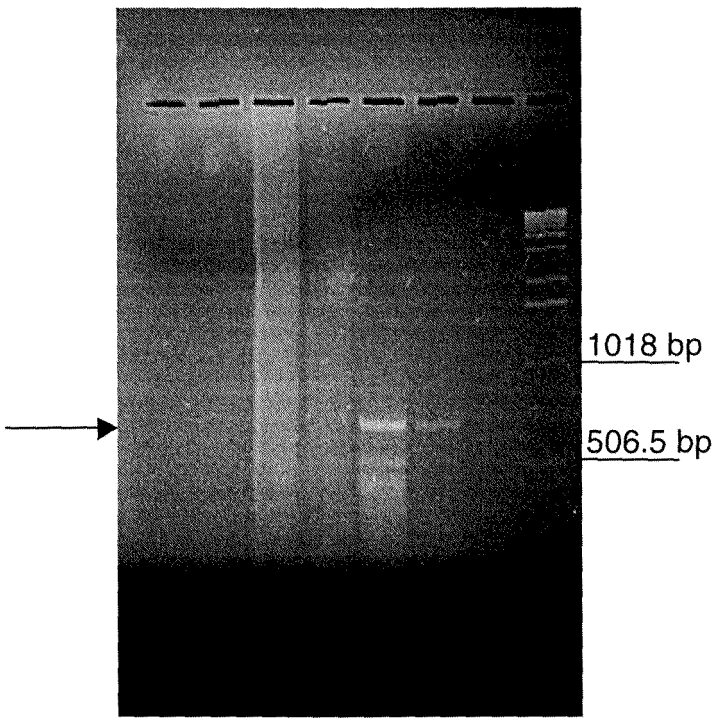

Figure 3.2.1 PCR amplification of putative ACS cDNAs using RT-generated cDNA templates from total RNA isolated from newly initiated leaves (leaf 1 and leaf 2). PCR products were separated on a 1.2% (w/v) agarose gel and visualised with ethidium bromide. Lanes (1) and (2) are separated products from the first round PCR of leaf 2 and leaf 1, respectively. Lanes (3) and (4) are those from the second round PCR using of the first round PCR products of leaf 2 and leaf 1 as templates, respectively. Lane (0) are the molecular size markers with two sizes indicated. The arrow indicates a 650 bp amplification product.

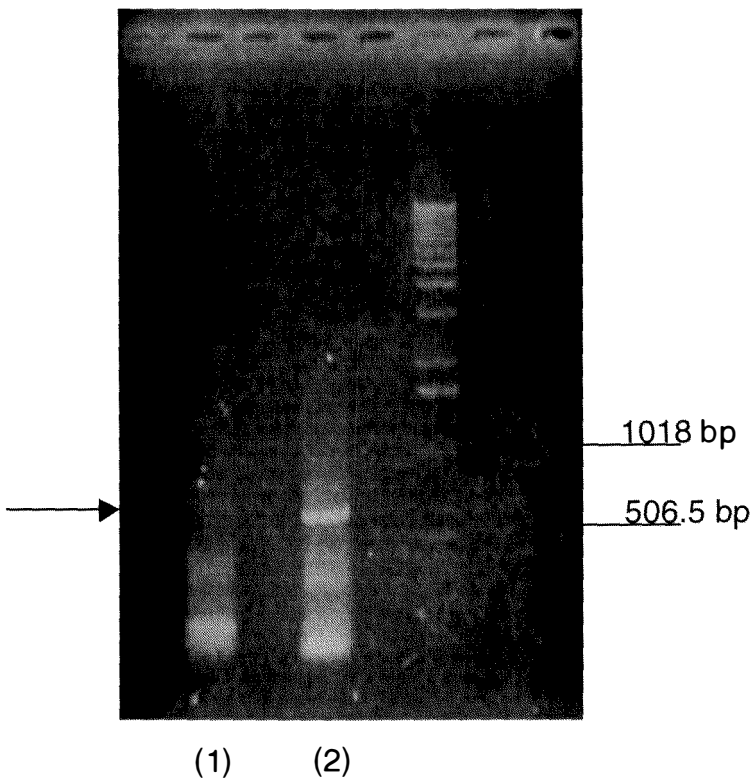

Figure 3.2.2 PCR amplification of putative ACS cDNAs using RT-generated cDNA templates from total RNA isolated from leaf 2. PCR products were separated on a 1.2% (w/v) agarose gel and visualised with ethidium bromide. Lane (1) is the product of second round PCR without cDNA templates (RNA templates) and Lane (2) is the product from the second round PCR using the first round PCR products as template. Lane (0) are molecular size markers with two sizes indicated. The arrow indicates a 650 bp amplification product.

and the second PCR, respectively. If any one of these two forward primers were used for two rounds of PCR, amplification of the 650 bp product did not occur (data not shown). This absolute requirement of two rounds of nested PCR may suggest either the ACS genes in leaf 1 and leaf 2 are expressed in relatively low abundance, or it could just be a consequence of the use of degenerate primers for PCR.

RT-PCR was also used to clone putative ACS genes expressed in the developing apex (Fig. 3.2.3). When cDNA templates were made from 1 μg or 3 μg of RT-treated poly(A)$^+$ mRNA isolated from the developing apex, no products were amplified from either cDNA template (Fig. 3.2.3). In contrast, PCR products of *ca.* 650 bp were successfully amplified with cDNA templates from 2 μg of poly(A)$^+$mRNA (Fig. 3.2.3, lane 3, 4 and 5). This result suggests that the ratio between cDNA templates and primers may be an important factor for PCR amplification. As well, the requirement of an increased amount of templates for the PCR may suggest even lower level of ACS gene expression in the developing apex, when compared with leaf 1 and leaf 2.

Each RT-PCR product of *ca.* 650 bp from leaf 2 was precipitated with ethanol and separated on a 1.2% (w/v) agarose gel (data not shown). The DNA of correct size was recovered from the gel, cloned into the pCR 2.1 vector using TA complementary matching, and the vectors were then transformed into *E. coli* strain DH5α . The presence of inserts in plasmids prepared from selected colonies was confirmed by EcoRI digestion (Fig. 3.2.4). Three sizes of inserts were obtained and the DNA sequences of each were determined.

Six DNA sequences were obtained and designated as ACS1, ACS2, ACS3, ACS4, ACS5 and ACS6. These sequences were divided into three groups (Table 3.2.1), according to sequence homology to ACSS, an ACS gene cloned from senescent leaves in white clover (Butcher, 1997). ACS3 and ACS5 belong to group I (685 bp), and these sequences show 92 to 94% homology to the reference sequence (ACSS). ACS1 was assigned to group II (674 bp)

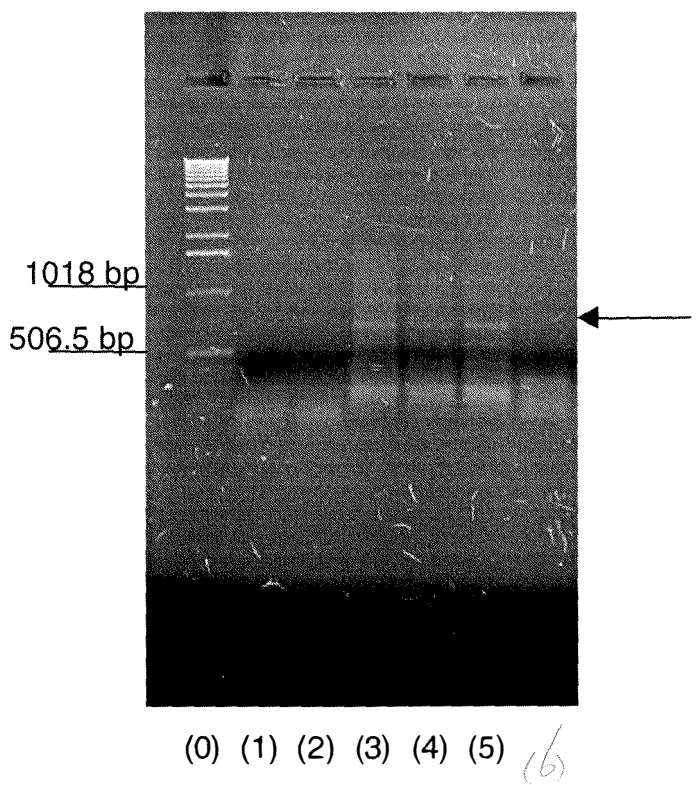

Figure 3.2.3 PCR amplification of putative ACS cDNAs using RT-generated cDNA templates from poly(A)$^+$mRNA isolated from the apex. Second round PCR products, amplified using two nested sets of degenerate primers (Table 2.4), were separated on a 1.2% (w/v) agarose gel and visualised with ethidium bromide. Lanes (1) and (2) are PCR products generated from cDNA templates from 1 μg poly(A)$^+$mRNA. Lanes (3), (4) and (5) are PCR products from cDNA generated from 2 μg poly(A)$^+$mRNA. Lane (6) are PCR products from cDNA templates generated from 3 μg poly(A)$^+$mRNA. Lane (0) are molecular size markers with two sizes indicated. The arrow indicates a 650 bp amplification product.

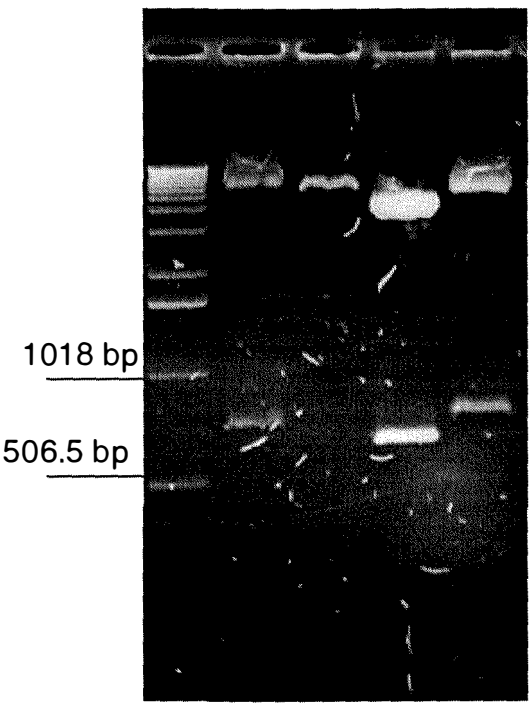

Figure 3.2.4 Cloning of cDNAs putatively encoding ACC synthase in a newly initiated leaf (leaf 2) of white clover using RT-PCR. Inserts obtained from EcoRI-digestion of pCR 2.1 plasmids containing putative ACC synthase sequences (leaf 2; Fig. 3.2.1, lane 3) were separated on a 1.2% (w/v) agarose gel and visualised with ethidium bromide. Lanes (1-4) are from four colonies of *E. coli*, grown on LB-Amp^{100} plate. Lane (2) represents a false positive colony. Lane (0) are molecular size markers with two sizes indicated.

with 72% homology to ACSS. ACS2, ACS4, and ACS6 were assigned to group III (700 bp), which show relatively low homology (64 to 65%) to ACSS (Table 3.2.1).

Table 3.2.1 Homology values of ACC synthase DNA sequences generated by RT-PCR in white clover with a reference sequence, ACSS*.

	Apex		Leaf 2	
	Sequence	Homology	Sequence	Homology
Group I (TRACS1)				
	ACS8	93%	ACS3	94%
			ACS5	92%
Group II (TRACS2)				
			ACS1	72%
Group III (TRACS3)				
	ACS7	64%	ACS2	64%
			ACS4	64%
			ACS6	65%

* ACC synthase gene cloned by RT-PCR with RT-generated cDNA templates made from total RNA isolated from senescent leaf tissues of white clover (Butcher, 1997).

Group I, II and III were redesignated as TRACS1, TRACS2 and TRACS3, respectively. The identification of these distinct groups indicates that the ACS genes expressed in leaf 2 might comprise more than one member of the putative ACS multigene family in white clover.

The *ca.* 650 bp PCR amplification products from the apex was also cloned into pCR 2.1 and transformed into *E. coli* DH5α. Two DNA sequences were generated from plasmids and designated as ACS7 and ACS8. The DNA sequences of ACS7 and ACS8 showed low homology with each other, but could be placed into group III (TRACS3) and group I (TRACS1) respectively, based on their nucleotide sequence homology to ACSS (Table 3.2.1).

3.2.1.2 Sequence analysis of ACS cDNA

The consensus nucleotide sequences of TRACS1, TRACS2 and TRACS3 are shown in figure 3.2.5, figure 3.2.6 and figure 3.2.7, respectively. The sequence homology of TRACS1 was 72% and 64% with TRACS2 and TRACS3, respectively. The homology between TRACS2 and TRACS3 was 63% (Table 3.2.2).

Table 3.2.2 Homology values of three ACS cDNAs identified in white clover.

	TRACS1	TRACS2	TRACS3
TRACS1	-	72%	64%
TRACS2	72%	-	63%
TRACS3	64%	63%	-

Searching GenBank database using the Blast-N programme revealed that the three TRACS genes showed high homology (70% to 79%) to ACS genes reported from other plant species (Table 3.2.3). This high similarity confirms that the RT-PCR-based gene cloning successfully generated ACS DNA homologues in white clover.

TRACS1 (680bp)

ACSR1F *GCCGAATTCATGGGNYTNGCNGARAAY*

ACSR2F *CTGGATCCGT WYCARGAYTA YCAYGG*

```
   1  CTGGATCCGT TCCAGGATTA TCACGGTTTA CCAGAGTTCA GAAATGCTGT GGTTAAATTC
        L  D  P   F  Q  D   Y  H  V  L   P  E  F   R  N  A   V  V  K  F
  61  ATGTTTAGAA CCAGAGGAAA CAGAGTAACA TTTGATCCTG ATCGTATTGT CAGGAGTGGT
        M  F  R   T  R  G   N  R  V  T   F  D  P   D  R  I   V  R  S  G
 121  GGAGCAACTG GAGCACATGA GGTTACTGCC TTTTGTTTGG CAGATCCTGG TGATGCTTTT
        G  A  T   G  A  H   E  V  T  A   F  C  L   A  D  P   G  D  A  F
 181  TTGGTACCTA CTCCTTACTA TCCAGGTTTC GATCGAGATT TGAGGTGGAG AACGGGAGTT
        L  V  P   T  P  Y   Y  P  G  F   D  R  D   L  R  W   R  T  G  V
 241  AAACTTGTTC CGGTTATCTG CGAAAGCGCG AATAATTTCA AATTAACAAA ACAAGCTTTA
        K  L  V   P  V  I   C  E  S  A   N  N  F   K  L  T   K  Q  A  L
 301  GAAGAAGCAT ATGAAAAGGC CAAAATTGAT AACATCAGAA TAAAAGGTTT ACTCATAACA
        E  E  A   Y  E  K   A  K  I  D   N  I  R   I  K  G   L  L  I  T
 361  AATCCTTCAA ATCCATTAGG CACAGTTATG GACAGAACCA CATTAAAAAC CGTTGTAAAT
        N  P  S   N  P  L   G  T  V  M   D  R  T   T  L  K   T  V  V  N
 421  TTCATCAACG AAAAGCGTAT TCATCTTATA AGCGATGAAA TTTACGCTGC AACGGTTTTT
        F  I  N   E  K  R   I  H  L  I   S  D  E   I  Y  A   A  T  V  F
 481  AGCCACCCAA GTTTCATAAG CATAGCTGAG ATCATAGAAA AAGAAACAGA CATCGAATGT
        S  H  P   S  F  I   S  I  A  E   I  I  E   K  E  T   D  I  E  C
 541  GGCCGTAACC TTGTTCACAT AGTTTACAGT CTTTCAAAAG ATATGGGATT CCCCGGTTTT
        G  R  N   L  V  H   I  V  Y  S   L  S  K   D  M  G   F  P  G  F
 601  AGAGTCGGTA TAATTTACTC TTACAATGAT ACCGTTGTTA ATTGCGCGCG CAAAATGTCA
        R  V  G   I  I  Y   S  Y  N  D   T  V  V   N  C  A   R  K  M  S
                                                                ATGTCN
 661  AGTTTCAGGT TAAGCTTGAG
        S  F  R   L  S  L
      AGYTTYRSNY TAAGCTTGAG ACSR6R
```

Figure 3.2.5 Nucleotide and deduced amino acid sequences of the protein-coding region of the consensus TRACS1 gene. Two sets of forward primers and a reverse primer (Table 2.4) used for RT-PCR are given in Italics.

TRACS2 (674bp)

ACSR1F *GCCGAATTCATGGGNYTNGCNGARAAY*

ACSR2F *CTGGATCCGT WYCARGAYTA YCAYGG*

```
     1  CTGGATCCGT TCCAGGATTA CCATGGATTG CCAGAATTCA GAAATGCTGT GGCAAATTTC
          L  D  P   F  Q  D   Y  H  G  L   P  E  F   R  N  A   V  A  N  F
    61  ATGTCAAAAG TGAGAGGTGG TAGGGTAAGA TTTGATCCTG ACCGTATATT GATGAGTGGT
          M  S  K   V  R  G   G  R  V  R   F  D  P   D  R  I   L  M  S  G
   121  GGAGCAACAG GGGCAAATGA ATTAATCATG TTCTGTTTGG CTGATCCTGG TGATGCCTTT
          G  A  T   G  A  N   E  L  I  M   F  C  L   A  D  P   G  D  A  F
   181  TTGGTTCCTA GCCCTTATTA TCCAGCATTT GTTCGTGATT TGTGTTGGAG AACCGGTGTG
          L  V  P   S  P  Y   Y  P  A  F   V  R  D   L  C  W   R  T  G  V
   241  CAACTAATTC CTGTCCAATG TCATAGCTCA AACAATTTCA AGATAACAAG AGAAGCACTT
          Q  L  I   P  V  Q   C  H  S  S   N  N  F   K  I  T   R  E  A  L
   301  GAAGAAGCTT ATATGAAAGC ACAAGAAAGA AACATCAATG TGAAAGGGTT AATCATAACA
          E  E  A   Y  M  K   A  Q  E  R   N  I  N   V  K  G   L  I  I  T
   361  AATCCATCAA ACCCTCTAGG AACAACAATA GAAAAAGAAA CACTAAAGAG CATAGTTAGT
          N  P  S   N  P  L   G  T  T  I   E  K  E   T  L  K   S  I  V  S
   421  TTCATCAATG AAAACAACAT TCATTTAGTT TGTGATGAAA TCTATTCCGG CACAGTTTTC
          F  I  N   E  N  N   I  H  L  V   C  D  E   I  Y  S   G  T  V  F
   481  GACACTCCGA AATACTTAAT TGTCGCCGAA GTTATACAAG AAATGGAAGA ATGCAAAAAA
          D  T  P   K  Y  L   I  V  A  E   V  I  Q   E  M  E   E  C  K  K
   541  GAACTCATTC ATATCATATA TAGTTTATCC AAAGACATGG GACTTCCTGG TTTCAGAGTC
          E  L  I   H  I  I   Y  S  L  S   K  D  M   G  L  P   G  F  R  V
   601  GGTTTAATTT ACTCTTACAA TGATACCGTT GTTAACTGCG CGCGCAAAAT GTCCAGCTTT
          G  L  I   Y  S  Y   N  D  T  V   V  N  C   A  R  K   M  S  S  F
                                                              AT GTCNAGYTTY
   661  ACGTTAAGCT TGAG
          T  L  S   L
        RSNYTAAGCT TGAG ACSR6R
```

Figure 3.2.6 Nucleotide and deduced amino acid sequences of the protein-coding region of the consensus TRACS2 gene. Two sets of forward primers and a reverse primer (Table 2.4) used for RT-PCR are given in Italics.

TRACS3 (704bp)

ACSR1F *GCCGAATTCATGGGNYTNGCNGARAAY*

ACSR2F *CTGGATCCGT WYCARGAYTA YCAYGG*

```
   1  CTGGATCCGT ACCAGGACTA CCACGGTCTC CCTTCATTCA AACAAGCATT GGTAGATTTC
        L  D  P    Y  Q  D    Y  H  G  L    P  S  F    K  Q  A    L  V  D  F
  61  ATGGCCGAGA TCAGAGGAAA CCGAGTTTCC TTTGATCCCA ACCATATAGT TCTCACTGCC
        M  A  E    I  R  G    N  R  V  S    F  D  P    N  H  I    V  L  T  A
 121  GCCTCTACTT CCGCAAACGA GACTCTAATG TTTTGTCTCG CCGAGAAAGG AGAAGCATTT
        A  S  T    S  A  N    E  T  L  M    F  C  L    A  E  K    G  E  A  F
 181  CTCCTTCCTA CTCCTTACTA TCCAGGATTT GATAGAGATC TTAAATGGAG AACTGGTGTT
        L  L  P    T  P  Y    Y  P  G  F    D  R  D    L  K  W    R  T  G  V
 241  GAGATTGTTC CAATACAATG CAATAGCTCC ACCAACTTTC AAATAACTGA ACAAGCATTA
        E  I  V    P  I  Q    C  N  S  S    T  N  F    Q  I  T    E  Q  A  L
 301  CAACAAGCAT ACAAAGATGC ACAAGAGCGC AACCTTAAAG TCAAAGGAGT AATGGTTACA
        Q  Q  A    Y  K  D    A  Q  E  R    N  L  K    V  K  G    V  M  V  T
 361  AACCCATCAA ACCCGTTAGG CACCACATTG TCAAGGAGTG AATTAAATCT TCTCGTTGAC
        N  P  S    N  P  L    G  T  T  L    S  R  S    E  L  N    L  L  V  D
 421  TTTATTGAAG AAAACAAAAA CATGCCATTT GATAAGCGAC GAGATTTACT CCGGGACTGT
        F  I  E    E  N  K    N  M  P  F    D  K  R    R  D  L    L  R  D  C
 481  TTTTTTCCTT CTCCAAGTTT TATCAGTGTT ATGGAAATCC TTAAGGAAAG AAATGACCTT
        F  F  P    S  P  S    F  I  S  V    M  E  I    L  K  E    R  N  D  L
 541  CAGGATTTCA AACACACTGA TAATATTTGC GAGAGAGTTC ATGTTGTCTA TAGTCTTTCC
        Q  D  F    K  H  T    D  N  I  C    E  R  V    H  V  V    Y  S  L  S
 601  AAAGACTTGG GTTTGCCAGG TTTCCGCGTT GGTGCACTTT ACTCCGAAAA CGATGAAGTT
        K  D  L    G  L  P    G  F  R  V    G  A  L    Y  S  E    N  D  E  V
 661  GTCGCAGCTG CAACCAAGAT GTCCAGCTTC GCCTTAAGCT TGAG
        V  A  A    A  T  K    M  S  S  F    A  L  S    L
                          AT GTCNAGYTTY RSNYTAAGCT TGAG ACSR6R
```

Figure 3.2.7 Nucleotide and deduced amino acid sequences of the protein-coding region of the consensus TRACS3 gene. Two sets of forward primers and a reverse primer (Table 2.4) used for RT-PCR are given in Italics.

In addition, each ACS gene had highest homology to different ACS genes reported in the database. For example, TRACS1 and TRACS3 were homologous to ACS2 (Accession No. AF016459) and ACS1 (Accession No. AF016458) from garden pea (*Pisum sativum*), respectively. TRACS2, however, did not show any significant homology to either sequence. This also suggests that the ACS genes generated by RT-PCR from developing tissue of white clover most likely encode more than one member of an ACS multigene family, so that more than one member of this ACS gene family may be expressed in these tissues.

Table 3.2.3 Comparison of the three ACS cDNAs identified in white clover with sequences available in the GenBank database (searched on 22nd, September 1999).

Reference sequence	Sequences with high homology	Accession No.
TRACS1	*Pisum Sativum* mRNA for ACC synthase (ACS2)	AF016459
	Glycine max mRNA for ACC synthase	X67100
	Vigna radiata ACC synthase mRNA (pAIM-1)	Z11613
	Carica papaya mRNA for ACC synthase (ACCS1)	AJ012577
	Lycopersicon esculentum ACC synthase (LE-ACS1b)	U72390
TRACS2	*Mangifera indica* ACC synthase mRNA (pMIA-1)	U22523
	Lycopersicon esculentum ACC synthase (LE-ACS6)	AB013100
	Solanum tuberosum ACC synthase mRNA (STACS5)	U70842
	Capsicum annum mRNA for ACC synthase (ACC1)	X82265
	Lycopersicon esculentum ACC synthase (LE-ACS1A)	U72389
TRACS3	*Vigna radiata* ACS mRNA (VRACS7)	U34987
	Pisum sativum mRNA for ACC synthase (ACS1)	AF016458
	Phaseolus vulgaris ACS gene (ACS1)	AF053355
	Vigna radiata ACS mRNA (VRACS6)	U34986
	Cucumis sativus CS-ACS3 mRNA for ACC synthase	AB006805

3.2.2 Expression of ACS genes during leaf ontogeny

Northern analysis was performed to determine the relative expression of the ACS genes in the developing apex and newly initiated leaves (leaf 1 and leaf 2). During the electrophoresis of RNA as part of northern analysis, it was observed that the rRNA profile changes during leaf development. For example, the rRNA profiles extracted from the developing apex or newly initiated leaves (leaf 1 and leaf 2) differ from those extracted from a mature green leaf (leaf 3; Fig. 3.2.8). Also, two to three times more poly(A)$^+$mRNA was isolated from the same amount of total RNA pool of the developing apex, when compared with mature green leaves (data not shown). This suggests that total RNA isolated from leaves at different developmental stages contain a different proportion of poly(A)$^+$ mRNA as well as a different rRNA profile. Therefore for northern anlysis, equal loading of poly(A)$^+$mRNA was used.

Two cDNA clones were used as probes, ACS3 and ACS6 (representing TRACS1 and TRACS3, respectively; Table 3.2.1). The probes were labeled with high specificity [α-P^{32}]-dCTP (6000 *Ci*/mmol) using the random priming system and 5 µg poly(A)$^+$mRNA, extracted from apex, leaf 1, and leaf 2, was used for northern analysis.

The TRACS1 probe did not hybridise to any separated mRNA species (data not shown). It may be the major ACS gene expressed in mature green and senescent leaf tissues of white clover, since a homologue (ACSS; Table 3.2.1) was cloned using RT-PCR from leaf tissue of the onset of senescence (Butcher, 1997). The TRACS3 probe hybridised to a mRNA of 1.95 kb (Fig. 3.2.9) and the level of hybridisation was significantly higher in leaf 2, suggesting the expression of this gene is higher in this tissue, when compared with the apex and leaf 1.

The expression pattern of TRACS3, however, does not correlate with the ACC content and ethylene production data, which are highest in the apex and lower in leaf 2 (Fig. 3.1.9; Fig. 3.1.10). To resolve this further, the expression pattern of TRACO2 has to be examined as well. In this thesis, no northern analysis was performed using TRACS2.

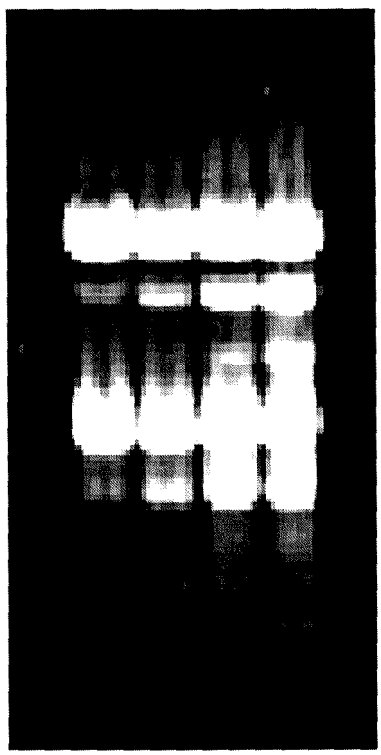

Figure 3.2.8 Total RNA, isolated from the tissue indicated, was separated on a 1.2 % (w/v) agarose-formaldehyde gel and stained with ethidium bromide.

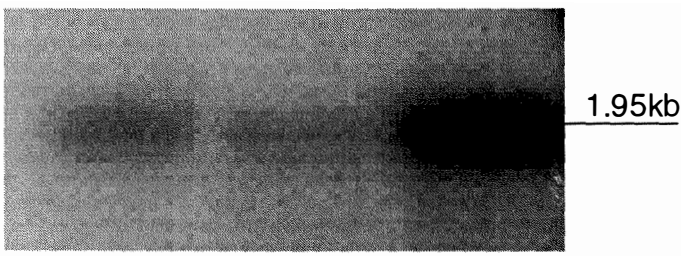

Figure 3.2.9 Expression of TRACS3 in the apex and newly initiated leaves (leaf 1 and leaf 2) determined by northern analysis. Five μg of poly(A)$^+$mRNA was separated on a 1.2 % (w/v) agarose-formaldehyde gel, blotted onto Hybond-N$^+$ with alkaline transfer buffer, probed with ^{32}P-labeled TRACS3 and washed at high stringency (0.1 X SSPE at 65 ^{o}C).

However, it is known that ACC is transport in plants (Jackson, 1985) and so it may be that ACC in the apex originates from other parts of the plant. Also, it has been reported that ACO activity is important to produce ethylene from developing tissue of *A. thaliama* (Smalle *et al.*, 1997a; Smalle *et al.*, 1997b).

Therefore, it is appropriate here to examine the gene expression of ACO (the enzyme which converts ACC to ethylene) in these tissues of white clover.

Part 3: Molecular cloning and characterisation of protein-coding regions of ACC oxidase genes in white clover

3.3.1 ACC oxidase genes in developing tissues of white clover

3.3.1.1 Cloning and sequencing of protein-coding regions of putative ACC oxidase genes expressed in the developing apex and a newly initiated leaf (leaf 2)

Putative ACO genes were amplified using RT-PCR with cDNA templates generated by RT-treatment of total RNA extracted from the developing apex (Fig. 3.3.1A) and a newly initiated leaf (leaf 2; Fig. 3.3.2A) of white clover. The PCR products of an expected size (*ca.* 800 bp) were amplified with two nested sets of degenerate primers provided by Professor Shang Fa Yang (UC, Davis) (First round with ACOF1 and ACOF2, second round ACOF2 and ACOR2; Table 2.4). The amplified product was only detected after two rounds of PCR, in common with ACS (section 3.2.1.1). This requirement for two rounds of PCR suggests that the expression of the putative ACO genes is not high in these tissues.

The PCR products were cloned into the pCR 2.1 vector and transformed into *E. coli* strain DH5α. Inserts were sized after EcoRI-digestion of plasmid DNA and DNA sequences of the inserts (*ca.* 800 bp) obtained.

Two inserts of the PCR products (Fig. 3.3.1B) generated from the apex were sequenced and designated as ACO1 and ACO2. The DNA sequences of ACO1 and ACO2 showed highest homology (99%) to each other, but much lower homology to TRACO2 (77%; Table 3.3.1) and TRACO3 (75%), ACO genes identified in mature green and senescent leaf tissues of white clover, respectively (Hunter, 1998; Hunter *et al.*, 1999).

ACO1 and ACO2 were, therefore, redesignated as TRACO1. The nucleotide and deduced amino acid consensus TRACO1 sequences, constructed from ACO1 and ACO2, are shown in figure 3.3.3.

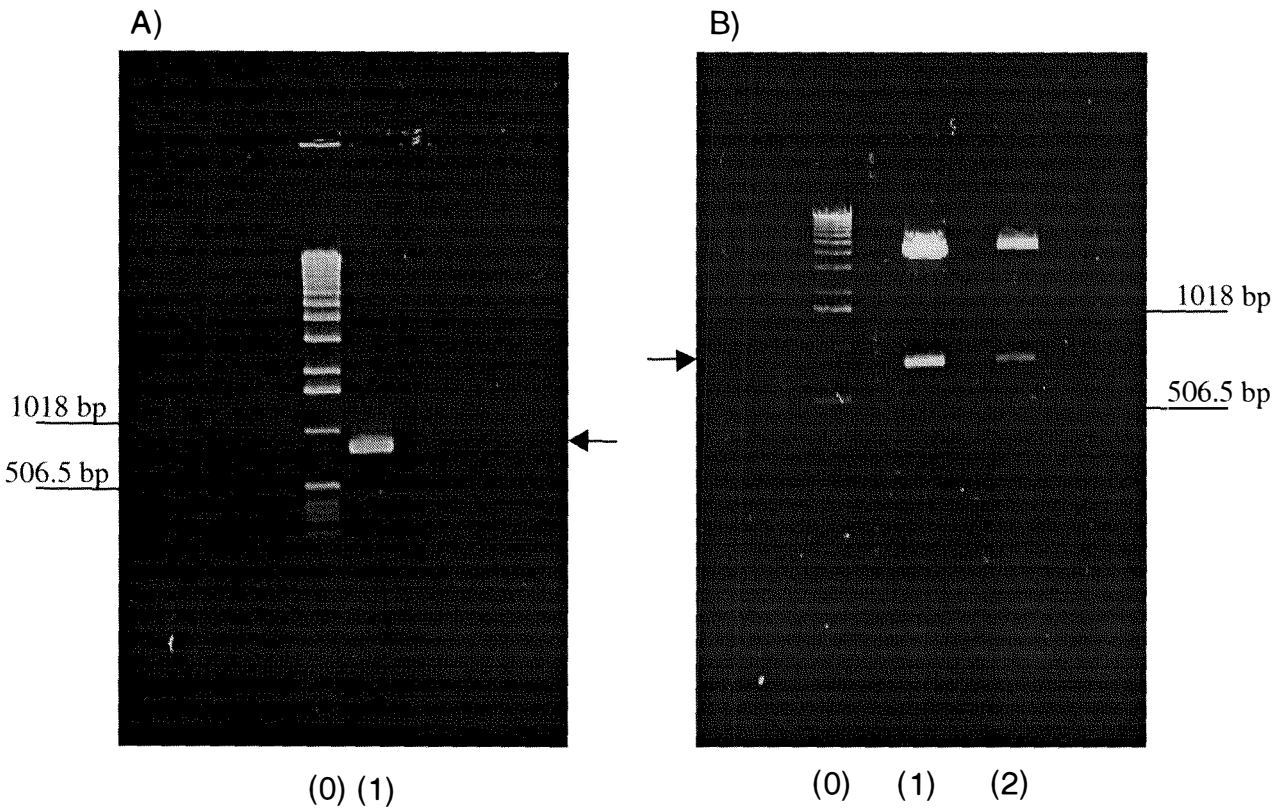

Figure 3.3.1 PCR amplification of a putative ACO cDNA using RT-generated cDNA templates from total RNA isolated from the apex. (A) PCR products (lane 1) were separated on a 1.2% (w/v) agarose gel and visualised with ethidium bromide. (B) Inserts obtained from EcoRI digestion of pCR 2.1 vectors containing putative ACC oxidase sequences (panel A lane 1) were separated on a 1.2% (w/v) agarose gel and visualised with ethidium bromide. Lanes (1) and (2) are digestion products of plasmids isolated from two *E. coli* colonies grown on LB-Amp^{100} plates. Lane (0) are molecular size markers with two sizes indicated. The arrows indicate a *ca.* 800 bp amplification product.

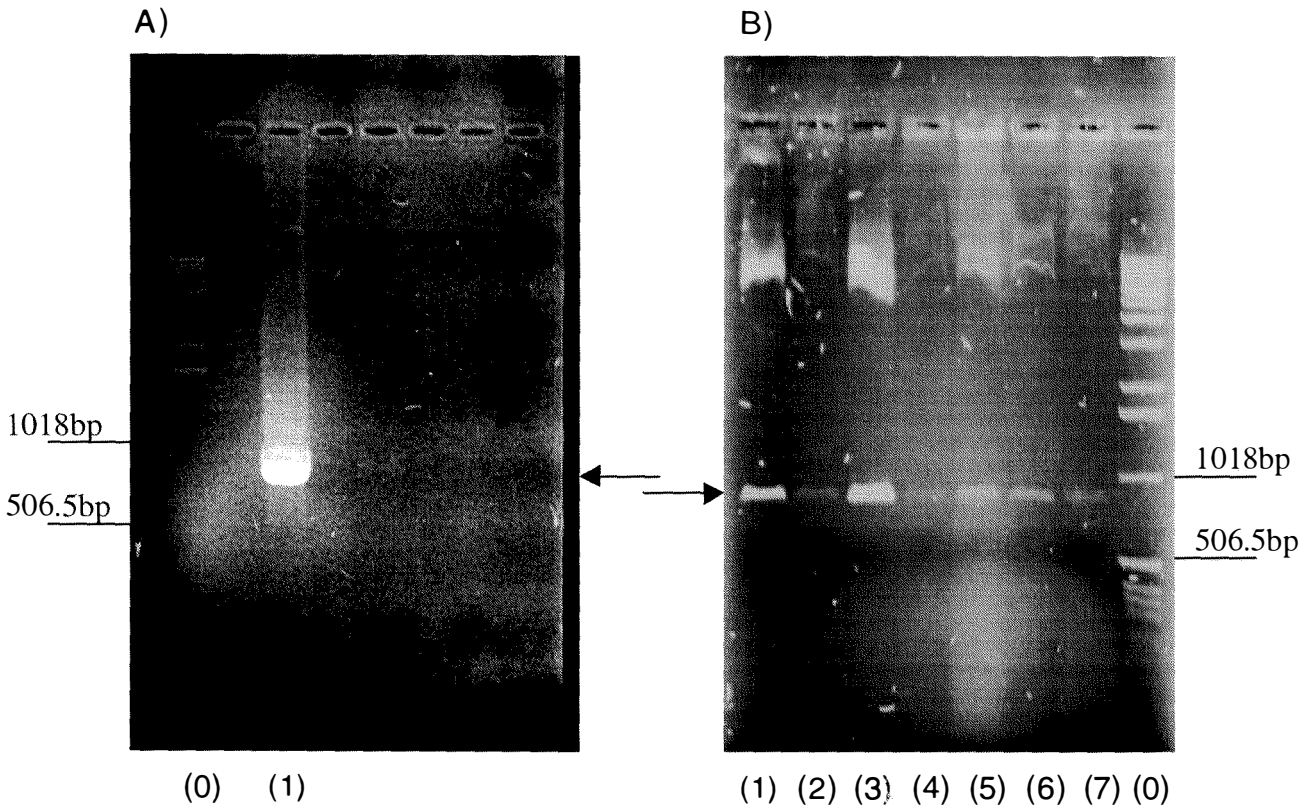

Figure 3.3.2 PCR amplification of putative ACO cDNAs using RT-generated cDNA templates from total RNA isolated from a newly initiated leaf (leaf 2). (A) PCR products (lane 1) were separated on a 1.2% (w/v) agarose gel and visualised with ethidium bromide. (B) Inserts obtained from EcoRI digestion of pCR 2.1 vectors containing putative ACC oxidase sequences (panel A lane 1) were separated on a 1.2% (w/v) agarose gel and visualised with ethidium bromide. Lane (1-7) are digestion products of plasmids isolated from 7 *E. coli* colonies grown on LB-Amp^{100} plates. Lane (0) are molecular size markers with two sizes indicated. The arrows indicate a *ca.* 800 bp amplification product.

Table 3.3.1 Homology values of partial protein-coding regions of ACC oxidase nucleotide sequences generated by RT-PCR in white clover with a reference, TRACO2*.

Apex		Leaf 2		
Sequence	Homology	Sequence	Homology	Nomenclature
ACO1	77%			TRACO1
ACO2	77%			
		ACO3	97%	TRACO2*
		ACO4	95%	
		ACO5	95%	
		ACO6	95%	
		ACO7	88%	TRACO3*

* ACC oxidase genes cloned by RT-PCR with RT-generated cDNA template from RNA isolated from mature green leaf tissue of white clover (Hunter, 1998).

Five inserts of the correct size for PCR products generated from leaf 2 were sequenced (Fig. 3.3.2B, lane 1, 3, 5, 6, and 7), and designated as ACO3, ACO4, ACO5, ACO6, and ACO7. Sequence alignment showed high homology (91-98 %) among these five DNA sequences to each other. When the ACO sequences, except ACO7, generated by RT-PCR from leaf 2 were aligned with that of TRACO2 (Hunter *et al.* 1999), homology values of 95-97% were obtained (Table 3.3.1). With this high sequence homology, this group of putative ACO sequences was redesignated as TRACO2. The nucleotide and deduced amino acid consensus TRACO2 sequences, constructed from the four ACO sequences, are shown in figure 3.3.4. This consensus sequence is identical to TRACO2 generated by RT-PCR from mature green leaves of white clover (Hunter, 1998; Hunter *et al.*, 1999)

TRACO1 (813bp)

ACOF1 *GAYGCNTGYSANA AYTGGGG*
ACOF2 *GCNTGYSANA AYTGGGGHTT*

```
   1  GCTTGCGAGA ATTGGGGCTT CTTTGAGTTG GTGAACCATG GAATATCTAT TGAGATGATG
        A  C  E    N  W  G    F  F  E  L    V  N  H    G  I  S    I  E  M  M
  61  GACAAAGTGG AGAAGCTCAC AAAAGATCAC TACAAGAAGT GTATGGAACA AAGGTTCAAA
        D  K  V    E  K  L    T  K  D  H    Y  K  K    C  M  E    Q  R  F  K
 121  GAAATGGTTT CAAGCAAAGG TTTGGAGTGT GTTCAGTCAG AAATAAATGA CTTAGATTGG
        E  M  V    S  S  K    G  L  E  C    V  Q  S    E  I  N    D  L  D  W
 181  GAAAGCACTT TCTTTTTGCG CCATCTTCCA TTTTCTAATA TTTCAGAGAT CCCAGATCTT
        E  S  T    F  F  L    R  H  L  P    F  S  N    I  S  E    I  P  D  L
 241  GATGATGATT ACAGGAAGAT AATGAAGGAA TTTGCACAAA AATTAGAGAA TCTGGCTGAG
        D  D  D    Y  R  K    I  M  K  E    F  A  Q    K  L  E    N  L  A  E
 301  GAACTTCTTG ACTTATTATG TGAGAATCTT GGGCTTGAAA AAGGGTATTT GAAGAAGGTG
        E  L  L    D  L  L    C  E  N  L    G  L  E    K  G  Y    L  K  K  V
 361  TTTTATGGTT CAAAGGGTCC AAACTTTGGT ACAAAAGTTA GTAACTATCC TCCTTGTCCT
        F  Y  G    S  K  G    P  N  F  G    T  K  V    S  N  Y    P  P  C  P
 421  AAGCCTGACC TTATTAAGGG ACTTAGAGCC CATACAGATG CTGGTGGCAT CATCCTTCTC
        K  P  D    L  I  K    G  L  R  A    H  T  D    A  G  G    I  I  L  L
 481  TTCCAAGATG ACAAAGTCAG TGGACTTCAG CTCCTCAAAG ATGACCAATG GATTGATGTC
        F  Q  D    D  K  V    S  G  L  Q    L  L  K    D  D  Q    W  I  D  V
 541  CCTCCAATGC GTCACTCTAT TGTCATCAAC CTTGGTGATC AACTTGAAGT CATAACAAAT
        P  P  M    R  H  S    I  V  I  N    L  G  D    Q  L  E    V  I  T  N
 601  GGGAAGTACA AGAGTGTGAT GCATAGAGTA ATTGCTCAAA CAGATGGTGC TAGAATGTCT
        G  K  Y    K  S  V    M  H  R  V    I  A  Q    T  D  G    A  R  M  S
 661  TTAGCTTCAT TCTATAATCC AAGTGATGAT GCTATCATTT CACCAGCACC AACTTTATTG
        L  A  S    F  Y  N    P  S  D  D    A  I  I    S  P  A    P  T  L  L
 721  AAGGAAAATG AAACAACAAG TGAAATTTAT CCAAAATTTG TGTTTGATGA TTACATGAAA
        K  E  N    E  T  T    S  E  I  Y    P  K  F    V  F  D    D  Y  M  K
 781  CTCTATATGG GATTAAAGTT CCAGGCCAAA GAG
        L  Y  M    G  L  K    F  Q  A  K    E
```

AARTT YCARGCNAAR GAR ***ACOR2***
AAR GARCCNMGNTTYGA ***ACOR1***

Figure 3.3.3 Nucleotide and deduced amino acid sequences of the protein-coding region of the consensus TRACO1 gene. The two nested sets of degenerated primers used for RT-PCR are given in Italics.

TRACO2 (804bp)

ACOF1 *GAYGCNTGYSANA AYTGGGG*
ACOF2 *GCNTGYSANA AYTGGGGHTT*

```
   1  GCATGCGAGA ATTGGGGCTT CTTTGAGCTG GTGAATCATG GCATATCTCA TGACTTAATG
        A  C  E   N  W  G   F  F  E  L   V  N  H   G  I  S   H  D  L  M
  61  GACACTGTGG AAAGGTTGAC AAAAGAACAC TACAGGATAT GCATGGAACA AAGATTCAAG
        D  T  V   E  R  L   T  K  E  H   Y  R  I   C  M  E   Q  R  F  K
 121  GATTTGGTGG CCAACAAAGG ACTAGAGGCT GTTCAAACTG AGGTCAAAGA CATGGACTGG
        D  L  V   A  N  K   G  L  E  A   V  Q  T   E  V  K   D  M  D  W
 181  GAGAGTACCT TCCACTTGCG TCACCTACCT GAGTCAAACA TTTCAGAGGT CCCTGATCTC
        E  S  T   F  H  L   R  H  L  P   E  S  N   I  S  E   V  P  D  L
 241  ACTGATGAAT ACAGGAAAGC AATGAAGGAA TTTGCTTTGA AGCTAGAGAA ACTAGCAGAG
        T  D  E   Y  R  K   A  M  K  E   F  A  L   K  L  E   K  L  A  E
 301  GAGCTGCTAG ACTTATTATG TGAGAATCTT GGACTAGAAA AGGGATACCT CAAAAAAGCC
        E  L  L   D  L  L   C  E  N  L   G  L  E   K  G  Y   L  K  K  A
 361  TTTTATGGAT CAAAGGGACC AACTTTTGGC ACCAAGGTTG CAAACTACCC TCCATGCCCA
        F  Y  G   S  K  G   P  T  F  G   T  K  V   A  N  Y   P  P  C  P
 421  AAACCAGACC TTGTAAAAGG TCTCCGAGCA CACACCGATG CCGGTGGAAT AATCCTCCTT
        K  P  D   L  V  K   G  L  R  A   H  T  D   A  G  G   I  I  L  L
 481  TTCCAAGATG ACAAAGTCAG TGGCCTTCAG CTTCTCAAAG ATGGTAAATG GGTAGATGTT
        F  Q  D   D  K  V   S  G  L  Q   L  L  K   D  G  K   W  V  D  V
 541  CCTCCCATGC ATCATTCCAT TGTCATCAAC CTTGGTGACC AACTCGAGGT AATAACAAAT
        P  P  M   H  H  S   I  V  I  N   L  G  D   Q  L  E   V  I  T  N
 601  GGTAAGTACA GGAGTGTGGA ACATCGTGTG ATAGCACAAA GTGATGGAAC AAGAATGTCC
        G  K  Y   R  S  V   E  H  R  V   I  A  Q   S  D  G   T  R  M  S
 661  ATAGCTTCAT TCTACAATCC TGGTAGTGAT GCTGTTATCT ATCCAGCAAC AACATTGATT
        I  A  S   F  Y  N   P  G  S  D   A  V  I   Y  P  A   T  T  L  I
 721  GAAGAGAATA ATGAAGTTTA CCCAAAATTT GTTTTTGAAG ATTACATGAA TCTTTATGCT
        E  E  N   N  E  V   Y  P  K  F   V  F  E   D  Y  M   N  L  Y  A
 781  GGATTAAAGT TTCAAGCTAA AGAA
        G  L  K   F  Q  A   K  E

          AART TYCARGCNAA RGAR ***ACOR2***
                       AA RGARCCNMGNTTYGA ***ACOR1***
```

Figure 3.3.4 Nucleotide and deduced amino acid sequences of the protein-coding region of the consensus TRACO2 gene. The two nested sets of degenerated primers used for RT-PCR are given in Italics.

However, the ACO7 sequence showed relatively low homology (88%) to that of TRACO2, whereas it showed much higher homology (97%) to that of TRACO3 (Table 3.3.1; Hunter *et al.*, 1999). Therefore, ACO7 was redesignated as TRACO3. The nucleotide and deduced amino acid sequences of TRACO3 (ACO7) are shown in figure 3.3.5. This consensus sequence is identical to TRACO3 generated by RT-PCR from senescent leaves of white clover (Hunter, 1998; Hunter *et al.*, 1999).

The nucleotide sequence homology of three putative ACO genes, designated as TRACO1, TRACO2 and TRACO3, in white clover are summarised in table 3.3.2. The sequence homology of TRACO1 is 77% and 75% with respect to TRACO2 and TRACO3. The homology between TRACO2 and TRACO3 is 84%.

Table 3.3.2 Homology values of protein-coding regions of three TRACO nucleotide sequences.

	TRACO1	TRACO2	TRACO3	Main tissue type used for isolation of RNA for RT-PCR
TRACO1	-	77	75	apex
TRACO2	77	-	84	leaf 2
TRACO3	75	84	-	leaf 2

The sequences generated from two different tissues (apex and leaf 2) of white clover suggest that three members of an ACO gene family may be differentially expressed in each tissue of white clover. The TRACO1 gene may be expressed predominantly in the apex, but the limited number of sequenced colonies (two sequences) cannot exclude the possibility of other ACO

TRACO3 (816bp)

ACOF1 *GAYGCNTGYSANAAYTGGGG*
ACOF2 *GCNTGYSANAAYTGGGGHTT*

```
   1  GCATGCCAGA ATTGGGGATT CTTTGAGCTG GTGAATCATG GCATACCTCA TGACCTTATG
        A  C  Q    N  W  G    F  F  E  L    V  N  H    G  I  P    H  D  L  M
  61  GACACATTGG AGAGATTGAC CAAAGAGCAC TACAGGAAAT GCATGGAGCA GAGGTTTAAG
        D  T  L    E  R  L    T  K  E  H    Y  R  K    C  M  E    Q  R  F  K
 121  GAATTGGTAT CAAGCAAAGG CTTAGATGCT GTCCAAACTG AGGTCAAAGA TATGGATTGG
        E  L  V    S  S  K    G  L  D  A    V  Q  T    E  V  K    D  M  D  W
 181  GAAAGTACCT TCCATGTTCG ACATCTCCCT GAATCAAACA TTTCAGAGCT CCCTGATCTC
        E  S  T    F  H  V    R  H  L  P    E  S  N    I  S  E    L  P  D  L
 241  AGTGATGAAT ACAGGAAGGT GATGAAGGAA TTTTCTTTGA GGTTAGAGAA GCTAGCAGAA
        S  D  E    Y  R  K    V  M  K  E    F  S  L    R  L  E    K  L  A  E
 301  GAGCTTTTGG ACTTGTTATG TGAGAATCTT GGACTTGAAA AAGGTTACCT CAAAAAGGCC
        E  L  L    D  L  L    C  E  N  L    G  L  E    K  G  Y    L  K  K  A
 361  TTCTATGGAT CAAGAGGACC AACTTTCGGC ACCAAGGTAG CCAACTACCC TCAATGCCCT
        F  Y  G    S  R  G    P  T  F  G    T  K  V    A  N  Y    P  Q  C  P
 421  AATCCAGAGC TGGTGAAGGG TCTCCGTGCT CACACCGATG CCGGTGGGAT CATCCTTCTC
        N  P  E    L  V  K    G  L  R  A    H  T  D    A  G  G    I  I  L  L
 481  TTCCAGGATG ACAAAGTCAG CGGCCTTCAG CTACTCAAAG ACGACGAGTG GATCGATGTT
        F  Q  D    D  K  V    S  G  L  Q    L  L  K    D  D  E    W  I  D  V
 541  CCCCCAATGC GTCACTCCAT TGTTGTCAAC CTTGGTGACC AGCTCGAGGT AATAACAAAT
        P  P  M    R  H  S    I  V  V  N    L  G  D    Q  L  E    V  I  T  N
 601  GGTAAATATA AGAGTGTGGA GCACCGTGTG ATAGCACAAA CAAATGGAAC AAGAATGTCT
        G  K  Y    K  S  V    E  H  R  V    I  A  Q    T  N  G    T  R  M  S
 661  ATAGCATCAT TCTACAACCC TGGAAGTGAT GCTGTAATCT ACCCTGCTCC AGAATTGTTG
        I  A  S    F  Y  N    P  G  S  D    A  V  I    Y  P  A    P  E  L  L
 721  GAAAAAGAAA CAGAGGAAAA AACCAATGTG TATCCTAAAT TTGTGTTTGA AGAGTACATG
        E  K  E    T  E  E    K  T  N  V    Y  P  K    F  V  F    E  E  Y  M
 781  AAGATCTATG CTGCTTTGAA ATTTCAAGCT AAGGAA
        K  I  Y    A  A  L    K  F  Q  A    K  E
```

AARTTYCARGCNAARGAR ***ACOF2***
AARGARCCNMGNTTYGA ***ACOR1***

Figure 3.3.5 Nucleotide and deduced amino acid sequences of the protein-coding region of the consensus TRACO3 gene. The two nested sets of degenerated primers used for RT-PCR are given in Italics.

genes being expressed in the apex. In leaf 2, it appears that both TRACO2 and TRACO3 are expressed with TRACO2 sequence comprising the majority of colonies generated from the RT-PCR reaction. TRACO3, known to be highly expressed in senescent leaf tissue (Hunter, 1998; Hunter *et al.*, 1999), appears not to be expressed abundantly in these tissues as determined by relative abundance in the RT-PCR generated sequences. However, further analysis of ACO gene expression was carried using northern hybridisation (section 3.3.3).

3.3.1.2 Sequence analysis of protein-coding regions of putative ACO genes

All three ACO genes in white clover were 70 to 80% homologous to the nucleotide sequences of ACO genes reported from other plant species in the GenBank database. The deduced amino acid sequences of all three ACO genes in white clover showed 84% identity to a consensus sequence constructed from ACO genes reported in the GenBank database (Fig. 3.3.6; Kadyrzhanova *et al.*, 1997). This high sequence identity at amino acid sequence level, as well as the nucleotide sequence level, confirms that ACO gene sequences were generated successfully from white clover using RT-PCR.

On comparison of the five sequences with high homology to each TRACO gene (Table 3.3.3), the gene sequences with highest homology to TRACO1 were very different from those with highest homology to TRACO2 and TRACO3. For example, TRACO2 and TRACO3 shared highest homology with an ACO gene in bean (*Phaseolus vulgaris*; Accession number AF053354), whereas TRACO1 showed highest homology to an ACO gene in pea (*Pisum sativum*; Accession number g398997), suggesting that TRACO1 is distinct from the other two ACO genes in white clover.

Phylogenetic analysis using the deduced amino acid sequences also confirmed that the two ACO genes generated from leaf 2, TRACO2 and TRACO3 were much closer to each other, when compared with TRACO1 generated from the developing apex (Fig. 3.3.7). TRACO2 and TRACO3 were clustered together with an ACO gene cloned from bean (PV-ACO). TRACO1 clustered with ACO genes cloned from pea seedlings (PS-ACO1).

Table 3.3.3 Comparison of the three ACO cDNAs identified in white clover with sequences available in the GenBank database (searched on 22nd, September 1999).

Reference sequence	Sequences producing high homology	Accession No.
TRACO1	*Pisum sativum* PS-ACO1	g398997
	Vigna radiata clone pVR-ACO1	U06046
	Vigna radiata clone pVR-ACO2	U06047
	Carica papaya ACC oxidase mRNA	U68215
	Cucumis sativus ACC oxidase2	AF033582
TRACO2	*Phaseolus vulgaris* ACC oxidase	AF053354
	Prunus perscica PAO1 mRNA	X77232
	Carica papaya ACC oxidase mRNA	U68215
	Vigna angularis mRNA for ACC oxidase	AB002667
	Petunia hybrida L ethylene forming enzyme	g169210
TRACO3	*Phaseolus vulgaris* ACC oxidase	AF053354
	Prunus perscica PAO1 mRNA	X77232
	Vigna angularis mRNA for ACC oxidase	AB002667
	Carica papaya ACC oxidase mRNA	U68215
	Passiflora edulis PE-ACO1 mRNA	AB015493

```
ACOCON   MENFPIINLEKLNGEERAATMEMIKD
TRACO1   ----------------------------
TRACO2   ----------------------------
TRACO3   ----------------------------

ACOCON   ACENWGFFELVNHGIPHELMDTVEKMTKEHYKKCMEQRFKELVASKGLEAVQAEVTDIDW
TRACO1   ..............SI.M..K...L..D...........M.S.....C..S.IN.L..
TRACO2   ..............S.D......RL.....RI.......D...N.......T..K.M..
TRACO3   ..Q............D....L.RL.....R..........S....D...T..K.M..

ACOCON   ESTFFLRHLPVSNISEVPDLDDEYREVMKDFAKRLEKLAEELLDLLCENLGLEKGYLKKA
TRACO1   ..........F.....I.....D..KI..E..QK..N.....................V
TRACO2   ....H.....E.........T....KA..E..LK.........................
TRACO3   ....HV....E.....L...S....K...E.SL..........................

ACOCON   FYGSKGPNFGTKVSNYPPCPKPDLIKGLRAHTDAGGIILLFQDDKVSGLQLLKDGQWIDV
TRACO1   ..................................................D.....
TRACO2   .......T.....A..........V.............................K.V..
TRACO3   ....R..T.....A...Q..N.E.V.............................DE....

ACOCON   PPMRNSIVVNIGDQLEVITNGKYKSVMHRVIAQTDGTRMSIASFYNPGSDAVIYPAPALV
TRACO1   ....H...I.L.........................A...L......SD..I.S...T.L
TRACO2   ...HH...I.L............R..E......S.....................TT.-
TRACO3   ....H.....L..............E.......N.....................E.L

ACOCON   EKLEAEKG-VYPKFVFDDYMKLYAGLKFQAKE
TRACO1   KEN.TTSE-I.............M........
TRACO2   --I.ENNE-.......E...N...........
TRACO3   ..ETE..TN.......EE...I..A.......

ACOCON   PRFEAMMAMESDPIATA
TRACO1   -----------------
TRACO2   -----------------
TRACO3   -----------------
```

Figure 3.3.6 Alignment of the deduced amino acid sequences from TRACO1, TRACO2 and TRACO3 with a consensus amino acid sequence (ACOCON in bold characters), constructed from 28 ACC oxidase genes in the GenBank database (Kadyrzhanova *et al.* 1997). Identical amino acid residues are indicated by (•), different residues are shown, and mismatching residues are indicated by (-) in the TRACO sequences.

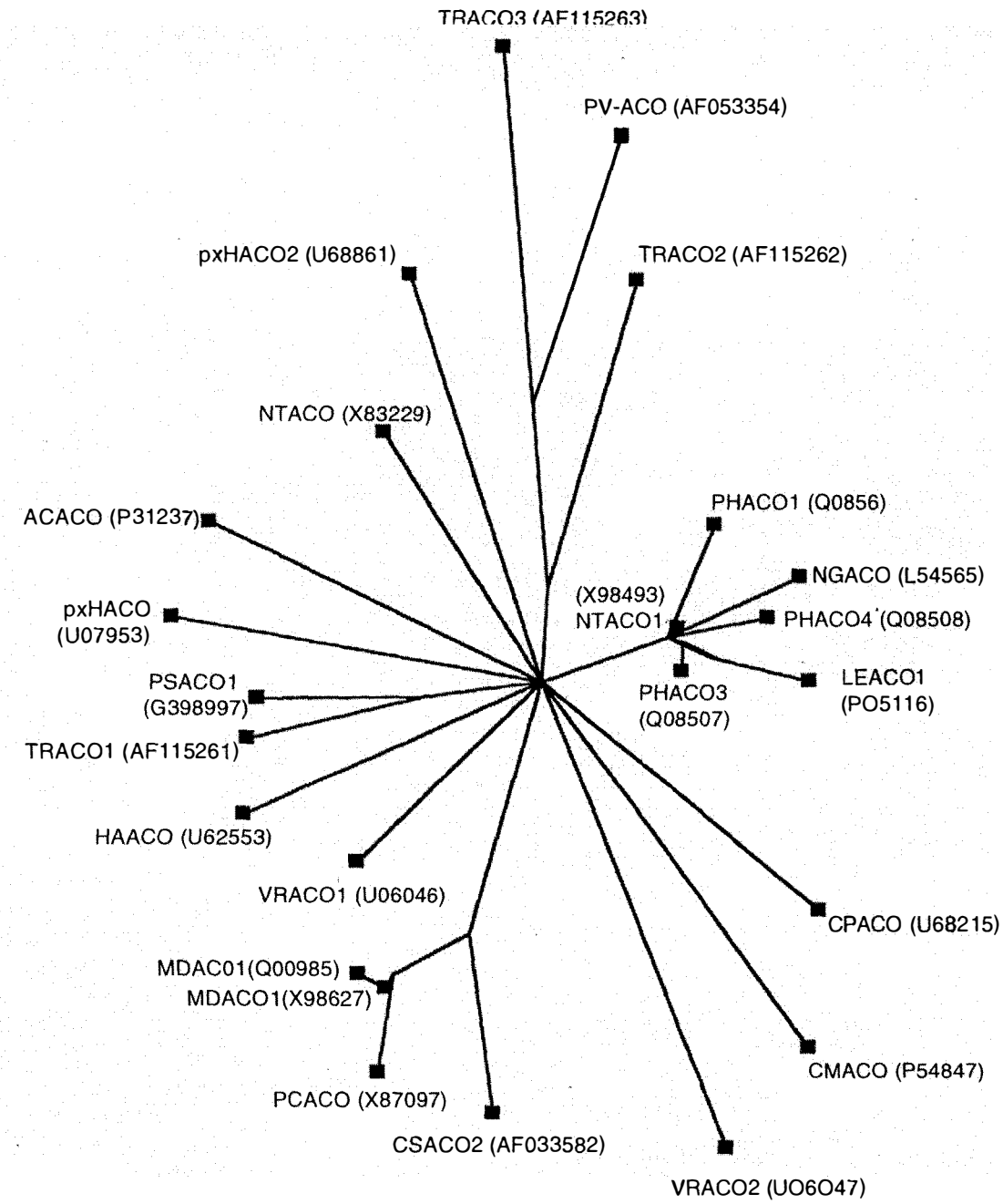

Figure 3.3.7 Phylogenetic analysis of the ACC oxidase amino acid sequences from white clover with other ACC oxidase genes in the GenBank database (searched on 22nd, September 1999). The accession number for each gene is given in parenthesis.

3.3.2 Expression of protein-coding regions of TRACO1 in *E.coli*

3.3.2.1 Expression and purification of TRACO1 protein in *E. coli*

The protein-coding region of TRACO1 was expressed in *E. coli* using the pPROEX-1 protein expression vector (Fig. 3.3.8). Transcription of the pPROEX-1 plasmid is designed to be under the (negative) control of the Lac gene inhibitor (lacIq), and hence when IPTG is added, transcription is induced. The expressed protein contains six consecutive His residues at the amino terminal, which facilitates purification using a nickel affinity column (Ni-NTA).

The protein-coding region of TRACO1 was amplified by PCR using a plasmid containing the TRACO1 gene (cf. Table 3.3.1; ACO1) as template. For the PCR, two modified primers (ACOFE and ACORH; Fig. 2.6) were designed based on ACOF2 and ACOR2 (Table 2.4) to produce an in-frame PCR product after digestion with EcoRI and Hind III. Products of *ca.* 800 bp were successfully generated after digestion of the PCR products with EcoRI and HindIII (Fig. 3.3.9A) and these were cloned into the polycloning sites on the pPROEX-1 vector and the vector was then transformed into *E. coli* strain DH5α. Plasmid was purified from transformed colonies expressing ampicilin resistance and the presence of inserts was confirmed by double digestion of the plasmid with EcoRI and Hind III (Fig. 3.3.9B). The pPROEX-1 plasmid containing the correct size (*ca.* 800 bp) inserts was then retransformed into *E. coli* strain TB1 and BL21, known as better foreign protein expression hosts, when compared to strain DH5α.

Protein expression was induced in both bacterial strains with IPTG treatment, and the expressed proteins were purified using the Ni-NTA column. Crude protein extracts from bacterial cell lysates and purified proteins after Ni-NTA column chromatography were separated using SDS-PAGE and visualised by CBB staining (Fig. 3.3.10). The column-purified protein fraction comprised a protein band of *ca.* 35 kD with a weaker protein band of *ca.* 28 kD (Fig. 3.3.10, lane 5). This low molecular weight protein band has been identified as a nickel-binding protein from *E. coli* (Dr. D. Hunter, IMBS, Massey University, *personal communication*).

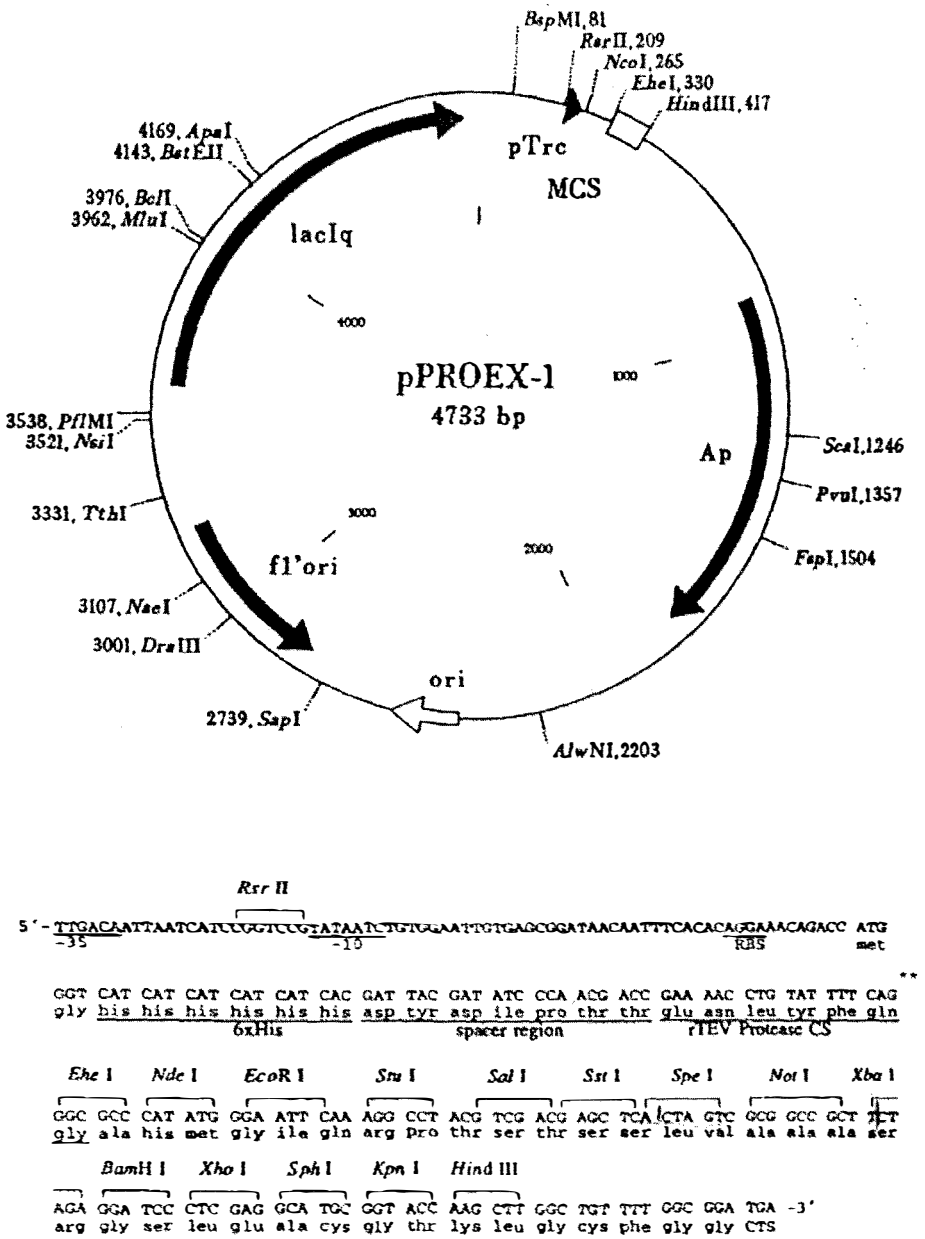

Figure 3.3.8 Map of the pPROEX-1 plasmid used for the expression of the TRACO1 cDNA in *E.coli*. The BamHI and HindIII sites, used for cloning TRACO1 cDNA in polycloning sites are shown in the vector sequence. The 6 X His repeats, used for purification of the expressed protein by Ni-NTA column chromatography are also shown in the vector sequence.

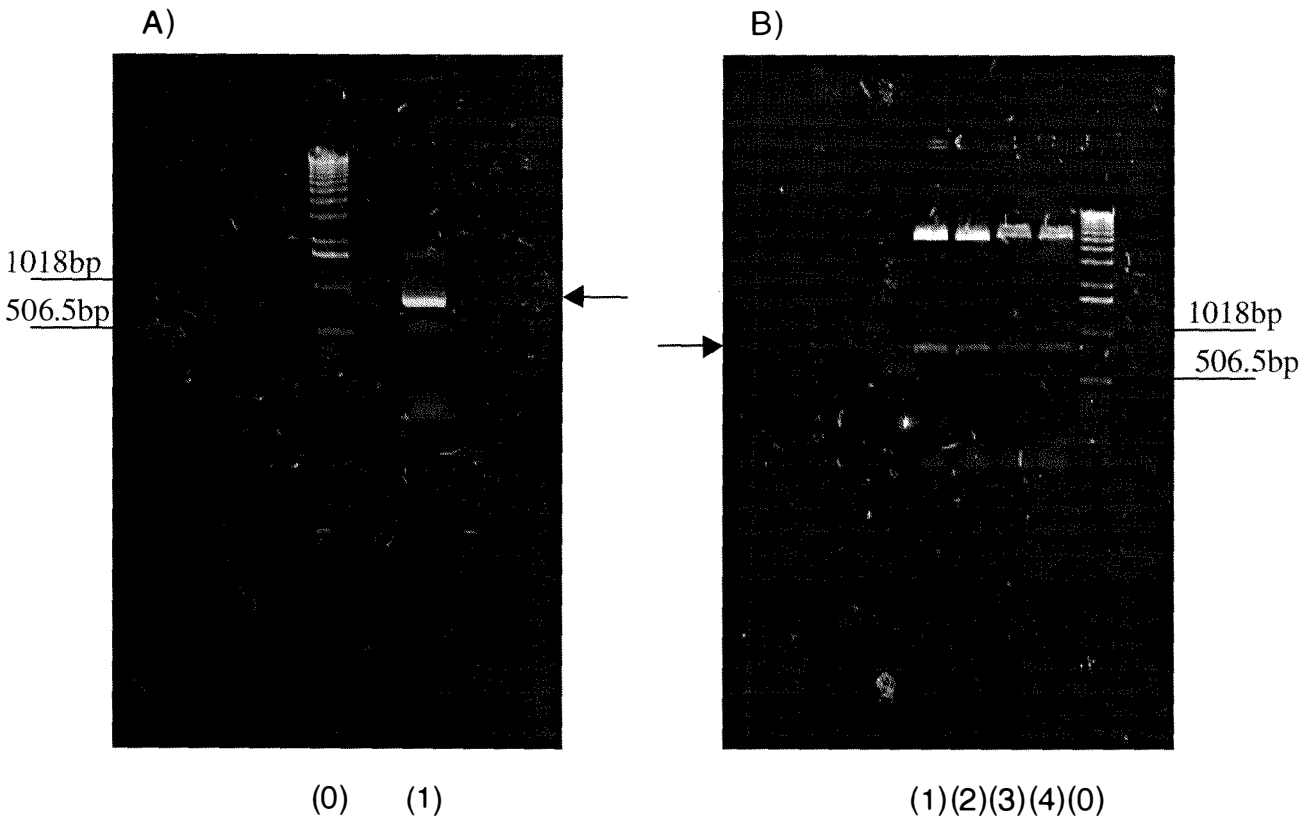

Figure 3.3.9 Cloning of TRACO1 cDNA into the pPROEX-1 vector. (A) PCR products amplified from ACO1 (Table 3.3.1) were separated on a 1.2% (w/v) agarose gel and visualised with ethidium bromide (lane 1). (B) Inserts, obtained from an EcoRI / HindIII double digestion of pPROEX-1 vectors containing the PCR product from (A), were separated on a 1.2% (w/v) agarose gel and visualised with ethidium bromide. Lane (1-4) are digestion products of plasmids isolated from 4 *E. coli* colonies grown on LB-Amp^{100} plates. Lane (0) are molecular size markers with two sizes indicated. Arrows indicate PCR products of *ca.* 800 bp.

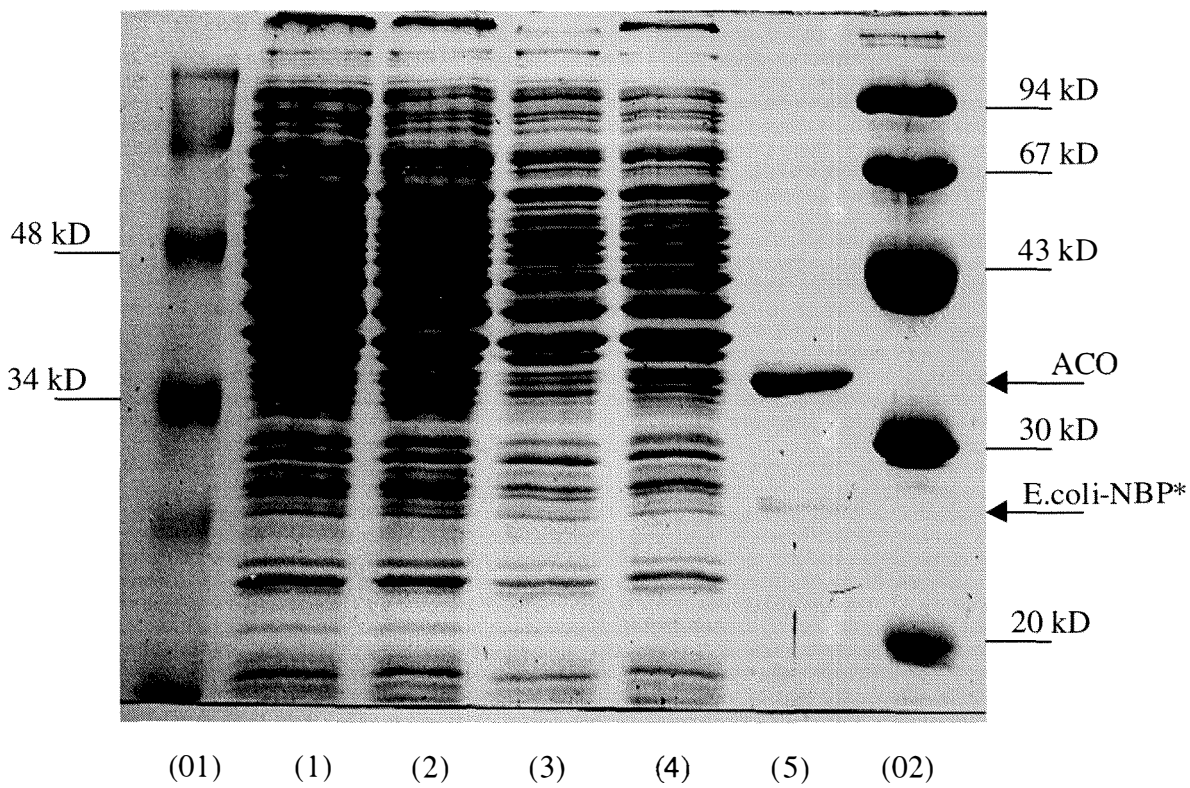

Figure 3.3.10 SDS-PAGE analysis of protein expression in two different strains of *E. coli* transformed with pPROEX-1 containing a TRACO1 insert. Total protein extracts from *E. coli* BL21 (1, 2) and TB1 (3, 4) were separated on a 16% (w/v) SDS-PAGE gel and proteins were visualised with Coomassie Blue staining. Lane (1), (3) and lane (2), (4) are protein extracts from uninduced and IPTG-induced *E. coli* cells, respectively. Lane (5) is a fusion protein from the induced *E. coli* TB1 cells (lane 4) purified using the Ni-NTA column. Lane (01) and (02) are two different molecular weight markers from Bio-Rad and Pharmacia, respectively, with molecular weights indicated. *E. coli-NBP is a nickel-binding protein in *E. coli.*

The protein band of *ca.* 35 kD is a putative protein product from the TRACO1 gene. This protein band (*ca.* 35 kD) appeared to be more discernible in the lane loaded with crude protein extracts from bacterial cell lysates induced by IPTG induction (Fig. 3.3.10 lane 4), when compared with bacterial cell lysates without IPTG induction (Fig. 3.3.10 lane 3). In addition, this induction of the *ca.* 35 kD protein expression was highest in *E. coli* strain TB1 (Fig. 3.3.10, lane 4), when compared with strain BL21 (Fig. 3.3.10 lane 2), and hence the TB1 strain was used as the *E. coli* host for expressing TRACO1 protein in this study.

3.3.2.2 Characterisation of ACO protein purified from transformed *E. coli*

Proteins expressed from pPROEX-1 vectors have a recognition site (ENLYFQ) for the TEV protease situated between the six consecutive His residues and the N-terminal of the expressed fusion protein (Fig. 3.3.8). So, 21 N-terminal amino acids of the expressed protein will be cleaved by TEV protease with a calculated molecular weight of *ca.* 2.5 kD. Since the Ni-column purified protein expressed in bacterial cells (*E. coli* strain TB1) transformed with a pPROEX-1 vectors containing TRACO1 had *ca.* 35 kD (Fig. 3.3.11 lane a), the protein digested with TEV protease should be *ca.* 32.5 kD.

To confirm that the IPTG-induced protein expression was the TRACO1 gene product, the Ni-NTA column purified protein was first characterised using the TEV protease (Fig. 3.3.11). When the purified protein of *ca.* 35 kD was digested with TEV protease, a protein band of *ca.* 32 kD was discerned (Fig. 3.3.11, lane 2). This indicates that the protein of 35 kD is a gene product originating from the pPROEX1 vector with the TRACO1 gene as an insert.

Purification of the expressed protein after digestion with the protease was undertaken using the Ni-NTA column by applying the protease-digested protein to the column. Without six consecutive His residues, the protease-digested protein should pass through the column without binding. However, the protein band was not discerned in the lane loaded with Ni-NTA column eluates without immidazole elution buffer (Fig. 3.3.11 lane 4), which implied

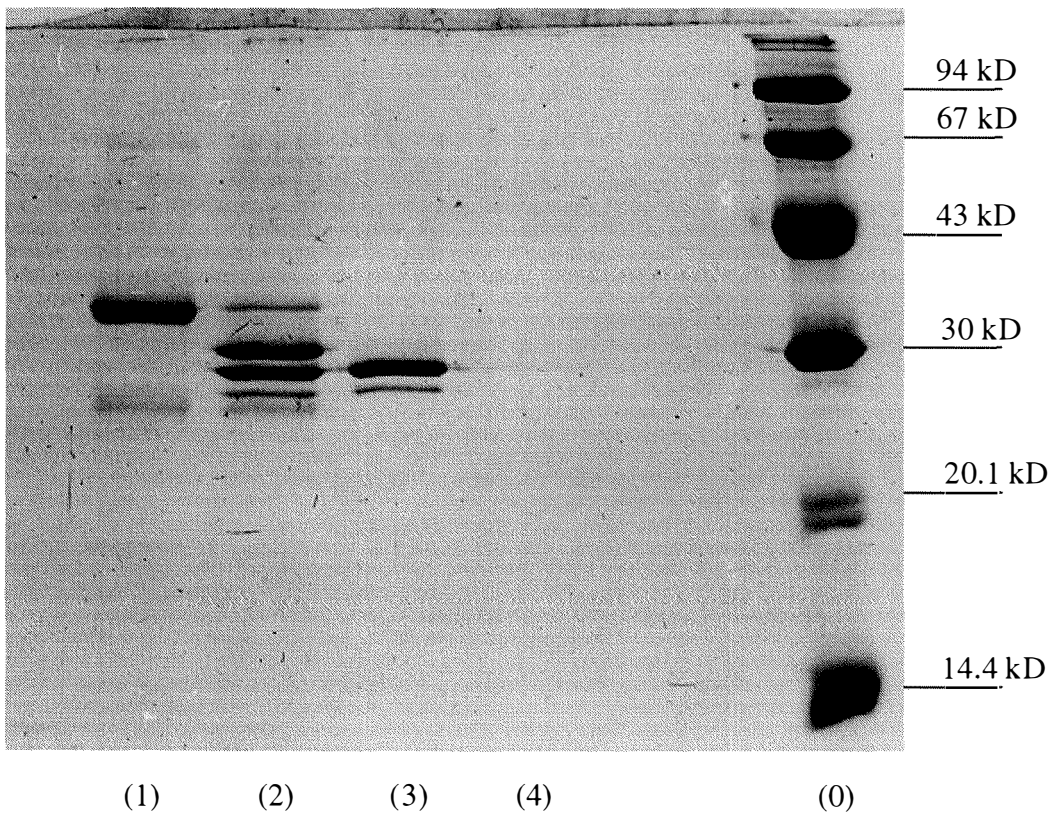

Figure 3.3.11 SDS-PAGE analysis of the expressed TRACO1 protein digested with TEV protease. Protein samples expressed and Ni-NTA column purified from *E. coli* TB1 cells (Fig. 3.3.10, lane 5) were digested with TEV protease and separated on a 16% (w/v) SDS-PAGE gel, and visualised with Coomassie Blue staining. Lane (1) is the purified fusion protein before TEV protease treatment. Lane (2) is the fusion protein digested with TEV protease. Lane (3) is the TEV protease. Lane (4) is TEV protease-digested protein after passage through the Ni-NTA column. Lane (0) are molecular weight markers from Pharmacia, with molecular weights indicated.

that the digested protein did not lose its affinity to the Ni-NTA column. The expressed protein may still bind to the column since hydrophobicity of the protein can mediate protein binding to the column, which is made of hydrophobic Sephadex beads.

However, evidence to confirm that the expressed protein was the gene product of TRACO1 was achieved by amino acid sequencing. For this, the Ni-NTA column purified protein was separated on a 16% (w/v) SDS-PAGE gel (Fig. 3.3.12) and gel slices containing the stained protein bands of *ca.* 35 kD were excised. The protein was digested with trypsin and then a peptide fragment was sequenced as Phe-Val-Phe-Asp-Asp-Tyr (Fig. 3.3.13). This peptide sequence was found in the deduced amino acid sequence of TRACO1 (Fig. 3.3.3; Fig. 3.3.13). This results confirms that the Ni-NTA column purified protein expressed from the pPROEX-1 vector is the gene product of TRACO1.

In addition, the deduced amino acid sequence of TRACO1 was further analysed to identify important amino acid residues and its putative secondary structures for ACO protein function (using Protein Prediction 2 programme; EMBL, Heidelberg, Germany) (Fig. 3.3.14). The deduced amino acid sequence of TRACO1 starts from Ala^{27}, when compared with a consensus amino acid sequence constructed from ACO genes reported in the GenBank database (Kadyrzhanova *et al.* 1997). However, the sequence contains residues proposed as important conserved sites which might be related to the enzyme function, such as lysine (K^{144}, K^{158}, K^{172}, K^{198}, K^{293}, K^{299}), histidine (H^{177}, H^{234}) and aspartic acid (D^{179}). The analysis of secondary structure indicates that there are sequences comprising α-helixes and β-sheets with a typical leucine zipper motif (F^{117}, L^{124}, L^{131}, L^{138}), which is widely conserved in ACO proteins reported from other plants. The leucine zipper motif is known as a site of protein-protein interactions for the dimerisation of proteins.

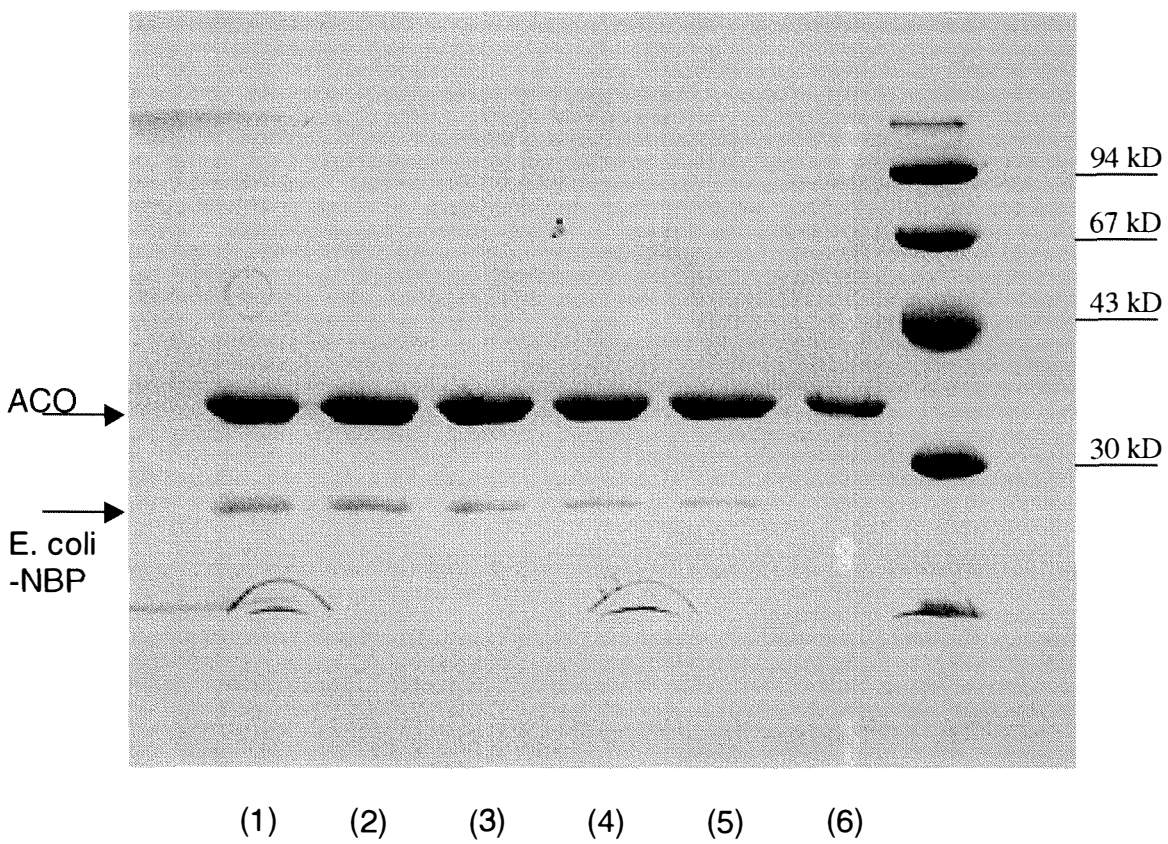

Figure 3.3.12 SDS-PAGE preparation for protein sequencing of TRACO1. Ten µg (lane 1-5) and 5 µg (lane 6) of Ni-NTA column purified protein from *E. coli* TB1 (Fig. 3.3.10, lane 5) were separated on a 16% (w/v) SDS-PAGE gel and visualised with Coomassie Blue staining. Lane (0) are molecular weight markers from Pharmacia, with molecular weights indicated. E. coli-NBP is a nickel-binding protein in *E. coli*.

```
TRACO1                                  [27]ACENWGFFELVNHGISIEMMDKVE
PS-ACO1     MENFPIVDMGKLNTEDRKSTMELIKD.........C...........T..

TRACO1      KLTKDHYKKCMEQRFKEMVSSKGLECVQSENDDLDWESTFFLRHLPFSNI
PA-ACO1     ....E.............AT.........D.............V.S.

TRACO1      SEIPDLDDDYRKIMKEFAQKLENLAEELLDLLCENLGLEKGYLKKVFYGS
PS-ACO1     ............V.....L...E.....................A....

TRACO1      KGPNFGTKVSNYPPCPKPDLIKGLRAHTDAGGIILLFQDDKVSGLQLLKD
PS-ACO1     ................E.............................

TRACO1      DQWIDVPPMRHSIVINLGDQLEVITNGKYKSVMHRVIAQTDGARMSLASF
PS-ACO1     ............................................I...

TRACO1      YNPSDDAIISPAPTLLKENETTSEIYPKFVFDDYMKLYMGLKFQAKE[297]
PS-ACO1     ...G...V....S........-..V.....................PRF

TRACO1
PS-ACO1     EAMMKAMSSVKVGPVVSI
```

Figure 3.3.13 Alignment of deduced amino acid sequences from TRACO1 and PS-ACO1 (the ACO gene sequence with the highest homology to TRACO1; Accession No. M98357). The amino acid sequence obtained by peptide sequencing after trypsin-digestion of TRACO1 is highlighted with a grey background. Identical amino acid residues are indicated by (•), different residues are shown, and mismatching residues are indicated by (-) in the PS-ACO1 sequence.

```
TRACO1  ACENWGFFELVNHGISIEMMDKVEKLTKDHYKKCMEQRFKEMVSSKGLECVQSEINDLDW
Protein LLLL..EEEE.LLLL.HHHHHHHHHHHHHHHHHHHHHHHHHHH.LLL.EE.........

TRACO1  ESTFFLRHLPFSNISEIPDLDDDYRKIMKEFAQKLENLAEELLDLLCENLGLEKGYLKKV
Protein H.......LLLLLLLLLLLLL.HHHHHHHHHHHHHHHHHHHHHHHHHHH.LLL.HHHHHHH

TRACO1  FYGSKGPNFGTKVSNYPPCPKPDLIKGLRAHTDAGGIILLFQDDKVSGLQLLKDDQWIDV
Protein ..LLLLL..EEEE.LLLLLLLHHHHHHHHHHLLLL.EEEEE.LLLLL..EE..LL.EEE.

TRACO1  PPMRHSIVINLGDQLEVITNGKYKSVMHRVIAQTDGARMSLASFYNPSDDAIISPAPTLL
Protein LLLLLEEEEE.LL.EEEE.LLLL.....EEEE.LLL..EEEEE..LLLLL....LL....

TRACO1  KENETTSEIYPKFFVFDDYMKLYMGLKFQAKE|
Protein .........L......HHHHHHHHHHHHH.LL|
```

Figure 3.3.14 Prediction of secondary structure of TRACO1 using the Protein Prediction 2 programme (EMBL, Heidelberg, Germany). Predicted secondary structures are shown as H, α-helix motif; E, β-sheet motif; L, looping motif. Amino acids proposed as critical residues for ACO activity are given in bold characters. Amino acid phenylalanine (F) and three leucines (L) residues, proposed as a putative Leu zipper motif, are indicated with a grey background.

3.3.3 Expression of ACO genes during leaf ontogeny

ACO gene expression, using northern analysis, has been characterised in the developing apex and newly initiated leaves (Leaf 1, 2 and 3) of white clover (Fig. 3.3.15). Three cDNA clones comprising protein-coding regions, ACO1, ACO3 and ACO7 clones were used as probes representing TRACO1, TRACO2 and TRACO3, respectively (Table 3.3.1). The specificity of the probes labeled with ^{32}P-dCTP was first tested by Southern analysis using cDNA probes as templates (data not shown). Under the conditions used, each gene probe hybridized specifically to each corresponding template, even though these clones shared high homology (77 to 88%) in terms of their nucleotide sequences (Table 3.3.2). For northern analysis, 2 µg of poly(A)$^+$mRNA extracted from the developing apex, leaf 1, leaf 2 and leaf 3 was used and separated through a 1.2% (w/v) agarose-formaldehyde gel.

The TRACO1 probe hybridised to a band of 1.35 kb almost exclusively in the developing apex (Fig. 3.3.15A) and the TRACO2 probe hybridised to a band of 1.35 kb in the newly initiated leaf tissue (Fig. 3.3.15B). The TRACO3 probe did not hybridise significantly to any mRNA confirming that the expression of this ACO gene is not high in developing tissues (Fig. 3.3.15C).

A residual level of TRACO2 expression was detected in the apex. This could be due to the cross-hybridisation under the conditions used between TRACO1 transcripts and the TRACO2 probe, because of high homology, or it could reflect a low level of TRACO2 expression in the apex. Likewise, the residual expression of TRACO1 in leaf 1 may either be low abundance of mRNA or cross hybridisation. To investigate this further, more gene-specific probes are required.

TRACO3 expression in the newly initiated leaves (leaf 1, 2 and 3) was further characterised using an extended exposure time for autoradiography (21 days) (Fig. 3.3.16B). With the extended exposure, TRACO3 was observed to hybridise to two transcripts of 1.17 kb and 1.35 kb, with the lower molecular weight RNA species (1.17 kb) more abundant (Fig. 3.3.17A). Hybridisation to the 1.35 kb transcript was low in leaf 1 and leaf 2, but relatively high in leaf 3.

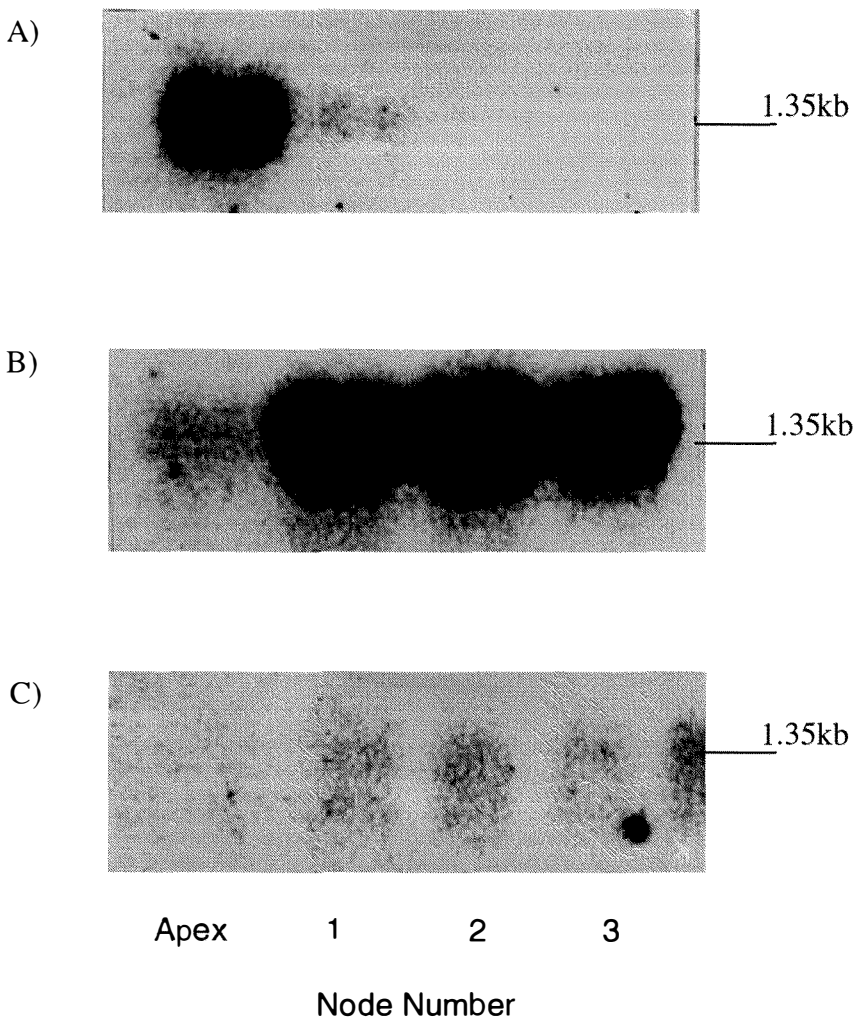

Figure 3.3.15 Expression of ACC oxidase genes in the developing apex and newly initiated leaves determined by northern analysis. Two μg of poly(A)+mRNA was separated on a 1.2% (w/v) agarose-formaldehyde gel, blotted onto Hybond-N^+ with alkaline transfer buffer, and probed with ^{32}P-labeled TRACO1, (A); TRACO2, (B) and TRACO3, (C). Membranes were washed at high stringency (0.1 X SSPE at 65 ^{o}C) and exposed to X-ray film for 16 hr.

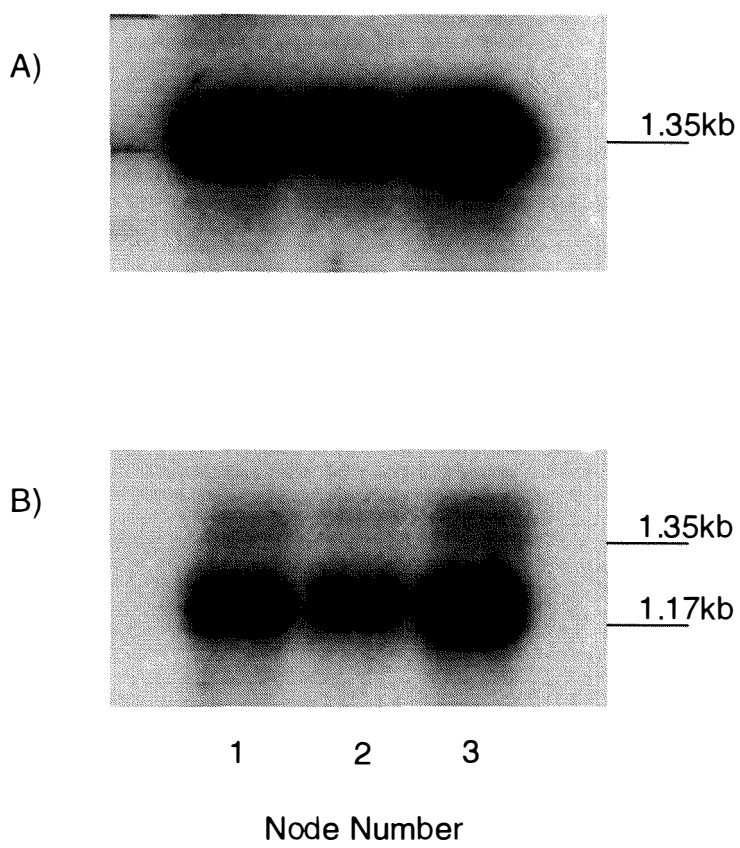

Figure 3.3.16 Expression of ACC oxidase genes in newly initiated leaves determined by northern analysis using an extended exposure time. Two μg of poly(A)$^+$mRNA was separated on a 1.2% (w/v) agarose-formaldehyde gel, blotted onto Hybond-N$^+$ with alkaline transfer buffer, and probed with ^{32}P-labeled TRACO2, (A) and TRACO3, (B). Membranes were washed at high stringency (0.1 X SSPE at 65 ^{o}C) and exposed to X-ray film for 21 days.

It is not clear whether both transcripts (1.17 kb and 1.35 kb) originate from TRACO3 or from closely related genes, which are recognised by cross-hybridisation due to the high homology of the sequences in protein-coding regions of ACO genes (Table 3.3.2).

To further examine TRACO3 gene expression, a gene-specific probe is required to reduce the chance of cross-hybridisation. Specific probes, comprising the 3'-untraslated regions of each gene were, therefore, cloned and used for further gene expression studies (section 3.4.3).

Part 4: Molecular cloning and characterisation of 3'-untranslated regions (UTRs) of ACC oxidase genes in white clover

3.4.1 Cloning and sequencing of 3'-UTRs of ACC oxidase genes expressed in the developing apex

The 3'-UTRs of ACO genes in white clover were generated using 3'-RACE. Two sets of nested forward primers (ACOF3 and ACOF6) were designed for two rounds of PCR (Table 2.4) and these were based on the nucleotide sequences encoding the protein-coding region of TRACO1 (Fig. 3.3.3; Fig. 3.4.2). The nested primer, ACOF6 was designed as the forward primer for the second round PCR and was based on a sequence starting at the 5th nucleotide of ACOF3 (Table 2.4). Also, two sets of nested forward primers (ACOF4 and ACOF7) and a forward primer (ACOF5) were designed to amplify the 3'-UTRs of TRACO2 and TRACO3, respectively by D. Hunter (Table 2.4). Oligo-d(T)/adapter sequences (ADPT) (Table 2.4) were used as the reverse primer to amplify all 3'-UTRs.

3.4.1.1 TRACO1

A series of products ranging from *ca.* 400 bp to *ca.* 900 bp were amplified using 3'-RACE from cDNA templates generated by RT-treatment of poly(A)$^+$mRNA isolated from the developing apex (Fig. 3.4.1A lane 1). Two rounds of PCR using the same forward primers (either ACOF3 or ACOF6) failed to significantly amplify a DNA band of the expected size (Fig. 3.4.1A lane 2 and 3). Even though the sequence of the ACOF6 primer starts only at the 5th nucleotide of ACO3F, this nested primer system clearly improves the specificity of 3'-RACE for TRACO1.

The *ca.* 700 bp 3'-RACE product was predicted as the size of the reading frame plus 3'-UTR of TRACO1, since most ACO genes contain ca. 200 to 300 bp as their 3'-UTR sequences (Imaseki, 1999). So the products were cloned into the pCR 2.1 vector, transformed into *E. coli* DH5α, plasmids containing inserts of the expected size were identified by EcoRI digestion (Fig. 3.4.1B; lane 1, 2, 3) and the nucleotide sequences of the inserts determined (Fig. 3.4.2).

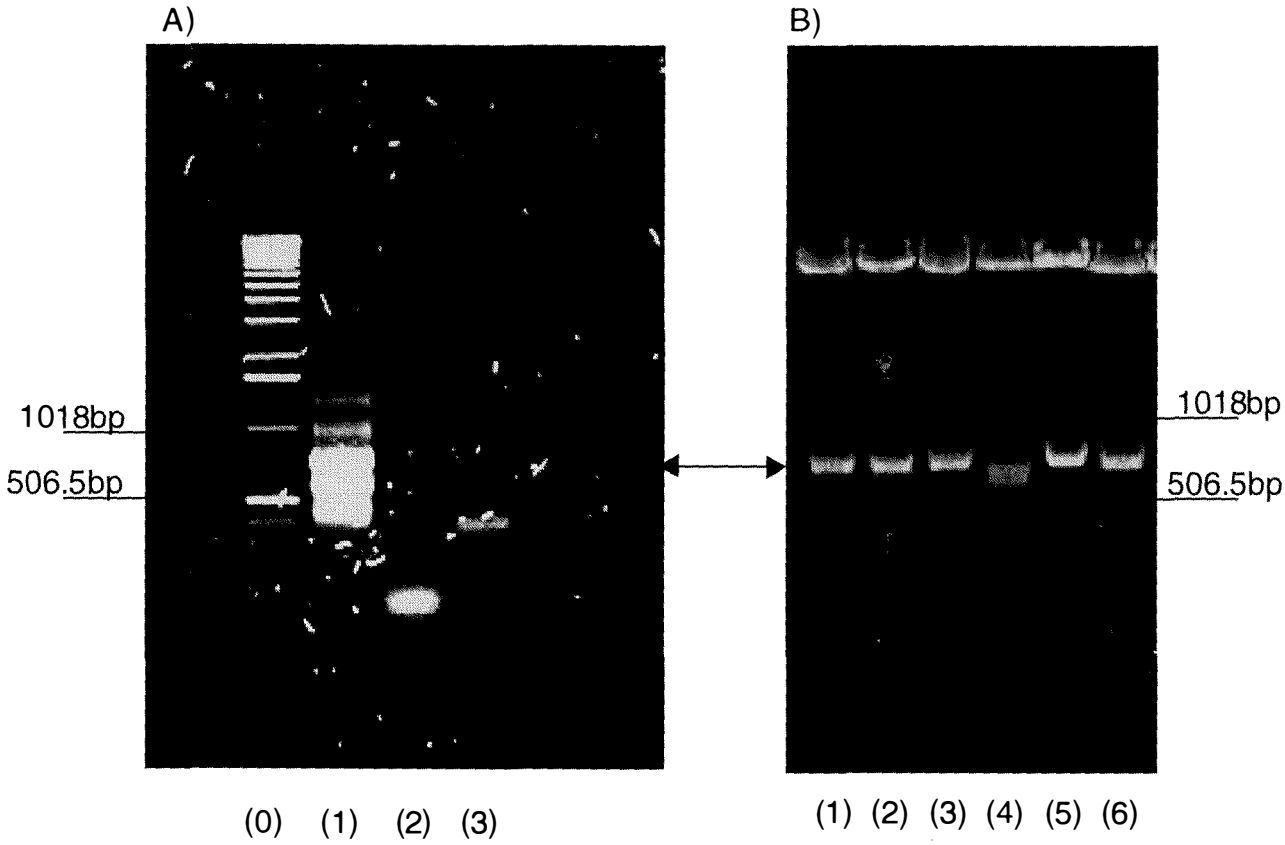

Figure 3.4.1 PCR amplification of the 3'-UTR of TRACO1 using RT-generated cDNA templates from poly(A)$^+$m RNA isolated from the apex. (A) PCR products were separated on a 1.2% (w/v) agarose gel and visualised with ethidium bromide. Lane (1), ACOF3 for the first round and ACOF6 for the second round PCR, as the 5'-primers; lane (2), ACOF3 as the 5'-primer for two rounds, and lane (3), ACOF6 as the 5'-primer for two rounds. Lane (0) are molecular size markers with two sizes indicated. (B) Inserts obtained from EcoRI digestion of pCR 2.1 vectors containing putative 3'-UTRs of TRACO1 were separated on a 1.2% (w/v) agarose gel and visualised with ethidium bromide. Lanes (1-6) are from 6 colonies of *E. coli*, grown on LB-Amp^{100} plates. Two molecular sizes are indicated. Arrows indicate *ca.* 700 bp PCR amplification products.

Figure 3.4.2

A. Schematic of the TRACO1 gene generated by RT-PCR (813 bp) and 3'-RACE (716 bp). The eTRACO1 represents a combination of the two sequences, comprising a 876 bp reading frame and 301 bp 3'-UTR.

B. Nucleotide and deduced amino acid sequences of TRACO1 including the protein-coding region and 3'-UTR. The 5'-primer sequences are indicated by underlining (ACOF3) and by italics (ACOF6) for first round and second round PCR for 3'-RACE, respectively. The 5'-primer sequence used for amplification of cDNA gene-specific probes is indicated by a grey background. The 3'-primer sequences for both 3'-RACE and cDNA probe amplification are indicated by bold italics.

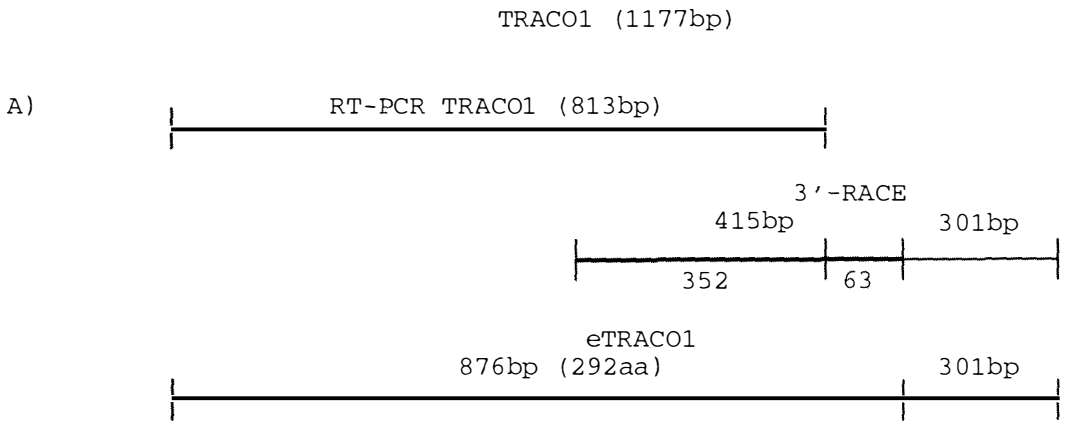

B)

```
   1  GCTTGCGAGA ATTGGGGCTT CTTTGAGTTG GTGAACCATG GAATATCTAT TGAGATGATG
        A  C  E  N  W  G  F  F  E  L  V  N  H  G  I  S  I  E  M  M
  61  GACAAAGTGG AGAAGCTCAC AAAAGATCAC TACAAGAAGT GTATGGAACA AAGGTTCAAA
        D  K  V  E  K  L  T  K  D  H  Y  K  K  C  M  E  Q  R  F  K
 121  GAAATGGTTT CAAGCAAAGG TTTGGAGTGT GTTCAGTCAG AAATAAATGA CTTAGATTGG
        E  M  V  S  S  K  G  L  E  C  V  Q  S  E  I  N  D  L  D  W
 181  GAAAGCACTT TCTTTTTGCG CCATCTTCCA TTTTCTAATA TTTCAGAGAT CCCAGATCTT
        E  S  T  F  F  L  R  H  L  P  F  S  N  I  S  E  I  P  D  L
 241  GATGATGATT ACAGGAAGAT AATGAAGGAA TTTGCACAAA AATTAGAGAA TCTGGCTGAG
        D  D  D  Y  R  K  I  M  K  E  F  A  Q  K  L  E  N  L  A  E
 301  GAACTTCTTG ACTTATTATG TGAGAATCTT GGGCTTGAAA AAGGGTATTT GAAGAAGGTG
        E  L  L  D  L  L  C  E  N  L  G  L  E  K  G  Y  L  K  K  V
 361  TTTTATGGTT CAAAGGGTCC AAACTTTGGT ACAAAAGTTA GTAACTATCC TCCTTGTCCT
        F  Y  G  S  K  G  P  N  F  G  T  K  V  S  N  Y  P  P  C  P
 421  AAGCCTGACC TTATTAAGGG ACTTAGAGCC CATACAGATG CTGGTGGCAT CATCCTTCTC
        K  P  D  L  I  K  G  L  R  A  H  T  D  A  G  G  I  I  L  L
 481  TTCCAAGATG ACAAAGTCAG TGGACTTCAG CTCCTCAAAG ATGACCAATG GATTGATGTC
        F  Q  D  D  K  V  S  G  L  Q  L  L  K  D  D  Q  W  I  D  V
 541  CCTCCAATGC GTCACTCTAT TGTCATCAAC CTTGGTGATC AACTTGAAGT CATAACAAAT
        P  P  M  R  H  S  I  V  I  N  L  G  D  Q  L  E  V  I  T  N
 601  GGGAAGTACA AGAGTGTGAT GCATAGAGTA ATTGCTCAAA CAGATGGTGC TAGAATGTCT
        G  K  Y  K  S  V  M  H  R  V  I  A  Q  T  D  G  A  R  M  S
 661  TTAGCTTCAT TCTATAATCC AAGTGATGAT GCTATCATTT CACCAGCACC AACTTTATTG
        L  A  S  F  Y  N  P  S  D  D  A  I  I  S  P  A  P  T  L  L
 721  AAGGAAAATG AAACAACAAG TGAAATTTAT CCAAAATTTG TGTTTGATGA TTACATGAAA
        K  E  N  E  T  T  S  E  I  Y  P  K  F  V  F  D  D  Y  M  K
 781  CTCTATATGG GATTAAAGTT TCAAGCTAAA GAGCCTAGAT TTGAAGCTAT GATGAAAGCA
        L  Y  M  G  L  K  F  Q  A  K  E  P  R  F  E  A  M  M  K  A
 841  ATGTCAAGTG TTGATGTGGG ACCAGTAGTA AGCATATGAA AAAAGCATAT TATTAGATTG
        M  S  S  V  D  V  G  P  V  V  S  I
 901  ATTATGTGTG GTTTTGTTAA TAAGCTGAGT TTATTAAGCG ATTATTAGTG TTTGGTTTGG
 961  TGTTTATTTA TTATTATAAT TGGTATGACT TATGAGAGGT TAAGATCATG CAGTCTAAAG
1021  GTGTTGTTAT TAAAGTTTAT AATAAAGTAT GATTAATGGT TGATTTTAGA TTGGGTGTGA
1081  TGACTGATTA GTGTTGTTGG TTGGAAGATT AACTGGTTAA TTAAGTTATT GAAATGTGAT
1141  GTAATACTGT TTTATAAAAC CAAAAAAAAA AAAAAAATTAGCTGCAGTAGGATCCAC
```

The size of the 3'-RACE products of TRACO1 was 716 nucleotides, which comprised 415 nucleotides encoding for protein-coding region and 301 nucleotides encoding for 3'-UTR (Fig. 3.4.2A). The 352 nucleotides at the 5'-end of the 3'-RACE product overlapped with the protein-coding region sequence in TRACO1 and so confirmed that 3'-UTR generated using 3'-RACE was TRACO1. The nucleotide and deduced amino acid sequences obtained from a combination of ACO sequences generated by RT-PCR and 3'-RACE for TRACO1 are shown in figure 3.4.2B.

3.4.1.2 TRACO2

The 3'-UTR of TRACO2 was generated from the developing apex using 3'-RACE (Fig. 3.4.3). A double round PCR using two nested sets of forward primers (ACOF4 and ACOF7; Table 2.4), with cDNA templates generated by RT-treatment of either 5 μg of total RNA or 1 μg of poly(A)$^+$mRNA, amplified a major product of *ca.* 400 bp (Fig. 3.4.3A, lane 2 and 4). A higher relative yield of the 400 bp product was obtained from two rounds, when compared with a single round of PCR (Fig. 3.4.3A, lane 1 and 3). In addition, when 5 μg of total RNA was used to generate cDNA templates by RT treatment, a double round PCR amplified a DNA band of the expected size (*ca.* 400 bp) at a high yield as well as other smaller bands (Fig. 3.4.3A, lane 2). This high yield was not demonstrated with cDNA templates generated by RT-treatment of 1 μg of poly(A)$^+$ mRNA (Fig. 3.4.4A, lane 4).

The 400 bp 3'-RACE products were cloned into the pCR 2.1 vector and transformed into *E. coli* DH5α. Inserts were then identified by EcoRI digestion of plasmids purified from bacterial colonies selected on LB-Amp^{100} plates (Fig. 3.4.3B). Even though these plasmids were prepared from bacterial colonies expressing ampicilin resistance, some did not contain 3'-RACE products as inserts. This was probably caused by self-ligation of the pCR 2.1 vector after degradation of the 3'-T overhangs at the cloning sites.

Inserts of an expected size were sequenced and revealed 416 nucleotides as the 3'-RACE product which comprised 166 nucleotides encoding for protein-coding region and 250 nucleotides encoding for 3'-UTR (Fig. 3.4.4A). A 106 bp sequence at the 5'-end of the 3'-RACE product overlapped with the protein-coding region of TRACO2 and so confirmed that the 3-UTR of TRACO2 was cloned successfully. The nucleotide and deduced amino acid

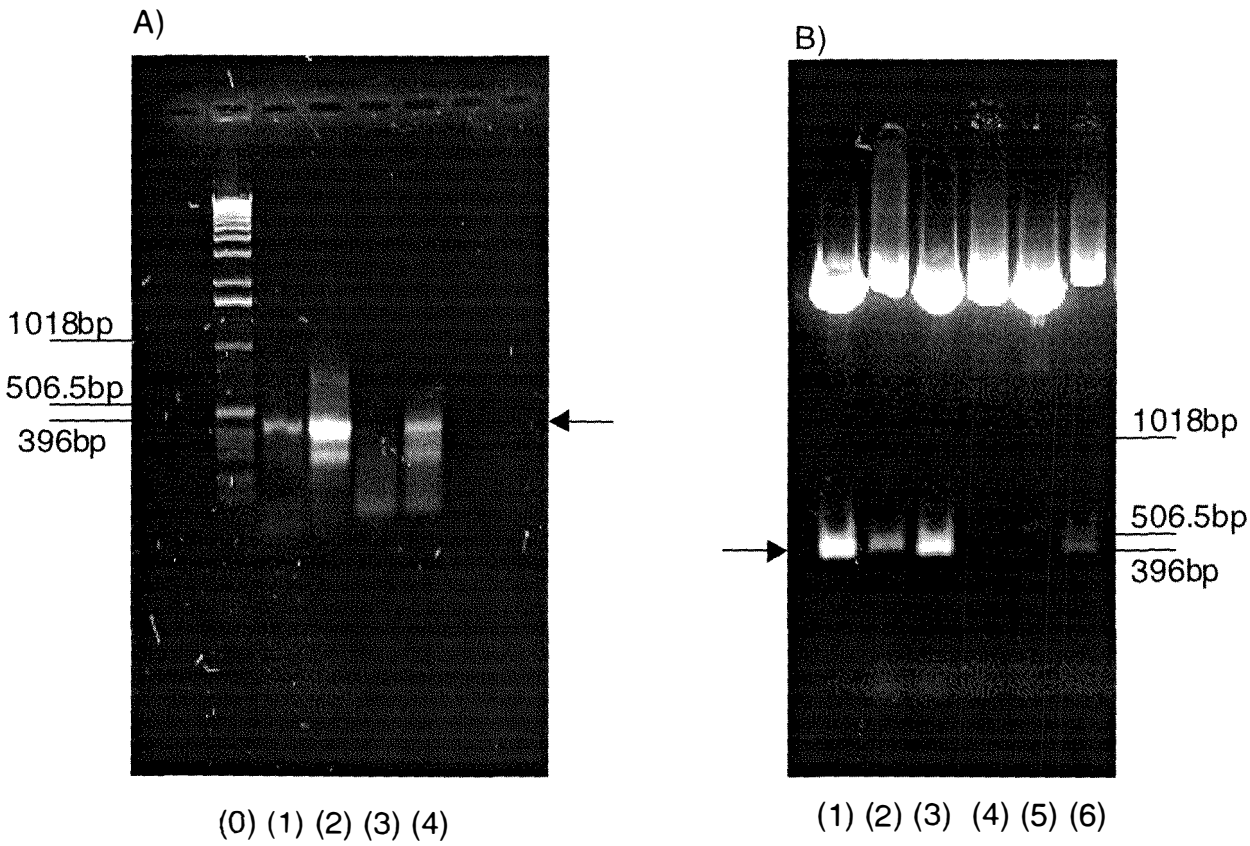

Figure 3.4.3 PCR amplification of the 3'-UTR of TRACO2 using RT-generated cDNA templates from poly(A)$^+$m RNA isolated from the developing apex. (A) PCR products were separated on a 1.2% (w/v) agarose gel and visualised with ethidium bromide. Lanes (1), (3) and (2), (4) are products from the first and the second round PCR, respectively. Five µg of total RNA (lanes 1 and 2) and 1 µg of poly(A)$^+$mRNA (lanes 3 and 4) were used as templates for cDNA synthesis. Lane (0) are molecular size markers with three sizes indicated. (B) Inserts obtained from EcoRI digestion of pCR 2.1 vectors containing putative 3'-UTRs of TRACO1 were separated on a 1.2% (w/v) agarose gel and visualised with ethidium bromide. Lanes (1-6) are from 6 colonies of *E. coli*, grown on LB-Amp^{100} plates. Arrows indicate *ca.* 400 bp PCR amplification products.

Figure 3.4.4

A. Schematic of the TRACO2 gene generated by RT-PCR (804 bp) and 3'-RACE (416bp). The eTRACO2 represents a combination of the two sequences, comprising a 864 bp reading frame and 250 bp 3'-UTR.

B. Nucleotide and deduced amino acid sequences of TRACO2 including the protein-coding region and 3'-UTR. The 5'-primer sequences are indicated by underlining (ACOF4) and by italics (ACOF7) for first round and second round PCR for 3'-RACE, respectively. The 5'-primer sequence used for amplification of cDNA gene-specific probes is indicated by a grey background. The 3'-primer sequences for both 3'-RACE and cDNA probe amplification are indicated by bold italics.

A)

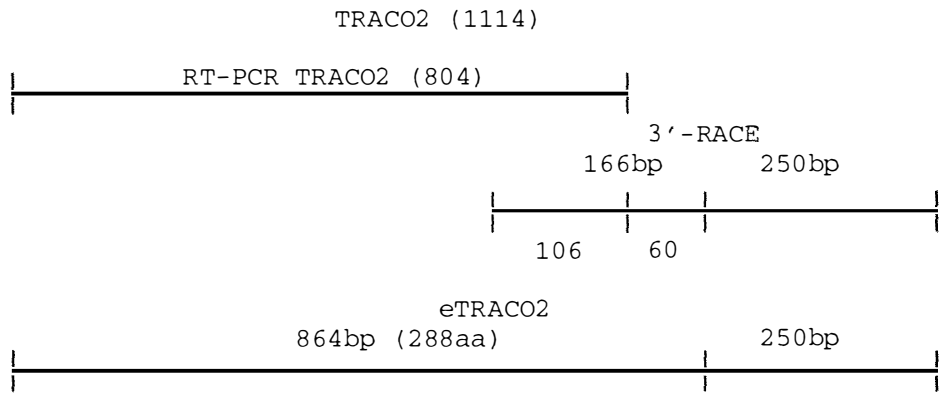

B)

```
   1  GCATGCGAGA ATTGGGGCTT CTTTGAGCTG GTGAATCATG GCATATCTCA TGACTTAATG
        A  C  E  N  W  G  F  F  E  L  V  N  H  G  I  S  H  D  L  M
  61  GACACTGTGG AAAGGTTGAC AAAAGAACAC TACAGGATAT GCATGGAACA AAGATTCAAG
        D  T  V  E  R  L  T  K  E  H  Y  R  I  C  M  E  Q  R  F  K
 121  GATTTGGTGG CCAACAAAGG ACTAGAGGCT GTTCAAACTG AGGTCAAAGA CATGGACTGG
        D  L  V  A  N  K  G  L  E  A  V  Q  T  E  V  K  D  M  D  W
 181  GAGAGTACCT TCCACTTGCG TCACCTACCT GAGTCAAACA TTTCAGAGGT CCCTGATCTC
        E  S  T  F  H  L  R  H  L  P  E  S  N  I  S  E  V  P  D  L
 241  ACTGATGAAT ACAGGAAAGC AATGAAGGAA TTTGCTTTGA AGCTAGAGAA ACTAGCAGAG
        T  D  E  Y  R  K  A  M  K  E  F  A  L  K  L  E  K  L  A  E
 301  GAGCTGCTAG ACTTATTATG TGAGAATCTT GGACTAGAAA AGGGATACCT CAAAAAAGCC
        E  L  L  D  L  L  C  E  N  L  G  L  E  K  G  Y  L  K  K  A
 361  TTTTATGGAT CAAAGGGACC AACTTTTGGC ACCAAGGTTG CAAACTACCC TCCATGCCCA
        F  Y  G  S  K  G  P  T  F  G  T  K  V  A  N  Y  P  P  C  P
 421  AAACCAGACC TTGTAAAAGG TCTCCGAGCA CACACCGATG CCGGTGGAAT AATCCTCCTT
        K  P  D  L  V  K  G  L  R  A  H  T  D  A  G  G  I  I  L  L
 481  TTCCAAGATG ACAAAGTCAG TGGCCTTCAG CTTCTCAAAG ATGGTAAATG GGTAGATGTT
        F  Q  D  D  K  V  S  G  L  Q  L  L  K  D  G  K  W  V  D  V
 541  CCTCCCATGC ATCATTCCAT TGTCATCAAC CTTGGTGACC AACTCGAGGT AATAACAAAT
        P  P  M  H  H  S  I  V  I  N  L  G  D  Q  L  E  V  I  T  N
 601  GGTAAGTACA GGAGTGTGGA ACATCGTGTG ATAGCACAAA GTGATGGAAC AAGAATGTCC
        G  K  Y  R  S  V  E  H  R  V  I  A  Q  S  D  G  T  R  M  S
 661  ATAGCTTCAT TCTACAATCC TGGTAGTGAT GCTGTTATCT ATCCAGCAAC AACATTGATT
        I  A  S  F  Y  N  P  G  S  D  A  V  I  Y  P  A  T  T  L  I
 721  GAAGAGAATA ATGAAGTTTA CCCAAAATTT GTTTTTGAAG ATTACATGAA TCTTTATGCT
        E  E  N  N  E  V  Y  P  K  F  V  F  E  D  Y  M  N  L  Y  A
 781  GGATTAAAGT TTCAAGCTAA AGAACCAAGA TTTGAAGCAT TTAAGGAATC ATCAAATGTT
        G  L  K  F  Q  A  K  E  P  R  F  E  A  F  K  E  S  S  N  V
 841  AAACTTGGTC CAATTGCAAC AGTTTAATTA TGTGTTACTA TAAATAAATA AAAAATAATA
        K  L  G  P  I  A  T  V
 901  TAAATATATG TTAACATGTT TGTTTAAGTG GAAGCAAGCA AAGTAAAAAA AAGCTTAAAG
 961  TCAAGTGCAT AAGTTTCTCA AATTAGTATG TAGTTGTTTA CTTACTATAT AGTGAGTGAT
1021  GTGATGTGAT TTTCTTGTAT TATTTGTGGA AAAAGTAATA TCAATGTTCA ATATAATAAT
1081  AAATATATTA TTCAAGTAAA AAAAAAAAAA AAAATTAGCTGCAGTAGGTCCACA
```

sequences obtained from a combination of ACO sequences generated by RT-PCR and 3'-RACE for TRACO2 are shown in figure 3.4.4B.

3.4.1.3. TRACO3

The 3'-UTR of TRACO3 was also amplified using 3'-RACE from cDNA templates generated by RT-treatment of RNA isolated from apex tissue (Fig. 3.4.5). First round PCR did not amplify any significant DNA bands using cDNA templates generated from either 1 μg poly(A)$^+$RNA or 5 μg total RNA (data not shown). However, PCR with cDNA templates made from 5 μg total RNA using the ACO2F primer (Table 2.4) as the 5'-sense primer for two rounds PCR amplified a major DNA band of *ca.* 350 bp (Fig. 3.4.5A).

The 3'-RACE products were cloned into the pCR 2.1 vector, and transformed into *E. coli* DH5α, even though the size of the 3'-RACE products were smaller (*ca.* 350 bp) than predicted (*ca.* 500 bp). The 3'-RACE product of *ca.* 350 bp was designated as 3'-RACE1 product. Plasmids containing these inserts were identified by EcoRI digestion and sequenced (Fig. 3.4.5B). At least two sizes of interest were obtained, but only the longest of these (Fig 3.4.5, lane 6) was the 3'-UTR sequence from TRACO3. The other products comprised sequences that did not match with reading frame sequences of any ACO genes.

The sequence comprises 359 nucleotides in total, which consists of 92 nucleotides encoding the 3'-UTR with 267 nucleotide encoding the protein-coding region (Fig. 3.4.6A). A 243 bp sequence at the 5'-end of 3'-RACE1 overlapped with the protein-coding region sequence generated by RT-PCR and so confirmed that the 3'-UTR of TRACO3 was successfully cloned using 3'-RACE.

However, an amplified product of *ca.* 500 nucleotides (*ca.* 300 nucleotide for 3'-UTS) was predicted originally from 3'-RACE of TRACO3. As such the 3'-UTRs of TRACO1 and TRACO2 generated by the 3'-RACE system were 301 bp and 250 bp, respectively. Therefore, the 92 bp cloned at the first attempt was hypothesised not to be the full-length 3'-UTR of TRACO3. Two additional attempts to clone an extended 3'-UTR of TRACO3 were undertaken, but only the *ca.* 90 bp sequence was cloned (data not shown). However, an extended size of 3'-UTR from TRACO3 was able to be cloned using 3'-RACE (the product

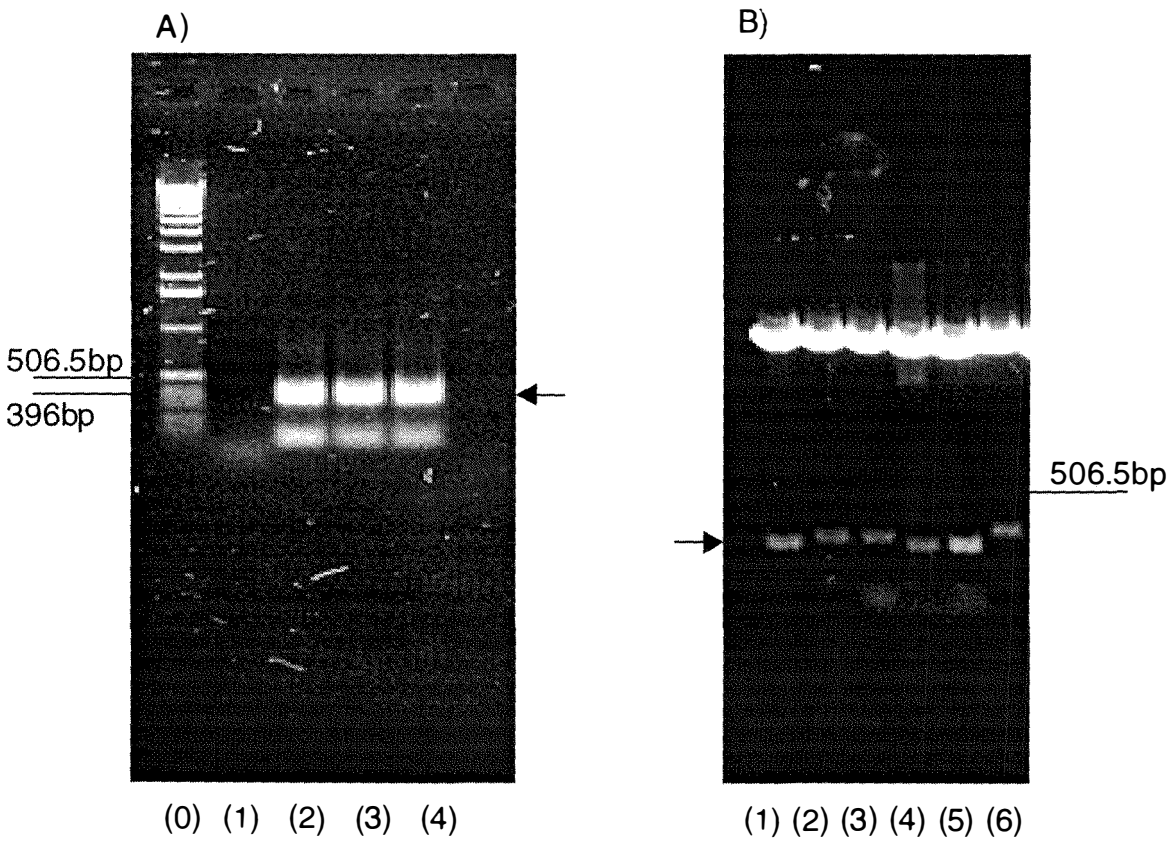

Figure 3.4.5 PCR amplification of the 3'-UTR of TRACO3 using RT-generated cDNA templates from poly(A)$^+$m RNA isolated from the developing apex. (A) PCR products were separated on a 1.2% (w/v) agarose gel and visualised with ethidium bromide. Lanes (1), (2), (3), and (4) are products from the second round PCR using of 0 µl, 2 µl, 5 µl, and 10 µl of the first round PCR as templates. Lane (0) are molecular size markers with two sizes indicated. (B) Inserts, obtained from EcoRI digestion of pCR 2.1 vectors containing putative 3'-UTRs of TRACO1, were separated on a 1.2% (w/v) agarose gel and visualised with ethidium bromide. Lanes (1-6) are from 6 colonies of *E. coli*, grown on LB-Amp^{100} plates. Arrows indicate *ca.* 350 bp PCR products.

Figure 3.4.6

A. Schematic of TRACO3 gene generated by RT-PCR and 3'-RACE. The RACE1 is the 3'-UTR of TRACO3 generated from the apex and the RACE2 is the 3'-UTR of TRACO3 generate from a senescent leaf tissue (leaf 12; Hunter, 1998). The eTRACO3 is a combined sequence of the reading frame and longest 3'-UTR.

B. Nucleotide and deduced amino acid sequences of TRACO3 including the protein-coding region and 3'-UTR. The 5'-primer sequences are indicated by underlining (ACOF5) used for two rounds PCR. The 5'-primer sequence used for amplification of cDNA gene specific probes is indicated by shaded characters. The 3'-primer sequences for both 3'-RACE and cDNA probe amplification are indicated by bold italics. The site of truncation to generate the 3'-UTR from the apex (at 932 bp) is marked by underlined bold italics.

A)

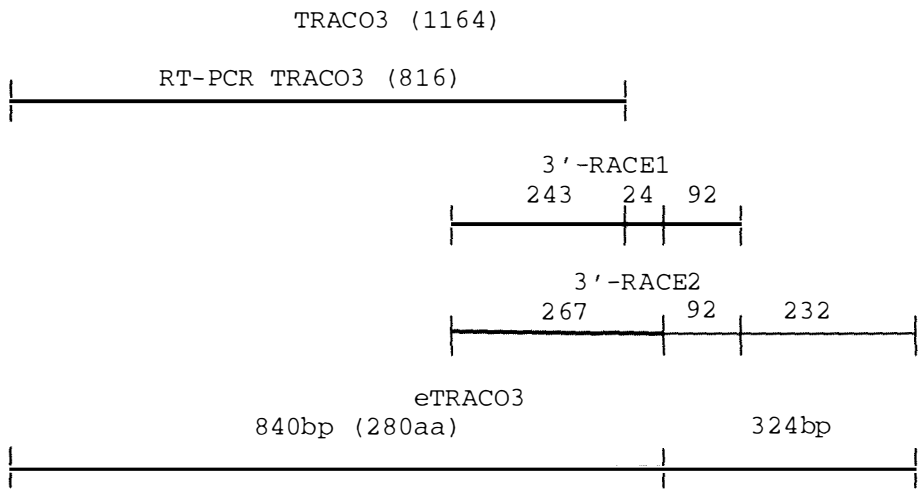

B)

```
   1 GCATGCCAGA ATTGGGGATT CTTTGAGCTG GTGAATCATG GCATACCTCA TGACCTTATG
       A  C  Q   N  W  G   F  F  E  L   V  N  H   G  I  P   H  D  L  M
  61 GACACATTGG AGAGATTGAC CAAAGAGCAC TACAGGAAAT GCATGGAGCA GAGGTTTAAG
       D  T  L   E  R  L   T  K  E  H   Y  R  K   C  M  E   Q  R  F  K
 121 GAATTGGTAT CAAGCAAAGG CTTAGATGCT GTCCAAACTG AGGTCAAAGA TATGGATTGG
       E  L  V   S  S  K   G  L  D  A   V  Q  T   E  V  K   D  M  D  W
 181 GAAAGTACCT TCCATGTTCG ACATCTCCCT GAATCAAACA TTTCAGAGCT CCCTGATCTC
       E  S  T   F  H  V   R  H  L  P   E  S  N   I  S  E   L  P  D  L
 241 AGTGATGAAT ACAGGAAGGT GATGAAGGAA TTTTCTTTGA GGTTAGAGAA GCTAGCAGAA
       S  D  E   Y  R  K   V  M  K  E   F  S  L   R  L  E   K  L  A  E
 301 GAGCTTTTGG ACTTGTTATG TGAGAATCTT GGACTTGAAA AAGGTTACCT CAAAAAGGCC
       E  L  L   D  L  L   C  E  N  L   G  L  E   K  G  Y   L  K  K  A
 361 TTCTATGGAT CAAGAGGACC AACTTTCGGC ACCAAGGTAG CCAACTACCC TCAATGCCCT
       F  Y  G   S  R  G   P  T  F  G   T  K  V   A  N  Y   P  Q  C  P
 421 AATCCAGAGC TGGTGAAGGG TCTCCGTGCT CACACCGATG CCGGTGGGAT CATCCTTCTC
       N  P  E   L  V  K   G  L  R  A   H  T  D   A  G  G   I  I  L  L
 481 TTCCAGGATG ACAAAGTCAG CGGCCTTCAG CTACTCAAAG ACGACGAGTG GATCGATGTT
       F  Q  D   D  K  V   S  G  L  Q   L  L  K   D  D  E   W  I  D  V
 541 CCCCCAATGC GTCACTCCAT TGTTGTCAAC CTTGGTGACC AGCTCGAGGT AATAACAAAT
       P  P  M   R  H  S   I  V  V  N   L  G  D   Q  L  E   V  I  T  N
 601 GGTAAATATA AGAGTGTGGA GCACCGTGTG ATAGCACAAA CAAATGGAAC AAGAATGTCT
       G  K  Y   K  S  V   E  H  R  V   I  A  Q   T  N  G   T  R  M  S
 661 ATAGCATCAT TCTACAACCC TGGAAGTGAT GCTGTAATCT ACCCTGCTCC AGAATTGTTG
       I  A  S   F  Y  N   P  G  S  D   A  V  I   Y  P  A   P  E  L  L
 721 GAAAAAGAAA CAGAGGAAAA AACCAATGTG TATCCTAAAT TTGTGTTTGA AGAGTACATG
       E  K  E   T  E  E   K  T  N  V   Y  P  K   F  V  F   E  E  Y  M
 781 AAGATCTATG CTGCTTTGAA ATTTCAAGCT AAGGAACCAA GATTTGAAGC ACTGAAAGCA
       K  I  Y   A  A  L   K  F  Q  A   K  E  P   R  F  E   A  L  K  A
 841 TGAAATGTGA ATTTGGGTTC AATTGCAATT GTTTTGAATT TAAACAAGTA ACATAAAATA
 901 GGCAAAGATG CATGTGCTCC TCAAATGAAA ATAATAAAAA ATAGATTTAA ATATGATGCG
 961 AGTCATGCAA ATATATTATG TGTTAGTTTT TGTAAGTTTA TTTTTAATAG ATAAACGAAA
1021 TGTGTGTTAA TACAAATTCA CACAGTAAAT TGAAGGGATT AGAGTTCGAA CATCGGTTAT
1081 GGTGTCAGAC TCATTTTGGC TTTGTAATTT TCTTTTTTTT TGCTTGAGTT CAACTCGTAT
1141 AAATTTAAAA AAAAAAAAAA AAAATTAGCTGCAGTAGGATCCA
```

was designated as 3'-RACE2; Fig. 3.4.6A) with cDNA templates generated by RT-treatment of RNA isolated from leaf 14 (Hunter, 1998). In that study, the use of 3'-RACE also revealed two smaller size products with the smallest one of these corresponding to the fragment (92 bp) generated using 3'-RACE from the apex. The nucleotide sequences of the longest 3'-UTR (324 bp) of TRACO3 is shown with the site of truncation to release the shorter sequence (92 bp) cloned from the apex (Fig. 3.4.6B). Also, the deduced amino acid sequence obtained from a combination of ACO sequences generated by RT-PCR and 3'-RACE for TRACO3 is shown in figure 3.4.6B.

The 232 nucleotides difference between 3'-RACE1 and 3'-RACE2 may account for the size difference between the two transcripts (1.1 kb and 1.35 kb) detected, when the protein-coding region of TRACO3 was used as a probe in northern analysis (Fig. 3.3.16). However, for further gene expression studies, the longer 3'-UTR of TRACO3 was used as probe, because it was the main species expressed in leaf 14 where TRACO3 expression was maximal when determined by northern analysis (Hunter *et al.*, 1999).

It is also interesting to note that only TRACO1 was generated by RT-PCR with degenerate primers using cDNA template generated by RT-treatment of mRNA isolated from the apex (section 3.3.1.1). However, 3'-RACE products were generated for all three ACO genes with gene-specific primers from mRNA isolated from the apex, although the 3'-UTR of TRACO3 was truncated. This result may suggest that PCR using gene-specific primers is more sensitive when compared with using degenerate primers.

3.4.1.4 Sequence analysis of ACO cDNA

The extended deduced amino acid sequences [the combination of the RT-PCR generated reading frame (protein-coding region) and the residual 3'-reading frame obtained by 3'-RACE] of TRACO1, TRACO2 and TRACO3 (Fig. 3.4.2; Fig. 3.4.4; Fig. 3.4.6.) were aligned (Fig. 3.4.7). The number of extended deduced amino acids for TRACO1, TRACO2 and TRACO3 were 292, 288, and 280, respectively, and the sequence homology was 81%, 78%, and 85% respectively in terms of comparison between TRACO1 and TRACO2, TRACO1 and TRACO3,

```
TRACO1   (  27)   ACENWGFFELVNHGISIEMMDKVEKLTKDHYKKCMEQRFKEMVSSKGLEC
TRACO2   (  27)   ...............HDL..T..R...E..RI.......DL.AN....A
TRACO3   (  27)   ..Q............PHDL..TL.R...E..R.........L......DA

TRACO1   (  77)   VQSEINDLDWESTFFLRHLPFSNISEIPDLDDDYRKIMKEFAQKLENLAE
TRACO2   (  77)   ..T.VK.M......H.....E.....V...T.E...A...F.L...KL..
TRACO3   (  77)   ..T.VK.M......HV....E.....L...S.E...V...FSLR..KL..

TRACO1   ( 127)   ELLDLLCENLGLEKGYLKKVFYGSKGPNFGTKVSNYPPCPKPDLIKGLRA
TRACO2   ( 127)   ....L......L.....K.A.......T...K.A..........VK....
TRACO3   ( 127)   ....L......L.....K.A....R..T...K.A...Q..N.E.VK....

TRACO1   ( 177)   HTDAGGIILLFQDDKVSGLQLLKDDQWIDVPPMRHSIVINLGDQLEVITN
TRACO2   ( 177)   HTD...................K.GK.V.....H...............
TRACO3   ( 177)   HTD...................K..E............V...........

TRACO1   ( 227)   GKYKSVMHRVIAQTDGARMSLASFYNPSDDAIISPAPTLL-KENETTSEI
TRACO2   ( 227)   ...RS.EH.....S..T...I......GS..V.Y..T..I-E..---N.V
TRACO3   ( 227)   ....S.EH......N.T...I......GS..V.Y...E..E..T.EKTNV

TRACO1   ( 276)   YPKFVFDDYMKLYMGLKFQAKEPRFEAMMKAMSSVDVGPVVSI
TRACO2   ( 273)   ......E...N..A..K...K.......-F.ES.N.KL..IATV
TRACO3   ( 277)   ......EE...I.AA.K...K......-------------LKA
```

Figure 3.4.7 Alignment of deduced amino acid sequences from TRACO2 and TRACO3 with that of TRACO1 as the reference sequence. Identical amino acid residues are indicated by (•), different residues are shown, and mismatching residues are indicated by (-) in the TRACO2 and TRACO3 sequences.

Critical residues for ACO activity are F^{117}, $L^{124, 131, 138}$, a putative Leu zipper motif; $H^{177, 234}$ D^{179}, putative Fe^{2+} binding site; $K^{144, 158, 172, 198, 293, 299}$, putative CO_2 binding sites (Kadyrzhanova *et al.* 1997).

and TRACO2 and TRACO3, respectively. The aligned sequences in figure 3.4.7 also indicate that those amino acids, proposed as critical residues for ACO function, are highly conserved in all three sequences.

Alignment analysis of the DNA sequences encoding the 3'-UTRs showed 55 to 61% homology to each other (Table 3.4.1), confirming that the 3'-UTR sequences were more divergent when compared with the protein-coding regions of the three genes (cf. Table 3.3.2).

Table 3.4.1 Homology values of 3'-UTRs of three TRACO nucleotide sequences.

	Reference sequence		
	TRACO1	TRACO2	TRACO3
TRACO1	-	61	55
TRACO2	61	-	59
TRACO3	55	59	-

Further this divergence was represented by short unique gene-specific sequences within each 3'-UTR as well as single base pair differences (Fig. 3.4.8). Therefore, the 3'-UTRs were considered to be more useful for further analysis of ACO gene expression using northern hybridisation.

```
TRACO1  TATGATGAAAGCAATGTCAAGTGTTGATGTGGGACCAGTAGTAAGCATATGAAAA--AAG
TRACO2  AT.T.A.G..T..---....A....A.AC.T..T...A.T.C..----------------
TRACO3  ---AC.........---.G..A...GA..T....TT..A.T.C..TTG.T.TG..TTT..A

TRACO1  CA--TATTATTAGATTGATTATGTGTGGTTTTGTTAATAAGCTGAGTTTATTAAGCGAT-
TRACO2  ----------C..T..A..........--.AC.A.A....----------.A...AAA..A
TRACO3  ..AG..AC..A.A..A.GCA.A.-A..CA.G..C.CC.C.AA...AAA..A...AAA..A

TRACO1  ----TATTAGTGTTTGGTTTGGTGTTTATTTATTAT----TATAATTGGTATG---ACTT
TRACO2  A---...A.A.A.A..T.AACA.....G..----------...G...A.---------
TRACO3  GATT..AATA..A.GC.AG.CA..CAA..A......GTGT..GTT..T...A.TTT.T..

TRACO1  ATGAGAGGTTAAGATCATGCAGTCTAAAGGTGTTGTTATTAAAGTTTATAATAAAGTATG
TRACO2  ---GC.A.CA...TAA.AAA.AG..T..A..CAA..GCA...GT..CTC..ATT......
TRACO3  T.A.T..A.A..----------.G...T...-.....A..C.AA.--.C.C.C....AA

TRACO1  ATTAATGGTTGATTT--T----AGATTGGGTGTGATGACTGATTAGTGTTGTTGGTTGGA
TRACO2  --..G.T...T.C..AC.----.T..A.T.A.....----------...A...GAT..TCT
TRACO3  T.G..G..A.T.GAG--.TCGA.C..C..T.A..G..T.A..C.CA.T...---------

TRACO1  AGATTAACTGGTTAATTAAGTTATTGAAATGTG--ATGTAATACTG----TTTTATAAAA
TRACO2  T.TA.T.T.T..GG.AA....A..ATC.....TCA..A.....A.AAATA.A....TC..
TRACO3  ------G..TTG.....TTC..T..TTTTGC.T--GA..TCA...C----G.A..A.TTT

TRACO1  CC-A
TRACO2  GTA.
TRACO3  AA-.
```

Figure 3.4.8 Alignment of nucleotide sequences of 3'-UTRs from TRACO2 and TRACO3 with that of TRACO1 as the reference sequence. Identical nucleotide sequences are indicated by (•), different sequences are shown, and mismatching sequences are indicated by (-) in the TRACO2 and TRACO3 sequences.

3.4.2 The multigene family of ACO in white clover

3.4.2.1 Three gene-specific probes using 3'-UTRs of ACO genes

Gene-specific probes were prepared using PCR with gene specific primers (Table 2.4) designed to amplify the 3'-UTR from each of the three ACO genes. The probes were 347 bp, 270 bp and 360 bp for TRACO1, TRACO2 and TRACO3, respectively. The specificity of probes was examined initially by Southern hybridization, using 50 ng of each 3'-UTR sequence immobilised onto a nylon membrane (Fig. 3.4.9). Each of the three gene specific probes, labeled with ^{32}P–dCTP, hybridised only to the corresponding 3'-UTR sequences, indicating that each gene specific probe was capable of discriminating each 3'-UTR template under the conditions used for hybridisation. Therefore, these 3'-UTRs were used as gene-specific probes in genomic Southern analysis and in northern analysis for gene expression studies.

3.4.2.2 Genomic Southern analysis

With the three gene-specific probes tested for specificity under the hybridisation conditions to be used, genomic Southern analysis was used to confirm that the three ACO genes cloned originated from the white clover genome. Genomic DNA (10 μg), extracted from mature green leaf tissue (leaf 4 and leaf 5) was digested with three restriction enzymes (EcoRI, Hind III and XbaI), and probed with ACO gene-specific 3'-UTR probes (Fig. 3.4.10). The hybridisation patterns for TRACO1 and TRACO3 were successfully demonstrated. The unique banding patterns suggested that TRACO1 and TRACO3 were encoded by different genes in white clover genome. Multiple hybridisation bands observed for TRACO1 may be a consequence of the allotetraploid white clover genome. However, a hybridisation pattern for TRACO2 was not achieved under the conditions used, even with 3-fold more DNA (30 μg) (data not shown). This was probably due to the fact that ^{32}P-dCTP was used for DNA labeling, but the 3'-UTR of TRACO2 has a high AT content (Fig. 3.4.8). Also, the relatively low Tm of the short probe (*ca.* 270 bp) of TRACO2 may have been unstable during hybridisation. When P^{32}-dATP was used for labeling with an extended probe (415 bp) comprising the 250 bp 3'-UTR and 165 bp protein-coding region of TRACO2, a unique hybridisation pattern with multiple bands was revealed, when compared with the TRACO1 and TRACO3 patterns (Hunter *et al.*, 1999).

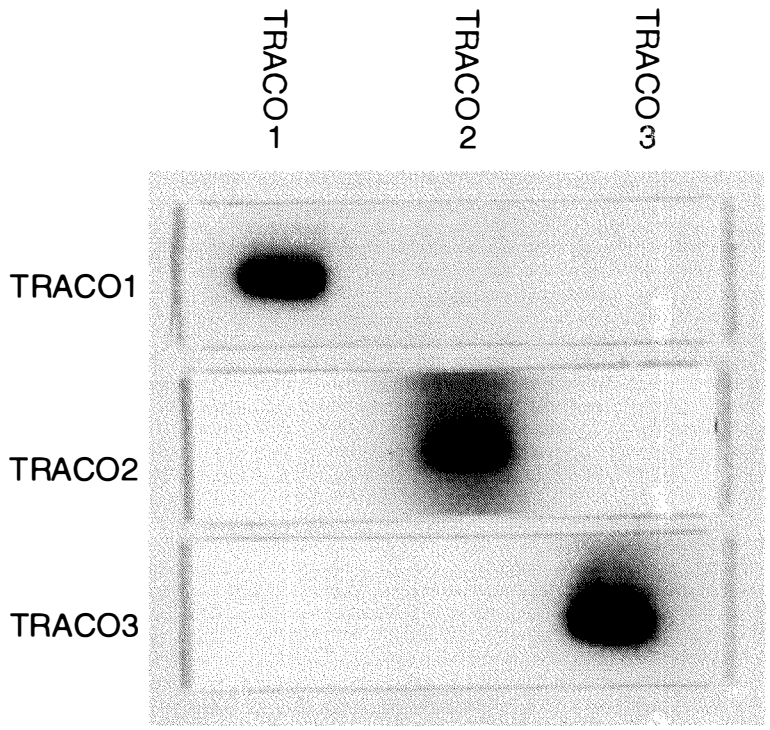

Figure 3.4.9 Southern analysis to determine the specificity of 3'-UTRs as gene-specific probes. Three separate membranes were prepared. Fifty ng of the 3'-UTR from each gene was separated on a 1.2% (w/v) agarose gel and blotted onto N^+-Hybond membrane with alkaline transfer buffer. Each membrane was hybridized with one of three ^{32}P-labeled 3'-UTR sequences (as indicated), washed at a high stringency (0.1X SSPE at 65 ^{o}C) and exposed to X-ray film for 15 min.

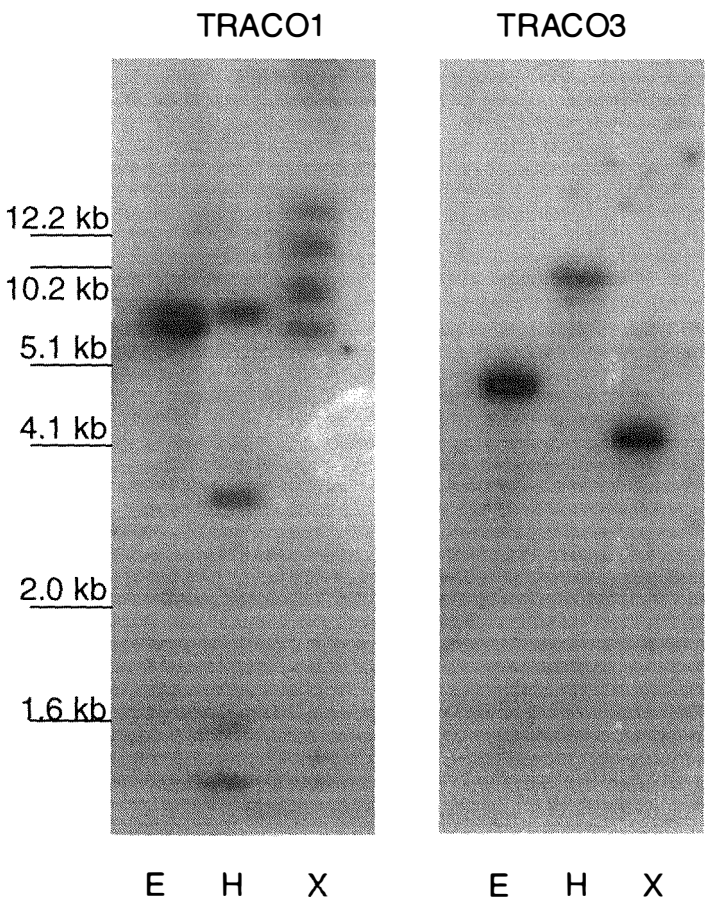

Figure 3.4.10 Southern analysis with genomic DNA using 3'-UTRs as probes. Ten μg of the genomic DNA was digested with EcoRI (E), HindIII (H), and XbaI (X) overnight, separated on a 0.8% (w/v) agarose gel and blotted onto N^+-Hybond membrane with alkaline transfer buffer. Each membrane was hybridized with ^{32}P-labeled TRACO1 and TRACO3 (as indicated), and exposed to X-ray film for 7 days. Molecular sizes are indicated.

Taken together, genomic Southern analysis indicates that each of three ACO genes are encoded by distinct genes in white clover.

3.4.3 Expression of ACO genes in white clover

3.4.3.1 Expression of ACO genes during early leaf development

The expression pattern of the three ACO genes during early leaf development has been characterised using northern analysis with gene-specific 3'-UTR probes (Fig. 3.4.11). Gene-specific probes of TRACO1 and TRACO2 hybridised to transcripts of 1.35 kb. TRACO1 was predominantly expressed in the developing apex, while TRACO2 was expressed in newly initiated leaves (leaf 1 and leaf 2) and in mature green leaves (leaf 3, leaf 4 and leaf 6), with maximum expression in newly initiated leaves. The residual expression of TRACO2 observed earlier in the apex, when the protein-coding region of the gene was used as a probe (figure 3.3.16), decreased markedly with the use of gene-specific probes. Expression of TRACO3 was barely detectable in younger leaf tissue with a slight induction in the later mature green leaves (leaf 3-6). In this northern only a 1.35 kb transcript was recognised. The overall expression pattern of ACO genes using gene-specific probes confirmed the expression pattern determined using the protein-coding region probes (section 3.3.3.2).

3.4.3.2 Organ-specific ACO gene expression

The gene expression pattern of TRACO1 and TRACO2 in other plant parts was studied using 1 µg of poly(A)$^+$mRNA extracted from floral buds (enclosed floral buds before flowering), the apex and axillary buds (buds taken from axils of node 3 and 4), mature green petioles, mature green nodes (portions including node and root primordium), mature green internodes, and roots (root tissues including root hairs and tips grown in vermiculate potting mix) (Fig. 3.4.12).

The gene-specific 3'-UTR TRACO1 hybridised to a transcript of 1.35 kb in the apex and axillary buds as well as roots, with higher hybridisation in the roots. TRACO2 hybridised to the same size transcript extracted from mature green petioles, mature green nodes, inter-nodes and roots, again with the highest hybridisation signal from the roots.

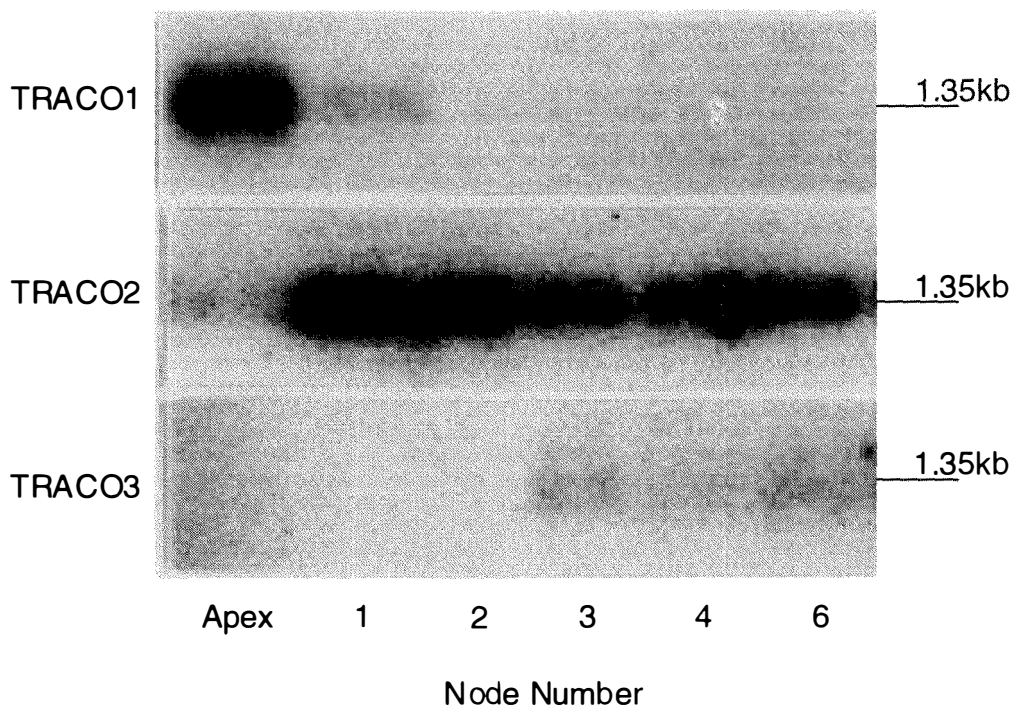

Figure 3.4.11 Expression of ACC oxidase genes in leaf tissue at different stages of development determined by northern analysis using 3' UTRs as probes. Two µg of poly(A)$^+$mRNA was separated on a 1.2 % (w/v) agarose-formaldehyde gel, blotted onto Hybond-N$^+$ with alkaline transfer buffer, probed with ^{32}P-labeled 3'-UTR of TRACO1, TRACO2 and TRACO3 (as indicated), and washed at high stringency (0.1 X SSPE at 65 ^{o}C). The membrane was exposed to X-ray film for 7 days.

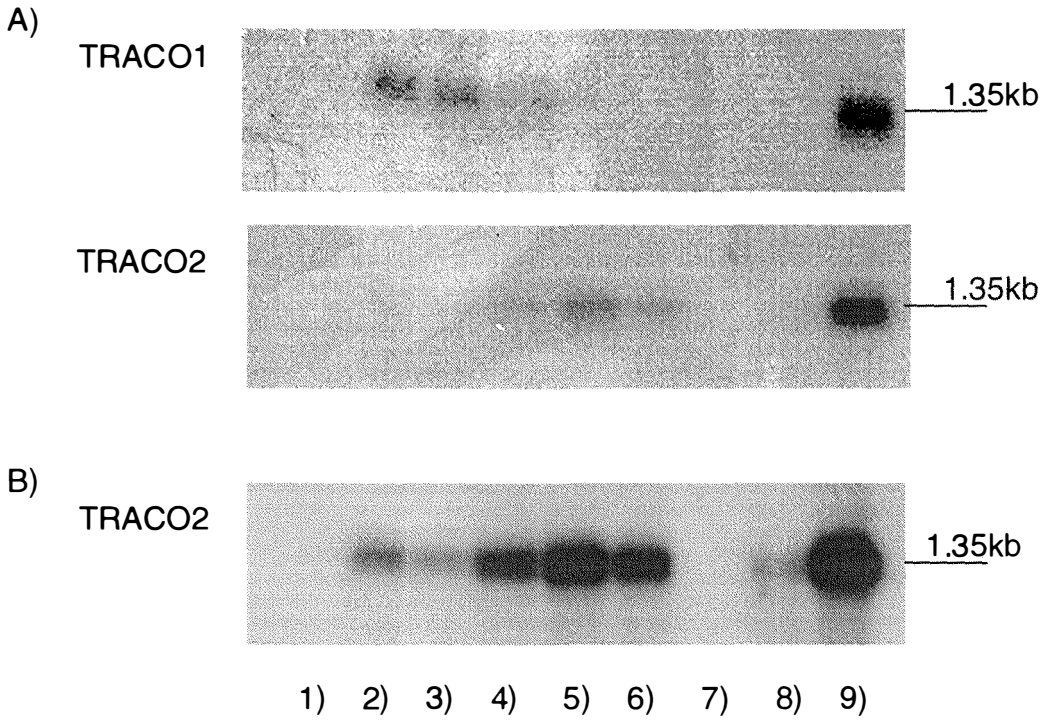

Figure 3.4.12 Expression of ACC oxidase genes in various tissues of white clover determined by northern analysis with 3'-UTRs as probes. One μg of poly(A)$^+$mRNA was isolated from floral buds (1); axillary buds (2); apical buds (3); mature green petiole (4); mature green inter-nodes (5); mature green nodes (6); senescent leaf 12 (8) and roots (9). Lane (7) was not loaded with RNA. Sample RNA was separated on a 1.2% (w/v) agarose-formaldehyde gel, blotted onto Hybond-N$^+$ with alkaline transfer buffer, probed with ^{32}P-labeled TRACO1 and TRACO2 (as indicated). Membranes were washed at high stringency (0.1 X SSPE at 65 ^{o}C) and exposed to X-ray film for 16 hr (A) and 21 days (B).

In summary, TRACO1 was expressed in developing vegetative bud tissues (apical and axillary buds), whereas TRACO2 was expressed mainly in the mature green vegetative tissues such as petiole, node and internodes. The root appeared to express both TRACO1 and TRACO2 to a higher extent, although the root was not divided into meristematic, elongating or mature tissues. Floral buds did not express either TRACO1 or TRACO2.

Extended exposure (21 days) of the membrane hybridised with TRACO2 demonstrated that expression is relatively higher in internodes and roots, when compared with petiole and node tissues (Fig. 3.4.12). Also, a basal level of TRACO2 expression was detected in the apical and axillary buds, but the level was about the same level as in senescent leaves (Leaf 12).

Part 5: Expression of ACO proteins in white clover

3.5.1. Characterisation of three polyclonal antibodies produced against proteins expressed from three TRACO genes using bacterial system

Polyclonal antibodies (PAbs) to the TRACO1 gene product, expressed using the pPROEX-1 vector in *E. coli* and purified using the Ni-NTA affinity column (section 3.3.2.2), were raised in rats (Table 3.5.1). Also, antibodies against expressed proteins of TRACO2 and TRACO3 were produced in rabbits and rats, respectively, by Dr. D. Hunter (IMBS, Massey University). Each antibody raised against TRACO1, TRACO2 and TRACO3 gene products, was designated as PAb1, PAb2 and PAb3, respectively.

Table 3.5.1 Summary of PAbs produced against three TRACO fusion proteins expressed and purified from *E. coli* strain TB1.

ACO gene	ID of PAb	Inoculated animal	Producer
TRACO1	PAb1	rat	Yoo, S-D
TRACO2	PAb2	rabbit	Hunter, DA
TRACO3	PAb3	rat	Hunter, DA

3.5.1.1 Characterisation of PAbs using TRACO proteins expressed in *E. coli*

Antibody specificity and cross reactivity of PAb1 was determined using Ni-NTA column-purified TRACO proteins expressed in *E. coli* (Fig. 3.5.1). Using western analysis, PAb1 specifically recognised a single protein band of *ca.* 35 kD in the TRACO1 lane after a development time of 1 min, whereas negligible recognition was detected in the lanes loaded

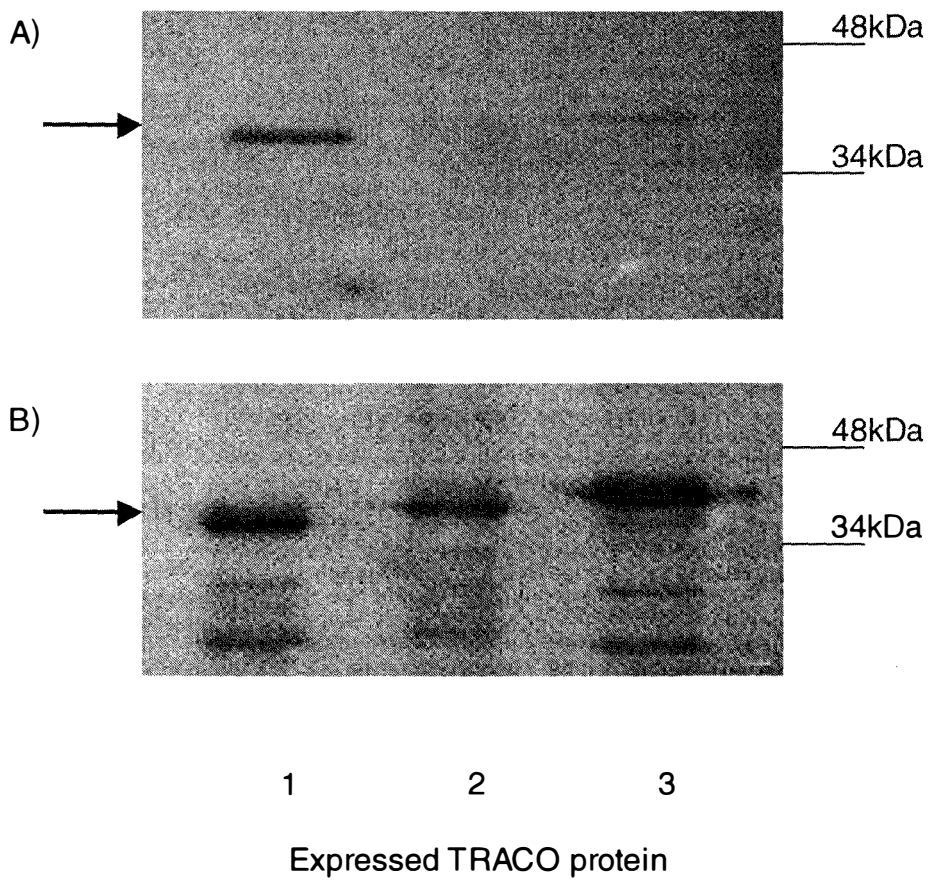

Figure 3.5.1 Western analysis of TRACO1, TRACO2 and TRACO3 proteins with PAb1. Five hundred ng of expressed ACO protein purified from *E. coli* was separated using 16% (w/v) SDS-PAGE and electroblotted onto PVDF membrane. Membranes were developed for 1 min (A) or 15 min (B). Arrows indicate antibody recognition of *c*a. 35 to 37 kD proteins. Two molecular weights are indicated.

with TRACO2 and TRACO3 proteins (Fig. 3.5.1A). However, when the developing time was extended to 15 min, PAb1 recognised multiple bands in the all three lanes with major recognition of *ca.* 35 to 37 kD proteins, which are the putative sizes for TRACO gene products expressed in *E. coli* (Fig. 3.5.1B).

The size difference between TRACO2 and TRACO3 most likely resulted from differences in the sequences generated by RT-PCR (TRACO2, 804 bp, which codes for 268 amino acids; TRACO3, 816 bp, which codes for 272 amino acids). However, the shortest size of the TRACO1 protein recognised by PAb1 cannot simply be explained by its size calculated from the DNA sequence (813bp, which encode for 271 amino acids).

In section 3.3.2.1, TRACO1 cDNA fragments of *ca.* 800bp, digested with two restriction enzymes, were cloned into pPROEX-1 vectors and the correct size of inserts were generated from the plasmids prepared from bacterial cells selected on LB-Amp^{100} plates (Fig. 3.3.9). It may be that a premature stop-codon was inserted during the in-frame amplification of TRACO1 for cloning into pPROEX-1. The TRACO1 gene inserted into the vector was not resequenced but sufficient amino acid sequence was obtained only to confirm that an in-frame protein was expressed (Fig 3.3.13). It may be that TRACO1 protein expressed in *E. coli* is relatively labile to prokaryotic proteinase.

In terms of cross-reactivity of the antibodies, the aligned amino acid sequences deduced from the three ACO genes show very similar putative protein epitopes, when the proteins are used as antigens (Fig. 3.5.2). In theory, looping regions between two adjacent β-sheets, the so called head-of-hairpin structure, are known to be antigenic (Branden and Tooze, 1991). These structures were very much identical in the amino acid sequences deduced from the three TRACO genes, due to the fact that primary and secondary structures of the proteins were conserved (Fig. 3.3.14) and may explain the cross-reactivity of the TRACO PAbs observed.

```
TRACO1   ACENWGFFELVNHGISIEMMDKVEKLTKDHYKKCMEQRFKEMVSSKGLEC
TRACO2   ................HDL..T..R...E..RI.......DL.AN....A
TRACO3   ..Q............PHDL..TL.R...E..R.........L......DA

TRACO1   VQSEINDLDWESTFFLRHLPFSNISEIPDLDDDYRKIMKEFAQKLENLAE
TRACO2   ..T.VK.M......H.....E.....V...T.E...A.....L...K...
TRACO3   ..T.VK.M......HV....E.....L...S.E...V....SLR..K...

TRACO1   ELLDLLCENLGLEKGYLKKVFYGSKGPNFGTKVSNYPPCPKPDLIKGLRA
TRACO2   ..................A.......T.....A..........V.....
TRACO3   ..................A....R..T.....A...Q..N.E.V.....

TRACO1   HTDAGGIILLFQDDKVSGLQLLKDDQWIDVPPMRHSIVINLGDQLEVITN
TRACO2   ............DDKVSG....KDGK.V..PPMHH.....LGDQ.....N
TRACO3   ............DDKVSG....KDDE....PPMRH...V.LGDQ.....N

TRACO1   GKYKSVMHRVIAQTDGARMSLASFYNPSDDAIISPAPTLL-KENETTSEI
TRACO2   GKYRSVE......SDGT...I...YNPGSDAV.Y..T..I-E..---N.V
TRACO3   GKYKSVE......TNGT...I...YNPGSDAV.Y...E..E..T.EKTNV

TRACO1   YPKFVFDDYMKLYMGLKFQAKE
TRACO2   ......E...N..A........
TRACO3   ......EE...I.AA.......
```

Figure 3.5.2 Alignment of the deduced amino acid sequences from TRACO2 and TRACO3 with that of TRACO1 as the reference sequence. Identical amino acid residues are indicated as (•), different residues are shown, and missing residues are indicated as (-). Amino acids in bold characters represent putative antigenic sites (Branden and Tooze, 1991), based on the prediction of secondary structure from each protein sequence (Protein Prediction 2 programme, EMBL, Heidelberg, Germany).

Taken together, these polyclonal antibodies appear to be useful as either for ACO isoform-specific recognition using a shorter developing time (1 min ≥) or for collective ACO protein recognition using a longer developing time (≥ 15 min) in a tissue at a time. However, when complex protein extracts were separated using SDS-PAGE and probed with PAbs, development time in excess of 15 min was always required to discern antibody recognition.

3.5.2 Expression of ACO proteins in the developing apex and leaf tissues

3.5.2.1 Characterisation of ACO protein accumulation with PAb1

Western analysis was performed using PAb1 to characterise the pattern of TRACO1 protein expression during early leaf development using protein extracts after 30% to 90% (w/v) ammonium sulphate fractionation (Fig. 3.5.3). PAb1 recognition was specifically discerned as a high molecular weight complex of ≥ 103 kD in protein extracts from the apex. The complex comprised a higher molecular weight band, which accumulated predominantly in protein extracts from the apex. Its recognition was dramatically reduced in protein extracts from leaf 1 and it was not discerned in those from leaf 2 onwards. Recognition of the lower molecular weight band was also high in the apex and then slowly decreased to be lowest by leaf 6.

When western analyses were repeated with pre-stained high range molecular weight markers, a reproducible antigen-antibody complex of ≥ 205 kD was recognised (Fig. 3.5.4). Recognition, which was highest in the apex, comprised a doublet protein band in this tissue, and then a single band of ≥ 205 kD, which was recognised with decreasing intensity from leaf 1 to leaf 6.

This protein complex hardly entered a 16% (w/v) SDS-PAGE gel as did the high molecular maker protein of 205 kD (data not shown). Therefore, 8-15% (w/v) SDS-PAGE gradient gels or 10% (w/v) SDS-PAGE gels were used for further analysis of this protein.

3.5.2.2 Characterisation of ACO protein accumulation by PAb2

Western analysis, using PAb2, determined that the antibody recognised a protein band of *ca.* 36 kD in protein extracts after 30%-90% (w/v) ammonium sulphate fractionation from the apex to leaf 8 (Figure 3.5.5). The extent of recognition by PAb2 was higher in the extracts from

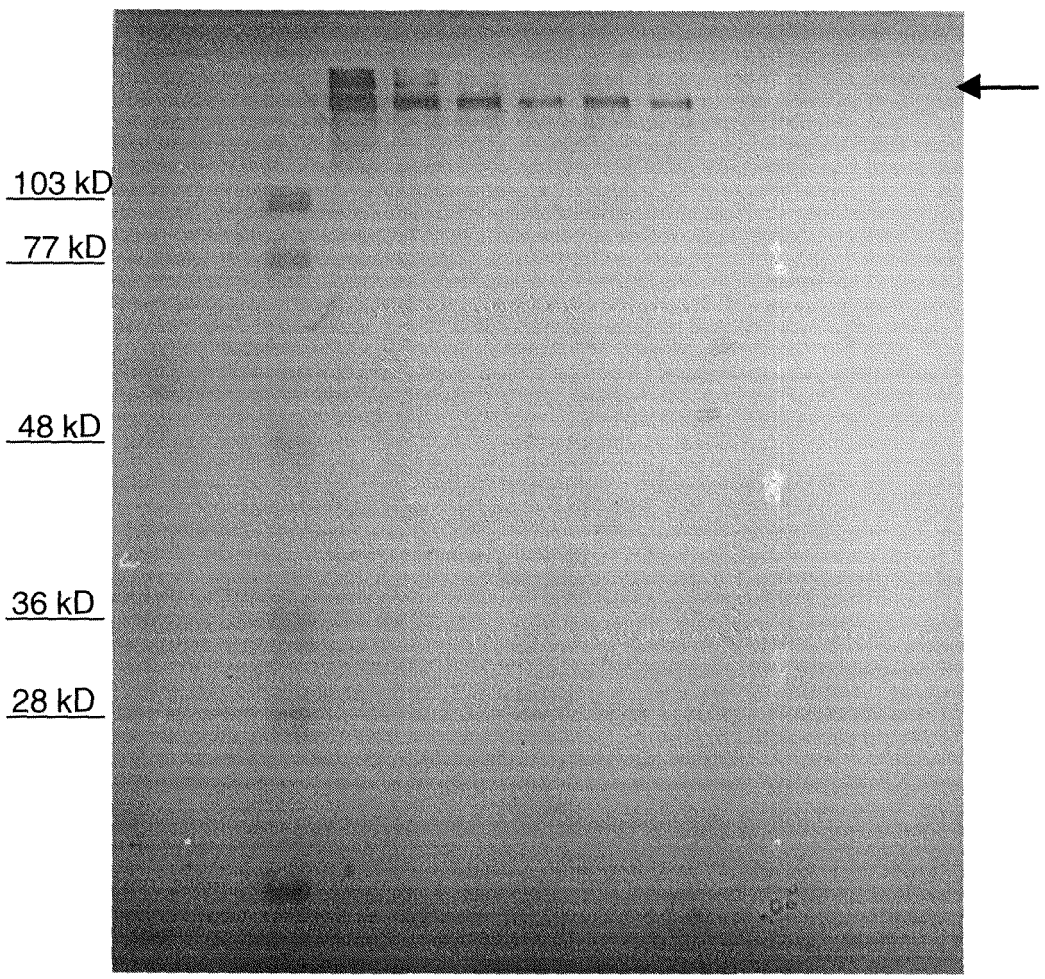

Figure 3.5.3 Western analysis, using PAb1, of ACO protein expression in the apex, and newly initiated and mature green leaves. Protein extracts (150 μg), fractionated with 30-90% (w/v) saturated ammonium sulphate, were separated on a 8-15% (w/v) gradient SDS-PAGE gel and electroblotted onto PVDF membrane. Lane (0) are pre stained molecular weight markers from Bio-Rad, with molecular weights indicated. The arrow indicates PAb1 recognition of a high molecular weight protein complex.

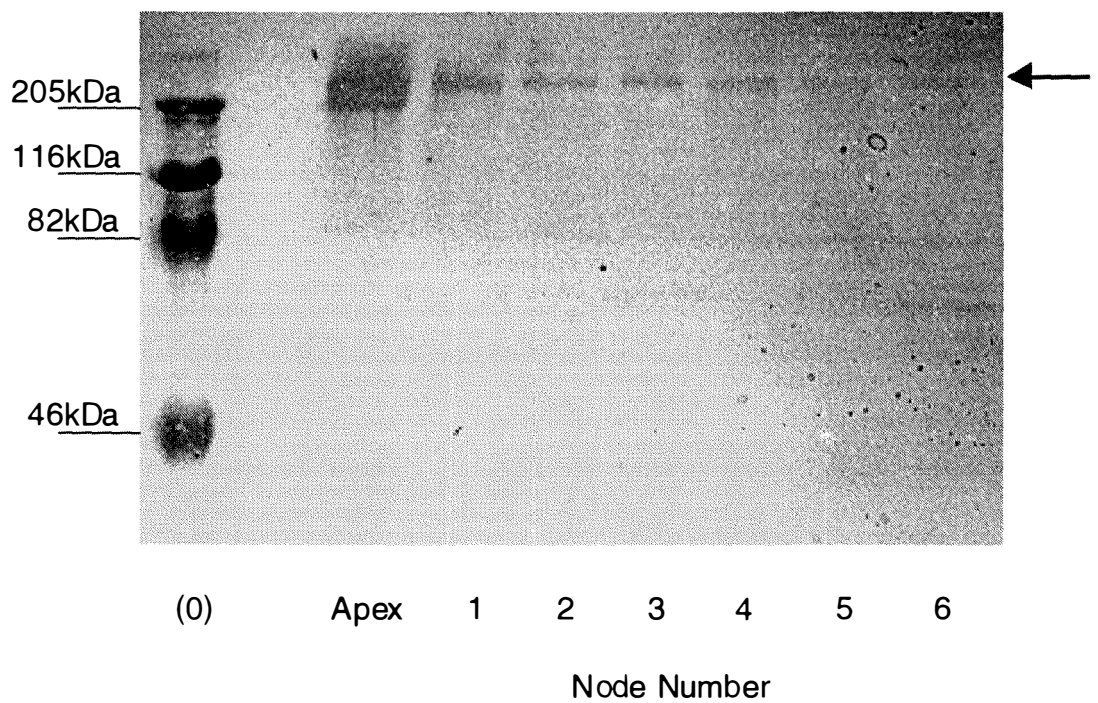

Figure 3.5.4 Western analysis, using PAb1, of ACO protein expression in the apex and newly initiated and mature green leaves. Protein extracts (150 μg), fractionated with 30-90% (w/v) saturated ammonium sulphate, were separated on a 8-15% (w/v) gradient SDS-PAGE gel and electroblotted onto PVDF membrane. Lane (0) are pre stained molecular weight markers from Bio-Rad (High Range) with molecular weights indicated. The arrow indicates PAb1 recognition of a *ca.* 205 kD protein complex.

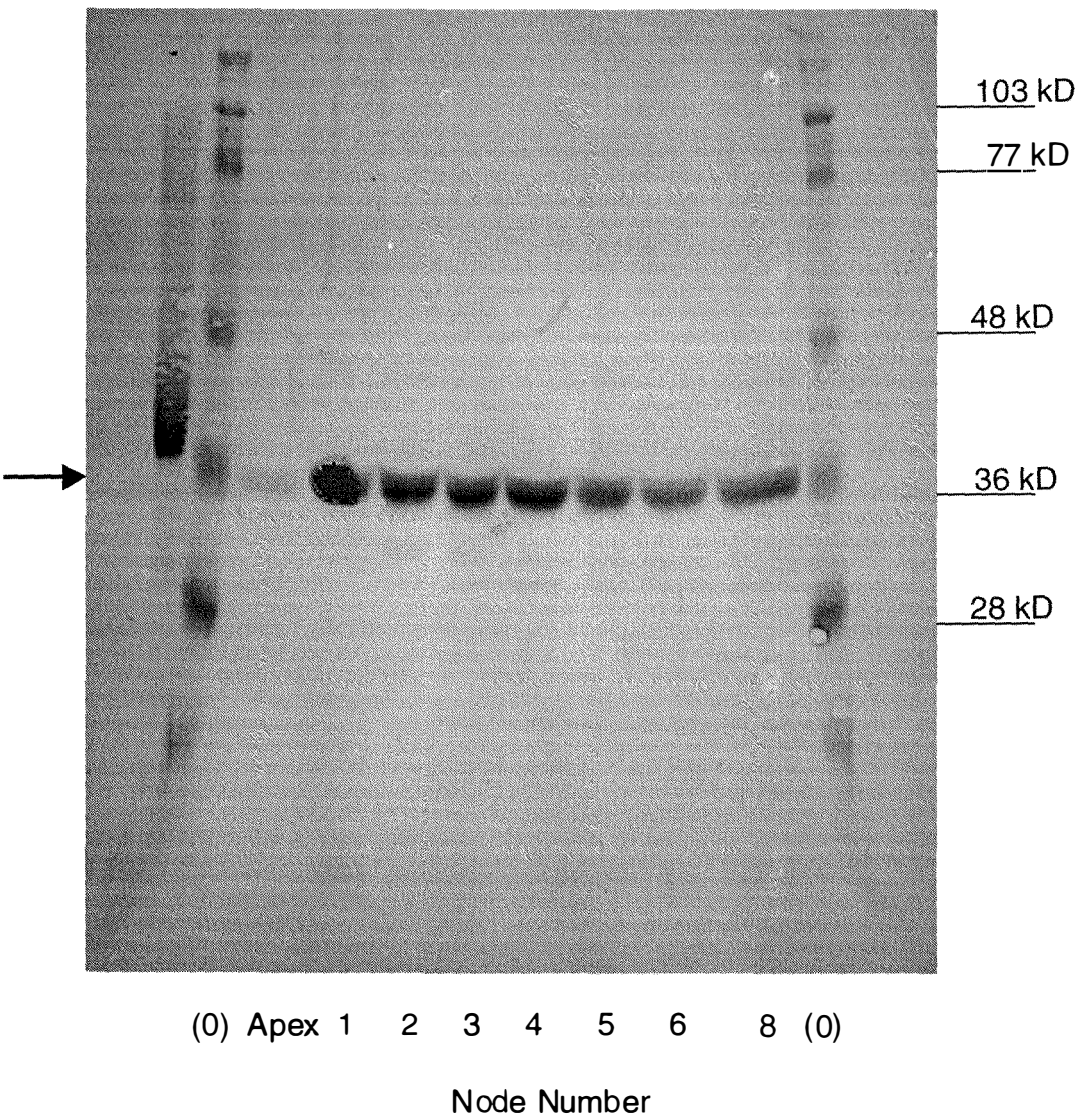

Figure 3.5.5 Western analysis, using PAb2, of ACO protein expression in the apex, and newly initiated and mature green leaves. Protein extracts (150µg), fractionated with 30-90% (w/v) saturated ammonium sulphate, were separated on a 8-15% (w/v) gradient SDS-PAGE gel and electroblotted onto PVDF membrane. Lane (0) are pre-stained molecular weight markers from Bio-Rad, with molecular weights indicated. The arrow indicates PAb2 recognition of a *ca.* 36 kD protein.

newly initiated leaves (leaf 1 and leaf 2) and just fully expanded mature green leaves (leaf 3 and leaf 4), when compared with protein extracts from the apex and the later mature green leaves (leaf 5, leaf 6 and leaf 8). So, expression of TRACO2 protein is highest during early leaf development (newly initiated leaves and just fully expanded leaves), a pattern which correlates well with ACO activity, *in vitro* (Fig. 3.1.12) and roughly with TRACO2 gene expression (Fig. 3.3.15; 3.4.11).

3.5.3 Expression of ACO protein in different organs of white clover

The pattern of ACO protein expression in various organs of white clover was examined by western analysis using PAb1 and PAb2 (Fig. 3.5.6; Fig. 3.5.7). Western analysis using PAb1 was performed with protein extracts from various plant organs of white clover (Fig. 3.5.6). PAb1 recognised the high molecular weight (≥ 205 kD) protein in extracts from bud tissues including the apex, axillary buds and floral buds and also from leaf 1. Although the protein recognised was about the same molecular weight as shown in figure 3.5.3, the double banding pattern was not observed using the mini-gel system with 20 µg of crude protein extracts (root: 5 µg) (Fig. 3.5.6), when compared with using the 8-15% gradient gel with 150 µg of a 30-90% (w/v) saturated ammonium-sulphate fraction of protein extracts (Fig. 3.5.3 and Fig. 3.5.4). This may be a reflection of the superior separation obtained with gradient gels. Nevertheless, recognition of the high molecular weight protein was consistent with that observed previously where the protein is shown to occur in developing bud tissues.

PAb1 also recognised protein bands of *ca.* 47 kD in leaf tissues. This protein band was also recognised by PAb2 but with a reduced intensity (Fig. 3.5.7). The different level of recognition between the two antibodies may be due to different developing times. Because PAb1 and PAb2 were raised against antigens sharing almost identical primary and secondary protein structures, a high level of cross-reactivity between the two polyclonal antibodies is expected (Fig 3.5.1B). The antigen of *ca.* 47 kD is one of antigens recognised by both PAb1 and PAb2, but the size of the protein is larger than the a monomeric protein encoded by TRACO transcripts of 1.35 kb. It is not certain yet how the 47 kD protein is related to the TRACO gene products.

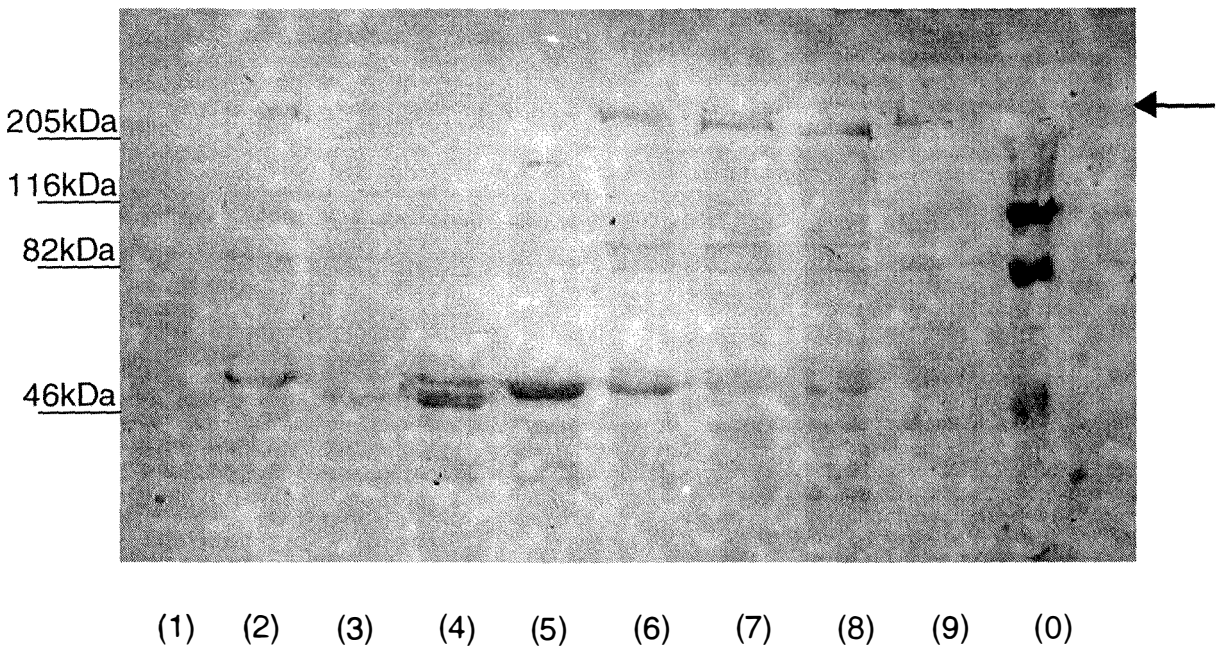

Figure 3.5.6 Western analysis, using PAb1, of ACO protein expression in various plant parts of white clover. Crude proteins were extracted from roots (1); petiole (2); leaf 12 (3); leaf 6 (4); leaf 2 (5); leaf 1 (6); apex (7); axillary buds (8) and floral buds (9). Twenty μg (lane 1, 5 μg) of the protein extracts were separated on 10% (w/v) SDS-PAGE and electroblotted onto PVDF membrane. Lane (0) is molecular weight markers from Bio-Rad, with molecular weights indicated. The arrow indicates PAb1 recognition of a *ca.* 205 kD protein.

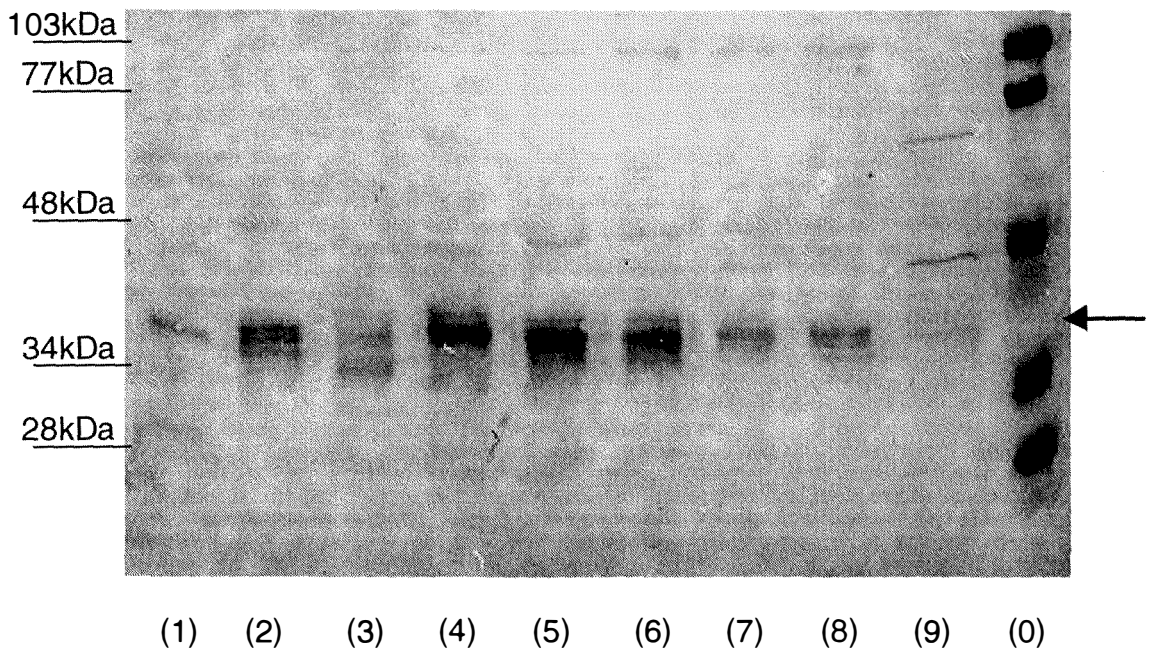

Figure 3.5.7 Western analysis, using PAb2, of ACO protein expression in various plant parts of white clover. Crude proteins were extracted from roots (1); petiole (2); leaf 12 (3); leaf 6 (4); leaf 2 (5); leaf 1 (6); apex (7); axillary buds (8) and floral buds (9). Twenty μg (lane 1, 5 μg) of the protein extracts were separated on 10% (w/v) SDS-PAGE and electroblotted onto PVDF membrane. Lane (0) is molecular weight markers from Bio-Rad, with molecular weights indicated. The arrow indicates PAb2 recognition of proteins in the 34 kD-38 kD range.

Although a PAb1-recognised protein is too large (*ca.* 205 kD) to be a monomeric ACO, the correlation between the pattern of gene expression and protein expression of TRACO1 led us to characterise the apex-specific antigens further by using immuno-precipitation and immunoaffinity-based purification (cf. section 3.5.4).

PAb2 recognised a protein band of *ca.* 36 kD in protein extracts from various plant organs including apical and axillary buds, mature green leaves, petioles and roots (Fig. 3.5.7). In common with results shown in figure 3.5.5, the extent of PAb2 recognition was highest in newly initiated leaf tissue (leaf 1 and leaf 2) and mature green leaf tissue (leaf 6). In addition to recognition of a *ca.* 36 kD protein band in these samples, closely related protein doublets or triplets were discerned. In this thesis, no further characterisation has been undertaken to determine the immunological relevance of these proteins. Recognition of *ca.* 36 kD protein band was reduced in senescent leaf tissue (leaf 12), where two protein bands (*ca.* 36 kD and *ca.* 32 kD) were recognised. No further characterisation of the *ca.* 32 kD has been undertaken. PAb2 also recognised a protein band of *ca.* 36 kD in protein extracts from mature green petioles with an intensity of the recognition similar to that of leaf 1. A lower level of PAb2 recognition was discerned with protein extracts from apical and axillary buds, which is again consistent with the results shown in figure 3.5.5. PAb2 recognition was also clearly discerned with only 5 μg of protein extracts from roots (other tissues were loaded with 20 μg protein), indicating that the root accumulates a high level of TRACO2 proteins.

3.5.4.Characterisation of apex-specific antigen

3.5.4.1 The use of the enzyme-linked immunosorbent assay (ELISA)

ELISA was used to determine the specificity of PAb1 recognition in protein extracts from the apex (Fig. 3.5.8). PAb1 recognised the TRACO1 protein (1.5 μg) expressed in *E. coli* at a 1:5000 dilution, but recognition of a control protein (Bovine serum albumin; 20 μg) was at a background level for all dilution used. When protein extract from the apex (20 μg) was coated onto the micro-plate, PAb1 recognition was detectable at a dilution factor of 1:100.

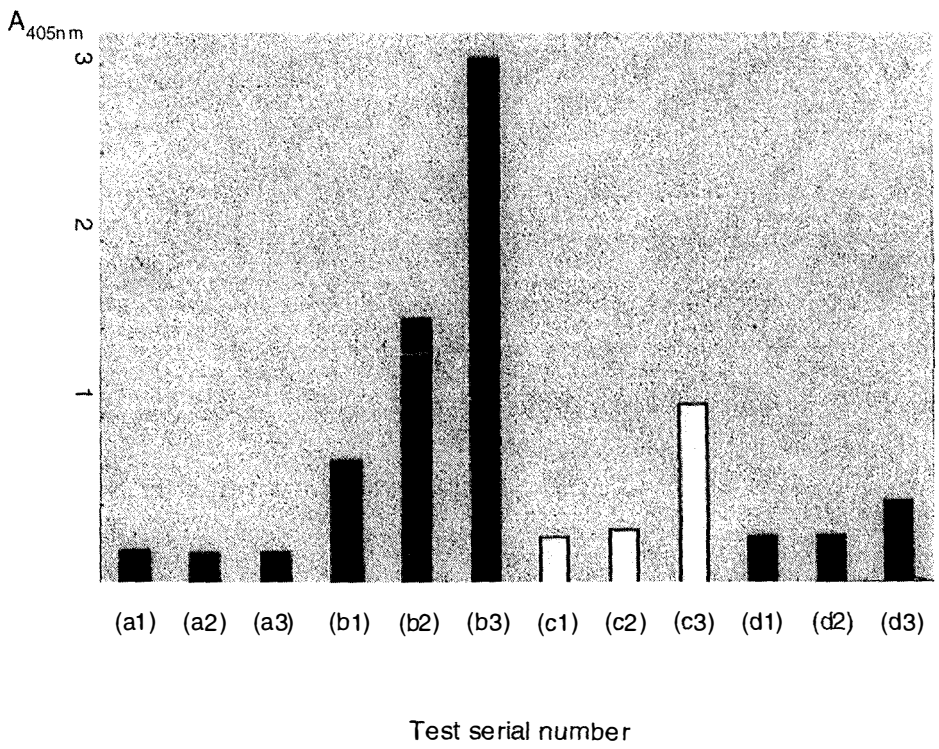

Figure 3.5.8 ELISA using purified PAb1 IgG. Ni-NTA column purified TRACO1 (15 µg) expressed in *E. coli*, BSA (200 µg) and crude extracts from apex (20 µg) and leaf 5 (20 µg) were prepared in coating buffer and a 200 µL aliquot coated onto the micro-plate.

(a1), BSA control, 1:5000; (a2), BSA control, 1:1000; (a3), BSA control, 1:100
(b1), TRACO1-E , 1:5000; (a2), TRACO1-E, 1:1000; (a3), TRACO1-E, 1:100
(c1), Apex, 1:5000; (c2), Apex, 1:1000; (c3),apex , 1:100
(d1), Leaf 5, 1:5000; (d2), Leaf 5, 1:1000; (d3), Leaf 5, 1:100
Dilution factor indicates PAb1 IgG in coating buffer

At this dilution factor, PAb1 recognition of the apex extract was higher than mature green leaf (leaf 5). Some PAb1 recognition with protein extracts from mature green leaf may be caused by the nature of polyclonal antibodies used.

The requirement for a relatively large amount of apex protein extract and the relatively low level of recognition by PAb1 suggests either that the ACO protein expression is not very high in the tissue or the PAb1 antibody does not recognise the native ACO protein as well as it does using western analysis with SDS-PAGE. It may be significant that the antibody was produced by immunising proteins solubilised from *E. coli* with SDS (section 2.4.8.4).

3.5.4.2 Immunoprecipitation using protein-G beads

Protein G-beads were used to purify the apex-specific antigen using immuno-precipitation (Fig. 3.5.9). PAb1 was first incubated with protein extracts from the apex for 1 hr at room temperature and any antibody : antigen complexes coupled to protein-G beads and collected using centrifugation. The precipitates were then separated on a 10% (w/v) SDS-PAGE and protein bands visualised by CBB staining.

A protein band of high molecular weight (*ca.* 205 kD) was discerned with proteins co-precipitated with the PAb1-coupled beads (Fig. 3.5.9, lane 1), which was not present in the lane loaded with the purified PAb1 alone (Fig. 3.5.9, lane 2). These results suggest that the high molecular weight protein band is linked to the antigen, which was recognised by PAb1 using western analysis (cf. Fig. 3.5.3; Fig. 3.5.4). However, there are other protein bands discernable by CBB staining in the proteins co-precipitated with the PAb1-coupled beads. Most of these will be PAb1 immunoglobulin proteins, since they were also visible in the lane loaded with PAb1 (Fig. 3.5.9, lane 2). Others are plant proteins, which may share epitopes with PAb1.

Western analysis was performed with proteins co-precipitated with the protein G beads (Fig. 3.5.10). The antigen-antibody complex of *ca.* 205 kD was discerned in lanes loaded with the protein precipitates (Fig. 3.5.10, lane 4) as well as with protein extracts from the apex (Fig. 3.5.10, lanes 1 and 2). PAb1 recognition of the *ca.* 205 kD protein was not observed in lanes

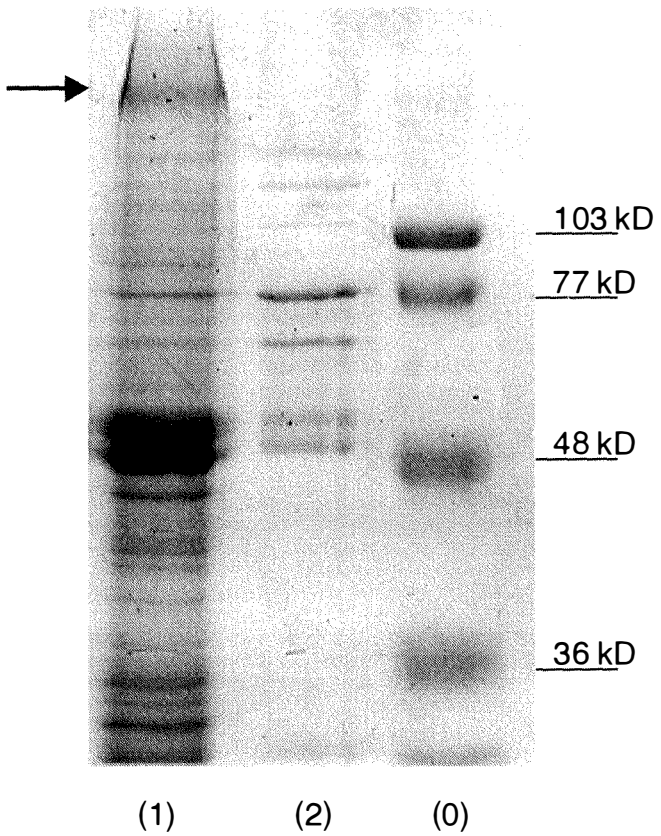

Figure 3.5.9 SDS-PAGE analysis of apical tissue-specific antigens immuno-precipitated with PAb1. Immuno-precipitated proteins from the developing apices were separated on 10% (w/v) SDS-PAGE and the gel was stained with Coomassie Blue. Lane (1) is protein immuno-precipitated with protein-G beads. Lane (2) is PAb1. Lane (0) are molecular weight markers from Bio-Rad, with molecular weights indicated. The arrow indicates a putative protein band of *ca.* 205 kD.

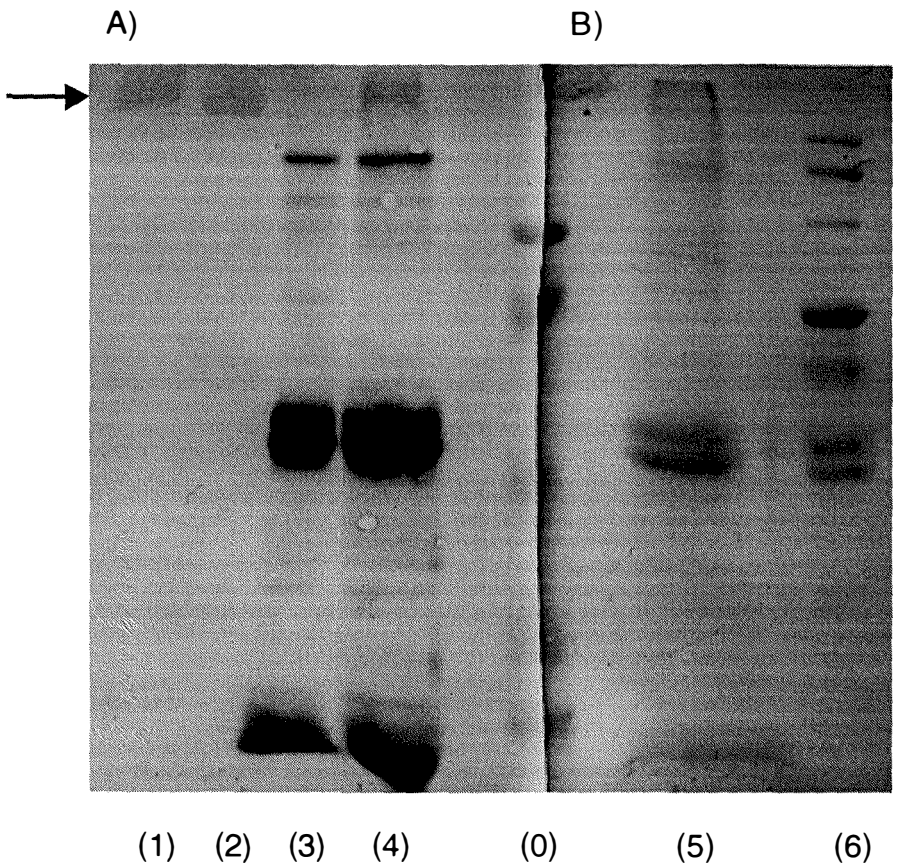

Figure 3.5.10 Analysis of the apex-specific *ca.* 205 kD protein using immuno-precipitation. Immuno-precipitated proteins with protein G beads coupled with PAb1were separated on a 8-15% (w/v) gradient SDS-PAGE gel, electroblotted onto PVDF membrane, and the membrane either used for western analysis with PAb1 (A) or stained with Coomassie Blue (B). Lane (1) and (2) are apex extracts. Lane (3) are PAb1 precipitated with protein G beads. Lane (4) and (5) are proteins immuno-precipitated with protein G beads. Lane (6) are PAb1. Lane (0) are pre-stained molecular weight markers from Bio-Rad. The arrow indicates PAb1 recognition of a *ca.* 205 kD protein.

loaded with the PAb1-coupled protein G beads before incubation with a protein extract from the apex (Fig. 3.5.10, lane 3), even though other lower molecular weight bands were discernable.

The other half of the membrane was stained with a modified CBB staining to visualise the corresponding bands recognised by western analysis with PAb1. However, visualisation by CBB staining was not as clear as by western analysis, suggesting that the protein is not very abundant in the apex extracts. Several attempts to purify the high molecular weight antigen in protein extracts from the apex were made, but not enough protein was obtained for protein sequencing. The need for these repeats suggests that the antigen exist at a low level in the apex, even though its expression is specific to this tissue. To collect enough of the antigen for protein sequencing, larger scale purification using an immuno-affinity column was adopted.

3.5.4.3 Bulk purification of *ca.* 205 KD antigens using PAb1 affinity column

An immuno-affinity column was prepared using CNBr-activated Sephadex coupled with PAb1. A protein extract from the apex was passed though the column and bound proteins eluted at two pH values, pH 11 and pH 2.5. The eluates were separated on 10% (w/v) SDS-PAGE gels and visualised by CBB staining. The purpose of this experiment was to purify enough of the high molecular weight antigen from the apex for protein sequencing.

When the CNBr-activated Sephadex resin was coupled with the purified PAb1, the gel mix was subjected to SDS-PAGE (Fig. 3.5.11). Several protein bands were discerned by CBB staining (Fig. 3.5.11, lane 2), but these bands could not be discerned in the resin before the coupling reaction (Fig. 3.5.11, lane 1), indicating that antibody coupling was successful. However, differences could not be detected between lanes loaded with resin examined before (Fig. 3.5.11, lane 2) and after (Fig. 3.5.11, lane 3) apex protein extracts were applied to the column, and also with the resin after eluting bound proteins (Fig. 3.5.11, lane 4). It may be that PAb1 immunoglobulin proteins bound to the resin are in vast excess when compared with any apex protein bound. As well, the high molecular weight antigen was not discernable by CBB staining in the lane loaded with the column eluates (Fig. 3.5.11, lane 5).

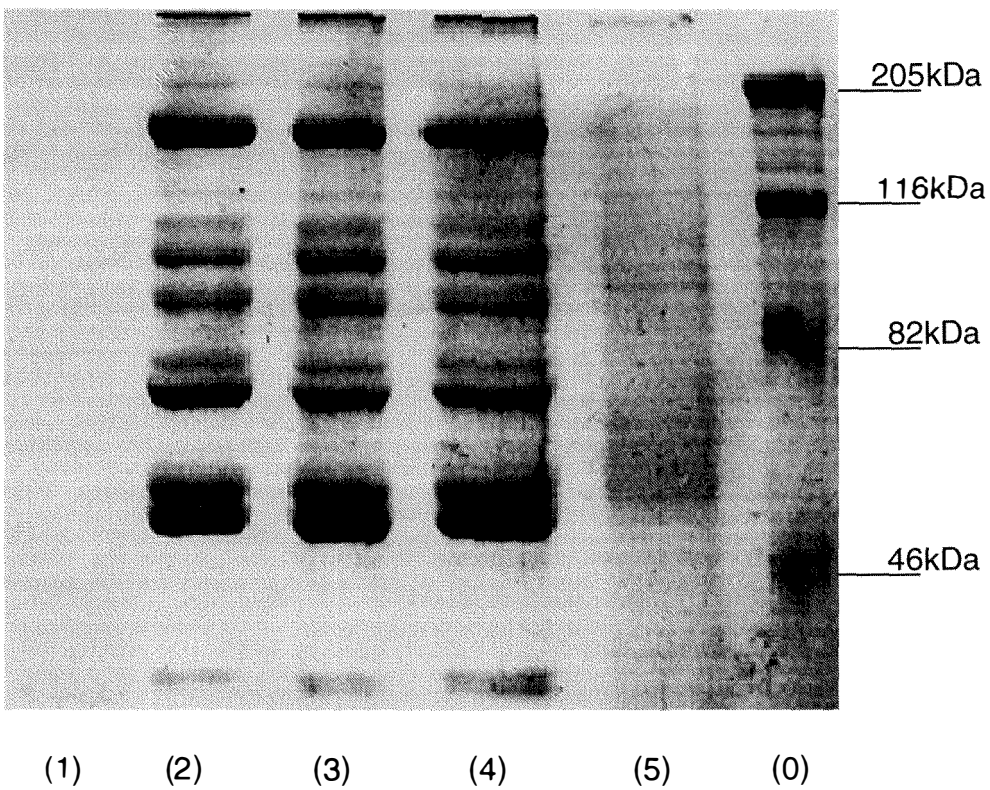

Figure 3.5.11 Analysis of a CNBr-activated Sepharose affinity column coupled with PAb1 using 10% (w/v) SDS-PAGE and Coomassie Blue staining. Lane (1), CNBr-Sephalose resin; (2), the resin coupled with PAb1; (3), PAb1-coupled resin with bound apex proteins; (4) PAb1-coupled resin after protein elution at two extreme pH values; (5), protein eluates from the column. Lane (0) are protein molecular weight markers from Bio-Rad, with molecular weights indicated.

When silver staining was used to visualise any protein in eluates from the PAb1-affinity column, protein bands corresponding to *ca.* 205 kD were visualised (Fig. 3.5.12).

This result also confirmed that silver staining is highly sensitive, because the protein of *ca.* 205 is discernible, and also it recognised a residual amount of proteins which had overflowed into the next well during loading (lane between lane (0) and lane (1) was empty originally).

To find out whether these high molecular weight protein bands were also recognised by PAb1, western analysis was performed using a membrane blotted from the other half of the gel. However, no antigen-antibody complex was detected from the lanes loaded with the column eluates by PAb1 (data not shown). It may be that the antigens lose their affinity for PAb1, particularly after elution from the affinity column at two extreme pH values (pH 2.5 and pH 11).

Nevertheless, several lanes of a 10% (w/v) SDS-PAGE gel were loaded with the column eluates and visualised with silver staining (data not shown). Gel slices containing the proteins of *ca.* 205kD were excised and amino acid sequencing using trypsin-digested peptides attempted, but no sequence was obtained.

All these results suggest that expression of the PAb1-recognised antigen in the apex occurs at a low level. To identify the antigen by its protein sequence, bulk scale protein purification may be required.

Figure 3.5.12 SDS-PAGE and silver staining of apex proteins purified by the PAb1 immuno-affinity column. Proteins eluted from the immuno-affinity column (Fig. 3.5.11, lane 5) were separated on a 8-15% (w/v) gradient SDS-PAGE gel and visualised with silver staining. Lane (1) are proteins eluted from the column. Lane (0) are molecular markers from Pharmacia. The arrow indicates a *ca.* 205 kD protein.

Part 6: Molecular characterisation of differential expression of ACC oxidase genes expressed in mature green leaves of white clover

3.6.1 Wounding-induced expression of ACC oxidase genes

3.6.1.1 Excised leaf wounding system

Changes in ACO gene expression in response to excision-induced wounding in the mature green leaves of white clover were characterised by northern analysis using gene-specific 3'-UTR probes (Fig. 3.6.1). Initially, the expression of all three ACO genes in white clover was examined, but TRACO1 gene expression was not detectable in mature green leaves in response to any of the treatments used in this section as well as in the following sections. This confirms earlier observations (Fig. 3.3.15; Fig. 3.4.11) which show a very low level of expression using both coding region as probe and the gene-specific 3'-UTR of TRACO1 as probe. So, further analysis using mature green leaf tissue was carried out with TRACO2 and TRACO3, which were differentially expressed during leaf ontogeny in white clover (TRACO2, mature green leaf-associated ACO gene; TRACO3, senescent leaf-associated ACO gene).

In respect to excision of leaf tissue, a transient increase in ethylene production was reported by D. Hunter (1998), and hence Purafil (an ethylene-binding compound) was added to the incubation system to reduce the level of atmospheric ethylene. Northern analysis revealed that over the time course used (12 hr), the transcript abundance of TRACO2 decreased after excision, whereas that of TRACO3 increased, with detection first at *ca.* 1.5 hr after excision.

3.6.1.2 Intact leaf wounding system

The wound-induced TRACO2 and TRACO3 expression was also examined in mature green leaves attached to the stolon (Fig. 3.6.2). In this experiment, the induction level of TRACO3 gene expression was significantly reduced, in terms of the intensity of hybridised band, when compared with excised tissue. A slight increase of TRACO3 transcript abundance was detected at 4 hr after wounding, which was delayed when compared with the 1.5 hr induction observed in the excision-wounded leaves (cf. Fig. 3.6.1), after which the transcript level returned to background level at 18 hr after wounding.

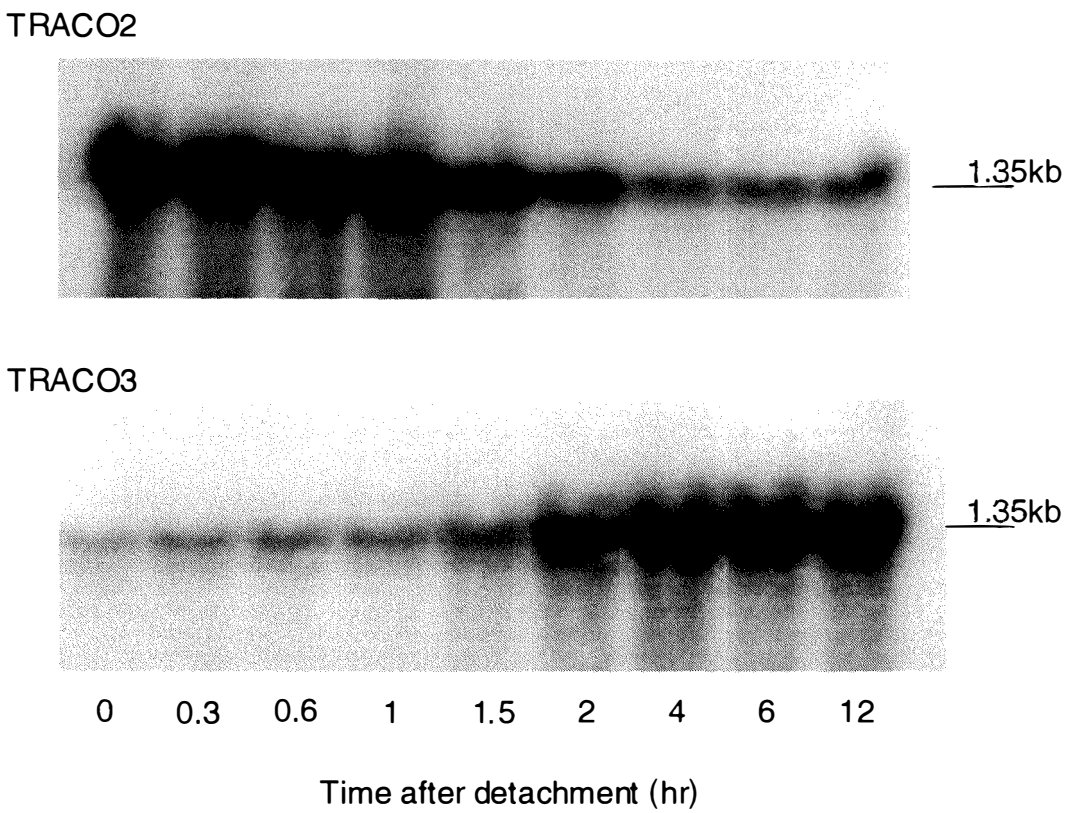

Figure 3.6.1 Time course of wounding by excision-induced gene expression of ACC oxidase in mature green leaves determined by northern analysis using 3'- UTRs as probes. Forty μg of total RNA extracted from the wounded (excised) tissues was separated on a 1.2 % (w/v) agarose-formaldehyde gel, blotted onto Hybond-N^+ with 20 X SSPE overnight, and probed with ^{32}P-labeled TRACO2 and TRACO3. The membranes were washed at a high stringency (0.1 X SSPE at 65 ^{o}C) and exposed to X-ray film for 4 days.

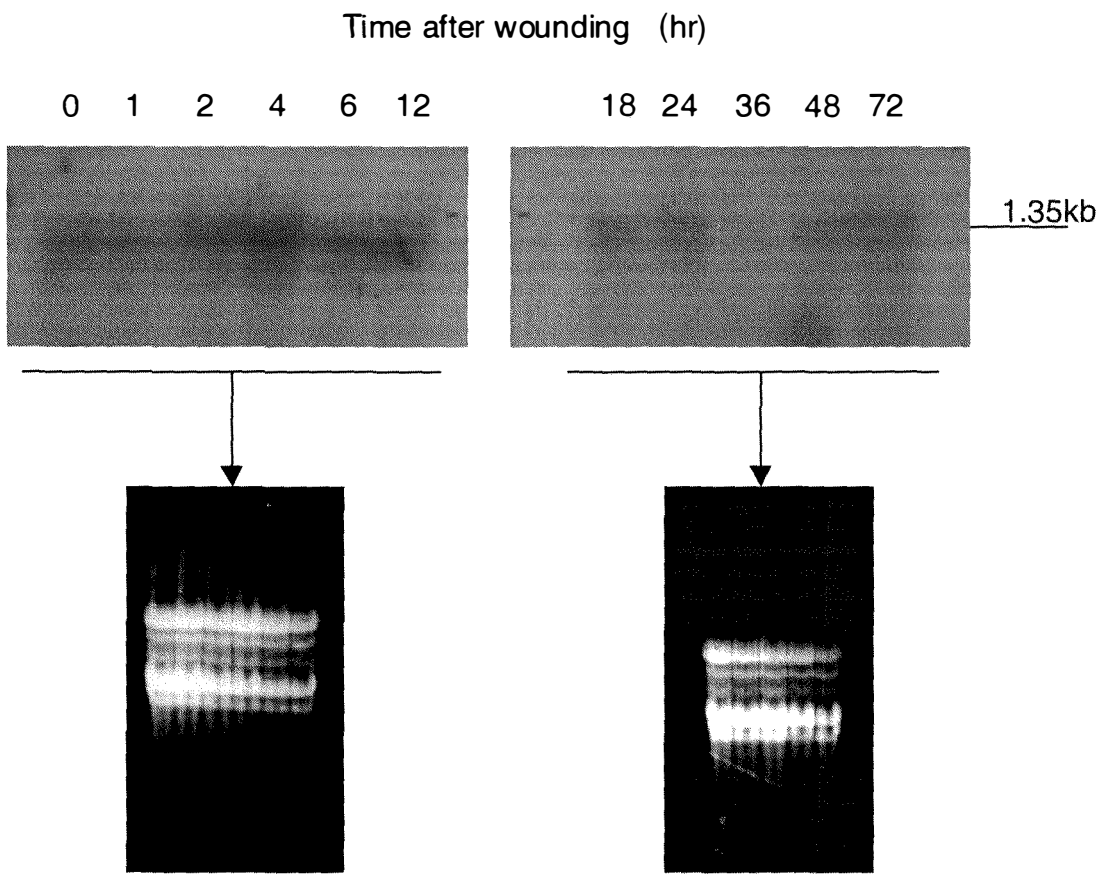

Figure 3.6.2 Time course of wounding-induced TRACO3 gene expression in attached mature green leaves determined by northern analysis with the 3'- UTR as probe. Forty μg of total RNA extracted from wounded leaves on the stolon was separated on a 1.2 % (w/v) agarose-formaldehyde gel, blotted onto Hybond-N^+ with 20 X SSPE overnight, and probed with ^{32}P-labeled TRACO3. The membrane was washed at a high stringency (0.1 X SSPE at 65°C) and exposed to X-ray film for 4 days. RNA stained by ethidium bromide is shown as a gel loading control.

Results from both wounding experiments suggest that wound induces the expression of TRACO3 gene in mature green leaves of white clover. Ethidium bromide-stained rRNA species indicated that RNA sample loading was not entirely equal between lanes, but it could not affect the interpretation of TRACO3 expression determined by northern analysis.

3.6.1.3 Wounding of intact leaves and AVG treatment

To determine if changes in ACC content, produced by the activity of ACC synthase, regulates the wound-induced TRACO3 gene expression, gene expression of TRACO2 and TRACO3 was examined using wounded intact mature green leaves pretreated with AVG (an inhibitor of ACC synthase activity) (Fig. 3.6.3). TRACO2 gene expression remained constant over the time course, while the AVG pretreatment induced the expression level of TRACO3 at 0 hr in mature green leaf tissue. TRACO3 gene expression increased at 12 to 18 hr after wounding, and then decreased to undetectable level at 72 hr after wounding.

Although the pattern of gene expression was complicated by a high level of TRACO3 expression in response to AVG treatment, the induction of TRACO3 expression by wounding was reproduced in the AVG-pretreated wounded intact leaves. The induction was transient as was observed in the wounded intact leaves without AVG pretreatment (cf. Fig. 3.6.2) and maximal induction was delayed further (12 to 18 hr after wounding) with AVG treatment, when compared to the time of induction in the wounded intact leaves without AVG pretreatment (2 to 4 hr after wounding).

In addition, the observation of steady expression of TRACO2 in this expression suggests that the down-regulation of TRACO2 in excised wound tissue may only be induced in mature green leaves, which age or senesce as a the consequence of detachment from the stolon.

3.6.2 Ethylene-induced expression of ACO genes

The series of wounding experiments indicated that the expression TRACO3 gene (the senescence-associated ACO gene) increases in response to wounding in mature green leaf tissue of white clover. However, an involvement of the transient endogenous ethylene

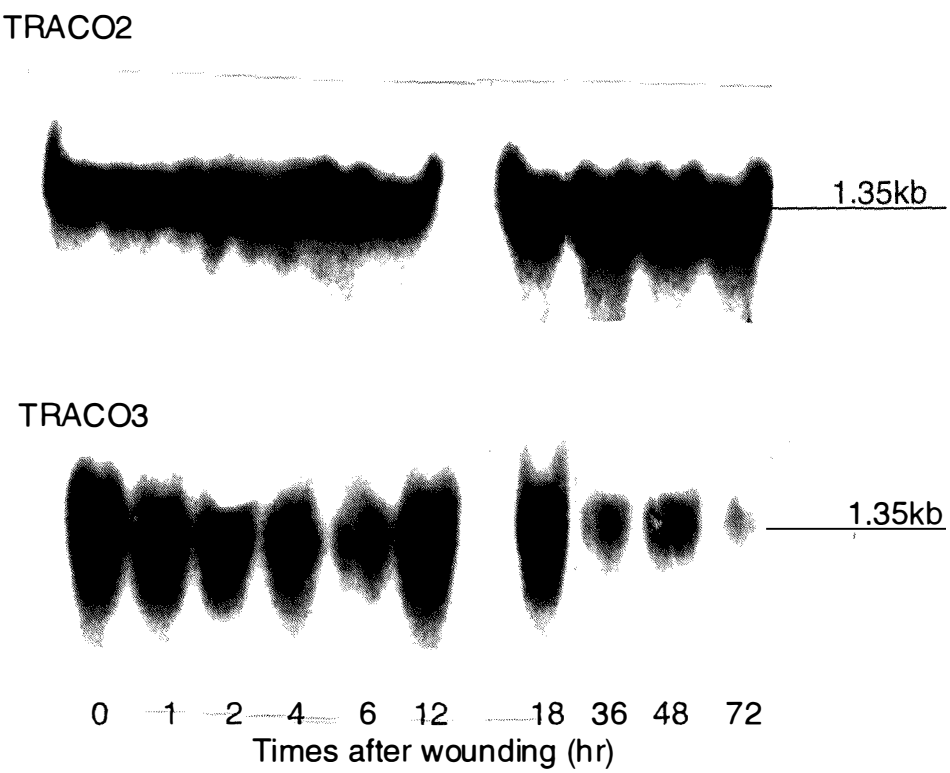

Figure 3.6.3 Time course of wound-induced gene expression of ACC oxidase determined by northern analysis using 3- UTRs as probes in attached mature green leaves pretreated with AVG. Forty mg of total RNA extracted from wounded leaves pretreated with AVG was separated on a 1.2 % (w/v) agarose-formaldehyde gel, blotted onto Hybond-N^+ with 20 X SSPE overnight, and probed with ^{32}P-labeled TRACO2 and TRACO3 (as indicated). The membranes were washed at a high stringency (0.1 X SSPE at 65 ^{o}C) and exposed to X-ray film for 4 days. The same membrane has been probed first with TRACO2 and then TRACO3. The membrane was stripped between probes using boiling washing buffer (0.1 X SSPE).

produced by wounding in regulating this induction cannot be excluded. Although any ethylene, which evolves from the tissue should be absorbed by Purafil, it may be that endogenous ethylene may still be able to mediate a response before it is absorbed. Thus gene expression induced by wounding should be examined further in terms of its relationship with transient ethylene production. To do this, changes in TRACO gene expression in response to ethylene treatment were characterised by northern analysis using both excised mature green leaves and intact mature green leaves.

3.6.2.1 Ethylene treatment with excised mature green leaves

In response to 10 μL L^{-1} ethylene treatment of excised mature green leaves, TRACO2 gene expression transiently increased 0.3 to 0.6 hr after ethylene treatment and then decreased gradually over the 12 hr time course (Fig. 3.6.4). This early transient induction of TRACO2 gene expression was not observable without ethylene treatment (Fig. 3.6.1). TRACO3 gene expression, however, increased continuously over the same time course after 1.5 hr duration as was observed in excision-wounded leaves (Fig. 3.6.1). The overall pattern of TRACO2 and TRACO3 gene expression was more or less similar to that observed in excision-wounded leaves (Fig. 3.6.1).

If any of changes in TRACO2 or TRACO3 expression was regulated by wound-induced ethylene, the time at which the changes of the gene expression is first observed would be expected to be earlier with ethylene treatment. The very similar kinetics of TRACO2 gene expression and TRACO3 gene expression in the excised mature green leaf system with and without applied ethylene suggests that the differential induction is under control of wounding-induced factors (tissue-ageing), rather than ethylene.

3.6.2.2 Ethylene treatment with intact mature green leaves

As discussed earlier, the use of excised green tissue cannot exclude the involvement of transiently evolved endogenous ethylene, produced by wounding in regulating the induction of TRACO3 gene expression. This is because ethylene produced by wounding in cells accumulates within the tissue before it evolves out of the tissue and is trapped by Purafil (Penmetsa and Cook, 1997).

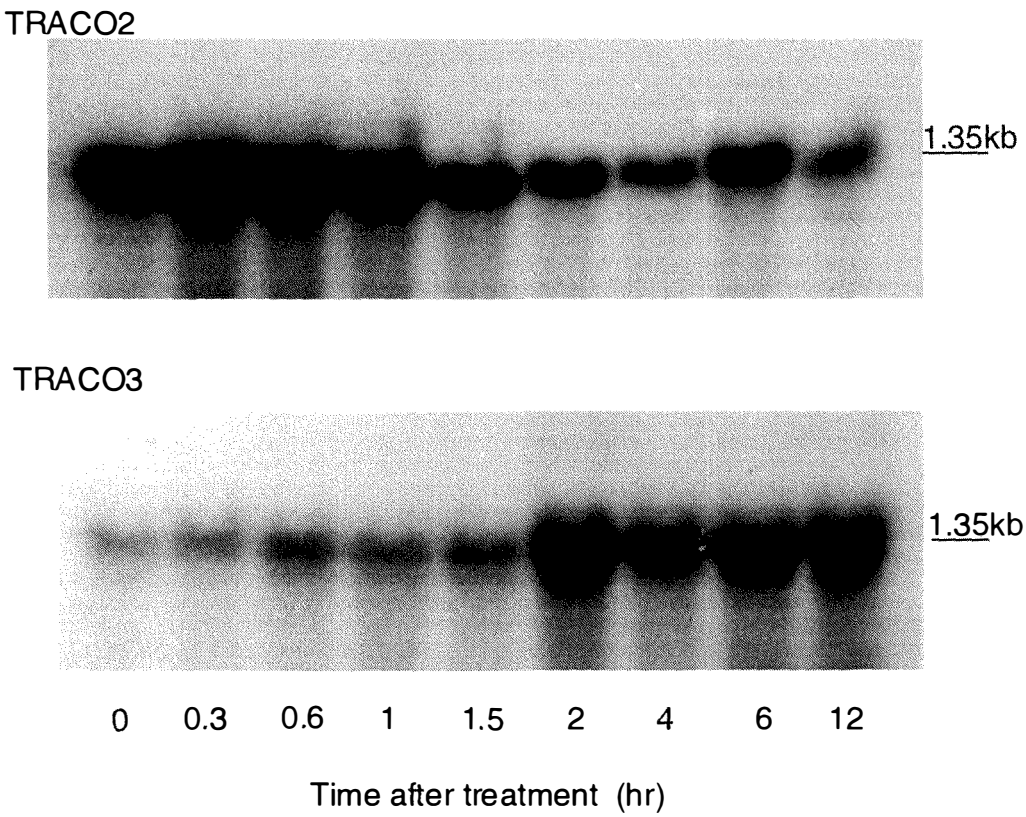

Figure 3.6.4 Time course of ethylene-induced gene expression of ACC oxidase in excised mature green leaf tissue determined by northern analysis using 3'-UTRs as probes. Total RNA was extracted from the leaves treated with ethylene (10 μL L^{-1}) at each time point. Forty μg of total RNA was separated on a 1.2 % (w/v) agarose-formaldehyde gel, blotted onto Hybond-N^+ with 20 X SSPE overnight, and probed with ^{32}P-labeled TRACO2 and TRACO3 (as indicated). The membranes were washed at a high stringency (0.1 X SSPE at 65 ^{o}C) and exposed to X-ray film for 7 days.

Therefore, if wound-induced ethylene triggers ACO gene expression before it evolves from the tissue, the tissue may become saturated in terms of responsiveness to ethylene and therefore is not competent to respond further to the applied ethylene. If this occurred, the induction time of TRACO3 would not occur earlier in response to the applied ethylene. Thus, to uncouple the effects of wounding and wound-induced ethylene on changes in TRACO2 and TRACO3 gene expression in mature green leaves, non-wounded whole plant tissue was used to examine the effect of ethylene.

When ethylene (10 $\mu L\ L^{-1}$) was applied to whole plants, TRACO2 gene expression increased over the time course of the experiment (Fig.3.6.5). However, this induction pattern was not detected in the control (non-ethylene treated tissue; Fig. 3.6.5). TRACO3 gene expression was not detectable at any of the time points examined (data not shown). This result suggests that the induction of TRACO3 gene expression was caused by wound-induced factors, and the induction of TRACO2 gene expression was induced in response to applied ethylene in mature green leaves of white clover. Moreover, it can be confirmed that the transient induction of TRACO2 expression observed at the early time (0.3 to 0.6 hr) after ethylene treatment to the excised tissues (Fig. 3.6.4) was most likely a response of the mature green tissue to the applied ethylene.

3.6.2.3 Ethylene and 1-MCP

To confirm the ethylene effects on the induction of TRACO2 in mature green leaves, ethylene action was blocked by pretreatment with a specific ethylene action inhibitor, 1-MCP before ethylene treatment.

The 1-MCP pretreated white clover plants displayed an ethylene-insensitive phenotype when treated with ethylene in terms of non-epinastic curvature of leaves (Fig. 3.6.6). The same phenotype change was monitored in three independent experiments. Nevertheless, the induction of TRACO2 expression was not blocked by pretreatment with 1-MCP (Fig. 3.6.5C) and gene expression still increased in response to applied ethylene in mature green leaves.

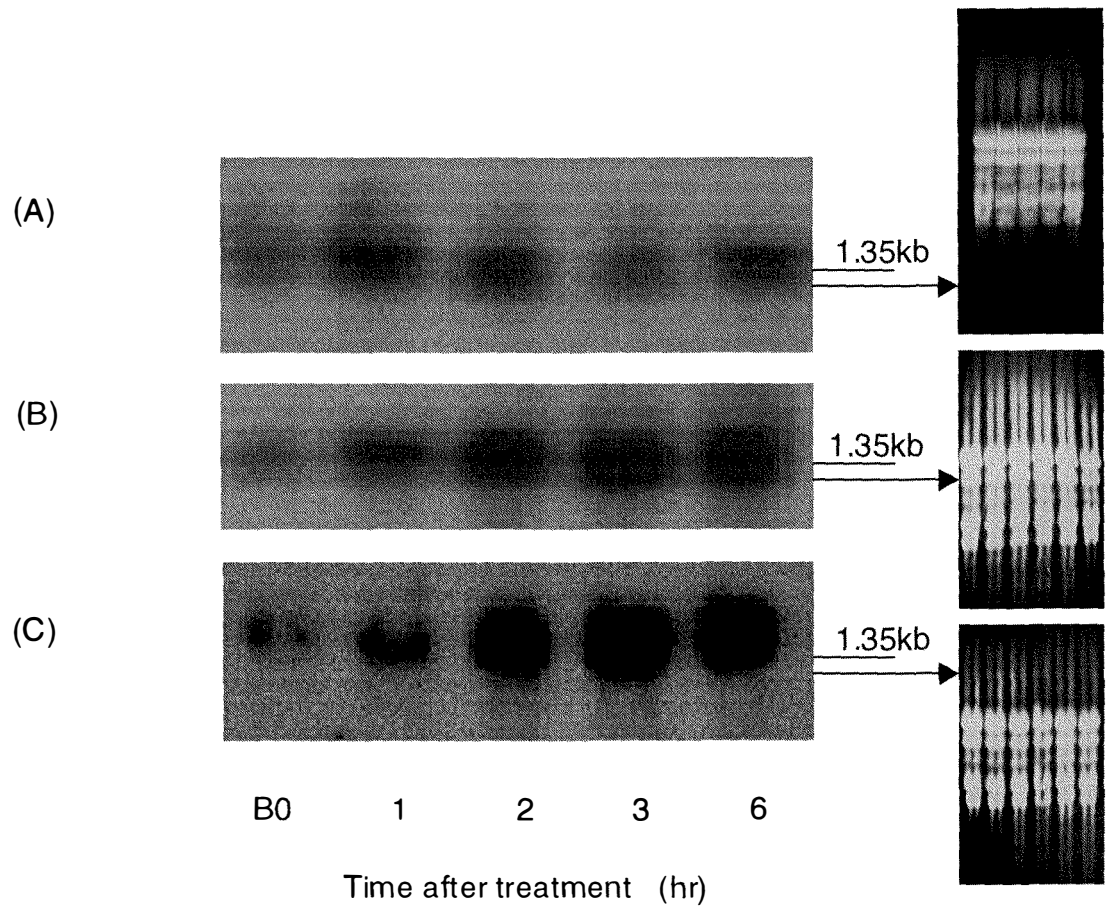

Figure 3.6.5 Time course of ethylene-induced TRACO2 gene expression determined by northern analysis using 3'- UTRs as probes in the mature green leaf tissue on the stolon, pretreated with 1-MCP. Total RNA was extracted from mature green leaves treated with (A), (-) 1-MCP (-) ethylene; (B), (-) 1-MCP (+) 10 μL L^{-1} ethylene, and (c), (+) 2 μL L^{-1} MCP (+) 10 μL L^{-1} ethylene. Forty μg of total RNA was separated on a 1.2 % (w/v) agarose-formaldehyde gel, blotted onto Hybond-N^+ with 20 X SSPE overnight, and probed with ^{32}P-labeled TRACO2. The membranes were washed at a high stringency (0.1 X SSPE at 65 ^{o}C) and exposed for 4 days. Lane B0 is from leaf tissue before 1-MCP treatment. RNA stained by ethidium bromide is shown as a gel loading control.

Figure 3.6.6 Response of leaves to (A), 10 μL L^{-1} ethylene and (B), 2 μL L^{-1} 1-MCP + 10 μL L^{-1} ethylene. Arrows highlight the epinastic (A), and non-epinastic (B) response.

A.

B.

To confirm that this does not happen because of unsaturated ethylene receptors, a range of 1-MCP concentrations was used (Fig. 3.6.7). TRACO2 gene expression increased in response to applied ethylene at a concentration of 0.5 μL L^{-1} (Fig. 3.6.7A), and. neither 0.02 μL L^{-1} nor 3 μL L^{-1} of 1-MCP pretreatment for 1 hr before the ethylene treatment could block the induction (Fig. 3.6.7B and C). Indeed, 1-MCP pretreatment more likely enhanced the induction of TRACO2 expression in mature green leaves of white clover.

3.6.3 IAA and AVG treatments of mature green leaves

Changes in TRACO gene expression in response to auxin treatment was determined by northern analysis using whole plants sprayed with 100 μM IAA (Fig. 3.6.8). This was of interest because IAA effects on vegetative tissue have been shown to be mediated by IAA-induced ethylene in many cases. Therefore, we would expect changes in TRACO gene expression in response to IAA treatment to be similar to the ethylene-treatment.

The IAA-treated whole plants demonstrated leaf curvature that is similar to a phenotype of ethylene-treated plants. This was not observed on control plants treated with the spray mixture without IAA (data not shown). This phenotypic response probably indicates that this IAA-induced response in mature green leaves is more likely mediated by ethylene and production of the hormone is induced by IAA, rather than by any of the other chemicals in the spray mixture.

TRACO2 gene expression was induced 3 hr after IAA treatment (Fig. 3.6.8A), and the induction was not observed in control plants (treated with spray mixture without IAA; data not shown). The TRACO2 induction indirectly supports the notion that ethylene may mediate the IAA effect on TRACO2 gene expression, because this gene is responsive to ethylene in mature green leaves. Changes in TRACO3 gene expression were not detected in this tissue (data not shown).

To determine the involvement of ACC synthase activity in induction of TRACO2 expression by IAA, expression was also examined in mature green leaves of white clover sprayed with a

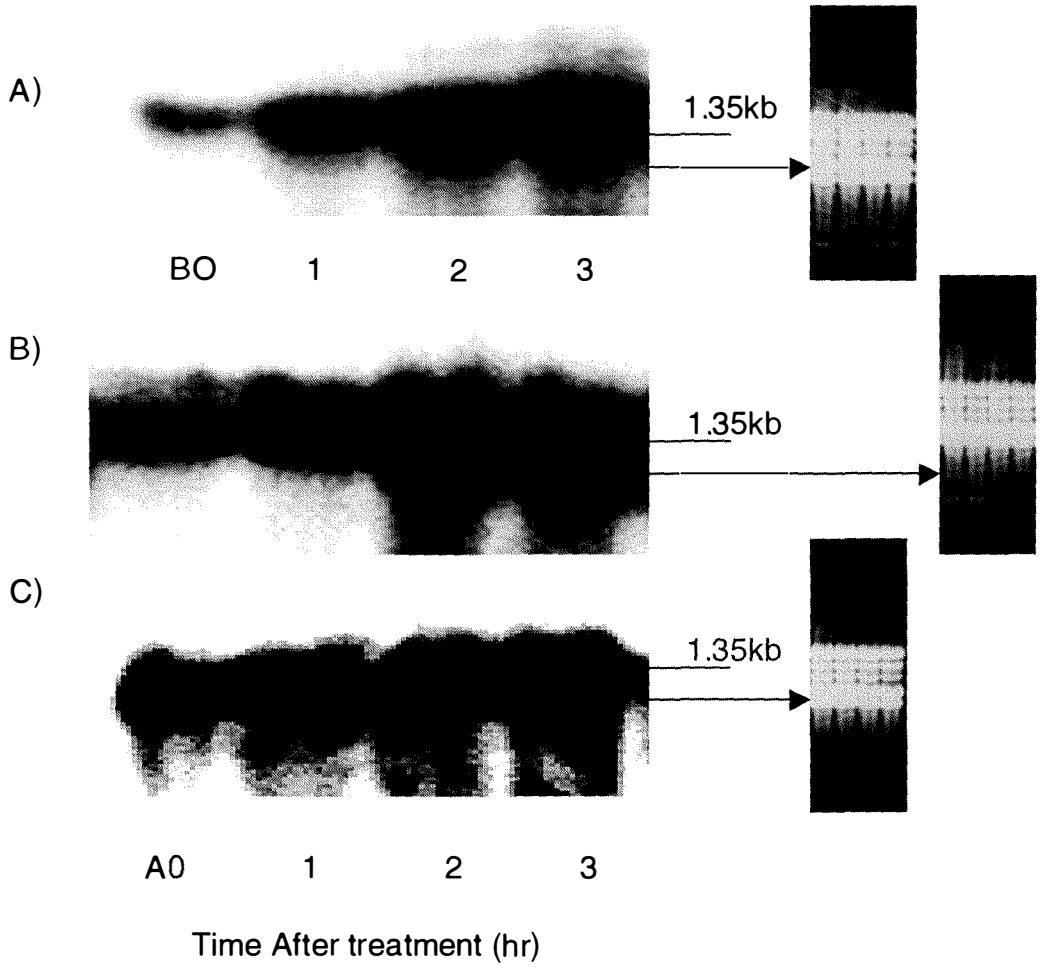

Figure 3.6.7 Time course of TRACO2 gene expression, determined by northern analysis using 3'- UTRs as probes in mature green leaf tissue on the stolon, pretreated with 1-MCP for 1 hr. Total RNA was extracted from mature green leaves treated with (A), (-) 1-MCP (+) 0.5 μL L^{-1} ethylene; (B), (+) 0.02 μL L^{-1} 1-MCP (+) 0.5 μL L^{-1} ethylene, and (c), (+) 3 μL L^{-1} MCP (+) 0.5 μL L^{-1} ethylene. Forty μg of total RNA was separated on a 1.2 % (w/v) agarose-formaldehyde gel, blotted onto Hybond-N^+ with 20 X SSPE overnight, and probed with ^{32}P-labeled TRACO2. The membranes were washed at a high stringency (0.1 X SSPE at 65 ^{o}C) and exposed to X-ray film for 4 days. Lanes B0 and A0 are RNA extracted from leaf tissue before and after 1-MCP treatment, respectively. RNA stained by ethidium bromide is shown as gel loading control.

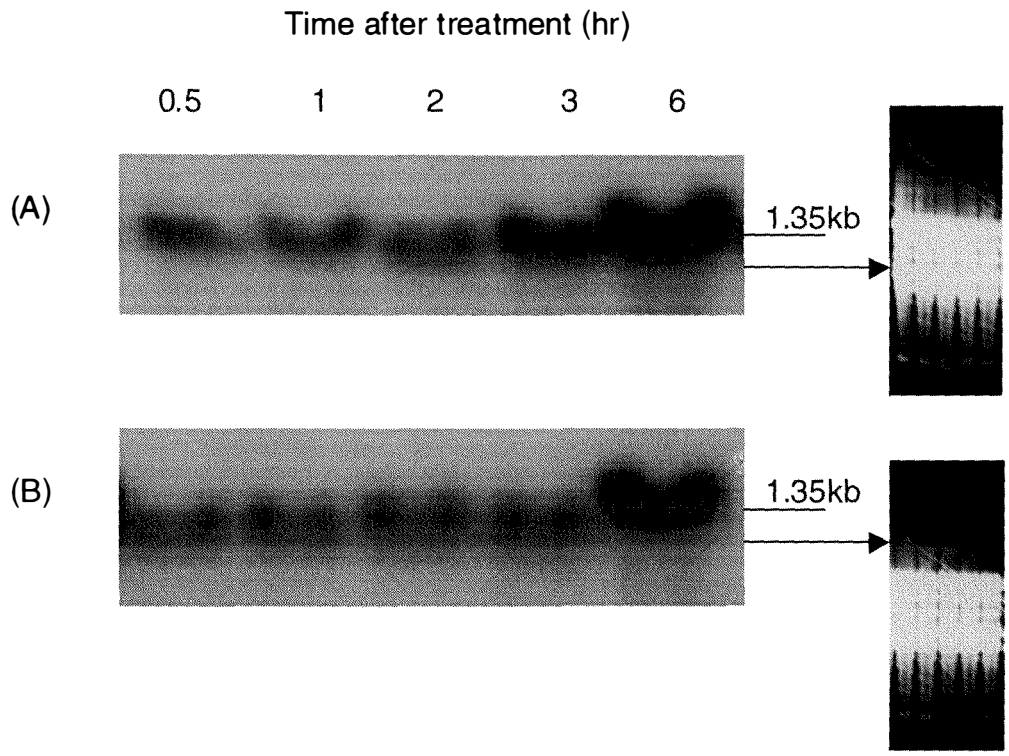

Figure 3.6.8 Time course of IAA-induced gene expression of TRACO2 determined by northern analysis using 3'- UTRs as probes in mature green leaf tissue on the stolon. Total RNA was extracted from mature green leaves treated with (A), (+)IAA (-)AVG and (B), (+)IAA (+)AVG. Thirty μg of total RNA was separated on a 1.2 % (w/v) agarose-formaldehyde gel, blotted onto Hybond-N^+ with 20 X SSPE overnight, and probed with ^{32}P-labeled TRACO2. The membranes were washed at a high stringency (0.1 X SSPE at 65 ^{o}C) and exposed to X-ray film for 4 days. RNA stained by ethidium bromide is shown as a gel loading control.

mixture of IAA and AVG. TRACO2 gene expression was induced in response to the treatment (Fig. 3.6.8B). However, the induction was not obvious until 6 hr after IAA treatment, and the extent of expression was reduced by co-treatment with AVG.

Chapter 4 Discussion

4.1 White clover clonal growth in the model system and ethylene production

The clonal growth of white clover was used in this thesis to provide an ideal model system for the characterisation of leaf development in this plant (Fig. 3.1.1). While the focus of this thesis was concerned with ethylene biosynthesis at the apex and newly initiated leaves, further analysis of the clonal growth system was undertaken. Basic physiological data (leaf fresh weight, leaf area and photosynthetic activity) demonstrated that leaves at each node can be categorised broadly into three developmental stages together with the developing apex: the young expanding stage, the mature green stage and the senescent stage. It appears that leaf 1 and leaf 2 are still expanding, whereas leaf 3 has almost reached full size in terms of leaf fresh weight and leaf area. However, after leaf 14 in the growth conditions used, leaf fresh weight decreases steadily, but leaf area decreases dramatically (Fig. 3.1.2). The steady change of fresh weight may be caused by some accumulation of inorganic substances in the senescent leaves. This is consistent with the observation that leaf fresh weight actually increases as the leaf senesces, when it was determined using leaf discs excised from the basal part of leaf blades at each node (Fig. 3.1.3). Overall, leaf development on the model stolon system is balanced between initiation of leaf tissue at the apex and senescence of leaves at the basal portion of stolons. So a constant number of mature green leaves are present, as well as developing tissue (apex and newly initiated leaves) and senescent tissue.

Chlorophyll content has been used to examine changes in photosynthetic capacity during leaf ontogeny (Butcher, 1997; Hunter, 1998). The observations in this thesis also confirmed that the chlorophyll content increases during leaf expansion stage (apex, leaf 1 and leaf 2) to reach to a maximum level, and remains high during mature green stage (leaf 3 to leaf 14), and then decreases as the rate of degradation overtakes the rate of synthetic processes, when the leaf starts to show visible signs of senescence after leaf 14 (Fig. 3.1.4).

Sestak (1985) observed that the rate of chlorophyll synthesis per unit leaf area or dry matter was high during the early mature green leaf stage, after which it slowed. In addition, the ontogenetic changes in chlorophyll amount and chlorophyll a/b ratio appeared to be affected by

the physiological status of the leaf, e.g. leaf hydration level, photoperiod, wavelength of radiation, seed spacing and mineral nutrition. Therefore, all measurements of changes in chlorophyll content during leaf ontogeny should be determined using plants grown in a uniform environment (Sestak, 1985).

Butcher (1997) examined the clonal growth of white clover in two different locations, which differed in terms of photoperiod and temperature. These environmental factors did affect the rate of leaf development such that different numbers of leaves in each of three leaf developmental stages during stolon growth were observed in each environment. However, within the same environment, a consistent pattern of leaf development along the stolon was observed. This observation supports the notion that leaf development is a genetically programmed process, which can interact with environmental factors.

In addition to chlorophyll content, measurements of chlorophyll fluorescence and CO_2 gas exchange rate have been used to examine photosynthetic activity in leaves at each node. Measurements of chlorophyll fluorescence (photochemical efficiency of PSII) demonstrates an identical trend to that of changes in chlorophyll content during leaf ontogeny in white clover (Fig. 3.1.7). Therefore, either measurement of chlorophyll content or chlorophyll fluorescence can be used as an indicator of the leaf ontogeny, particularly for mature green and senescent leaf tissue.

Although measurements of CO_2 gas exchange rate show a similar trend to changes in both chlorophyll content and chlorophyll fluorescence, the gas exchange rate appears to decrease earlier (after leaf 12) than those of chlorophyll content and chlorophyll fluorescence (after leaf 14; Fig. 3.1.6; Fig. 3.1.7). This is probably due to an increase in respiration rate of the leaf tissue just before the onset of visual leaf senescence, rather than a net decrease of leaf photosynthesis rate. To confirm this, the respiration rate of the leaf tissue has to be determined further. Therefore, measurement of CO_2 gas exchange rate cannot be interpreted directly as photosynthetic activity for leaves at each node.

Oh *et al.* (1996) reported that measurement of chlorophyll fluorescence (photochemical efficiency of PSII) was a reliable parameter of functional leaf senescence. Moreover, the

authors observed that a cytokinin-induced delay of leaf senescence of *A. thaliana* was accompanied by maintenance of chlorophyll content, but the photochemical efficiency of PSII decrease, suggesting that chlorophyll content alone might lead to misinterpretation of the onset of senescence.

The process of senescence has long been an interesting area of study in plants, as well as other living organisms (Bleecker, 1998). For leaf senescence, loss of chlorophyll has been reported as one of the very early events, followed by the remobilisation of chloroplast proteins and membrane lipids as nitrogen and carbon sources, respectively, to growing plant parts or into storage forms (Buchanan-Wollaston, 1997; Nam, 1997).

With a particular interest in changes that occur during leaf senescence, data of chlorophyll fluorescence have been calculated further to monitor changes in photochemical efficiency of PSII in the leaf tissue (Table 3.1.1; Fig. 3.1.8). When leaf tissues were divided into four stages of leaf development according to their chlorophyll content and node number (newly initiated leaves, mature green leaves, onset of senescence and senescent leaves), more photon energy was observed to be converted into non photochemical forms (non photochemical quenching; Npq), probably as light or heat emission in senescent leaves. Thus photochemical yield (Fv'/Fm') is apparently much lower in the senescent leaf tissue, when compared with non-senescent leaf tissue.

The changes of chlorophyll fluorescence in naturally senescing leaves of white clover are consistent with observations in senescing peach leaves after pathogen (*Taphrina deformans*) infection (Raggi, 1991). In that study, leaf senescence was studied with respect to the changes in photochemical efficiency of PSII of the infected leaves. The damaged PSII in the pathogen-infected leaves, which was indicative of the progress of leaf senescence, resulted in an increase of Npq with the decrease in photochemical yield. These results suggest that a loss of photosynthetic activity of leaf tissue is most likely related to the initiation of the leaf tissue senescence in white clover. This is also consistent with the proposal that an age-related factor causes chloroplast breakdown in photosynthetic tissues, and the senescence programme is then initiated in the tissue (Hensel *et al.*, 1993).

A high level of ethylene production is associated with senescent leaf tissue of white clover (Fig 1.5) (Butcher, 1997; Hunter, 1998) and ethylene production associated with organ senescence has been well documented in the literature (Yang and Hoffman, 1984; Reid, 1995). More recently, the involvement of ethylene in leaf senescence has been examined using transgenic tomato plants containing an anti-sense construct of the LE-ACO1 gene, causing a reduction of endogenous ethylene production (John *et al.*, 1995). These plants showed delayed initiation of leaf senescence, which supports the view that ethylene plays a role in senescence. In addition, the role of ethylene in leaf senescence was also supported by observations of the ethylene-insensitive *etr1* mutant of *A. thaliana* (Bleecker *et al.*, 1988). The mutant plants demonstrated an obvious delay of leaf senescence by one or two weeks, compared to wild type. A further characterisation of senescence in *etr1* mutants revealed that initiation of senescence-associated gene (SAG) expression was delayed in the mutant, but when it did occur the intensity of gene expression was similar to wild type plants (Grbic and Bleecker, 1995). Together, these studies confirmed that ethylene is neither necessary nor sufficient to cause leaf senescence, it only influences the timing. The significance of ethylene production from senescence leaf tissue of white clover and the molecular and biochemical regulation of its biosynthesis has been studied more fully by Butcher (1997), Hunter (1998) and Gong (1999). This thesis is concentrated primarily with ethylene biosynthesis at the apex.

Butcher (1997) and Hunter (1998) reported a significantly higher level of ethylene production from the developing apex and newly initiated leaves as well as from senescent leaves of white clover. So, the pattern of ethylene production is biphasic during leaf ontogeny in white clover. In this study, rates of ethylene production, both *in vivo* and *in vitro*, have also been confirmed to be high in the developing tissues (the apex and newly initiated leaves) of white clover, when compared with mature green leaves (Fig 3.1.9; Fig 3.1.10). In addition, measurements of ethylene production, *in vitro*, has been undertaken over a 11 hr period after leaf excision (AE) and revealed further that constitutive ethylene production from the developing apex and leaf 1 was significantly higher, when compared with leaf 2 and leaf 3 (data not shown).

It has also been shown that the rate of ethylene production, *in vitro*, increased 3 hr AE in the apex and newly initiated leaves (leaf 1 and leaf 2), but did not increase in fully expanded mature

green leaves (leaf 3 and leaf 4) (Fig. 3.1.10). This increased rate of ethylene production probably corresponds to stress-induced ethylene production. Tomato petioles, starting at 40 min, produced an ethylene peak at 2 to 3 hr AE (Boller and Kende, 1980) or pea epicotyls produced an ethylene peak at 2 to 3 hr AE (Saltveit and Dielley, 1978). However, it is interesting to note that the developing apex and leaf tissues are rather sensitive to the excision-induced wounding, when compared with the fully expanded mature green leaf tissue, in terms of ethylene production. It may be that specific factors involved in ethylene biosynthesis or evolution predominantly occur during the early development of the apex and leaf tissues of white clover (alternatively, it is simply possible that an increased rate of ethylene production in mature green leaves was lost, because of the 2 hr detection interval).

High ethylene production from developing tissue has also been reported in several other plant species. For example, Osborne (1991) reported *ca.* four-fold higher ethylene production from developing leaf tissue, compared to fully expanded mature leaf tissue in *Phaseolus vulgaris,* and a similar pattern of ethylene production has also been observed from *Nicotiana tobaccum* (Aharoni *et al.*, 1979), *Olea europaea* (Lavee and Martin, 1981) and *Prunus serrulata* (Roberts and Osborne, 1981).

In white clover, ethylene production from the apex and newly initiated leaves may be involved in controlling early leaf development. A role for ethylene in regulating leaf development has been characterised thoroughly using leaf explants of sunflowers, which show a biphasic growth response to applied ethylene (Lee and Reid, 1997). In that study, in a low concentration of applied ethylene, leaf expansion was facilitated, whereas growth rate was reduced in response to a high concentration of applied ethylene. The authors suggested, therefore, that high concentrations of ethylene act as an inhibitor of leaf tissue expansion, but a certain basal level is necessary for leaf tissue growth. However, there is no evidence yet for ethylene affecting early growth and development of leaf tissue in white clover, and further experiments on the role of ethylene in this tissue are needed.

Nevertheless, it is possible to determine the molecular mechanisms which regulate the production of higher levels of ethylene at the apex and newly initiated leaves and this was the major aim of this thesis. A parallel study has been undertaken recently with mature and senescent leaf tissue of white clover (Hunter, 1998). As a first step, the genes encoding the ethylene biosynthetic enzymes, ACS and ACO have been cloned and their patterns of gene expression and protein accumulation characterised in the apex and newly initiated leaves, together with mature green leaves of white clover.

4.2 Characterisation for ACS during the early development of leaf tissue in white clover

4.2.1 Molecular characterisation of the ACS gene family

The level of ACS gene expression is known to be very low in plant tissues. Even in ripening tomato fruit tissue, which produces a large amount of ethylene, ACS protein accumulation was calculated to be less than 0.0001% of total protein (Bleecker *et al.*, 1986). As another illustration, screening of a cDNA library made from ripening kiwifruit failed to isolate any ACS genes expressed, even though kiwifruit is one of the climacteric fruits (fruit ripening is normally associated with a large amount of ethylene production as well as increased rate of respiration) (Whittaker *et al.*, 1997).

This supports the notion that ACS gene expression during fruit ripening is still very low, in spite of its high ethylene production in at least these two species. However, three ACS genes in ripening kiwifruits could be successfully identified using the RT-PCR approach. Therefore, RT-PCR was used to isolate ACS genes expressed in the apex and newly initiated leaves of white clover.

For ACS gene sequences reported in the GenBank database, at least eight regions (six out of eight conserved sequence boxes are shown in Fig. 4.1) of the primary sequences are highly conserved, even though the nucleotide and deduced amino acid sequences of these genes show significant diversity (usually 55% to 75%; Imaseki, 1999). So, in this thesis, two rounds of PCR were performed with nested degenerate primers based on conserved deduced amino acid sequences in box 2 and box 7 of ACS genes.

```
          BOX 2                          BOX 3
ACSCON    FQDYHGLP          FCLADPGDAFLVPSPYYAAFDRDLKWRT
TRACS1    .....V..          .............T...PG.....R...
TRACS2    ........ - 39 -   ............TS...P..V...C...
TRACS3    Y.......          ....EK.E...L.T...PG.........

                BOX 4              BOX 5
ACSCON          TNPSNPLGT          IHLICDEIYS
TRACS1          ......... - 18 -   ....S....A - 33 -
TRACS2  - 41-   ......... - 18 -   ...V...... - 31 -
TRACS3          ......... - 25 -   .RD.LR.~~~ - 37 -

            BOX 6                  BOX 7
ACSCON    SLSK*DMGLPGFRVG          MSSFGL
TRACS1    ....*...F......          ....R.
TRACS2    ....*.......... - 14 -   ....T.
TRACS3    ....*.L........          ....A.
```

Figure 4.1 Alignment of deduced amino acid sequences in conserved boxes of ACS genes reported in GenBank database (from Imaseki, 1999). Identical amino acid residues are indicated as (•), different residues are given, and missing residues are indicated as (-). K* : a pivotal lysine amino acid residue for ACS function.

A *ca.* 650 bp product was amplified using cDNA templates made from either RT-treated total RNA isolated from leaf 1 and leaf 2 (Fig. 3.2.1), or poly(A)$^+$mRNA from the developing apex (Fig. 3.2.3). RT-PCR has been widely used as a rapid method of cloning ACS transcripts. For example, Yip *et al.* (1992) isolated four PCR clones from tomato fruits or fruit cells after a single round of PCR. In comparison, two rounds of PCR with nested primers is always necessary to amplify a DNA band in white clover leaf tissue, probably suggesting that ACS expression is lower in leaf tissue from this plant species, when compared with tomato fruit tissue. Furthermore, the amplification of PCR products from apex tissue required more cDNA template made from poly(A)$^+$mRNA, when compared to leaf 1 and leaf 2 (Fig. 3.2.3). This suggests even lower expression of ACS in the developing apex when compared with leaf 1 and leaf 2 of white clover.

The PCR products amplified from white clover were sequenced and three ACS genes were designated as TRACS1 (Fig. 3.2.5), TRACS2 (Fig.3.2.6) and TRACS3 (Fig. 3.2.7) (Table 3.2.1), with the ACS gene sequences having 63% to 72% homology (Table 3.2.2). All three ACS sequences included 6 (boxes 2 to 7) of the conserved amino acid residue regions, which are reported as the structural core of ACS (Imaseki, 1999). Also, the Lys residue in box 6 (K*, Fig. 4.1), which is known to be an important amino acid residue for ACS function, is conserved in all three ACS genes identified in white clover. These observations of the TRACS sequences suggest that these are authentic ACS genes of white clover.

When the three ACS sequences were compared with genes reported in the GenBank database, the alignments also confirmed the PCR products as ACS gene sequences (Table 3.2.3). Moreover, different aligned sequence profiles for each ACS gene suggest that these ACS genes are most likely encoded by distinct genes in white clover.

In this thesis, northern analysis has been used to study ACS gene expression during the early leaf development. From isolation of poly(A)$^+$mRNA, it is evident that leaves at different developmental stages contain different proportions of poly(A)$^+$mRNA as well as a different rRNA profile (Fig 3.2.8). This was first observed in leaves of white clover by Butcher (1997)

and a similar observation has been reported from other gene expression studies during leaf senescence (Bleecker, 1998). The amount of rRNA changes during leaf senescence in higher plants, and so if a gene expression study is carried out with total RNA, then the actual level of expression can be misinterpreted.

Northern analysis was, therefore, performed using 5 µg of poly(A)$^+$mRNA extracted from the apex, leaf 1 and leaf 2 and two ACS genes, TRACS1 and TRACS3, used as probes (Fig. 3.2.8). TRACS1 gene expression was not detected by northern analysis, although the TRACS1 gene sequence was identified by RT-PCR from the same tissue. This probably implies that the expression level of TRACS1 gene is very low at the early developing stage of leaf tissue in white clover and maybe higher in mature green or senescent leaves. TRACS3 gene expression was detected in the apex and newly initiated leaves (leaf 1 and leaf 2), with a relatively higher expression in leaf 2.

Specific ACS gene expression in developing tissues has been reported from *A. thaliana* (Van Der Straeten *et al.*, 1992; Rodrigues-Pousada *et al.*, 1993; Rodrigues-Pousada *et al.*, 1996). The level of AT-ACC1 (ACS2) gene expression was examined using RT-PCR (Van Der Straeten *et al.*, 1992), and also its transcriptional activation was examined using transgenic plants of *A. thaliana* containing ACS2 promoter-GUS reporter gene constructs (Rodrigues-Pousada *et al.*, 1993). Both experiments indicated consistently that the ACS gene was highly expressed in the developing leaf and floral tissue. As well, characterisation of AT-ACC1 (ACS2) gene expression during rosette leaf development indicated that the gene expression was most likely related to the high level of IAA in the developing leaf tissue (Rodrigues-Pousada *et al.*, 1996).

Examination of the GenBank database shows that TRACS3 has highest homology to ACS genes expressed in response to IAA treatment of other plant species (PS-ACS1). This may suggest that TRACS3 is an ACS gene induced by the higher levels of endogenous IAA which are often reported to be associated with the early stage of leaf development (Osborne, 1991).

IAA-induced expression has also been reported for CM-ACS1 in winter squash (Nakagawa *et al.*, 1991), pBTAS2 (LE-ACS3) in tomato (Yip *et al.*, 1992), ACS2 and ACS4 in *A. thaliana* (Abel *et al.*, 1995; Rodrigues-Pousada *et al.*, 1996), and VR-ACS6 in mung bean (Yoon *et al.*, 1997; Yoon *et al.*, 1999). One of the common molecular responses of IAA-induced ACS gene expression in non-senescent vegetative tissue is that gene expression is further up-regulated by cytokinin, but down-regulated by ABA, methyl jasmonate and ethylene (Imaseki, 1999). It remains to be determined whether TRACS3 gene expression is responsive to IAA or other hormones in white clover.

A further study of ACS gene expression in white clover has been now carried out for all three TRACS genes (Trish Murray, IMBS, Massey University, *personal communication*). Northern analysis reveled that TRACS1 and TRACS2 are expressed in mature and senescent leaves, and using semi-quantitative RT-PCR with gene-specific primers, TRACS3 expression has been shown to be specific in the developing apex and newly initiated leaves. The three TRACS genes, therefore, appear to be differentially expressed during leaf ontogeny in white clover.

4.2.2 Characterisation of ACC accumulation

Accumulation of ACC (the product of ACS activity) coincides with ethylene production in the developing tissues (Fig. 3.1.11). The amount of ACC in the developing apex and a newly initiated leaf tissue (leaf 1) was comparatively larger than measured in a mature green leaf tissue (leaf 6), and corresponds to the high level of ethylene production from these tissues. However, the difference in ACC content (*ca.* 1.5-fold) between the apex and mature leaf 6 is not as much as the difference in ethylene production (*ca.* 5 to 6-fold) between the two tissues. Although the expression of at least one ACS gene (TRACS3) has been detected in the apex in this thesis, and by Murray (*personal communication*), the relative abundance of the gene transcript, or ACS enzyme activity in the apex has not been determined.

A further possibility to explain the discrepancy is that ACO activity may play an important role in regulating ethylene production at the apex, rather than ACS activity. ACO activity has been reported as the controlling factor in producing IAA-induced ethylene production, which

regulates hypocotyl elongation of light-grown seedlings of *A. thaliana* (Smalle *et al.*, 1997a; Smalle *et al.*, 1997b). Enhanced hypocotyl elongation and the promotion of primary leaf emergence was induced by IAA, but this effect was blocked by silver ions (an ethylene action inhibitor) or Co^{+} (an ACO activity inhibitor). This suggests that the action of IAA is mediated through ethylene. However, the hypocotyl response was not hindered by AVG (an ACS activity inhibitor), indicating that ACS activity is not an important factor for the ethylene production. Instead, ethylene production is more likely to be promoted by an increase in ACO activity. Therefore, it was important to investigate ACO gene expression and its enzyme activity as a putative rate-controlling step of ethylene production during the early leaf development of white clover.

4.3 Characterisation for ACO during the early development of leaf tissue in white clover

4.3.1 Molecular characterisation of ACO gene family

The reading-frames (protein-coding regions) of ACO genes were cloned from the apex (Fig. 3.3.1) and a newly initiated leaf (leaf 2; fig. 3.3.2) using two rounds of PCR with nested degenerate primers. This absolute requirement for two rounds of PCR for the amplification is in common with ACS amplification, and probably suggests that the level of ACO gene expression in leaf tissue of white clover might not be as high as reported from other tissues in other plant species.

Based on nucleotide sequence homology, the ACO genes can be categorised into three groups designated as TRACO1 (Fig 3.3.3), TRACO2 (Fig. 3.3.4), and TRACO3 (Fig. 3.3.5) (Table 3.3.1). In many plants, ACO genes have been reported to comprise multigene families, which tend to be smaller than ACS gene families. For example, four genes in tomato (Barry *et al.*, 1996; Nakatsuka *et al.*, 1998), four genes in petunia (Tang *et al.*, 1993), three genes in melon (Lasserre *et al.*, 1996), three genes in sunflower (Liu *et al.*, 1997), three genes in tobacco (Kim *et al.*, 1998), two genes in mung bean (Kim and Yang, 1994), and two genes in broccoli (Pogson *et al.*, 1995) have been identified.

Using RT-PCR, the TRACO1 gene was identified exclusively in the apex, whereas the TRACO2 and TRACO3 genes were amplified from leaf 2, with a higher frequency of TRACO2 clones (as transformed colonies) identified (Table 3.3.1; Table 3.3.2). The TRACO3 gene was amplified with higher frequency from cDNA templates made from RNA isolated from senescent leaves (leaf 12; Hunter, 1998). The frequency of gene clones from a PCR product in this system could be related to the level of expression of each ACO gene in a tissue, suggesting that TRACO1 gene expression occurs mainly in the apex, TRACO2 gene expression in leaf 2 (a newly initiated leaf), and TRACO3 gene expression in leaf 12 (a senescent leaf).

The 3'-UTR of each ACO gene has also been cloned using 3'-RACE with the 5'-primers, based on reading-frame sequences obtained from TRACO genes, and 3'-adaptor primers (Fig. 3.4.1; Fig. 3.4.3; Fig. 3.4.5). Successful DNA amplification of 3'-UTRs of TRACO genes was obtained by single round PCR, and a second round of PCR further amplified the products. In senescent leaves, a second round PCR was also not necessary for cloning the 3'-UTR of TRACO3 (Hunter, 1998). This may imply that the use of gene-specific primers increases the sensitivity of amplification using PCR.

It is interesting that the 3'-RACE system amplified the 3'-UTRs of all three TRACO genes with cDNA templates made from RNA isolated from the apex (Table 3.4.1), even though RT-PCR only detected the reading-frame of TRACO1 from this tissue (Table 3.3.2). Moreover, the 3'-UTRs of TRACO1 (Fig. 3.4.2) and TRACO2 (Fig. 3.4.4) were 301 bp and 250 bp, respectively, but the 3'-UTR of TRACO3 (Fig. 3.4.6) from the apex was only 92 bp. Previously, Hunter (1998) reported that 3'-UTRs of TRACO3 cloned from senescent leaves were three different sizes of 92 bp, 172 bp and 324 bp, suggesting that the truncated TRACO3 3'-UTR is the only one expressed in the apex.

Three different ACO transcripts, which only differed in terms of size of the 3'-UTR were also observed from screening a cDNA library made from submerged rice internode mRNA (Mekhedov and Kende, 1996). The authors proposed that ACO genes might be transcribed through alternative polyadenylation processing. So, further characterisation is required to

determine if alternative polyadenylation is a part of TRACO3 gene transcription processing during leaf ontogeny in white clover.

The three TRACO gene sequences in white clover show high homology in their reading-frames (Table 3.3.2), but much lower homology in the 3'-UTRs (Table 3.4.1). This is consistent with observations from other ACO genes reported in the GenBank database. Imaseki (1999) summarised these as comprising long clusters of conserved sequences spanning over two-thirds of the reading-frame with significant divergence only in the N-terminal 20 amino acids and the C-terminal 10 to 12 amino acids.

Examination of the deduced amino acid sequences of the three ACO genes in white clover also revealed that these sequences contain amino acid residues known to be critical for ACO activity (Kadyrzhanova *et al.*, 1997), indicating that these ACO genes probably encode for functionally active ACO proteins (Fig. 3.4.7).

Information obtained from the GenBank database indicates that the TRACO1 gene matches to a set of ACO genes which are distinct from those matched with the TRACO2 and TRACO3 genes (Table 3.3.3). Further, phylogenetic analysis shows that the TRACO1 may be encoded by an ACO gene which is evolutionarily distant from those of TRACO2 and TRACO3 (Fig. 3.3.7).

The TRACO1 gene had highest homology with pPE8 (PS-ACO1) (Peck *et al.*, 1993) (Fig. 3.3.13). PS-ACO1 was cloned by a combination of PCR amplification and screening of a cDNA library made with poly(A)$^+$mRNA isolated from apical hooks of etiolated pea seedlings treated with 100 μM IAA for 4 hr. The high level of sequence homology between TRACO1 and PS-ACO1 may imply that both ACO genes encode for similar ACO proteins in terms of biochemical characteristics, and are functionally equivalent in plant development.

Expression studies of three TRACO genes during early leaf development of white clover have been conducted using both reading-frame (Fig. 3.3.15) and 3'-UTR (Fig. 3.4.11) regions as

probes in northern analysis. Hybridisation with both probes indicated that the TRACO1 gene is expressed almost exclusively in the developing apex and the TRACO2 gene is expressed in leaf tissues, with relatively higher expression in newly initiated leaves. However, neither reading-frame nor 3'-UTR probes of TRACO3 hybridised to RNA extracted from early developing tissues over the expose time used normally (reading-frame probes, 16 hr; 3'-UTR probes, 7 days). This result suggests either that TRACO3 gene is not expressed in these tissues, or its expression is under the limit of detection (see below).

The almost exclusive expression of the TRACO1 gene in the developing apex should be further characterised to determine in which cells or tissues the ACO gene is expressed in the apex. As is shown in figure 4.2, the apex includes various organs such as the shoot apical meristem, the stolon elongation zone, leaf primordia and also axillary buds. Therefore, because of this tissue heterogeneity, it will be interesting to determine if all tissues express TRACO1 in the apex.

Residual TRACO1 gene expression is also observed in the newly initiated leaves, which implies that the ACO gene may be expressed in the young leaf primordial tissue in the apex. Its expression is probably then turned off when the developing leaf emerges from the apical sheath to start rapid expansion. If the TRACO1 gene is turned off when TRACO2 gene expression is induced in the newly initiated expanding leaves, a gene silencing mechanism might be involved. This may be a co-suppression type (Kooter et al., 1999; Wassenger and Pelisser, 1999), since in terms of sequences TRACO1 and TRACO2 are highly similar genes. However, until tissue localisation of TRACO1 is determined in the leaf primordial tissue, such a mechanism can only exist as speculation.

The localisation of TRACO1 gene expression in the apex can be determined using *in situ* hybridisation. This technique has been used in the study of the localisation of PS-ACO1 gene expression in apical hook tissue of pea seedlings (Peck *et al.*, 1998). An asymmetrical distribution of PS-ACO1 transcripts was observed between the inner and outer parts of the

Figure 4.2 Apical structure of white clover.
Shoot apical meristem (0), leaf primordium (1), developing leaflet (2), axillary bud (3), and stolon elongation zone (4) are indicated.

apical hook such that cortical cells of the inner part of the apical hook expressed a relatively higher level of the ACO gene (and higher ACO enzyme activity, *in vitro*). The hybridisation also showed clearly that gene expression was absent in the epidermal cells and confirmed an earlier observation that epidermal cells do not produce ethylene (Todaka and Imaseki, 1985). Although *in situ* hybridisation has been successfully used to localise the expression of many plant genes, it may be difficult to localise specific TRACO gene expression in the apex tissue of white clover. This is because the three ACO genes in white clover show high sequence homology. For example, some TRACO2 gene expression is always detected in the apex, together with TRACO1. Moreover, the amount of ACO gene expression in the apex is uncertain, but is probably very low.

As a preliminary study of *in situ* hybridisation, anti-sense transcripts of TRACO1 (*ca.* 700 bp including the 3'-UTR) were labeled, *in vitro,* with [α-P^{32}]-UTP and used for northern analysis (data not shown). The TRACO1 riboprobe was hybridised in Church hybridisation solution, containing 50 % (v/v) formamide at 65 ^{o}C and washed at high stringency (0.05 X SSPE at 65 ^{o}C). However, the anti-sense riboprobe of TRACO1 demonstrated cross-hybridisation with TRACO2 transcripts in the mature leaf tissues, indicating that the riboprobe would not discriminate TRACO1 expression from the TRACO2 expression in the apex using these hybridisation conditions. A more sensitive method might be required with an ability to discriminate each gene transcript and to visualise gene expression on the tissue sections. An *in situ* RT-PCR with gene specific primers, which has been used to localise *myb*-like regulatory gene expression in endosperm of maize seeds, may be a useful option (Bombelli *et al.*, 1998).

The TRACO2 gene is mainly expressed in mature green leaves and the maximum expression is associated with newly initiated leaves (Fig. 3.3.15; Fig. 3.4.11). This TRACO2 gene expression gradually decreases as the leaf ages. From a study of leaf senescence with the white clover model growth system, Hunter *et al.* (1999) reported that TRACO2 gene expression ceased around the onset of chlorophyll break down, with increased ethylene production following soon after.

TRACO3 gene expression was not initially detected in the apex and newly initiated leaves examined in this study (Fig. 3.3.15; Fig. 3.4.11). TRACO3 gene expression is reported to begin before the onset of chlorophyll break down and then increases during leaf senescence, coinciding with senescence-associated ethylene production (Hunter *et al.*, 1999). However, an attempt to detect any low level TRACO3 gene expression in the developing leaves was made by exposing the RNA membrane probed with the reading-frame of TRACO3 for an extended time (Fig. 3.3.16). When membrane exposure was extended to 21 days, the TRACO3 probe clearly hybridised to two transcripts of 1.17 kb and 1.35 kb, with greater signal associated with the 1.17 kb transcript. However, over the same exposure time, the TRACO2 reading-frame probe hybridised to a single transcript of 1.35 kb.

Two transcripts hybridising to the reading-frame of TRACO3 was also reported in the gene expression study of TRACO3 during leaf maturation and senescence in white clover (Hunter, 1998). In that study, when 2 μg of poly(A)$^+$mRNA extracted from mature leaves and senescent leaves was used, the TRACO2 gene probe hybridised to a transcript of 1.35 kb. However, the TRACO3 probe hybridised to two transcripts of 1.35 kb and 1.17 kb, suggesting that there might be a further ACO gene, sharing high sequence homology to TRACO3, and which is expressed in a similar manner to TRACO3 during leaf senescence. This assumption led to the cloning of the 3'-UTR of the ACO gene, which is proposed to have less sequence homology, and hence should reduce cross-hybridisation. During cloning of the 3'-UTR of the TRACO3 gene from senescent leaves, three sizes of 3'-RACE products were amplified (cf. section 4.3.1), suggesting that the 1.17 kb RNA transcript could be a TRACO3 transcript with the shortest 3'-UTR generated by an alternative polyadenylation process. However, when using the longest 3'-UTR of TRACO3 as gene-specific probe, northern analysis revealed a single band of 1.35 kb. Hunter (1998) speculated that if the 1.17 kb was a TRACO3 gene transcript with a truncated 3'-UTR, the probe should have hybridised to the 1.17 kb transcript as well. Thus, the 1.17 kb transcript was concluded not to be a TRACO3 gene transcript, and was probably detected through cross-hybridisation by the reading-frame probe of TRACO3 (Hunter, 1998). Because the longest 3'-UTR clone was used as probe for northern analysis, if the 1.17 kb gene transcript was a TRACO3 gene transcript with a shorter 3'-UTR, then this transcript could

only hybridise with *ca.* 128 bp of the 3'-UTR probe (this was most likely even shorter, because the random priming system was used for probe-labeling). Whereas, the 1.35 kb transcript would hybridise to the whole 360 bp of the probe. Therefore, the hybridisation complex with the truncated portion (*ca.* 128 bp) would be very unstable because of its predictable low Tm, and hence the complex could be washed off by the high stringency washing used in that study. So, the initial conclusion which excludes the possibility of the 1.17 kb transcript as the TRACO3 gene may be premature. The possibility of the unstable hybridisation complex should be examined further with lower stringency washing using a probe labeling systems which ensure production of full-length probes, such as end labeling or PCR labeling. The argument that the 1.17 kb transcript is the TRACO3 gene is supported further by the observation of the shorter 3'-UTR (92 bp) of the TRACO3 gene identified by 3'-RACE from the apex. The difference of 232 bp between the longest 3'-UTR from TRACO3 (324 bp) and the shortest (92 bp) could account for the difference in observed transcript sizes (1.35 kb and 1.17 kb). In northern blots performed in this thesis (Fig. 3.4.11), the TRACO3 3'-UTR probe recognised a transcript of 1.35kb with greater intensity of signal when compared with 1.17 kb transcript.

Taken that the 1.17 kb transcript is a TRACO3 gene, it can be speculated that alternative polyadenylation occurs to produce the transcript with the shorter 3'-UTR in the early leaf developing stage, and the transcript with the longer 3'-UTR in the later senescent stage of leaf development.

It has been reported that transcripts with short 3'-UTRs, caused by premature polyadenylation are unstable and are degraded rapidly by RNase, when compared to those with longer 3'-UTRs (Abler and Green, 1996; De Rocher *et al.*, 1998; Diehn *et al.*, 1998;). So, alternative polyadenylation of TRACO3 gene transcripts may occur as part of the regulatory mechanism of ACO gene expression during leaf development. This can be examined further by performing 3'-RACE with TRACO3 gene-specific primers, using cDNA templates made from RNA isolated from leaf tissues at different developmental stages.

It is also interesting to note that 3'-RACE of the TRACO1 gene amplified products of a range of sizes (Fig. 3.4.1). One of them (ca. 700 bp) was sequenced and confirmed to the 3'-UTR of TRACO1. However, it may be that these other products represented differentially polyadenylated transcripts of this gene. This was not investigated in this thesis.

In white clover, TRACO1 gene expression, which occurs almost exclusively in the developing apex was also detected in axillary buds, but not in floral buds (Fig. 3.4.12). This organ-specific TRACO1 expression in developing vegetative bud tissues may control ethylene production, which probably regulates the early development of leaf tissue (Lee and Reid; 1997).

The mature green leaf tissue-associated TRACO2 gene expression was also detected in petiole, internode, and node tissues, with a relatively higher expression in the internode. Expression of both TRACO1 and TRACO2 was detected in roots, although discrimination of this expression in root meristems, root elongation zone, lateral roots and root hairs was not determined.

Differential expression of the ACO gene family has also been characterised in several plant species (Nadeau *et al.*, 1993; O'Neil *et al.*, 1993; Tang *et al.*, 1993; Tang *et al.*, 1994; Barry *et al.*, 1996; Barry *et al.*, 1997; Guis *et al.*, 1997; Lasserre *et al.*, 1997; Liu *et al.*, 1997; Kim *et al.*, 1998; Jin *et al.*, 1999). In sunflowers, the ACCO1 gene is expressed highly in apical buds and roots, and is also expressed in the hypocotyl and cotyledon at a lower level (Liu *et al.*, 1997). This ACCO1 gene expression is very similar to TRACO1 gene expression in the apex and roots of white clover. However, the ACCO1 probe used in that expression study cross-hybridised with two other similar gene transcripts (ACCO2 and ACCO3), so the gene expression pattern visualised by this probe probably reflects the expression pattern of all three ACO genes rather than any specific ACO gene.

Thus RT-PCR was used for more specific gene expression. Only a basal level of ACCO3 gene expression was detected in the roots, hypocotyls and leaves. However, the ACCO1 gene was mainly expressed in the roots. This ACO gene expression is similar to TRACO1 in white clover, but the specific ACCO1 expression using RT-PCR was not determined in the apex in the study. The ACCO2 gene was highly expressed in leaf tissue and so the ACCO2 gene in

sunflower may be related to the TRACO2 gene expression in white clover. From observations in tobacco (Kim *et al.*, 1998), pNG-ACO2 gene is expressed constitutively in leaf tissue, together with mature stem tissue, whereas pNG-ACO1 and pNG-ACO3 genes are expressed highly in senescent leaf tissue as well as roots. Also, in mung bean plants (Jin *et al.*, 1999), the VR-ACO1 gene is expressed in leaf and stem at a reduced level, and etiolated hypocotyl and roots at a relatively higher level. However, specific gene expression in the apex has not been determined in these studies.

In melon, three ACO genes are shown to be differentially expressed in an organ-specific and/or a development-specific manner (Guis *et al.*, 1997). The CM-ACO2 gene was only detected in etiolated hypocotyls, whereas CM-ACO1 and CM-ACO3 genes were detected in leaf and root tissues by RT-PCR. Only CM-ACO1 was detected in melon fruits by RT-PCR. When RT-PCR is used as a quantitative method to measure gene expression, it should include internal controls for amplification (as it was in the gene expression studies in sunflowers; Liu *et al.*, 1997). However, such internal controls were not included in the study of ACO gene expression in melon. Gene expression of CM-ACO1 and CM-ACO3 has been characterised using GUS-promoter activity assays in leaf tissue of melon plants (Lassere *et al.*, 1997). CM-ACO3 promoter activity is relatively high in mature green leaves, and hence its gene expression pattern is reminiscent of TRACO2 gene in white clover. However, CM-ACO1 promoter activity increases during leaf senescence. So this pattern of gene expression is close to TRACO3 gene expression in white clover. Even though differential expression of ACO genes in melon has been thoroughly characterised, the expression of any of the CM-ACO genes has not been examined in the apex. In tomato fruits, LE-ACO1 and LE-ACO3 are also expressed differentially (Barry *et al.*, 1996; Barry *et al.*, 1997). The LE-ACO1 gene is induced at the breaker stage and remains at a high expression level throughout fruit ripening. The LE-ACO3 gene is expressed only transiently at the breaker stage and then its expression is reduced to a basal level. These expression patterns in tomato fruits are similar to those in senescent leaf tissue in tomato plants and suggest that LE-ACO1 is similar to TRACO3. However, as yet, the gene expression of any of the LE-ACO genes has not been examined in the vegetative apex of

tomato. The specific ACO gene expression in the apex of white clover, is to the author's knowledge the first such demonstration in the literature (see Hunter *et al.*, 1999).

In white clover, neither the TRACO1 gene nor the TRACO2 gene was expressed in floral tissue of white clover (Fig. 3.4.12). In other plant species, differential expression of ACO genes has been reported in floral tissue in a tissue-specific and/or development-specific manner. In tomato flowers, for example, the LE-ACO1 gene is expressed in all floral organs but its expression is highest in petal and style/stigma tissue after pollination (Barry *et al.*, 1996). LE-ACO2 gene expression is highly induced in the anther at the pollen-release stage (anthesis), but then expression decreases. The LE-ACO3 gene is highly expressed throughout flower development and senescence, except in the sepal tissue. This differential expression of ACO genes during flower development is also observed in orchid (Nadeau *et al.*, 1993; O'Neil *et al.*, 1993) and petunia (Tang *et al.*, 1993; Tang *et al.*, 1994).

By deduction from these studies, it is most likely that the TRACO3 gene may be expressed in floral tissue of white clover, because flowers from other species have been shown to express a senescence-related ACO gene (Fluhr and Mattoo, 1996; Imaseki, 1999). However, ACO expression should be thoroughly examined in each floral tissue as well as at each floral developmental stage to more precisely characterise the expression of ACO genes in this organ of white clover.

Taken together, the TRACO genes identified in this study appear to be expressed constitutively in white clover, but members of the TRACO gene family are also differentially expressed in various organs at various developmental stages. This differential expression of the ACO multigene family can be interpreted as an adaptive process so as to express the appropriate ACO isoform in any particular environment of each organ at a specific developmental stage. It has been observed that ACO enzyme activity is primarily controlled at the transcriptional level, whereas ACS enzyme activity is also modified at a post-transcriptional level (Spaun *et al.*,1990; Spaun *et al.*,1994). Therefore, differential ACO gene expression may be necessary to produce a particular ACO isoform in a particular organ at a particular developmental stage.

Finlayson *et al.* (1998) reported that ACO isoforms may exist in an organ-specific manner. They observed that ACO enzyme activity characterised in roots was distinct from that characterised in leaf tissue of corn or sunflower and proposed that each of these tissues requires a distinct ACO isoform to cope with different environmental conditions, with main differences in CO_2 and O_2 concentrations. These environmental factors are known to act as an enhancer (CO_2) or a necessary cosubstrate (O_2) of ACO enzyme activity. In that study, ACO enzyme activity, *in vitro*, in root extracts was much less affected by CO_2, compared to those from leaf extracts in both plant species (Finlayson *et al.*, 1998). These different biochemical properties of ACO activity in two protein extracts indicates the presence of at least two different ACO isoforms, although no further protein purification studies was undertaken.

Therefore, to examine if differential expression of ACO genes in white clover is related to expression of ACO isoforms in an organ- or a development-specific manner, this study was extended to the characterisation of ACO proteins in white clover.

4.3.2 Biochemical characterisation of ACO protein expression

Characterisation of ACO protein in white clover has been examined with ACO activity, *in vitro* (Fig. 3.1.12; Fig. 3.1.13), and ACO protein accumulation using polyclonal antibodies, which were raised against TRACO proteins expressed in *E. coli* (Fig. 3.3.10; Table 3.5.1).

ACO activity, *in vitro*, is relatively higher in mature leaves (leaf 3 or leaf 4), compared to those in the developing apex and newly initiated leaves (Fig 3.1.12). This extractable ACO activity, *in vitro*, coincides closely with the expression of the TRACO2 gene (Fig. 3.3.15; Fig. 3.4.11). Moreover, PAb2 (the polyclonal antibody raised against the TRACO2 gene product) recognised a *ca.* 36 kD protein (Fig. 3.5.5), which is within the range reported for ACO proteins from other plant species (Dong *et al.*, 1992; Dupille *et al.*, 1993; Pirruning *et al.*, 1993; Rombaldi *et al.*, 1994; Liu *et al.*, 1997; Jin *et al.*, 1999). The relative protein accumulation also coincides with TRACO2 gene expression (Fig. 3.3.15; Fig. 3.4.11).

In contrast to PAb2, PAb1 (the polyclonal antibody raised against the TRACO1 gene product), recognised a *ca.* 205 kD protein complex, which is expressed predominantly in the apex (Fig. 3.5.3; Fig. 3.5.4). A higher molecular weight protein was expressed almost exclusively in the

apex and a slightly lower molecular weight protein, the expression of which was highest in the apex but was also detectable as declining in recognition in leaf 1 to 6. Even though the size of either of these proteins cannot be a product transcribed directly from a 1.35 kb transcript, the expression pattern of the complex, particularly the higher molecular weight protein, coincided with the gene expression pattern of TRACO1 (Fig. 3.3.15; Fig. 3.4.11). It may be that this protein is highly abnormal in terms of its migration using SDS-PAGE or a multimerization of the TRACO1 protein may also be an explanation. However, the protein extracts were run on SDS-PAGE in reducing conditions after 2-mercaptoethanol treatment with boiling, so disulfide bond-based mutimerization of the protein should be excluded.

Although, the possibility of ACO protein complex with other proteins cannot be discounted. The TRACO1 gene had highest homology with PS-ACO1 (Peck *et al.*, 1993) (Fig. 3.3.13). Analysis of the PS-ACO1 gene sequence reveals a typical Leu zipper protein motif, containing Leu residues every seven amino acids from Phe^{117} to Leu^{138} (Phe^{117}AlaLeuaLysLeuGleGle Leu^{124}AlaGleGleLeuLeuAspLeu^{131}LeuCysGleAsnLeuGlyLeu^{138}) which may be involved with protein-protein interaction. This protein motif has also been recognised on other ACO proteins as well as E8 protein (a tomato ripening-related protein), which are classified together as the dioxygenase family in plants. Binding of other cellular proteins to this motif may be a mechanism by which the TRACO1 gene product increases in size.

It is also possible that some epitopes recognised by PAb1 on other proteins are simply shared with those of the TRACO1 protein, and this protein is present predominantly in bud-related tissues. The TRACO1 polyclonal antibodies cross-reacted with other TRACO protein products expressed in *E. coli* (Fig. 3.5.1), which suggests that an ACO isoform recognised by PAb1 will most likely be recognised by PAb2 or PAb3. However, both PAb2 and PAb3 failed to recognise the high molecular weight antigen species, suggesting that this high molecular weight antigen may not be an ACO isoform (TRACO1 protein), even though the pattern of antigen abundance is broadly consistent with TRACO1 gene expression.

Nevertheless, with the observation of a consistent pattern between PAb1-recognised antigen accumulation and TRACO1 gene expression, immuno-affinity purification using both protein G beads and a CNBr-activated Sepharose column was carried out to identify the antigen by

protein sequencing (Fig. 3.5.9; Fig. 3.5.10; Fig. 3.5.11, Fig. 3.5.12). Including ELISA (Fig. 3.5.8), all immunology-based assays indicated that the PAb1-recognised antigens are specifically expressed in the apex. However, the amino acid sequence of the peptide was not obtained following trypsin digestion. This was most likely because of the low yield of protein obtained by the affinity column, indicating that the antigen might be present at an extremely low level in the apex.

Purification of TRACO2-related antigen in mature green leaf tissue was also attempted using PAb2-coupled affinity column in the same way (Deming Gong, IMBS, Massey University, *personal communication*). However, peptide sequencing was not possible with the purified proteins. Because the immuno-affinity purification has been used routinely to identify unknown antigens (McManus and Osborne, 1990a; McManus and Osborne 1990b), the failure of this technique in this thesis may be because the expression level of the antigen (ACC oxidase) in the apex and leaf tissues is much less than expected. Alternatively, the ACO protein expressed in *E. coli* was immunised as SDS-denatured proteins, while immuno affinity column chromatography relies on the antibody recognising the protein in its native state. It may be, therefore, that the PAb1 antibodies have a very low affinity for the native ACO protein. The comparatively low dilution (1:100) of white clover leaf extracts used in ELISA (Fig. 3.5.8) offers support for this suggestion.

ACO activity, *in vitro*, in the apex is only about 60% of ACO activity, *in vitro*, measured in leaf 4 (Fig. 3.1.12). It may be that extractable ACO activity from the apex does not correlate directly with ethylene production from the tissue or it could be due to assaying ACO enzyme activity, *in vitro*, under sub-optimised conditions for the ACO from the apex.

A similar decrease in ACO activity, *in vitro*, was observed in senescent leaves of white clover, although the expression of the TRACO3 gene and ethylene production increase in this tissue (Hunter, 1998). So, further purification of ACO proteins in mature green and senescent leaf tissue of white clover has been conducted by Deming Gong (IMBS, Massey University, *personal communication*). Protein extracts from mature green leaves and senescent leaves

were subjected to hydrophobic chromatography, followed by gel filtration and ion exchange column chromatography. This purification revealed one ACO isoform in mature green leaves and two ACO isoforms from senescent leaves with distinct molecular sizes. Also, biochemical characterisation of two ACO of the isoforms (one from mature green leaves, and the other from senescent leaves) indicated that the optimum pH for ACO activity assay, *in vitro* for a senescent leaf-related ACO (pH 8.5) differs from the mature green leaf-related enzyme (pH 7.5). From the identification of optimised assay conditions for each ACO isoform in white clover, these conditions were applied to measure ACO activity, *in vitro*, in crude protein extracts from senescent leaf tissue, but no ACO activity, *in vitro* was measured. Therefore, it has been concluded that the assay of ACO activity, *in vitro*, to detect senescence-related ACO isoforms requires at least partial purification using hydrophobic column chromatography. But once this partial purification has been achieved, there is clear evidence that ACO activity, *in vitro*, has increased in accordance with TRACO3 gene expression in the senescent leaf tissue of white clover (D. Gong, *personal communication*).

In common with the assay of ACO activity, *in vitro*, in senescent leaf tissue of white clover, it is likely that characterisation of ACO activity, *in vitro*, associated with TRACO1 gene expression in the apex may also require a partially purified protein preparation. It may then be possible to determine the optimal assay conditions and characterise the specific biochemical properties of the ACO isoform expressed in the apex. Preliminary purification of ACO isoforms from the apex showed that a *ca.* 205 kD antigen-antibody complex (identified by western analysis) was co-eluted from a hydrophobic column with fractions containing ACO activity (D. Gong, *personal communication*). This result indicates that the high molecular weight antigen might have some similarity with ACO proteins in terms of the hydrophobicity of the protein. Further purification using FPLC is, therefore, required to identify the antigen in the apex of white clover.

Some studies, in which the differential expression of ACO genes have been examined in other plant species, have been extended to examine ACO enzyme activity, *in vitro*, and protein accumulation. In tomato plants (Barry *et al.*, 1996), when LE-ACO1 and LE-ACO3 gene

expression is highly induced in wounded leaf tissue, senescent flower tissue, and ripening fruit tissue, extractable ACO activity, *in vitro*, increases about 4- to 5-fold higher in wounded leaves and senescent flowers, and 20-fold higher in ripening fruits (breaker+3 days stage).

A concerted change of ACO gene expression and ACO activity was also observed in petals of carnation flowers during vase storage (Vries *et al.*, 1994). ACO gene expression is not detected in fresh flowers, but it increases rapidly at day 6 to reach a maximum at day 9 and then decreases. Extractable ACO activity from the tissue follows the gene expression pattern precisely. ACO activity, *in vivo,* is comparatively lower than activity, *in vitro,* but the changing pattern is more or less consistent. The less activity by *in vivo* assay is proposed to be due to sub-optimisation of the activity assay conditions. However, the consistent changes in the pattern of ACO activity and ACO gene expression clearly demonstrates that petal senescence-associated ACO genes encode functional ACO proteins, which produces ethylene in this tissue.

ACO activity, *in vitro* was also measured in various organs of white clover and was highest in roots (27.87 ± 2.31 nL C_2H_4 mg protein^{-1} hr^{-1}), then petioles (7.40 ± 0.25 nL C_2H_4 mg protein^{-1} hr^{-1}), floral buds (5.71 ± 2.33 nL C_2H_4 mg protein^{-1} hr^{-1}) and axillary buds (5.43 ± 0.09 nL C_2H_4 mg protein^{-1} hr^{-1}), internode (2.70 ± 0.06 nL C_2H_4 mg protein^{-1} hr^{-1}) and node (2.67 ± 0.07 nL C_2H_4 mg protein^{-1} hr^{-1}) extracts (Fig. 3.1.12). The activity data matched protein accumulation patterns recognised by the PAb2 (*ca.* 36 kD) and may again reflect the specificity of the enzyme assay (Fig. 3.5.7). So, a more detailed characterisation of assay conditions maybe required for each tissue.

In addition, PAb1 recognised the high molecular weight protein consistently from bud-related tissues including the apex, axillary buds and floral buds (Fig. 3.5.6). PAb1 recognition of the antigen in floral buds does not coincide with TRACO1 gene expression, since this gene was not detectable in floral bud tissue (as determined by northern analysis; Fig. 3.4.12). The discrepancy between protein recognition by PAb1 and gene expression of TRACO1 here may suggest that PAb1-recognised antigen is most likely not a gene product of TRACO1. It may be

an antigen sharing epitopes with TRACO1 protein, which is expressed predominantly in bud-related tissue, such as the apex, axillary buds, and floral buds.

From these studies of ACO activity, *in vitro*, and ACO protein accumulation, compared with ACO gene expression, it is clear that ACO is present in almost all plant organs of white clover. Furthermore, TRACO proteins appear to be expressed in an organ- or a development-specific manner, probably to mediate environmentally tailored ACO activity in each tissue.

4.4 Molecular characterisation of ACO gene expression in mature green leaves

ACO gene expression in white clover has been characterised using mature green leaves to examine responses of the gene expression to wounding and ethylene, which are identified as induction factors of ACO gene expression in many plants (Kende, 1993; Fuhr and Mattoo, 1996; Imaseki, 1999).

In these experiments, excised mature green leaf tissue of white clover displayed changes in TRACO2 and TRACO3 gene expression, which are similar to those reported by Hunter *et al* (1999) that occur during leaf maturation and senescence. TRACO2 gene expression decreased, but TRACO3 increased with time after leaf tissue-excision from the stolon (Fig. 3.6.1). Wounding of mature green leaves attached to stolons also demonstrated an induction of TRACO3 gene expression, but it was delayed when compared to excised leaf tissue and eventually decreased (Fig. 3.6.2). However, the down-regulation of TRACO2 gene expression was not observed in wounded attached mature green leaves (data not shown). Both wounding experiments indicate the TRACO3 gene expression is responsive to wounding, whereas the down-regulation of TRACO2 gene expression only occurs as the leaf ages after tissue detachment.

It has been reported that wounding signals induce expression of ACS genes and enzyme activity to produce stress-ethylene in many plant species, including winter squash (Nakajima *et al.*, 1988; Nakajima *et al.*, 1990), zucchini (Huang *et al.,* 1991), *A. thaliana* (Liang *et al.*, 1992) and tomato (Lincoln *et al.*, 1993). Furthermore, characterisation of a wound-induced

ACS gene (WSACS2) isolated from winter squash has shown that active oxygen species (AOS) caused by wounding are most likely involved in the induction of the WSACS2 gene expression *ca.* 2 to 3 hr after wounding (Watanabe and Sakai, 1998). However, an increase in PS-ACS2 gene expression in pea seedlings was observed only 10 min after wounding (Peck and Kende, 1998). The induction of PS-ACS2 gene expression was no different when RNA was isolated from tissue at the wounding site or tissue 4 cm removed from the wounding site, suggesting that a hydraulic or an electronic signal might mediate the rapid wound response in the tissue.

To unravel a possible involvement of ACS activity in the induction of TRACO3 gene expression by wounding, a preliminary experiment with attached wounded leaves pretreated with AVG (an ACS activity inhibitor) was undertaken (Fig. 3.6.3). Although the plants pretreated with AVG expressed a higher level of TRACO3 gene expression at the beginning of wounding, wound-induced TRACO3 gene expression appears to be delayed by the AVG treatment, suggesting that the TRACO3 gene expression may be mediated through an increase in ACS activity.

Wound-induced ACO gene expression and the enzyme activity have been reported in many other plant species (Hyodo *et al.*, 1993; Kim and Yang *et al.*, 1994; Barry *et al.*, 1996; Bouquin *et al.*, 1997; Liu *et al.*, 1997). Kim and Yang (1994) characterised the effects of wounding on VR-ACO1 gene expression in mung bean hypocotyl. Wound-induced VR-ACO1 gene expression was blocked by treatment with the ethylene action inhibitor, 2,5-norbornadiene, suggesting that ethylene most likely mediates the wounding response in this tissue.

In tomato leaf tissue, LE-ACO1 gene expression was induced by wounding, together with increases of extractable ACO activity and polyclonal antibody-recognised ACO protein accumulation (Barry *et al.*, 1996). In addition, Simpson *et al.* (1998) demonstrated that both LE-ACO1 gene expression and ethylene production can be elicited by short oligo-garacturonides (DP 4-6), which are considered to be major cell wall degradation products caused by wounding from pathogen infection, insect damage, or mechanical perturbation (Nothnagel *et al.*, 1983; Takahashi and Jaffe, 1984; Ryan, 1987). This result implies that the

short oligosaccharides may induce the gene expression of LE-ACO1. However, it has not been examined whether ethylene mediates the oligosaccharide signal to induce LE-ACO1 gene expression in tomato.

In hypocotyls of sunflower (Liu *et al.*, 1997), wound-induced ACCO1 gene expression was not induced by ethylene treatment (as ethephon). Moreover, the ACCO1 gene expression was up-regulated in response to either silver thiosulphate (STS) or silver nitrate, which are known to be inhibitors of ethylene action. However, it has not been determined if any other member of the ACO gene family can be induced by ethylene in sunflowers.

The inducibility of TRACO gene expression in response to ethylene has also been determined to examine if ethylene is involved in up-regulation of wound-induced TRACO3 gene expression in white clover. Overall changes of TRACO2 and TRACO3 gene expression in excised mature leaf tissue are not altered by applied ethylene: the expression of TRACO2 declines, while the expression of TRACO3 increases with time (Fig. 3.6.4). However, when mature green leaf tissue attached to the stolon is used to eliminate wounding caused by excision, only TRACO2 gene expression is increased by the ethylene treatment, but there is no induction of TRACO3 expression (Fig. 3.6.5; Fig. 3.6.7). These results indicate that ethylene induces TRACO2 gene expression in mature green leaves, whereas wounding or ageing-related facors induce TRACO3 gene expression, and these factors are not simply replaced by ethylene in mature green leaf tissue. Therefore, transient ethylene production by wounding appears not to be an inducing factor for the up-regulation of TRACO3 gene expression.

Ethylene-induced ACO gene expression has been also reported from other plant species, including avocado fruit (Starrette and Laties, 1993), mung bean hypocotyls (Kim *et al.*, 1997), and pea seedlings (Peck and Kende; 1995; Kwak and Lee, 1997; Peck *et al.*, 1998). This ACO gene expression is proposed to lead to further ethylene production, termed autocatalytic ethylene biosynthesis (Fluhr and Mattoo, 1996). Studies on ethylene involvement in the regulation of ACO gene expression in melon leaf tissue have shown that CM-ACO1 (an ACO gene associated with organ senescence and fruit ripening) is induced separately by either wounding or ethylene (Bouquin *et al.*, 1997). Sequence analysis of the CM-ACO1 gene

promoter region have revealed putative *cis*-elements for both wounding or ethylene response, so it is proposed that the CM-ACO1 gene may be induced in melon plants by ethylene and wounding directly, but independently. Therefore, induction of ACO gene expression in white clover by ethylene or wounding differs from melon. TRACO2 gene expression is induced in response to ethylene, whereas TRACO3 gene expression by wounding or wounding-induced tissue ageing. However, the possibility that ethylene enhances TRACO3 gene expression in senescent or wounded tissues cannot be excluded.

TRACO2 gene expression is also induced in mature green leaves by IAA treatment of whole plants (Fig. 3.6.8). The induction is delayed or reduced by co-treatment with AVG, indicating that IAA affects ACS activity and then the immediate (ACC) or final (C_2H_4) products of ACS activity probably induce TRACO2 gene expression.

From the study of IAA-induced expression of genes coding for ethylene biosynthetic enzymes in pea seedlings (Peck and Kende, 1995; Peck and Kende, 1998), two ACS genes, PS-ACS1 and PS-ACS2 were induced specifically by IAA within 30 min and 15 min, respectively. However, PS-ACO1 was induced 2 hr after IAA treatment. The IAA-induced gene expression of pS-ACO1 was also reversibly blocked by the ethylene action inhibitor, 2,5-norbornadiene. From the inhibition studies, together with the longer lag time for induction of ACO gene expression, it is proposed that the IAA-effect on ACO gene induction is mediated by the rapid induction of ACS gene expression and ACS activity, which increases the cellular concentration of ACC. Then, the increased ACC is immediately converted to ethylene by a basal level of ACO in the tissue, and so this ethylene synthesized *de novo*, in turn, induces the later ACO gene expression.

In white clover, the pattern of IAA-induced TRACO2 gene expression coincides with PS-ACO1 induction by IAA in pea seedlings. The induction of TRACO2 gene expression requires *ca.* 3 hr, and is delayed and reduced by inhibiting ACS activity using AVG. Also, the nature of TRACO2 gene expression, which is responsive to ethylene, supports the notion that IAA-induced TRACO2 gene expression is mediated by ethylene in mature green leaves of white clover, in common with IAA-induced PS-ACO1 expression in pea seedlings. It may be that

IAA in the apex induces ACS activity and the ACC product is converted to ethylene by the TRACO1 isoform, which then induces the expression of TRACO2.

In this study, 1-MCP (an ethylene action inhibitor) was used to confirm that TRACO2 gene expression is responsive to ethylene. 1-MCP has been used successfully to inhibit ethylene-induced effects on abscission of phlox flowers (Porat *et al.*, 1995b), wilting responses of cut carnations (Sisler *et al.*, 1996a), or ripening of tomato and banana fruits (Sisler *et al.*, 1996b). It also showed a substantial reduction or complete inhibition of ethylene production from carnation flowers (Sisler *et al.*, 1996a) or pollinated *Phalaenopsis* flowers (Porat *et al.*, 1995a). All these effects were achieved with a concentration as low as 1 nL L^{-1}. However, it has also been observed that growing vegetative tissue requires a much higher concentration to block ethylene effects (Sisler and Sereck, 1997). For example, treatment with 40 nL L^{-1} of 1-MCP for 6 hr was required for the retardation of pea seedling growth.

The 1-MCP treatment conditions used in this thesis were 20 nL L^{-1} to 3000 nL L^{-1} for 0.5 hr to 1 hr. Leaf tissue, pretreated with 1-MCP before ethylene treatment, showed an inhibition of the ethylene-induced leaf epinastic response (Fig. 3.6.6). Inhibition of this ethylene-induced phenotypic change was also reported for 1-MCP treated tomato leaf tissue (Cardinale *et al.*, 1995). Therefore, 1-MCP used here appears to be functioning as an ethylene action inhibitor. However, northern analysis demonstrated that 1-MCP induced TRACO2 gene expression in attached leaves (Fig. 3.6.5; Fig. 3.6.7) and TRACO3 gene expression in excised tissue (Hunter, 1998).

There are a few studies which report that ethylene action inhibitors can block ethylene responses at the physiological or phenotypic level, but an actual increase in ethylene production can be measured (Reid, 1995). For example, silver ions reversed the ethylene effect of promoting root formation in sunflower hypocotyls, but it also enhanced ethylene production from this tissue (Liu *et al.*, 1990; Liu and Reid, 1992). Research with another type of ethylene action inhibitor, diazocyclopentadien (DACP) revealed that tomato fruit ripening was almost completely blocked by pretreatment of DACP, but those fruits still produced a high level of

ethylene when the fruit-ripening stage began (Imaseki, 1999). These observations may imply a complicated relationship between ethylene biosynthesis and ethylene responsiveness. In summary, the ethylene effect on TRACO2 gene expression was unable to be confirmed using 1-MCP. To confirm the ethylene effect, it might require other ethylene action inhibitor (e.g. 2,5-norbornadiene) or the use of ethylene-insensitive mutants (e.g. transgenic plants containing mutant constructs of the ethylene receptor gene; Penmetsa and Cook, 1997; Wilkinson *et al.*, 1997; Knoester *et al.*, 1998; Lund *et al.*, 1998; Hoffman *et al.*, 1999).

To explain the independent induction pattern of TRACO2 and TRACO3 gene expression in response to wounding and ethylene, two recent publications may be relevant (Chao *et al.*, 1997; Solano *et al.*, 1998) and a hypothetical model of nuclear events by ethylene response is proposed in figure 4.3.

The EIN3 gene has been identified as a transcriptional factor represented as a small gene family (EIN3-like1, 2, and3) in *A. thaliana.* (Chao *et al.*, 1997). Over-expression of the gene was sufficient to induce some ethylene responses in the absence of ethylene. So, ethylene induces EIN3 transcription and the EIN3 protein binds to a specific DNA region, called a primary ethylene responsive element, found in 5'-flanking regions of some ethylene responsive genes, including E4, and LE-ACO1 in tomato (Montgomery, 1993; Blume and Grierson, 1997), GST1 in carnation (Itzhaki *et al.*, 1994), and also ERF1 in *A. thaliana* (Solano *et al.*, 1998).

ERF1 is another transcription factor, shown to be induced by ethylene in *A. thaliana* but its expression is dependent upon the presence of functional EIN3 in the nucleus (which is the primary ethylene responsive gene). The ERF1 protein then binds to a secondary ethylene responsive element, the so called GCC box, in 5'-flanking regions of down stream of other genes such as PDF 1.2 (Penninckx *et al.*, 1996), basic-chitinase (Shinsh *et al.*, 1995), and hookless1 (Lehman *et al.*, 1996). These genes are ethylene responsive through the ethylene induction of EIN3 expression and EIN3 induction of ERF1.

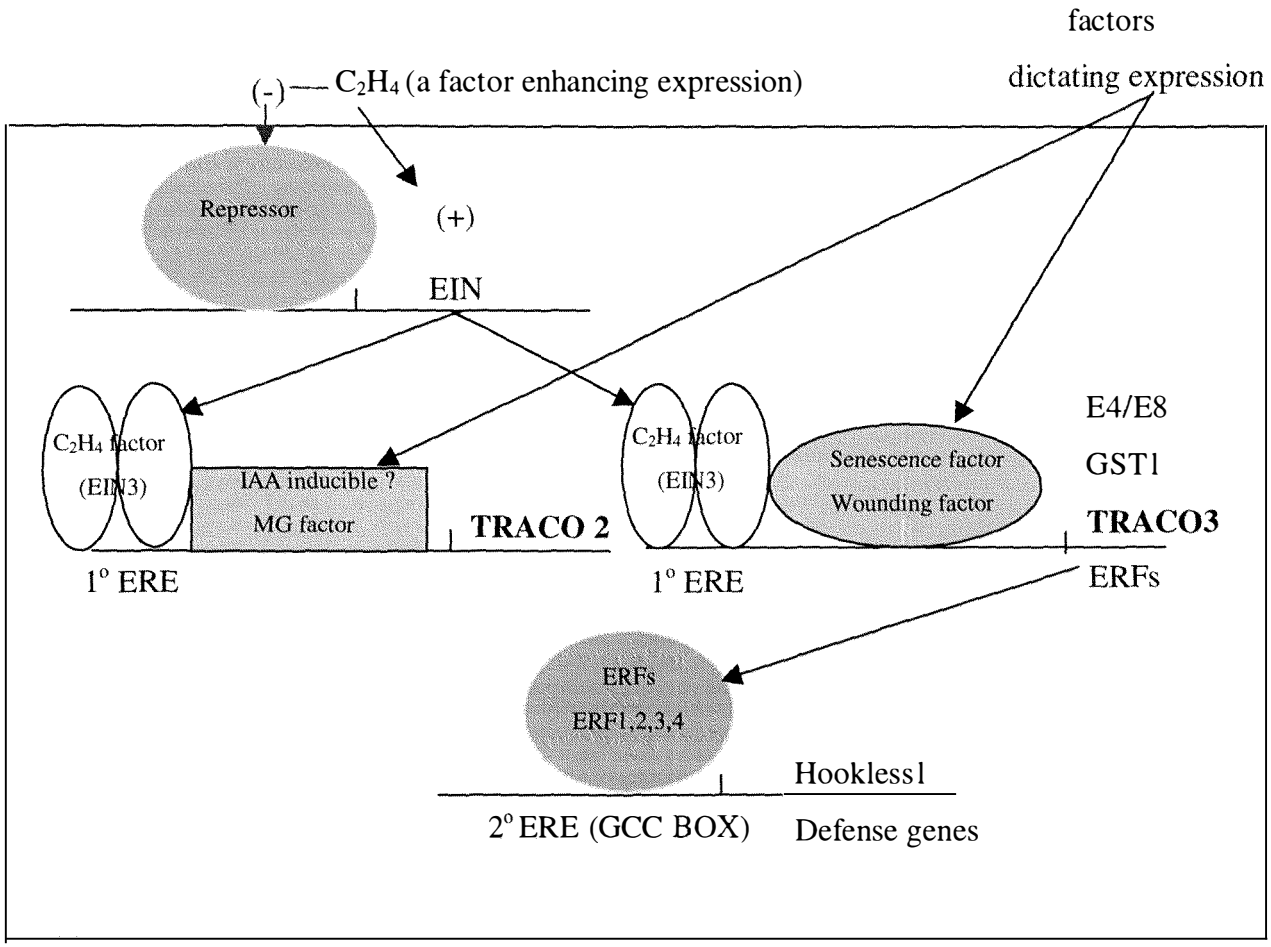

Figure 4.3 Hypothetical model of nuclear events in response to ethylene (modified from Solano *et al.*, 1998).

From the results in this thesis, it can be speculated that TRACO2 and TRACO3 genes may be induced by a factor (or factors) which are distinct from ethylene (Fig.4.3). This is supported from the study of ERF gene (a primary target gene) expression in wounded tobacco leaves. Wounding of the leaf blade induces the expression of ERF genes without ethylene, suggesting that the gene expression is independent of ethylene signal. However, by ethylene the

expression of ERF genes (at least ERF1 and ERF4) was further enhanced and resulted in the induction of basic-chitinase gene (a secondary target gene) in the tissue (Susuki *et al.*, 1998).

In mature leaf tissue of white clover, whatever ACO gene is expressed by unknown factor (e.g. TRACO2 in mature green tissue; TRACO3 under stress condition), ethylene probably promotes the gene expression of the ACO genes as primary target genes through the induction of functional EIN3 proteins. It can be speculated that the lack of TRACO3 gene expression by ethylene in mature green leaves may be a result of the absence of wounding or senescence-factors, which activate TRACO3 gene expression in this tissue.

Once expression of an ACO gene is activated, ethylene can enhance the expression through the mechanism that the ethylene-induced EIN3 proteins bind to the primary ERE of the ACO gene to co-operate the transcription. The demonstration of enhanced TRACO3 gene expression by ethylene in wounded leaves could support this model, but this was not examined in this thesis. This is also supported further by the notion that ethylene acts as a promoting factor of organ senescence or pathogen-infected symptoms, rather than an inducer of these physiological processes in plants (Grbic and Bleecker, 1996; Lund *et al.*, 1998).

This model, however, should not rule out other possible factors involved in regulating ethylene-responsive gene expression. For example, OBF (ocs element binding factor) proteins in *A. thaliana* interact directly with the GCC binding proteins to maximise PR gene expression in response to ethylene (Buttner and Singh, 1997). Also, nitrilase-like proteins have been reported as proteins which sequester GCC box-binding proteins in the cytosol of tobacco plants to control down-stream ethylene-responsive gene expression (Xu *et al.*, 1998). Many reports indicate that ethylene-responsive gene expression is much more complicated than outlined in the hypothetical model (Fig. 4.3).

The expression of TRACO2 and TRACO3 can be used as a useful system to define the tissue factors that probably dictate regulation of plant growth and development.

4.5 Summary and future studies

Ethylene production from developing leaf tissues, including the apex and newly initiated leaves of white clover has been investigated. To investigate the molecular basis of this ethylene production, genes encoding the ethylene biosynthetic enzymes, ACS and ACO, have been cloned. Reading frame sequences of three ACS genes have been identified using RT-PCR with degenerate primers and designated as TRACS1, TRACS2, and TRACS3. Gene expression studies using northern analysis revealed that the TACS3 gene is predominantly expressed in the early leaf developmental stages with maximum expression in leaf 2 (an actively expanding leaf). In contrast, TRACS1 gene transcripts are not detectable during early leaf development.

Three ACO genes, including reading-frame sequences and 3'-untranslated regions have been identified using a combination of RT-PCR and 3'-RACE. Gene expression studies using northern analysis showed that the TRACO1 and TRACO2 genes were expressed predominantly during early leaf development. Expression of the TRACO1 gene was predominantly in the developing apex, whereas TRACO2 gene was expressed mainly in newly initiated leaves and mature green leaves, with maximum TRACO2 gene expression in the newly initiated expanding leaves of white clover. TRACO3 gene expression was not in any developing tissue using the same hybridisation conditions and autoradiography developing time as used for TRACO1 and TRACO2. However, a longer exposure time revealed the hybridisation of the reading frame to two transcripts of 1.17 kb and 1.35 kb with expression higher in 1.17 kb. The occurrence of two transcripts could cause through differential polyadenylation and may represent a mechanism of controlling the expression of this gene during early leaf development of white clover.

The TRACO1 gene (the apex-related ACO gene) was also expressed in axillary buds, but TRACO2 gene expression (the mature leaf-related ACO gene) was detected in mature inter-node, node, and petiole tissue. Both TRACO1 and TRACO2 genes were highly expressed in roots of white clover.

Polyclonal antibodies were raised against TRACO1 and TRACO2 gene products in *E. coli* and designated as PAb1 and PAb2, respectively. ACO protein accumulation as a 36.4 kD was detected by PAb2 and ACO activity, *in vitro* corresponded to TRACO2 gene expression. PAb1

recognised a protein of 205 kD, the accumulation of which coincided with TRACO1 gene expression in an apex-specific manner.

Characterisation of the two ACO genes expressed in the leaf tissue has shown that ethylene induces TRACO2 gene expression, whereas wounding or wounding-induced tissue ageing induces TRACO3 gene expression in mature green leaves.

As a summary of differential expression of ACO genes during leaf development, it can be proposed that the high ethylene production at the apex is mediated by the TRACO1 gene product. This ethylene production may trigger TRACO2 gene expression in the expanding leaves and expression decreases as the leaf ages. In response to (as yet unidentified) age-related factors, TRACO3 gene expression is induced to produce the senescence-associated ethylene in leaves.

In terms of future studies, the expression of the TRACO1 gene has to be localized to determine which cells or tissues in the apex are expressing the gene. The use of *in situ* RT-PCR will be an option to localise specific TRACO gene expression.

The differential expression of TRACO2 and TRACO3 during leaf development also provides the opportunity to investigate the molecular mechanisms underlying gene expressions regulated by developmental signals. For example, cloning of the 5'-regulatory regions of these ACO genes should unravel specific or universal *cis*-elements controlling gene expression, according to developmental or tissue-specific signals. Further characterisation of the 5'-regulatory regions of the ACO genes should be a means of identifying some pivotal regulatory proteins specifically induced or associated with the *cis*-elements.

Bibliography

Abel S and Theologis A. 1996. Early genes and auxin action. Plant Physiology. 111: 9-17

Abel S, Nguyen MD, Chow W, and Theologis A. 1995. ACS4, a primary indoleacetic acid-responsive gene encoding 1-aminocyclopropane-1-carboxylate synthase in *Arabidopsis thaliana*. Journal of Biological Chemistry 270(32): 19093-19099

Abeles FB, Morgan PW and Saltveit ME. 1992. Ethylene in Plant Biology. Academic Press Inc., San Diego

Abeles FB. 1973. Ethylene in Plant Biology. Academic press Inc., San Diego

Abler ML and Green PJ. 1996. Control of mRNA stability in higher plants. Plant Molecular Biology 32: 63-78

Aharoni N, Liberman M, and Sisler H. 1979. Pattern of ethylene production in senescing leaves. Plant Physiology 64: 796-800

Alonso JM, Hirayama T, Roman G, Nourizadeh S and Ecker JR. 1999. EIN2, a bifuntional tranducer of ethylene and stress response in *Arabidopsis*. Science 284: 2148-2152

Arteca JM and Arteca RN. 1999. A multi-responsive gene encoding 1-aminocyclopropane-1-carboxylate synthase (ACS6) in mature *Arabidopsis* leaves. Plant Molecular Biology 39: 209-219

Barlow JN, Zhang Z, John P, Baldwin JE and Schofield CJ. 1997. Inactivation of 1-aminocyclopropane-1-carboxylic acid oxidase involves oxidative modifications. Biochemistry 36(12): 3563-3569

Barry CS, Blume A, Hamilton A, Fray R, Payton S, Alpuchie-Solis A and Grierson D. 1997. Regulation of ethylene synthesis and perception in tomato and its control using gene technology. In Kanelis AK, Chang C, Kende H and Grierson D, eds, Biology and Biotechnology of the Plant Hormone Ethylene. NATO ASI Series, Kluwer Academic Publishers, Dordrecht, The Netherlands, pp 299-306

Barry CS, Blume B, Bouzayen M, Cooper W, Hamilton AJ, and Grierson D. 1996. Differential expression of the 1-aminocyclopropane-1-carboxylate oxidase gene family of tomato. The Plant Journal 9(4): 525-535

Bennet M, Kieber JJ, Giraudat J and Morris P. 1998. Hormone regulated development. In Anderson M and Roberts J, eds, Arabidopsis. Sheffield Academic Press Ltd. England, pp 107-150

Bewley JD and Black M. 1994. Seeds: Physiology of development and germination, 2nd Ed. Plenum Press, New York, NY

Bleecker AB and Schaller GE. 1996. The mechanism of ethyleen perception. Plant Physiology 111: 653-660

Bleecker AB, Esch JJ, Hall AE, Rodriguez FI and Binder BM. 1998. The ethylene-receptor family from Arabidopsis: structure and function. Philosophical Transactions of Royal Society of London Biological Sciences 353(1374): 1405-1412

Bleecker AB, Estelle MA, Somerville C and Kende H. 1988a. Insensitive to ethylene conferred by a dominant mutation in *Arabidopsis thaliana*. Science 241: 1086-1089

Bleecker AB, Kenyon WH, Somerville SC and Kende H. 1986. Use of monoclonal antibodies in the purification and characterization of 1-aminocyclopropane-1-carboxylate synthase, an enzyme in ethylene biosynthesis. Proceedings of the National Academy of Sciences, USA 83: 7759-7759

Bleecker AB, Robinson G and Kende H. 1988b. Studies on the regulation of 1-aminocyclopropane-1-carboxylate synthase in tomato using monoclonal antibodies. Planta 173: 385-390

Bleecker AB. 1998. The evolutionary basis of leaf senescence: method to the madness? Current Opinion in Plant Biology 1: 73-78

Bleecker AB. 1999. Ethylene perception and signaling: an evolutionary perspective. Trends in Plant Sciences 4(7): 269-274

Blume B and Grierson D. 1997. Expression of ACC oxidase promoter-GUS fusion in tomato and *Nicotiana plumbaginifolia* regulated by developmental and environmental stimuli. The Plant Journal 12(4): 731-746

Blume B, Barry CS, Hamilton AJ, Bouzayen M and Grierson D. 1997. Identification of transposon-like elements in non-coding regions of tomato ACC oxidase genes. Molecular and General Genetics 254: 297-303

Boller T and Kende H. 1980. Regulation of wound ethylene. Nature 286: 259-260

Bombelli L, Doneda L, Tonelli C and Dolfini S. 1998. In situ reverse transcrption-PCR in plant tissues. Elsevier Trends Journals Technical Tips Online T/01229

Botella JR, Arteca JM, Schlagnhaufer CD, Arteca RN and Phillips AT. 1992b. Indentification and characterization of a full-length cDNA encoding for an auxin-induced 1-amino-cyclopropane-1-carboxylate synthase from etiolated mung bean hypocotyl segments and expression of its mRNA in response to indole-3-acetic acid. Plant Molecular Biology 20: 425-436

Botella JR, Schlagnhaufer CD, Arteca J, Arteca RN and Phillips AT. 1993. Identification of two new members of the 1-aminocyclopropane-1-carboxylate synthase-encoding multigene family in mung bean. Gene 123: 249-253

Botella JR, Schlagnhaufer CD, Arteca RN, and Phillips AT. 1992a. Identification and characterization of three putative genes for 1-aminocyclopropane-1-carboylate synthase from etiolated mung bean hypocotyl segments. Plant Molecular Biology 18: 793-797

Bouquin T, Lasserre E, Pradier J, Pech J-C and Balague C. 1997. Wound and ethylene induction of the ACC oxidase melon gene CM-ACO1 occurs via two direct and independent transduction pathways. Plant Molecular Biology 35: 1029-1035

Bowles D. 1998. Signal transduction in the wound response of tomato plants. Philosophical Transactions of Royal Society of London-Biological Sciences 353: 1495-1510

Bradstatter I and Kieber JJ. 1998. Two genes with similarity to bacterial response regulators are rapidly and specifically induced by cytokinin in Arabidopsis. The Plant Cell 10: 1009-1019

Branden C and Tooze J. 1991. Introduction to protein structure. Garland Pub. NY

Buchanan-Wollaston V. 1997. The molecular biology of leaf senescence. Journal of Experimental Botany 48: 181-199

Butcher SM, Fountain DW, and McManus MT. 1996. Leaf senescence and clonal growth of white clover. Agronomy Society of New Zealand Special Publication No. 11 Glassland Research and Practice series No. 6: 171-173

Butcher SM. 1997. Ethylene biosynthesis during leaf maturation and senescence in white clover. Ph.D. Thesis, Department of Plant Biology and Biotechnology, Massey University, Palmerston North, New Zealand

Buttner M and Singh KB. 1997. *Arabidopsis thaliana* ethylene-responsive element binding protein (AtEBP), an ethylene-inducible, GCC box DNA-binding protein interacts with an ocs element binding protein. Proceedings of National Academy of Sciences, USA 94: 5961-5966

Cardinale FC, Jennings JC and Anderson JC. 1995. Use of the ethylene action inhibitor 1-methylcyclopropene to study the role of ethylene in elicitor induced ethylene biosynthesis in tomato leaves. Plant Physiololy (Suppl.) 108: 140

Chang C and Meyerowitz EM. 1995. The ethylene hormone response in *Arabidopsis*: An eukaryotic two-component signaling system. Proceedings of National Academy of Sciences, USA 92: 4129-4133

Chang C and Shockey JA. 1999. The ethylene response pathway: Signal perception to gene regulation. Current Opinion in Plant Biology 2: 352-358

Chang C, Kwok SF, Bleecker AB, and Meyerowitz EM. 1993. *Arabidopsis* ethylene-response gene ETR1: Similarity of product to two-component regulators. Science 262:539-544

Chang C. 1996. The ethylene signal transduction pathway in *Arabidopsis*: An emerging paradigm? Trends in Biochemical Sciences. 20:129-133

Chao Q, Rothenberg M, Solano R, Roman G, Trezaghi W, and Ecker JR. 1997. Activation of the ethylene gas response pathway in Arabidopsis by the nuclear protein ETHYLENE-INSENSITIVE3 and related protein. The Cell 89: 1133-1144

Charng Y-Y, Chung M-C, Chou S-J, and Yang SF. 1998. Subcellular localization of ACC oxidase in apple fruit. The American Society of Plant Physiologists' meeting 98 Abstract No. 237

Chomczynski P. 1992. One-hour downward alkiline capillary transfer for blotting of DNA and RNA. Analytical Biochemistry 201: 134-139

Church GM and Gilbert W. 1984. Genomic sequencing. Proceedings of National Academy of Sciences, USA 81: 1991-1995

Clark KL, Larsen PB, Wang X and Chang C. 1998. Association of the arabidopsis CTR1 raf-like kinase with the ETR1 and ERS ethylene receptors. Proceedings of National Academy of Sciences 95: 5401- 5406

De Rocher EJ, Vargo-Gogola TC, Diehn SH and Green PJ. 1998. Direct evidence for rapid degradation of *Bacillus thuringiensis* toxin mRNA as a cause of poor expression in plants. Plant Physiology 117: 1445-1461

Destefano-Beltran LJC, Van Caeneghem W, Gielen J, Richard L, Van Montagu M and Ven Der Straeten D. 1995. Characterization of three members of the ACC synthase gene family in *Solanum tuberosum* L. Molecular General Genetics 246: 496-508

Diehn SH, Chiu, W-L, De Rocher EJ and Green PJ. 1998. Premature polyadenylation at multiple sites within a *Bacillus thuringiensis* toxin gene-coding region. Plant Physiology 117: 1433-1443

Dolan L. 1997. The role of ethylene in the development of plant form. Journal of Experimental Botany 48: 201-210

Dong JG, Fernandez-Maculet JC and Yang SF. 1992. Purification and charaterisation of 1-aminocyclopropane-1-carboxylate oxidase from apple fruit. Proceedings of National Academy of Sciences, USA 89: 9789-9793

Dong JG, Yip WK, and Yang SF. 1991. Monoclonal antibodies against apple 1-aminocyclopropane-1-carboxylate synthase. Plant and Cell Physiology. 32(1): 25-31

Drew MC. 1997. Oxygen deficiency and root metabolism: Injury and acclimation under hypoxia and anoxia. Annual Review of Plant Physiology and Plant Molecular Biology 48: 223-250

Dupille E and Zacarias L. 1996. Extraction and biochemical characterization of wound-induced ACC oxidase from citrus peel. Plant Science 114: 53-60

Dupille E, Rombaldi C, Leilievre J-M, Cleyet-Marel J-C, Pech J-C and Latche A. 1993. Purification, properties and partial amino-acid sequence of 1-aminocyclopropane-1-carboxylic acid oxidase from apple fruits. Planta 190: 65-70

Ecker JR. 1995. The ethylene signal transduction pathway in plants. Science 268: 667-675

Edelman L and Kende H. 1990. A comparison of 1-aminocyclopropane-1-carboxylate synthase *in vitro* translation product and *in vivo*-labeled proteins in ripening tomatoes. Planta 182: 635-638

Evens PT and Malmberg RL. 1989. Do polyamines have roles in plant development? Annual Review of Plant Physiology and Plant Molecular Biology 40: 235-269

Fernandez-Maculet JC and Yang SF. 1992. Extraction and partial characterisation of the ethylene-forming enzyme from apple fruit. Plant Physiology 99: 751-754

Finlayson SA, Reid DM and Morgan PW. 1997. Root and leaf specific ACC oxidase activity in corn and sunflower seedlings. Phytochemistry 45: 869-877

Fluhr R and Mattoo AK. 1996. Ethylene-biosynthesis and perception. Critical Reviews in Plant Sciences 15: 479-523

Fluhr R. 1998. Ethylene perception: from two-component signal transducers to gene induction. Trends in Plant Sciences 3: 141-146

Gamble RL, Coonfield ML, and Schaller GE. 1998. Histidine kinase activity of the ETR1 ethylene receptor from *Arabidopsis.* Proceedings of National Academy of Sciences, USA 95(13): 7825-78229

Gibbs RA. 1999. The weed paves the way. Nature Genetics 22: 219-220

Gomez-Lim MA, Valdes-Lopez V, Cruz-Hernandez A and Saucedo-Arias LJ. 1993. Isolation and characterization of a gene involved in ethylene biosynthesis from *Arabidopsis thaliana*. Gene 134: 217-221

Gong D. 1999. Characterisation of 1-aminocyclopropane-1-carboxylate (ACC) oxidase isoforms during leaf maturation and senescence in white clover (*Trifolium repens*, L). Ph.D. Thesis, Institute of Molecular BioSciences, Massey University, Palmerston North, New Zealand

Grbic V and Bleecker AB. 1995. Ethyleen regulates the timing of leaf senescence in *Arabidopsis*. The Plant Journal 8: 595-602

Greer DH, Laing WA and Campbell BD. 1995. Photosynthetic responses of thirteen pasture species to elevated CO2 and Temperature. Australian Journal of Plant Physiology 22: 713-722

Guis M, Bouquin T, Zegzouti H, Ayub R, Ben Amor M, Lasserre E, Botondi R, Raynal J, Latche A, Bouzayen M, Balague C and Pech JC. 1997. Differential expression of ACC oxidase genes in melon and physiological characterization of fruit expressing an antisense ACC oxidase gene. In Kanelis AK, Chang C, Kende H and Grierson D, eds, Biology and Biotechnology of the Plant Hormone Ethylene. NATO ASI Series, Kluwer Academic Publishers, Dordrecht, The Netherlands, pp. 327-337

Guzman P and Ecker JR. 1990. Exploiting the triple response of arabidopsis to identify ethylene related mutants. The Plant Cell 2: 513-523

Hall DO. 1993 Photosynthesis and production in a changing environment: a filed and laboratory manual. Chapman & Hall. London

Hamilton AJ, Bouzayen M, and Grierson D. 1991. Identification of a tomato gene for the ethylene-forming enzyme by expression in yeast. Proceedings of National Academy of Sciences, USA 88: 7434-7437

Hamilton AJ, Lycett GW and Grierson D. 1990. Antisense gene that inhibits synthesis of the ethylene in trangenic plants. Nature 346: 284-287

Harpham N, Bery A, Knee E, Rovedahoyos G, Raskin I, Sanders I, Smith A, Wood C and Hall M. 1991. The effect of ethylene on the growth and development of wild-type and mutants *Arabidopsis thaliana* (L.) Heynh. Annals of Botany 68: 55-61

Hensel LL, Grbic V, Baumgarten DA and Bleecker AB. 1993. Developmental and age-related processes that influence the longitivity and senescence of photosynthetic tissues in *Arabidopsis*. The Plant Cell 5 : 553-564

Henkens JAM, Rouwendal A, ten Have A and Woltering EJ. 1994. Molecular cloning of two different ACC synthase PCR fragments in carnation flowers and organ-specific expression of the corresponding genes. Plant Molecular Biology 26: 453-458

Herschman HR. 1991. Primary response genes induced by growth factors and tumer promoters. Annual Review of Biochemistry 60: 281-319

Hill CS and Treisman R. 1995. Transcriptional regulation by extracellular signals: Mechanisms and specificity. The Cell 80:199-211

Hirayama T, Kieber JJ, Hirayama N, Kogan M, Guzman P, Nourideh S, Alonso JM, Dailey WP, Dancis A and Ecker JR. 1999. RESPONSE-TO-ANTAGONIST1, a Menkes/Wilson disease-related copper transporter, is required for ethylene signaling in *Arabidopsis*. The Cell 97: 383-393

Hoffman T, Schmidt JS, Zheng X and Bent AF. 1999. Isolation of ethylene insensitive soybean mutants that are altered in pathogen susceptibility and gene-for gene disease resistance. Plant Physiology 119(3): 935-950

Hohenester E, White MF, Kirsch JF and Jansonius JN. 1994. Crystallization and preliminary X-ray analysis of recombinant 1-aminocyclopropane-1-carboxylate synthase from apple. Journal of Molecular Biology 243: 947-949

Hua J and Myerowitz EM. 1998. Ethylene responses are negatively regulated by a receptor gene family in *Arabidopsis thaliana.* The Cell 94(2): 261-271

Hua J, Chang C, Sun Q and Meyerowitz EM. 1995. Ethylene insensitivity conferred by Arabidopsis ERS gene. Science 269: 1712-1714

Hua J, Sakai H, Nourizadeh S, Chen QG, Bleecker AB, Ecker JR and Myerowitz EM. 1998. EIN4 and ERS2 are members of the ethylene putative receptor gene family in Arabidopsis. The Plant Cell 10: 1321-1332

Huang P-L, Parks JE, Rottmann WH and Theologis A. 1991. Two genes encoding 1-aminocyclopropane-1-carboxylate synthase in zucchini (*Cucurbita pepo*) are clustered and similar but differentially regulated. Proceedings of National Academy of Sciences, USA 88: 7021-7025

Hunter DA, Yoo SD, Butcher S and McManus MT. 1999. Expression of ACC oxidase during leaf ontogeny in white clover. Plant Physiology 120: 131-141

Hunter DA. 1998. Characterisation of ACC oxidase during leaf maturation and senescence in white clover (*Trifolium repens* L). Ph.D. Thesis, Institute of Molecular BioSciences, Massey University, Palmerston North, New Zealand

Huxtable S, Zhou H, Wong S, and Li N. 1998. Renaturation of 1-aminocyclopropane-1-carboxylate synthase expressed in *Escherichia coli* in the form of inclusion bodies into a dimeric and catalytically active enzyme. Protein Expression and Purification 12(3): 305-314

Hyodo H, Hashimoto C, Mrozumi S, Hu W and Tanaka K. 1993. Characterization and induction of the activity of 1-aminocyclopropane-1-carboxylate oxidase in the wounded mesocarp tissue of *Cucurbita maxima*. Plant and Cell Physiology 34(5): 667-671

Ievinsh G and Kreicbergs. 1992. Endogenous rhythmicity of ethylene production in growing intact cereal seedlings. Plant Physiology 100: 1389-1391

Imaseki H. 1999. Control of ethylene synthesis and metabolism. In Hooykass PJJ, Hall MA and Linnenga KR, eds, Biochemistry and Molecular Biology of Plant Hormone. Elsevier Science. B.V. , pp 209-245

Inskeep WP and Bloom PR. 1985. Extinction coefficients of chlorophyll a and b in N,N-dimethylformamide and 80 % acetone. Plant Physiology 77: 483-485

Itzhaki H, Maxson JM and Woodson W. 1994. An ethylene-responsive enhancer element is involved in the senescence-related expression of the carnation glutathione-S-transferase (GST1) gene. Proceedings of National Academy of Sciences, USA 91: 8925-8929

Jackson D. 1991. In situ hybridisation in plants. In Molecular Plant Pathology: A Practical Approach. (Eds, Bowles DJ, Gurr SJ, and McPherson M). pp 163-174. Oxford University Press

Jackson MB. 1985. Ethylene and responses of plants to soil waterlogging and submergence. Annual Review of Plant Physiology 36: 145-175

Jin E, Lee J-H, Park J-A and Kim WT. 1999. Temporal and spatial regulation of the expression of 1-aminocyclopropane-1-carboxylate oxidase by ethylene in mung bean (*Vigna radiata*). Physiologia Plantarum 105: 132-140

John I, Grake R, Farrell A, Cooper W, Lee P, Horton P and Grierson D. 1995. Delayed leaf senescence in ethylene deficient ACC oxidase antisense tomamto plants : Molecular and Physiological analysis. The Plant Journal. 7: 483-490

John P. 1997. Ethylene biosynthesis: The role of 1-aminocyclopropane-1-carboxylic acid (ACC) oxidase, and its possible evolutionary origin. Physiologia Plantarum 100(3): 583-592

Johnson PR and Ecker JR. 1998. The ethylene gas signal transduction pathway: a molecular perspective. Annual Review of Genetics 32: 227-254

Jung T, Cho MH and Kim WT. 1999. Induction of 1-aminocyclopropane-1-carboxylate oxidase mRNA by ethylene in mung bean roots: Possible involvement of phophoinositide and Ca^{2+} in ethylene signaling. The American Society of Plant Physiologists Annual Meeting Abstract No. 709

Kadyrzhanova DK, McCully TJ, Jaworski SA, Ververdis P, Vlachonasios KE, Murakami KG and Dilley DR. 1997. Structure-function analysis of ACC oxidase by site directed mutagenesis. In Kanelis AK, Chang C, Kende H and Grierson D, eds, Biology and Biotechnology of the Plant Hormone Ethylene. NATO ASI Series, Kluwer Academic Publishers, Dordrecht, The Netherlands, pp. 5-13

Kende H, Van Der Knaap E and Cho H-T. 1998. Deep water rice: A model plant to study stem elongation. Plant Physiology 118: 1105-1110

Kende H. 1983. Some concepts concerning the mode of action of plant hormones. In Meudt WJ, ed, Strategies of plant reproduction, Beltsville Agricultural Research Center Symposium No. 6. Allanheld, Osmun, NJ, pp 147-156

Kende H. 1993. Ethylene biosynthesis. Annual Review of Plant Physiology and Plant Molecular Biology 44: 283-307

Kepczynski J and Kepczynska E. 1997. Ethylene in seed dormancy and germination. Physiologia Plantarum 101: 720-726

Ketring DL. 1977. Ethylene and seed germination. In Khan AA, ed, Physiology and Biochemistry of Seed Dormancy and Germination. North holland Publishing Co., Amsterdam, pp 157-178

Kieber JJ and Ecker JR. 1993. Ethylene gas: it's not just for ripening any more. Trends in Gentics 9(10): 356-362

Kieber JJ, Rothenberg M, Roman G, Feldmann K and Ecker JR. 1993. CTR1, a negative regulator of the ethylene response pathway in Arabidopsis, encodes a member of the Raf family of protein kinases. The Cell 72:427-441

Kieber JJ. 1997a. The ethylene response pathway in arabidopsis. Annual Review of Plant Physiology and Plant Molecular Biology 48: 277-296

Kieber JJ. 1997b. The ethyleen signal transduction pathway in Arabidopsis. Journal of Experimental Botany 48(307): 211-218

Kim JH, Kim WT, Kang BG, and Yang SF. 1997a. Induction of 1-aminocyclopropane-1-carboxylate oxidase mRNA by ethylene in mung bean hypocotyls: involvement of both protein phosphorylation and dephosphorylation in ethylene signaling. The Plant Journal 11(3): 399-405

Kim WT and Yang SF. 1992. Turnover of 1-aminocyclopropane-1-carboxylic acid synthase protein in wounded tomato fruit tissue. Plant Physiology 100: 1126-1131

Kim WT and Yang SF. 1994. Structure and expression of cDNAs encoding 1-aminocyclopropane-1-carboxylate oxidase homologs isolated from excised mung bean hypocotyl. Planta 194: 223-229

Kim WT, Campbell A, Moriguchi T, Yi HC and Yang SF. 1997b. Auxin induced three genes encoding 1-aminocyclopropane-1-carboxylate synthase in mung bean hypocotyls. Journal of Plant Physiology 150: 77-84

Kim WT, Silverstone A, Yip WK, Dong JG and Yang FS. 1992. Induction of 1-aminocyclopropane-1-carboxylate synthase mRNA by auxin in mung bean hypocotyls and cultured apple shoots. Plant Physiology 98: 465-471

Kim YS, Choi D, Lee MM, Lee SH and Kim WT. 1998. Biotic and abiotic stress-related expression of 1-aminoacyclopropane-1-carbyxylate oxidase gene family in *Nicotiana glutinosa* L. Plant and Cell Physiology 39(6): 565-573

Knoester M, Van Loon LC, Van Den Heuvel J, Henning J, Bol JF and Linthorst HJM. 1998. Ethylene-insensitive tobacco lacks nonhost resistance against soil-born fungi. Proceedings of National Academy of Sciences, USA 95: 1933-1937

Kooter JM, Matzke MA and Meyer P. 1999. Listening to the silencing genes: transgene silencing, gene regulation and pathogen control. Trends in Plant Science 4(9): 340-347

Kuai J and Dilley DR.1992. Extraction, partial purification and characterization of 1-aminocyclopropane-1-carboxylic acid oxidase from apple fruit. Postharvest Biology and Technology 1(3): 203-211

Kwak S-H and Lee SH. 1997. The requirements for Ca^{2+}, protein phosphorylation and dephosphorylation for ethylene signal transduction in *Pisum sativum* L. Plant and Cell Physiology 38(10): 1142-1149

Laing WA, Greer DH, and Schnell TA. 1995. Photoinhibition of photosynthesis causes a reduction in vegetative growth rates of dwarf bean (*Phaseolus vulgaris*) plants. Australian Journal of Plant Physiology 22: 511-520

Lammli UK. 1970. Cleavage of structural proteins during the assembly of the bacteriophage T4. Nature 227: 680-685

Lassere E, Bouquin T, Hernandez JA, Bull J, Pech J-C and Balague C. 1996. Structure and expression of three genes encoding ACC oxidase homologs from melon (*Cucumis melo* L.). Molecular and General Genetics 251: 81-90

Lasserre E, Godard F, Bouquin T, Hernadez JA, Pech J-C, Roby D and Balague C. 1997. Differential activation of two ACC oxidase gene promoters from melon during plant development and in response to pathogen attack. Molecular and General Genetics 256: 211-222

Lavee S and Martin GC. 1981. Ethylene evolution from various developing organs of olive (*Olea euopaea*) after excision. Physiologia plantarum 51: 33-38

Lay VJ, Prescott AG, Thomas PG and John P. 1996. Heterologous expression and site-directed mutagenesis of the 1-aminocyclopropane-1-carboxylic acid oxidase from kiwi fruit. European Journal of Biochemistry 242(2): 228-234

Lee SH and Reid DM. 1997. The role of endogenous ethylene in the expansion of *Helianthus annuus* leaves. Canadian Journal of Botany 74: 501-508

Lehman A, Black R and Ecker JR. 1996. HOOKLESS1, an ethylene response gene is required for differential cell elongation in the Arabidopsis hypocotyl. The Cell 85 : 185-194

Lelievre J-M, Latche A, Jones B, Bouzayen M and Pech J-C. 1997. Ethylene and fruit ripening. Physiologia Plantarum 101: 727-739

Li N and Mattoo AK. 1994. Deletion of the carboxyl-terminal region of 1-amiocyclopropane-1-carboxylic acid synthase, a key protein in the biosynthesis of ethylene, results in catalytically hyperactive, monomeric enzyme. Journal of Biological Chemistry 269: 6908-6917

Li N, Huxtable S, Yang SF and Kung SD. 1996. Effect of N-terminal deletions on 1-aminocyclopropane-1-carboxylate synthase activity. FEBS 378: 286-290

Li N, Wiesman Z, Liu D and Mattoo AK. 1992. A functional tomato ACC synthase expressed in *Escherichia coli* demonstrates suicidal inactivation by its substrate S-adenosyl-methionine. Federation of European Biochemical Society 306: 103-107

Li Y, Feng L and Kirsch JF. 1997. Kinetic and spectroscopic investigations of wild-type and mutant forms of apple 1-aminocyclopropane-1-carboxylate synthase. Biochemistry 36(49): 15477-15488

Liang X, Abel S, Keller J, Shen N and Theologis A. 1992. The 1-aminocyclopropane-1-carboxylate synthase gene family of *Arabidopsis thaliana*. Proceedings of National Academy of Sciences, USA 89: 11046-11050

Liang X, Oono Y, Shen NF, Kohler C, Li K, Scolnik PA, and Theologis A. 1995. Chracterisation of two members (*ACS1* and *ACS3*) of the 1-aminocyclopropane-1-carboxylate synthase gene family of *Arabidopsis thaliana*. Gene 167: 17-24

Lincoln JE, Campbell AD, Oetiker J, Rottmann WH, Oeller PW, Shen NF and Theologis A. 1993. *LE-ACS4*, a fruit ripening- and wounding-induced 1-aminocyclopropane-1-carboxylate synthase gene of tomato (*Lycopersicon esculentum*). Journal of Biological Chemistry 268(26): 19422-19430

Liu J and Reid DM. 1992. Adventitious rooting in hypocotyls pf sunflower (*Helianthus annuus*) seedlings. IV. The role of changes in endogenous free and conjugated indole-3-acetic acid. Physiolgia Plantarum 86: 285-292

Liu J, Mukherjee I and Reid DM. 1990. Adventitious rooting in hypocotyls of sunflower (*Helianthus annuus*) seedlings. III. The role of ethylene. Physiologia. Plantarum 78: 268-276

Liu J-H, Lee-Tanmon SH and Reid DM. 1997. Differential and wound-inducible expression of 1-aminocyclopropane-1-carboxylate oxidase genes in sunflower seedlings. Plant Molecular Biology 34: 923-933

Lund ST, Stall RE and Klee HJ. 1998. Ethylene regulates the susceptible responses to pathogen infection in tomato. The Plant Cell 10: 371-382

Mabberley DJ. 1993. The Plant Book. Cambridge University Press, Cambridge

Manning, K. 1998. Detoxification of cyanide by plants and hormone action. Ciba Foundation Symposium 140 :92-110

Martin MN and Saftner RA. 1995. Purification and characterization of 1-aminocyclopropane-1-carboxylic acid N-malonyltransferase from tomato fruit. Plant Physiology 108: 1241-1249

Martin MN, Cohen JD and Saftner RA. 1995. A new 1- aminocyclopropane-1-carboxylic acid-conjugating activity in tomato fruit. Plant Physiology 109: 917-926

Mattoo AK and Suttle JC. 1991. The plant hormone Ethylene. CRC Press, Boca Raton, FL

Mattoo AK and White WB. 1991. Regulation of ethylene biosynthesis. In Mattoo AK and Suttle JC, eds, The plant hormone ethylene. CRC Press, Boca Raton, FL. pp 21-42.

McGarvey J and Christoffersen RE. 1992. Characterization and kinetic parameters of ethylene-forming enzyme from avocado fruit. Journal of Biological Chemistry 267: 5964-5967

McGrath R and Ecker JR. 1998. Ethylene signaling in Arabidopsis: Events from the membrane to the nucleus. Plant Phsiology and Biochemistry 36(1-2): 103-113

Mckeon TA, Fernandez-Maculet JC and Yang SF. 1995. Biology and Metabolism of Ethylene. In Davies PJ, 2nd ed, Plant Hormones : Physiology, Biochemistry and Molecular biology. Kluwer Academic Publishers, Dordrecht, The Nethelands, pp 118-139

McManus MT and Osbone DJ. 1990a. Identification of polypeptides specific to rachis abscission zone cells of *Sambucus nigra*. Physiol. Plant. 79: 471-478

McManus MT and Osbone DJ. 1990b. Evidence for the preferential expression of particular polypeptides in leaf abscission zones of the bean *Phaseolus vulgaris* L. J. Plant Physiol. 136: 391-397

Mehta A, Jordan R L, Anderson JD and Mattoo AK. 1988. Identification of a unique isoform of 1-aminocyclopropane-1-carboxylic acid synthase by monoclonal antibody. Proceedings of National Academy of Sciences, USA 85: 8810-8814

Meike DW, Cherry JM, Dean C, Rounsley SD and Koorneef M. 1998. *Arabidopsis thaliana*: a model plant for genome analysis. Science 282: 662-682

Mekhedov SL and Kende H. 1996. Submergence enhances expression of a gene encoding 1-aminocyclopropane-1-carboxylic acid oxidase in deep water rice. Plant and Cell Physiology 37(4): 531-537

Memelink J, Swords KM and Stahelin LA. 1994. Southern, northern and western blot analysis. 1994. In Gelvin SB and Schilperoot RA, 2 nd eds., Plant Molecular Biology Manual, p F-10, Kluwer Academic, London, UK

Meyerowitz EM. 1989. Arabidopsis, a useful weed. The Cell 56: 263-269

Michael SD, John MC and Amasino RM. 1994. Removal of polysaccharide from plant DNA by ethanol precipitation. BioTechniques 17(2): 274-276

Montgomery J, Pollard V, Deikman J and Fischer RL. 1993. Positive and negative regulatory regions control the spatial distribution of polygalacturonase transcription in tomato fruit pericarp. The Plant Cell 5: 1049-1062

Moran R and Porath D. 1980. Chlorophyll determination in intact tissues using N,N-dimethylformamide. Plant Physiology 65: 478-479

Morgan PW and Drew MC. 1997. Ethylene and plant response to stress. Physiologia Plantarum 100: 620-630

Moya-Leon M and John P. 1995. Purification and biochemical characterisation of 1-aminocyclopropane-1-carboxylate oxidase from banana fruit. Phytochemistry 39: 15-20

Nadeau JA., Zhang XS, Nair H and O'Neil S. 1993. Temporal and spatial regulation of 1-aminocyclopropane-1-carboxylate oxidase in the pollination-induced senescence of orchid flowers. Plant Physiology 103:31-39

Nakagawa N, Mori H, Yamazaki K and Imaseki H. 1991. Cloning of a complementary DNA for auxin-induced 1-aminocyclopropane-1-carboxylate synthase and differential expression of the gene by auxin and wounding. Plant and Cell Physiology 32(8): 1153-1163

Nakajima N, Mori H, Yamazaki K, and Imaseki H. 1990. Molecular cloning and sequence of a complementary DNA encoding 1-aminocyclopropane-1-carboxylate synthase induced by tissue wounding. Plant and Cell Physiology 31: 1021-1029

Nakajima, N., Nakagawa, N. and Imaseki, H. 1988. Molecular size of wound-induced 1-aminocyclopropane-1-carboxylate synthase from *Cucurbita maxima* Duch. and change of translatable mRNA of the enzyme after wounding. Plant and Cell Physiology 29(6): 989-998

Nakatsuka, A., Hironori, S.M., Shiomi, S., Nakano, R., Kubo, Y., and Inaba, A. 1998. Differential expression and internal feedback regulation of 1-aminocyclopropane-1-caroxylate synthase, 1-aminocyclopropane-1-carboxylate oxidase and ethylene receptor genes in tomato fruit during development and ripening. Plant Physiology 118: 1295-1305

Nam HG. 1997. The molecular genetic analysis of leaf senescence. Current Opinion in Biotechnology 8: 200-207

Nothnagel EA, McNeil M, Albershein P and Dell A. 1983. Host-pathogen interactions XXII. A galaturonic acid oligosaccharide from plant cell walls elicitors phytoalexins. Plant Physiology 71: 9916-926

O'Donnell PJ, Calvert C, Atzorn R, Wasternack C, Leyser HMO and Bowles DJ. 1996. Ethylene as a signal mediating the wound response of tomato plants. Science 274: 1914-1917

Oetiker JH, Olson DC, Shiu OY and Yang SF. 1997. Differential induction of seven 1-aminocyclopropane-1-carboxylate synthase genes by elicitor in suspension cultures of tomato (*Lycopersicon esculentum*). Plant Molecular Biology 34(2): 275-286

Oh SA, Lee SY, Chung IK, Lee C and Nam HG. 1996. A senescence-associated gene of *Arabidopsis thaliana* is distinctively regulated during natural ad artificially induced leaf senescence. Plant Molecular Biology 30: 739-754

Ohtsubo N, Mitsuhara I, Koga M, Seo S, Ohashi Y. 1999. Ethylene promotes the necrotic lesion formation and basic PR gene expression in TMV-infected tobacco. Plant and Cell Physiology 40 (8): 808-817

Olson DC, Oetiker JH and Yang SF. 1995. Analysis of LE-ACS3, a 1-aminocyclopropane-1-carboxylic acid synthase gene expression during flooding in the roots of tomato plants. Journal of Biological Chemistry 270: 14056-14061

Olson DC, White JA, Edelman L, Harkins RN and Kende H. 1991. Differential expression of two genes for 1-aminocyclopropane-1-carboxylate synthase in tomato fruits. Proceedings of National Academy of Sciences, USA 88: 5340-5344

O'Neil SD, Nadeau JA, Zhang XS, Bui AQ and Halevy AH. 1993. Interorgan regulation of ethylene biosynthetic genes by pollination. The Plant Cell 5: 419-432

O'Neil SD. 1997. Pollination regulation of flower development. Annual Review of Plant Physiology and Plant Molecular Biology 48: 547-574

Osborne DJ. 1991. Ethylene in plant ontogeny and abscission In Mattoo AK and Suttle JC, eds, The plant hormone ethylene. CRC Press. Boca Raton. FL CRC press, pp. 193-214

Park KY, Drory A and Woodson WR. 1992. Molecular cloning of a 1-aminocyclopropane-1-carboxylate synthase from senescing carnation flower petals. Plant Molecular Biology 18: 377-386

Peck SC and Kende H. 1995. Sequential induction of the ethylene biosynthetic enzymes by indole-3-acetic acid in etiolated peas. Plant Molecular Biology 28: 293-301

Peck SC and Kende H. 1998. Differential regulation of genes encoding 1-aminocyclopropane-1-carboxylate (ACC) synthase in etiolated pea seedlings: effects of indole-3-actic acid, wounding, and ethylene. Plant Molecular Biology 38(6): 977-982

Peck SC, Olson D and Kende H. 1993. A cDNA sequence encoding 1-aminocyclopropane-1-carboxylate oxidase from pea. Plant Physiology 101: 689-690

Peck SC, Pawlowski, K and Kende H. 1998. Asynmetric responsiveness to ethylene mediates cell elongation in the apical hook of peas. The Plant Cell 10: 713-720

Peiser G and Yang SF. 1998. Evidence for 1-(Malonylamino)-cyclopropane-1-carboxylic acid being the major conjugate of aminocyclopropane-1-caboxylic acid in tomato fruit. Plant Physiology 116: 1527-1532

Penmetsa RV and Cook DR. 1997. A legume ethylene insensitive mutant hyper infected by its rhizobial symbiont. Science 275: 527-530

Penninckx I, Eggmont K, Terras F, Thomma B, Desamblanx G, Buchala A, Metraux J, Manners J and Broekaert W. 1996. Phathogen-induced systemic activation of plant defensin gene in *Arabidopsis* follows a salicylic acid independent pathway. The Plant Cell 8: 2309-2323

Pirrung MC, Kaiser LM and Chen J. 1993. Purification and properties of the apple ethylene-forming-enzyme. Biochemistry 32: 7445-7450

Pogson BJ, Downs C and Davies KM. 1995. Differential expression of two 1-aminocyclo-propane-1-carboxylic acid oxidase genes in Broccoli after harvest. Plant Physiology 108: 651-657

Porat R, Halevy A, Serek M and Borochov A. 1995a. An increase in ethylene sensitivity following pollination is the intial event triggering an increase in ethylene production and enhanced senescnece of Phalaenopsis orchid flowers. Physiologia Plantarum 93: 778-784

Porat R, Shlomo E, Serek M, Sisler EC and Borochov A. 1995b. 1-methylcyclopropene inhibits ethylene action in cut phlox flowers. Postharvest Biology and Technology 6: 313-319

Raggi V. 1995. CO2 assimilation, respiration and chlorophyll fluorescence in peach leaves infected by *Taphrina deformans*. Physiologia Plantarum 93: 540-544

Ramassamy S, Olmos E, Bouzayen M, Pech J-C and Latche A. 1998. 1-aminocyclopropane-1-carboxylic acid oxidase of apple fruit is periplasmic. Journal of Experimental Botany 49(329): 1909-1915

Raz V and Fluhr R. 1992. Calcium requirement for ethylene-dependent responses. The Plant Cell 4: 1123-1130

Raz V and Fluhr R. 1993. Ethylene signal is transduced via protein phosphorylation events in plants. The Plant Cell 5: 523-530

Reid MS. 1995. Ethylene in plant growth, development and senescence. In Davies PJ, 2nd ed, Plant Hormones : Physiology, Biochemistry and Molecular biology. Kluwer Academic Publishers, Dordrecht, The Nethelands, pp 486-508

Reinhardt, D., Kende, H. and Boller, T. 1994. Subcellular localisation of 1-aminocyclo-propane-1-carboxylate oxidase in tomato cells. Planta 195: 142-146

Reuber S, Bornman JF and Weissenbock G. 1996. A flavonoid mutant of barley (Hordeum vulgare L.) exhibits increased sensitivity to UV-B radiation in the primary leaf. Plant, Cell and Environment 19: 593-601

Robert JA and Osborne DJ. 1981. Auxin and the control of ethylene production during the development and senescence of leaves and fruits. Journal of Experimental Botany 32(130): 875-887

Rodrigues-Pousada RA, De Rycke R, Dedonder A, Van Caneghem W, Engler G, Van Montague M and Van Der Straeten D. 1993. The *Arabidopsis* 1-aminocyclopropane-1-carboxylate synthase gene 1 is expressed during early development. The Plant Cell 5: 897-911

Rodrigues-Pousada RA, Van Caeneghem W, De Rycke R, Van Montagu M and Van Der Straeten D. 1996. Ethylene in the early development of *Arbidopsis*; developmental and hormonal controls of an ACC synthase gene. Journal of Experimental Botany (Lancaster meeting, Abstract Number P7.12)

Rodriguez FI, Esch JJ, Hall AE, Binder BM, Schaller GE and Bleecker AB. 1999. A copper cofactor for the ethylene receptor ETR1 from *Arabidopsis*. Science 283: 996-998

Roman G, Lubarsky B, Kieber JJ, Rothenberg M and Ecker JR. 1995. Genetic analysis of ethylene signal transduction in *Arabidopsis thaliana*, five novel mutant integrated into a stress response pathway. Gene 139: 1393-1409

Rombaldi C, Lelievre JM, Latche A, Petitprez M, Bouzayen M and Pech JC. 1994. Immunocytolocalization of 1-aminocyclopropane-1-carboxylic acid oxidase in tomato and apple fruits. Planta 192(4): 453-460

Rottmann WH, Peter GF, Oeller PW, Keller JA, Shen NF, Nagy BP, Taylor LP, Campbell AD and Theologis A. 1991. 1-aminocyclopropane-1-carboxylate synthase in tomato is encoded by a multigene family whose transcription is induced during fruit and florar senescence. Journal of Molecular Biology 222: 937-961

Ryan CA. 1987. Oligosaccharide signalling in plants. Annual Review of Cell Biology 3: 295-317

Sakai H, Hua J, Chen QG, Chang C, Medrano L, Bleecker AB and Myerowitz EM. 1998. ETR2 is an ETR1-like gene involved in ethylene signaling in Arabidopsis. Proceedings of National Academy of Sciences, USA 95: 5812-5817

Saltveit ME and Dilley DR. 1978. Rapidly induced wound ethylene from excised segments of etiolated Pisum Sativum cv.. Alaska I Characterization of the responses. Plant Physiology 61: 447-450

Sambrook J, Fritsch EF and Maniatis T. 1989. Molecular cloning: A laboratory manual, 2nd edn. Cold Spring Habor Laboratory Press. Cold Spring Harbor, NY

Sato T, Oeller PW and Theologis A. 1991. The 1-aminocyclopropane-1-carboxylate synthase of cucurbita. Journal of Biological Chemistry 266: 3752-3759

Sato T and Theologis A. 1989. Cloning the mRNA encoding 1-aminocyclopropane-1-carboxylate synthase, the key enzyme for ethylene biosynthesis in plants. Proceedings of National Academy of Sciences, USA 86: 6621-6625

Satoh S and Esashi Y. 1986. Inactivation of 1-aminocyclopropane-1-carboxylic acid synthase of etiolated mung bean hypocotyl segments by its substrate, S-adenosyl-L-methionine. Plant and Cell Physiology 27(2): 285-291

Satoh S and Yang SF. 1988. S-adenosylmethionine-dependent inactivation and radiolabeling of 1-aminocyclopropane-1-carboxylate synthase isolated from tomato fruits. Plant Physiology 88: 109-114

Schaller GE and Bleecker AB. 1995. Ethylene-binding sites generated in yeast expressing the Arabidopsis ETR1 gene. Science 270 :1809-1811

Schaller GE, Ladd AN, Lanahan MB, Spanbauer JM and Bleecker AB. 1995. The ethylene response mediator ETR1 from Arabidopsis forms a disulfide-link dimer. Journal of Biological Chemistry 270: 12526-12530

Schlagnhaufer CD, Glick RE, Arteca RN and Pell EJ. 1995. Molecular cloning of an ozone-induced 1-aminocyclopropane-1-carboxylate synthase cDNA and its relationship with a loss of rbcS in potato (*Solanum tuberosum* L.) plants. Plant Molecular Biology 28: 93-103

Sestak Z. 1985. Chlorophyll and cartenoids during leaf ontogeny. In Sestak Z, ed. Photosynthesis during leaf development, Academia, Prague, pp 76-106

Shaw JF, Chou YS, Chang RC and Yang SF. 1996. Characterization of the ferrous ion binding site of apple 1-aminocyclopropane-1-carboxylic acid oxidase by site-directed mutagenesis. Biochemistry and Biophysics Research Communication 225(3): 697-700

Shinshi H, Usami S and Ohme-Takagi M. 1995. Identification of an ethylene-responsive region in the promoter of a tobacco class I chitinase gene. Plant Molecular Biology 27: 923-932

Shiu OY, Oetiker JH, Yip WK and Yang SF. 1998. The promoter of LE-ACS7, an early flooding-induced 1-aminocyclopropane-1-carboxylate synthase gene of the tomato, is tagged by a Sol3 tranposon. Proceedings of National Academy of Sciences, USA 95: 10334-10339

Simpson SP, Ashford DA, Harvey DJ and Bowles DJ. 1998. Short chain oligogalaturonides induce ethylene production and expression of the gene encoding aminocyclopropane-1-carboxylic acid oxidase in tomato plants. Glycobiology 8(6) 579-583

Sisler EC and Serek M. 1997. Inhibitors of ethylene responses in plants at the receptor level: recent developments. Physiologia Plantarum 100: 577-582

Sisler EC, Dupille E and Serek M. 1996a. Effect of 1-methylcyclopropene on ethylene binding and ethylene action on cut carnations. Plant Growth Regulation 18: 79-86

Sisler EC, Serek M and Dupille E. 1996b. Comparison of cyclopropene, 1-methylcyclopropene and 3,3-dimethylcyclopropene as ethylene antagonists in plants. Plant Growth Regulation. 18:169-174

Smalle J and Van Der Straeten, D. 1997. Ethylene and vegetative development. Physiologia Plantarum 100: 593-605

Smalle J, Haegman M, Kurepa J, Van Montague M. and Van Der Straeten D. 1997a. Ethylene can stimulate *Arabidopsis* hypocotyl elongation in the light. Proceedings of National Academy of Sciences, USA 94: 2756-2761

Smalle J, Kurepa J, Haegman M, Van Montagu M and Van Der Straeten D. 1997b. Ethylene and Arabidopsis rosette development. In Kanelis AK, Chang C, Kende H and Grierson D, eds, Biology and Biotechnology of the Plant Hormone Ethylene. NATO ASI Series, Kluwer Academic Publishers, Dordrecht, The Netherlands, pp. 87-92

Smith JJ and John P. 1993. Activation of 1-aminocyclopropane-1-carboxylate oxidase by bicarbonate/carbon dioxide. Phytochemistry 32: 1381-1386

Smith JJ, Ververidis P and John P. 1992. Charaterisation of ethylene-forming enzyme partially purified from melon. Phytochemistry 31: 1484-1494

Smyth DR. 1990. *Arabidopsis thaliana* : A model plant for studying the molecular basis of morphogenesis. Astralian Journal of Plant Physiology 17: 323-331

Solano R and Ecker JR. 1998. Ethylene gas: perception, signaling and response. Current opinions in Plant Biology 1(5): 393-398

Solano R, Stepanova A, Chao Q and Ecker JR. 1998. Nuclear events in ethylene signaling: a transcriptional cascade mediated by ETHYLENE-INSENSITIVE3 and ETHYLENE-RESPONSE-FACTOR1. Genes and Development 12(23): 3703-3714

Spanu P, Boller T and Kende H. 1993. Differential accumulation of transcripts of 1-amino-cyclopropane-1-carboxylate synthase genes in tomato plants infected with *Phytophthora infestans* and in elicitor-treated tomato cell suspensions. Journal of Plant Physiology 141: 557-562

Spanu P, Felix G and Boller T. 1990. Inactivation of stress induced 1-aminocyclopropane-1-carboxylate synthase *in vivo* differs from substrate-dependent inactivation *in vitro*. Plant Physiology 93: 1482-1485

Spanu P, Grosskopf DG, Felix G and Boller T. 1994. The apparent turnover of 1-aminocyclopropane-1-carboxylate synthase in tomato cells is regulated by protein phosphorylation and dephosphorylation. Plant Physiology 106: 529-535

Spanu, P, Reinhardt D and Boller T. 1991. Analysis and cloning of the ethylene-forming enzyme from tomato by functional expression of its mRNA in *Xenopus* laevis oocytes. European Molecular Biology Organization Journal 10: 2007-2013

Starret DA and Laties GC. 1993. Ethylene and wound-induced gene expression in the preclimacteric phases of ripening avocado fruit and mesocarp discs. Plant Physiology 103: 227-234

Su LY, Liu Y and Yang SF. 1985. Relationship between 1-aminocyclopropane-1-carboxylatemalonyl-transferase and D-amino acid malonyltransferase. Phytochemistry 24: 1141-1145

Suzuki K, Suzuki N, Ohme-Takagi M and Shinshi H. 1998. Immediate early induction of mRNAs for ethylene-responsive transcription factors intobacco leaf strips after cutting. The Plant Journal 15(5): 657-665

Tabor CW and Tabor H. 1984. Methionineadenosyltranferase (S-adenosylmethionine synthetase) and S-adenosylmethioinine decarboxylase. Advanced Enzymology 56: 251-282

Takahashi H and Jaffe MJ. 1984. Thigmomorphogenesis; the relationship of mechanical perturbation to elicitor-like activity and ethylene biosynthesis. Physiologia Plantarum 61: 405-411

Tang X, Gomes AMTR and Woodson WR. 1994. Pistil-specific and ethylene-regulated expression of 1-aminocyclopropane-1-carboxylate oxidase genes in petunia flowers. The Plant Cell 6: 1227-1239

Tang X, Wang H, Bramer AS, and Woodson WR. 1993. Organnization and structure of the 1-aminocyclopropane-1-carboxylic acid oxidase gene family from Petunia hybrida. Plant Molecular Biology 23(6): 1151-1164

Tang, X. and Woodson, W. 1996. Temporal and spatial expression of 1-aminocyclopropane-1-carboxylate oxidase mRNA following pollination of immature and mature petunia flowers. Plant Physiol. 112 : 503-511

Tarun AS and Theologis A. 1998. Complementation analysis of mutants of 1-aminocyclopropane-1-carboxylate synthase reveals the enzyme is a dimer with shared active sites. Journal Biological Chemistry 273(20): 12509-12514

Tarun AS, Lee JS and Theologis A. 1998. Random mutagenesis of 1-aminocyclopropane-1-carboxylate synthase: a key enzyme in ethylene biosynthesis. Proceedings of National Academy of Sciences, USA 95(17): 9796-9801

Tayeh MA, Howe DL, Salleh HM, Sheflyan GY, Son JK and Woodard RW. 1999. Kinetic and mutagenetic evidence for the role of histidine residues in the *Lycopersicon esculentum* 1-aminocyclopropane-1-carboxylic acid oxidase. Journal of Protein Biochemistry 18(1): 55-68

Tear JM, Islam R, Flanagan R, Gallagher S, Davies MG, Grabau C. 1997. Measurement of nucleic acid concentrations using the DyNAQuant™ and the GeneQuant. BioTechniques 22(6): 1170-1174

Thomas RG. 1987. The structure of the mature plant, pp2-28 and Vegetative growth and development, pp31-62. In William, ed, White clover. CAP press, Sydney

Todaka I and Imaseki H. 1985. Epidermal cells do not contributed to auxin-induced ethylene production in mung bean stem sections. Plant and Cell Physiology 26: 865-871

Towbin H, Staehelin T and Gordo J. 1979. Electrophoric transfer of protein from polyacrylamide gel to nitrocellulose sheets: procedures and some applications. Proceedings of National Acdemy of Sciences USA 76: 4350-4354

Trebitsh T, Staub JE and O'Neil SD. 1997. Identification of a 1-aminocyclopropane-1-carboxylic acid synthase gene linked to the Female (F) locus that enhances female sex expression in cucumber. Plant Physiology 113: 987-995

Van der Straeten D, Djudzman A, Caeneghem WV, Smalle J. and Montagu MV. 1993. Genetic and physiological analysis of a new locus in arabidopsis that confers resistance to 1-aminocyclopropane-1carboxylic acid and ethylene and specifically affects the ethylene signal transduction pathway. Plant Physiology 102: 401-408

Van Der Straeten D, Rodrigues-Pousada RA, Villarroel R, Hanley S, Goodman HM, and Van Montagu M. 1992. Cloning, genetic mapping, and expression analysis of an *Arabidopsis thaliana* gene that encodes 1-aminocyclopropane-1-carboxylate synthase. Proceedings of National Academy of Sciences, USA, 89: 9969-9973

Van Der Straeten D, Van Wiemeersch L, Goodman HM and Van Montagu M. 1990. Cloning and sequence of two different cDNAs encoding 1-amino cyclopropane-1-carboxylate synthase in tomato. Proceedings of National Academy of Sciences, USA 87: 4859-4863

Ververdis P and John P. 1991. Complete recovery in vitro of ethylene-forming enzyme activity. Phytochemistry 30: 725-727

Vioque B and Castellano JM. 1998. *In vivo* and *in vitro* 1-aminocyclopropane-1-carboxylic acid oxidase activity in pear fruit: role of ascorbate and inactivation during catalysis. Journal of Agricultural Food Chemistry 46: 1706-1711

Vioque B. and Castellano JM. 1994. Extraction and biochemical characterization of 1-aminocyclopropane-1-carboxylic acid oxidase from pear. Physiologia Plantarum 90: 334-338

Vogel JP, Woeste KE, Theologis A and Kieber JJ. 1998. Recessive and dominant mutation in the ethylene biosynthetic gene ACS5 of *Arabidopsis* confers cytokinin insensitivity and ethylene overproduction, respectively. Proceedings of National Academy of Sciences, USA 95: 4766-4771

Vries MAN-D, Woltering EJ and De Vrije T. 1994.Partial characterization of carnation petal 1-aminocyclopropane-1-carboxylate oxidase. Journal of Plant Physiology 144: 549-554

Watanabe T and Sakai S. 1998. Effects of active oxygen species and methyl jasmonate on expression of the gene for a wound-inducible 1-amincyclopropane-1-carboxylate synthase in winter squash (*Cucurbita maxima*). Planta 206: 570-576

Wassengger M and Pelissrer T. 1999. Signaling in gene silencing. Trends in Plant Science 4(6): 207-208

White MF, Vasquez J, Yang SF and Kirsch JF. 1994. Expression of apple 1-aminocyclo-propane-1-carboxylate synthase in *Escherichia coli*: kinetic characterization of wild-type and active-site mutant forms. Proceedings of National Academy of Sciences, USA 91: 12428-12432

Whittaker DJ, Smith GS and Gardner RC. 1997. Expression of ethylene biosynthetic genes in *Actinidia chinesis* fruit. Plant Molecular Biology 34: 45-55

Wilkinson JQ, Lanahan MB, Clark DG, Bleecker AB, Chang C, Meyerowitz EM and Klee H. 1997. A dominant mutant receptor from Arabidopsis confers ethylene insensitivity in heterologous plants. Nature Biotechnology 15(5): 444-447

Woeste K and Kieber JJ. 1998. The molecular basis of ethylene signaling in Arabidopsis. Philosophical Transactions of Royal Society in London Biological Sciences 353: 1431-1438

Woodson WR, Park KY, Drory A, Larsen PB and Wang H. 1992. Expression of ethylene biosynthetic pathway transcripts in senescing carnation flowers. Plant Physiology 99: 526-532

Wurgler-Murphy SM and Saito H. 1997. Two-component signal transducers and MAPK cascades. Trends in Biochemical Sciences 22(5): 172-176

Xu P, Narasimhan MN, Samson T, Coca MA, Huh GH, Zhou J, Martin GB, Hasegawa PM and Bressan RA. 1998. A nitrilase-like protein interacts with GCC box DNA-binding proteins involved in ethylene and defense responses. Plant Physiology 118(3): 867-874

Yang SF and Dong JG. 1993. Recent progress in research of ethylene biosynthesis. Botanical Bulletin of Academia Sinica 34: 89-101

Yang SF and Hoffman NE. 1984. Ethylene biosynthesis and its regulation in higher plants. Annual Review of Plant Physiology 35: 155-189

Yip W, Dong J, Kenny JW, Thompson GA and Yang SF. 1990. Characterisation and sequencing of the active site of 1-aminocyclopropane-1-carboxylate synthase. Proceedings of National Academy of Sciences, USA 87: 7930-7934

Yip W, Dong J-G and Yang SF. 1991. Purification and characterization of 1-aminocyclopropane-1-carboxylate synthase from apple fruits. Plant Physiology 95: 251-257

Yip W, Moore T and Yang SF. 1992. Differential accumulation of transcripts for four tomato 1-aminocyclopropane-1-carboxylate synthase homologs under various conditions. Proceedings of National Academy of Sciences, USA 89: 2475-2479

Yip WK and Yang SF. 1988. Cyanide metabolism in relation to ethylene production in plant tissues. Plant Physiology 88: 473-476

Yoon IS, Mori H, Kim JH, Kang BG and Imaseki H. 1997. VR-ACS6 is an auxin-inducible 1-aminocyclopropane-1-carboxylate synthase in mung bean (*Vigna radiata*). Plant and Cell Physiology 38(3): 217-224

Yoon IS, Park D-H, Mori H, Imaseki H and Kang BG. 1999. Characterization of an auxin-inducible 1-aminocyclopropane-1-carboxylate synthase gene, VR-ACS6, of mung bean (*Vigna radiata* (L.) Wilczek) and hormonal interactions on the promoter activity in transgenic tobacco. Plant and Cell Physiology 40(4): 431-438

Yoshii H and Imaseki H. 1982. Regulation of auxin-induced ethylene biosynthesis. Repression of inductive formation of 1-aminocyclopropane-1-carboxylate synthase by ethylene. Plant and Cell Physiology 23: 639-649

Yu SJ, Kim S, Lee JS and Lee DH. 1998. Differential accumulation of transcripts for ACC synthase and ACC oxidase homologs in etiolated mung bean hypocotyls in response to various stimuli. Molecules and Cells 8(3): 350-358

Yu YB and Yang SF. 1979. Auxin-induced ethylene production and its inhibition by aminoethoxy vinylglycine and cobalt ion. Plant Physiology 64: 1074-1077

Zarembinski TI and Theologis A. 1994. Ethylene biosynthesis and action: a case of conservation. Plant Molecular Biology 26: 1579-1597

Zarembinski TI and Theologis A. 1993. Anaerobiosis and plant growth hormones induce two genes encoding 1-aminocyclopropane-1-carboxylate synthase in rice (*Oryza sativa* L.). Molecular and Biological Cells 4(4): 363-373

Zhang Z, Barlow JN, Baldwin JE and Schofield CJ. 1997. Metal catalyzed oxidastion and mutagenesis studies on the iron(II) binding site of 1-aminoacyclopropane-1-carboxylate oxidase. Biochemistry 36(50): 15999-16007

Zhang Z, Schofield CJ, Baldwin JE, Thomas P and John P. 1995. Expression, purification and charaterization of 1-aminocyclopropane-1-carboxylate oxidase from tomato in *Escherichia coli*. Biochemical Journal 307: 77-85

Zhou H, Huxtable S, Xin H and Li N. 1998. Enhanced high-level expression of soluble 1-aminocyclopropane-1-carboxylate synthase and rapid purification by expanded-bed adsorption. Protein Expression and Purification 14(2): 178-184

Appendix I: Histological analysis

1 Tissue fixation and wax embedding

Plant tissues were fixed by a method described by Jackson (1991). To prepare the fixative, PBS [7 mM Na_2HPO_4, 3 mM NaH_2PO_4 (pH 11), 130 mM NaCl] was prepared just before use, then incubated at 60 °C, and 4g of paraformaldehyde added and completely dissolved with occasional swirling. The fixing solution was cooled on ice and then the pH adjusted to 7.0 with concentrated H_2SO_4. Sample tissue was harvested and immediately immersed into excess fixing solution on ice, infiltrated by vaccum, and then stored in fresh fixing solution at 4 °C overnight. The fixed tissue was then transferred into cold 0.85% (w/v) NaCl on ice for 30 min with occasional swirling, then placed into plastic cassettes and dehydrated through an ethanol series of 35% (v/v), 45% (v/v), 55% (v/v), 70% (v/v), 85% (v/v) ethanol, each containing 0.85% (w/v) NaCl, then 95% (v/v) and 100% (v/v) ethanol, each for 90 min at each stage. The sample was then treated with 100 % (v/v) ethanol for 2 hr at room temperature, 50 % (v/v) ethanol: 50 % (v/v) Histoclear™II (national diagnostics, Atlanta, Georgia, USA) for 1 hr and then in three changes of 100 % (v/v) Histoclear™II. PARAPLAST chips (OXFORD Labware, St. Louis, USA) were then added to occupy approximately half the volume of the Histoclear™II and the mixture was incubated at room temperature overnight.

The sample with PARAPLAST chips was then incubated at 40-50 °C until the PARAPLAST chips dissolved completely and then the tissue was transferred into new molten PARAPLAST and incubated at 60 °C overnight. The PARAPLAST was renewed at 12 hr intervals for 4 days, and then a wax block was prepared by pouring some molten PARAPLAST in a metal mould and placing the sample of tissue at the centre, and then the mould was placed on chilled plates (LEICA EG1160; Leica Instruments GmbH, Nussioch, Germany) to solidify the PARAPLAST. After solidifying, wax (PARAPLAST) blocks were stored at 4 °C until required.

2 Tissue sectioning

The wax block was first cut to a trapezoid shape by blade, leaving about 2 mm of wax around the plant material. The sculptured wax block was fixed to the microtome (LEICA RM2145; Leica Instruments GmbH, Nussioch, Germany) and 8 µm sections cut and floated onto sterile

water incubated at 42 °C. The section was lifted onto glass slides (SUPERFROST®*PLUS; Biolab Scientific, NZ), excess water drained off and the slides then placed on a hotplate (45 °C; RaymondALamb, England) overnight before storage in a desiccater at room temperature until required.

3 Visualization of slides

Slides were stained with safranin and Fast Green to visualise lignified tissue and cytosol, respectively. One % (w/v) safranin was prepared in 70% (v/v) ethanol and 0.3% Fast Green was prepared in a 150 mL solution of 10% (v/v) clove oil, 10% (v/v) methyl cellasolve, 30% (v/v) glacial acetic acid, and 60% (v/v) ethanol. The staining procedure is outlined in table A.

Table A Staining procedure

Order	Treatment	Time
1.	HistoClear	10 min
2.	50% (v/v) HistoClear/50% (v/v) Ethanol	5 min
3.	100% (v/v) Ethanol	5 min
4.	100% (v/v) Ethanol	5 min
5.	95% (v/v) Ethanol	5 min
6.	85% (v/v) Ethanol	5 min
7.	70% (v/v) Ethanol	5 min
8.	Safranin	24 hr
9.	Water	briefly
10.	70% (v/v) Ethanol	5 min
11*.	0.5% (v/v) Picrinic acid	10 sec
12.	95% (v/v) Ethanol	2 min
13.	95% (v/v) Ethanol	10 sec
14.	Fast Green	5 min
15.	Clove Oil	briefly
16**.	Clove Oil/Ethanol/Histoclear	5-10 sec
17.	Histoclear	5 sec
18.	Histoclear	5 sec
19.	Histoclear	5 sec
20.	DPX mountant and mount cover slip	

* 0.5% (v/v) Picrinic acid: 0.5% picrinic acid in 95% (v/v) ethanol

** Clove Oil/Ethanol/Histoclear = 50:25:25

Emendations

Page iii	Line 3	*Trifolium*
	Line12	'isolated from either'
Page xxvi	Line 4	carboxylate
Page xxvi	Line 18	tetrazolium
Page xxvii	Line 2	pyridoxal
Page 4	Line 18	delete 'on'
Page 5	Line 13	delete 'full stop' and continue with 'because'
Page 7	Line 2	Meyerowitz
Page 7	Line 6	'not possible' replace 'unable'
Page 8	Line 5	mitogen
Page 9	Line 14	Shinshi
Page 11	Fig. 1.2	aminocyclopropane
Page 13	Line 3	'at' replace first 'after'
Page 14	Line 10	cells
Page 18	Line 5	delete 'by'
Page 22	Line 26	Meyerowitz
Page 25	Line 15	'a' replace 'as'
Page 36	Line 28	*Helianthus*
Page 41	Line 12	delete 'lowed'
Page 49	Line 6	'may be a'
Page 74	Line 15	quartz
	Line 17	Sambrook
Page 76	Line 8	Germany
Page 79	Line 11	The
Page 82	Line 8	agar
Page 110	Line 1	delete 'were'
Page 132	Table 3.2.3	*Pisum sativum*
Page 136	Line 3	*thaliana*
Page 150	Fig. 3.3.8	'EcoRI' replace 'BamHI' (second line)
Page 162	Line 5	untranslated
Page 182	Line 16	section 3.3.3
Page 190	Line 1	delete 'as'
Page 198	Fig. 3.5.8	'b2' and 'b3' replace 'a2' and 'a3' (second line)
Page 199	Line 19	discernible
Page 202	Line 3	discernible
Page 202	Line 9	exists
Page 202	Line 26	discernible
Page 209	Line 20	delete 'in this expression'
Page 229	Line 11	revealed
Page 224	Line 4	Dilley
Page 240	Line 25	Spanu *et al.*, 1990; Spanu *et al.*, 1994
Page 241	Line 1	Finlayson *et al.* (1997)
	Line 8	Finlayson *et al.*1997
Page 251	Line 23	Shinshi
Page 254	Line 7	TRACS3
Page 256	Line 14	transducer
	Line 32	ethylene
Page 257	Line 21	Identification
Page 258	Line 29	alkaline
Page 259	Line 8	characterisation
Page 260	Line 7	Ethylene
	Line 10	CO_2
	Line 19	field
Page 262	Line 8	'Drake' replace 'Grake'
	Line 9	tomato
	Line 16	phosphoinositide
Page 263	Line 3	ethylene
	Line 19	-1-carboxylate
	Line 35	'Laemmli' replace 'Lammli'
Page 264	Line 15	1-aminocyclopropane-1-
	Line 34	of
Page 266	Line 32	galacturonic
Page 267	Line 2	and
	Line 28	Asymmetric
	Line 36	Pathogen
Page 268	Line 8	CO_2
	Line 25	Roberts
Page 270	Line 8	transposon
	Line 9	oligogalacturonides
	Line 30	Characterisation
	Line 33	Australian
Page 271	Line 18	in tobacco
	Line 26	Organisation
Page 272	Line 1	'Teare' replace 'Tear'
	Line 4	Williams, W.M.
	Line 5	contribute
	Line 15	1-carboxylic
Page 272	Add '**Van Slogteren CMS, Hoge JHC, Hooykaas PJJ, Schilperoot RA**. 1983. Clonal analysis of heterogenec crown gall turmour tissues induced by wild type and shooter mutant strains of Agrobacterium tumefeciens- expr T-DNA genes. Plant Molecular Biology 2: 321-333'	